

NOVEL PINCER COMPLEXES OF TRANSITION METALS FOR REDUCTION OF  
CARBON DIOXIDE TO CARBON MONOXIDE AND CROSS COUPLING OF  
ARYL HALIDES

A Dissertation

by

CHANDRA MOULI PALIT

Submitted to the Office of Graduate and Professional Studies of  
Texas A&M University  
in partial fulfillment of the requirements for the degree of

DOCTOR OF PHILOSOPHY

Chair of Committee,	Oleg V. Ozerov
Co-Chair of Committee,	Francois P. Gabbai
Committee Members,	Michael B. Hall
	Mark T. Holtzapple
Head of Department,	Simon North

August 2016

Major Subject: Chemistry

Copyright 2016 Chandra Mouli Palit

## ABSTRACT

Carbon dioxide is a major anthropogenic greenhouse gas and one of the biggest causes of global climate change. Utilization of CO<sub>2</sub> to produce chemicals is an interesting proposition to mitigate its negative impact. However, the chemical inertness of CO<sub>2</sub> presents a challenge to its transformation into useful chemicals. Transition metal complexes supported by pincer ligands have proved successful previously for the activation of small molecules. Here, we report our investigations into the use of a Pd<sup>I</sup>-Pd<sup>I</sup> dimer [(<sup>F</sup>PNP)Pd]<sub>2</sub>, previously utilized by our group to activate molecules such as H<sub>2</sub>O, H<sub>2</sub>, NH<sub>3</sub>, O<sub>2</sub>, and to transform CO<sub>2</sub> into CO, a more widely used C1-feedstock for chemicals. Use of trimethylsilyl reagents proved vital for O-atom abstraction to produce CO, and an in-house CO trap, (<sup>Me</sup>PNP)Ir(Ph)(H) was used to quantify the amount of CO evolved.

Transition metal catalyzed cross coupling reactions have made synthesis of previously unattainable substrates possible, thus opening new avenues into new specialty chemicals, pharmaceuticals and agro chemicals. Group 10 metals, especially Pd have been used almost exclusively for these reactions in the past. The reasons for the popularity of these Pd catalysts are the versatility, functional group tolerance and wide substrate scope exhibited by them. More recently, however, metals outside group 10 such as Cu, Ir, Rh have found uses in these reactions. Especially, (POCOP)Rh systems previously reported by our group have been very useful in catalysis and mechanistic studies. Based on the success of these Rh catalysts and high natural abundance and low prices of cobalt, we envisioned the use of analogous Co systems as catalysts for catalytic cross coupling. With

that as our primary goal,  $\text{Co}^{\text{III}}$  complexes such as  $(\text{POCOP})\text{Co}(\text{Ar})(\text{X})$  and  $(\text{POCOP})\text{Co}(\text{Ar})(\text{SAr}')$  presumed to be part of the catalytic C-S coupling cycle have been isolated and their interchange has been probed. However, contrary to the observations in Rh, C-S RE is not observed in the thermolysis of  $(\text{POCOP})\text{Co}(\text{Ar})(\text{SAr}')$ ; instead  $\text{C}_{\text{Ar}}-\text{C}_{\text{ligand}}$  is the predominant reaction. A shift to the PNP ligands was made and indeed C-S RE is observed although accompanied by decomposition to  $(\text{PNP})\text{Co}^{\text{II}}$  species.

A relatively unexplored way of incorporating new functionality into pincer transition metal complexes is having multi-nuclear pincers that can be connected by different linkers to influence the degree of proximity and in turn the cooperativity between multiple metal sites. Such cooperativity can prove beneficial for reactions where one metal center is not enough. Here we have expanded the library of binuclear pincer ligands and complexes by reporting ligands of different steric bulk, linkers with incorporated functionality, and also metalation of these pincers with Ni and Pd.

## DEDICATION

“To my family for encouraging me to embark on this journey and to my friends for  
making the experience memorable”

## ACKNOWLEDGEMENTS

First and foremost, I would like to thank my committee chair and research advisor, Prof. Oleg Ozerov for his guidance over the past six years. I appreciate his invaluable guidance, detailed feedback and continues patience with me as I navigated my research projects and life in graduate school. I would also like to thank my committee members, Prof. Michael Hall, Prof. Francois Gabbai, and Prof. Mark Holtzapple for giving me advice and direction throughout my graduate school tenure.

Thanks also to the Ozerov research group members, who have played an important part in making me the chemist and the person that I am today. Their devotion, hard work and knowledge in chemistry have served as great examples for me to emulate over the years. I would specially like to thank Loren Press, Alex Kosanovich and Bryan Foley for the innumerable discussions about life outside chemistry that have shaped my world view. I am honored to mention the current and past Ozerov group members I had the pleasure of working with: Dr. Weixing Gu, Dr. Yanjun Zhu, Dr. Dan Smith, Dr. David Herbert, Dr. Jia Zhou, Dr. Morgan MacInnis, Dr. Rafael Huacuja, Dr. Rodrigo Ramirez, Dr. Sam Timpa, Dr. Chun-I Lee, Dr. Jillian Davidson, Billy McCulloch, Christina Bramell, Chelsea Mandell, Christopher Pell, Wei-Chun Shih, Soomin Park, Patrick Hubbard, Qingheng Lai, and Andy Yu.

Having the support of my incredible friends has made life in grad school easier. Masato Hirai, John Patrick, Andrew Brown, Brateen Shome, and Scott Winkler have been the best roommates and friends one could ask for over the years. Subrata Ghosh and his family

have reminded me of my own family at times and they have kept me connected to my roots.

On the note of family, I would like to express my immense love and gratitude to my parents and brother, who have stood with me all my life and whose confidence and belief in me helped me take on the challenge of graduate school and their support and love has been my rock through difficult times.

## NOMENCLATURE

OA	oxidative addition
RE	reductive elimination
<sup>i</sup> Pr	<i>iso</i> -propyl
<sup>t</sup> Bu	<i>tert</i> -butyl
dppf	bis(diphenylphosphino)ferrocene
tolyl	C <sub>6</sub> H <sub>4</sub> Me
S <sup>i</sup> Pr <sub>2</sub>	diisopropylsulfide
Ph	phenyl
Ar	aryl
py	pyridine
OAc	acetate
OTf	trifluoromethane sulfonate
L	ligand
THF	tetrahydrofuran
OEt <sub>2</sub>	diethylether
DMAP	4-(N,N-dimethylamino)pyridine
NCS	N-chlorosuccinimide
solv	solvent
NMR	Nuclear Magnetic Resonance

ESI-MS            Electrospray Ionization-Mass spectrometry

Ar<sup>Y</sup>                benzene ring with a para substituent Y



## TABLE OF CONTENTS

	Page
ABSTRACT .....	ii
DEDICATION .....	iv
ACKNOWLEDGEMENTS .....	v
NOMENCLATURE .....	vii
TABLE OF CONTENTS .....	ix
LIST OF FIGURES .....	xii
LIST OF TABLES .....	xxi
CHAPTER I INTRODUCTION AND LITERATURE REVIEW .....	1
1.1. General introduction to pincer ligands .....	1
1.2. Coupling catalyzed by transition metals .....	3
1.2.1 History of transition metal catalyzed coupling reactions .....	3
1.2.2. Mechanism of transition metal catalyzed coupling reactions .....	6
1.2.2.1 Classical mechanism of coupling reactions with palladium .....	7
1.2.2.2 Mechanism of coupling reactions with Rh.....	9
CHAPTER II REDUCTION OF CO <sub>2</sub> TO FREE CO BY A Pd <sup>I</sup> -Pd <sup>I</sup> DIMER .....	14
2.1. Introduction .....	14
2.2. Results and discussions .....	17
2.2.1. Overview of ( <sup>F</sup> PNP <sup>iPr</sup> ) ligand and past reactivity of [( <sup>F</sup> PNP)Pd-] <sub>2</sub> .....	17
2.2.2. Preliminary reactions of <b>201</b> with CO <sub>2</sub> and CS <sub>2</sub> .....	18
2.2.3. Reactions of <b>201</b> with CO <sub>2</sub> and Me <sub>3</sub> SiX reagents .....	20
2.2.4. Trapping of evolved CO with ( <sup>Me</sup> PNP)Ir(D)(C <sub>6</sub> D <sub>5</sub> ) .....	20
2.2.5. Control reactions .....	21
2.2.6. Mechanistic insight.....	22
2.3. Conclusion.....	24
2.4. Experimental details.....	24
2.4.1. General considerations .....	24
2.4.2. Estimation of number of moles of gases in J. Young NMR tube headspace .....	25
2.4.3. General procedure for preparation of a stock solution of (FNP)Me .....	25
2.4.4. In-situ generation of ( <sup>Me</sup> PNP)Ir(D)(C <sub>6</sub> D <sub>5</sub> ) ( <b>207D</b> ) from ( <sup>Me</sup> PNP)Ir(H)(Mes) ( <b>206</b> ). .....	26
2.4.5. Spectral details for some previously reported compounds.....	26

2.4.6. Reactions of $[(^F\text{PNP})\text{Pd}]_2$ ( <b>201</b> ) with $\text{CO}_2$ .....	27
2.4.7. Synthesis of $(^F\text{PNP})\text{Pd-C(S)S-Pd}(\text{PNP}^F)$ ( <b>203</b> ) and its reactions .....	33
2.4.8. Characterization of $(^{\text{Me}}\text{PNP})\text{Ir(H)(Ph)CO}$ ( <b>208</b> ) .....	37
2.4.9. CO trapping experiments .....	38
2.4.10. Control reactions .....	42
2.4.11. Synthesis of $(^F\text{PNP})\text{Pd-SiMe}_3$ ( <b>210</b> ) and its reactions .....	46

### CHAPTER III POCOP COBALT COMPLEXES RELEVANT TO CATALYTIC COUPLING AND REDUCTIVE ELIMINATION STUDIES.....49

3.1. Introduction .....	49
3.2. Results and discussion.....	53
3.2.1. Synthesis of $\text{Co}^{\text{II}}$ complexes.....	53
3.2.2. Synthesis of $\text{Co}^{\text{III}}$ complexes.....	55
3.2.3. X-ray structural studies .....	58
3.2.4. Discussion of spin states of (POCOP)Co compounds.....	62
3.2.5. Thermolysis and observation of $\text{C}_{\text{ligand}}-\text{C}_{\text{Ph}}$ reductive elimination from <b>316</b> .	63
3.3. Conclusion.....	66
3.4. Experimental details.....	66
3.4.1 General considerations .....	66
3.4.2. Synthesis of (POCOP) $\text{Co}^{\text{II}}$ compounds.....	67
3.4.3. Synthesis of (POCOP) $\text{Co}^{\text{III}}$ compounds.....	73
3.4.4. Reactions of (POCOP)Co(Ph)(X) complexes with alkyl reagents.....	80
3.4.5. Decomposition studies of (POCOP)Co(R)(X) complexes.....	83
3.4.6. Thermolysis of (POCOP)Co(Ph)(SPh) and analysis of the product mixture .	84
3.4.7. X-ray crystallography .....	88

### CHAPTER IV COBALT COMPLEXES OF PNP LIGANDS AND OBSERVATION OF C-S COUPLING .....93

4.1. Introduction .....	93
4.2. Results and discussions .....	94
4.2.1. Synthesis of PNP complexes of $\text{Co}^{\text{II}}$ .....	94
4.2.2. Synthesis of PNP complexes of Cobalt <sup>III</sup> .....	95
4.2.3. Structure discussion.....	97
4.2.4. Thermolysis experiments .....	98
4.2.5. Mechanistic studies .....	99
4.3. Conclusion and future experiments.....	102
4.4. Experimental details.....	103
4.4.1. General considerations .....	103
4.4.2. Synthesis of $(^{\text{Me}}\text{PNP}^{\text{iPr}})\text{Co}^{\text{II}}$ complexes .....	104
4.4.3. Synthesis of $(^{\text{Me}}\text{PNP}^{\text{iPr}})\text{Co}^{\text{III}}$ complexes .....	105
4.4.4. Synthesis of $(^{\text{Me}}\text{PNP}^{\text{iPr,Et}})$ ligand and its Co complexes .....	112
4.4.5. Thermolysis experiments .....	118

4.4.6. X-Ray crystallography .....	121
CHAPTER V BINUCLEAR PCN AND PNN LIGANDS AND THEIR PD AND NI COMPLEXES .....	122
5.1. Introduction .....	122
5.2. Results and discussion.....	124
5.2.1. Synthetic details for PCN complexes.....	124
5.2.2. Synthetic details for PNN complexes.....	126
5.2.3. Solid-State structures of complexes of the type ( <sup>R</sup> PCN-C <sub>n</sub> )MX and ( <sup>iPr</sup> PNN-C <sub>2</sub> )MX .....	127
5.3. Conclusions .....	130
5.4. Experimental .....	130
5.4.1. General considerations .....	130
5.4.2. Synthesis of PCN compounds with alkyl linkers .....	131
5.4.3. Synthesis of PNN compounds with alkyl linkers.....	155
5.4.4. Synthesis of PCN ligand and Ni complex with pendant amine linker .....	158
5.4.5. X-ray crystallography.....	161
CHAPTER VI SUMMARY AND CONCLUSIONS .....	166
REFERENCES.....	168

## LIST OF FIGURES

	Page
<b>Figure I.1</b> A typical pincer complex .....	1
<b>Figure I.2</b> Some typical pincer ligands with the acronyms used for them .....	2
<b>Figure I.3</b> Pd catalyzed C-C and C-heteroatom cross coupling reactions.....	4
<b>Figure I.4</b> Copper catalyzed coupling reactions.....	5
<b>Figure I.5</b> Generalized mechanism for coupling reactions using a $M^n/M^{n+2}$ cycle .....	6
<b>Figure I.6</b> (a) OA of aryl halides to $(PPh_3)_4Pd$ (b) OA of aryl halides to $Pd(0)$ complexes with bulky phosphines .....	7
<b>Figure I.7</b> (a) Catalytic cycle for Pd catalyzed coupling reactions (b) RE/OA via a concerted transition state .....	8
<b>Figure I.8</b> (a) OA of aryl halides to a $(PNP)Rh^I$ fragment (b) synthetic cycle for catalytic intermediates involving $(PNP)Rh$ .....	10
<b>Figure I.9</b> Comparison of ground state structures of $d^6$ Rh and $d^8$ Pd complexes prior to RE. ....	12
<b>Figure I.10</b> (a) Catalytic reactions with $(POCOP)Rh(H)(Cl)$ (b) Mechanism for catalytic coupling using $(POCOP)Rh$ catalysts .....	12
<b>Figure II.1</b> Comparison of the polarity and reactivity of $CO_2$ and $CO$ .....	15
<b>Figure II.2</b> Catalytic reduction of $CO_2$ to $CO$ by a $Cu(I)NHC$ catalyst using $(Bpin)_2$ ...	16
<b>Figure II.3</b> Pd catalysts for the reduction of $CO_2$ to $CO$ reported by Dubois .....	16
<b>Figure II.4</b> Previously reported reactivity of $[(^F PNP)Pd-]_2$ (201) with small molecules .....	18
<b>Figure II.5</b> Reactivity of 201 with $CO_2$ and $CS_2$ .....	19
<b>Figure II.6</b> Reactivity of 201 with $CO_2$ in the presence of $Me_3SiX$ .....	20
<b>Figure II.7</b> Synthesis of the in-situ trap 207D and its reaction with $CO$ .....	21
<b>Figure II.8</b> Reactions of 201 with $CO_2/Me_3SiX$ in the presence of 207D as a trap for $CO$ .....	21

<b>Figure II.9</b> Overall stoichiometry of the reaction and possible mechanisms.....	23
<b>Figure II.10</b> Synthesis of $(^F\text{PNP})\text{Pd}(\text{SiMe}_3)$ (210) from of $(^F\text{PNP})\text{PdCl}$ (204).....	24
<b>Figure II.11</b> $^{31}\text{P}\{^1\text{H}\}$ NMR (300 MHz, $\text{C}_6\text{D}_6$ ) spectrum of the reaction of $[(^F\text{PNP})\text{Pd-}]_2$ (201) with $\text{CO}_2$ and $\text{Me}_3\text{SiOTf}$ after heating for 18 h .....	28
<b>Figure II.12</b> $^{19}\text{F}$ NMR (300 MHz, $\text{C}_6\text{D}_6$ ) spectrum of the reaction of $[(^F\text{PNP})\text{Pd-}]_2$ (201) with $\text{CO}_2$ and $\text{Me}_3\text{SiOTf}$ after heating for 18 h.....	29
<b>Figure II.13</b> Silyl region of the $^1\text{H}$ NMR (300 MHz, $\text{C}_6\text{D}_6$ ) stacked spectra of the reaction of $[(^F\text{PNP})\text{Pd-}]_2$ (201) with $\text{CO}_2$ and $\text{Me}_3\text{SiOTf}$ showing conversion of $\text{Me}_3\text{SiOTf}$ (-0.05 ppm) into $(\text{Me}_3\text{Si})_2\text{O}$ (0.11 ppm) .....	29
<b>Figure II.14</b> $^{31}\text{P}\{^1\text{H}\}$ (300 MHz, $\text{C}_6\text{D}_6$ ) NMR spectrum of the reaction of $[(^F\text{PNP})\text{Pd-}]_2$ (201) with $\text{CO}_2$ and $\text{Me}_3\text{SiCl}$ after heating for 18 h .....	31
<b>Figure II.15</b> $^{19}\text{F}$ NMR (300 MHz, $\text{C}_6\text{D}_6$ ) spectrum of the reaction of $[(^F\text{PNP})\text{Pd-}]_2$ (201) with $\text{CO}_2$ and $\text{Me}_3\text{SiCl}$ after heating for 18 h.....	32
<b>Figure II.16</b> Silyl region of the $^1\text{H}$ NMR (300 MHz, $\text{C}_6\text{D}_6$ ) stacked spectra of the reaction of $[(^F\text{PNP})\text{Pd-}]_2$ (201) with $\text{CO}_2$ and $\text{Me}_3\text{SiCl}$ showing unreacted $\text{Me}_3\text{SiCl}$ (0.17 ppm), $(\text{Me}_3\text{Si})_2\text{O}$ (0.11 ppm) and unidentified resonance at 0.19 ppm .....	32
<b>Figure II.17</b> $^1\text{H}$ NMR (300 MHz, $\text{C}_6\text{D}_6$ ) spectrum of $(^F\text{PNP})\text{Pd-C(S)S-Pd(PNP}^F)$ (203) (minute impurities of $\text{Et}_2\text{O}$ ).....	34
<b>Figure II.18</b> $^{31}\text{P}\{^1\text{H}\}$ (300 MHz, $\text{C}_6\text{D}_6$ ) NMR spectrum of $(^F\text{PNP})\text{Pd-C(S)S-Pd(PNP}^F)$ (203) .....	34
<b>Figure II.19</b> $^{19}\text{F}$ NMR (300 MHz, $\text{C}_6\text{D}_6$ ) spectrum of $(^F\text{PNP})\text{Pd-C(S)S-Pd(PNP}^F)$ (203).....	35
<b>Figure II.20</b> $^{13}\text{C}\{^1\text{H}\}$ (300 MHz, $\text{C}_6\text{D}_6$ ) NMR spectrum of $(^F\text{PNP})\text{Pd-C(S)S-Pd(PNP}^F)$ (203) ( $\text{Pd-CS}_2\text{-Pd}$ resonates at 285.3 ppm) .....	35
<b>Figure II.21</b> $^{31}\text{P}\{^1\text{H}\}$ (300 MHz, $\text{C}_6\text{D}_6$ ) NMR spectrum of the reaction of $[(^F\text{PNP})\text{Pd-}]_2$ (201) with $\text{CO}_2$ and $\text{Me}_3\text{SiOTf}$ and $(^{\text{Me}}\text{PNP})\text{Ir(D)}(\text{C}_6\text{D}_5)$ (207D) as in-situ CO trap after heating for 18 h.....	39
<b>Figure II.22</b> $^{31}\text{P}\{^1\text{H}\}$ (300 MHz, $\text{C}_6\text{D}_6$ ) NMR spectrum of the reaction of $[(^F\text{PNP})\text{Pd-}]_2$ (201) with $\text{CO}_2$ and $\text{Me}_3\text{SiCl}$ and $(^{\text{Me}}\text{PNP})\text{Ir(D)}(\text{C}_6\text{D}_5)$ (207D) as in-situ CO trap after heating for 18 h.....	41

<b>Figure III.1</b> General $M^n/M^{n+2}$ for transition metal catalyzed coupling reactions between aryl halides with nucleophiles. ....	50
<b>Figure III.2</b> Examples of coupling reactions catalyzed by $Co^{II}$ halides.....	51
<b>Figure III.3</b> Comparison of proposed mechanisms for Chirik's system and our Rh catalysts.....	53
<b>Figure III.4</b> Synthesis of (POCOP)Co halide complexes .....	54
<b>Figure III.5</b> Synthesis of (POCOP)Co(R) compounds .....	55
<b>Figure III.6</b> Synthesis of (POCOP)Co(Cl) <sub>2</sub> (311) and (POCOP)Co(Cl) <sub>2</sub> (PMe <sub>3</sub> ) (312)..	56
<b>Figure III.7</b> (a) Synthesis of (POCOP)Co <sup>III</sup> compounds by 1 e- oxidation of (POCOP)Co(Ph) (b) Alternative synthesis of (POCOP)Co(Ph)(X) (c) Synthesis of (POCOP)Co(Ph)(SPh) .....	57
<b>Figure III.8</b> ORTEP drawing (50% probability ellipsoids) of (POCOP)Co(SPh) (309). Select atom labeling. Hydrogen atoms are omitted for clarity. Selected bond distances (Å) and angles (deg) for 309 follow: Co1-P1, 2.1816(8); Co1-P2, 2.1719(9); Co1-S1, 2.1706(8); S1-C1, 1.773(2); P1-Co1-P2, 161.86(2); C7-Co1-S1, 163.15(6); Co1-S1-C1, 119.89(7). ....	59
<b>Figure III.9</b> ORTEP drawing (50% probability ellipsoids) of (a) (POCOP)Co(Cl) <sub>2</sub> (311). Select atom labeling. Hydrogen atoms are omitted for clarity. Selected bond distances (Å) and angles (deg) for 311 follow: Co1-Cl1, 2.285(2); Co1-Cl2, 2.238(2); Co1-C1, 1.934(4), C1-Co1-C1, 110.3(1); C1-Co1-Cl2, 144.4(1); P1-Co1-P2, 159.10(3). (b) (POCOP)Co(Cl) <sub>2</sub> (PMe <sub>3</sub> ) (312). Select atom labeling. Hydrogen atoms are omitted for clarity. Selected bond distances (Å) and angles (deg) for 312 follow: Co1-P1, 2.263(1); Co1-P2, 2.270(1); Co1-P3, 2.303(1); Co1-C1, 1.969(5); Co1-Cl1, 2.258(1); Co1-Cl2, 2.253(1); P1-Co1-P2, 159.04(5); Cl1-Co1-Cl2, 179.21(5); Cl1-Co1-P1, 94.16(5); Cl1-Co1-P3, 91.52(5); P3-Co1-P1, 99.76(5).....	60
<b>Figure III.10</b> ORTEP drawing (50% probability ellipsoids) of (POCOP)Co(Ph)(I) (315). Select atom labeling. Hydrogen atoms are omitted for clarity. Selected bond distances (Å) and angles (deg) for 315 follow: Co2-P1, 2.210(2); Co2-P2, 2.204(2); Co2-I1, 2.601(2); Co2-C18, 1.907(3); Co2-C19, 1.940(3); P1-Co2-P2, 161.83(4); C18-Co2-I1, 155.19(9); C19-Co2-I1, 115.86(9); C18-Co2-C19, 88.9(1).....	61
<b>Figure III.11</b> ORTEP drawing (50% probability ellipsoids) of (POCOP)Co(Ph)(SPh) (316). Select atom labeling. Hydrogen atoms are omitted for clarity.	

Selected bond distances (Å) and angles (deg) for 316 follow: Co1-C25, 1.947(2); Co1-P3, 2.222(1); Co1-P1, 2.223(1); Co1-S1, 2.215(1); Co1-C1, 1.933(2); C1-Co1-C25, 89.54(8); C1-Co1-P3, 81.80(5); C1-Co1-P1, 80.24(5); C1-Co1-S1, 148.98(6); C25-Co1-S1, 119.96(6).....	61
<b>Figure III.12</b> (a) Expected electronic structure for 315 and 316 in square pyramidal geometry (b) (b) Expected electronic structure for 309 in square planar geometry .....	62
<b>Figure III.13</b> (a) Previously reported observations upon thermolysis of (POCOP)Rh(Ph)(SPh) (b) Expected observations for thermolysis of (POCOP)Co(Ph)(SPh) (c) Actual observations.....	64
<b>Figure III.14</b> Possibilities upon thermolysis of (POCOP)Co(Ph)(SPh) .....	65
<b>Figure III.15</b> <sup>1</sup> H NMR of (POCOP)CoCl (301) in C <sub>6</sub> D <sub>6</sub> .....	68
<b>Figure III.16</b> <sup>1</sup> H NMR of (POCOP)Co(Ph) (308) in C <sub>6</sub> D <sub>6</sub> . Minor residual pentane, toluene, and grease present. ....	72
<b>Figure III.17</b> <sup>1</sup> H NMR spectrum of (POCOP)Co(SPh) (309) in C <sub>6</sub> D <sub>6</sub> . Minor residual pentane present. ....	73
<b>Figure III.18</b> <sup>1</sup> H NMR spectrum of (POCOP)Co(Cl) <sub>2</sub> (311) in C <sub>6</sub> D <sub>6</sub> . Minor residual pentane and toluene present. ....	74
<b>Figure III.19</b> <sup>1</sup> H NMR of (POCOP)Co(Cl) <sub>2</sub> (PMe <sub>3</sub> ) (312) in C <sub>6</sub> D <sub>6</sub> . Minor residual pentane and toluene present.....	75
<b>Figure III.20</b> <sup>1</sup> H NMR spectrum of (POCOP)Co(Ph)(Cl) (313) in C <sub>6</sub> D <sub>6</sub> . Large amount of residual pentane present. ....	77
<b>Figure III.21</b> <sup>1</sup> H NMR spectrum of (POCOP)Co(Ph)(OAc) (314) in C <sub>6</sub> D <sub>6</sub> . Minor residual pentane and toluene present.....	78
<b>Figure III.22</b> <sup>1</sup> H NMR spectrum of (POCOP)Co(Ph)(SPh) (316) in C <sub>6</sub> D <sub>6</sub> . Minor residual pentane present.....	80
<b>Figure III.23</b> <sup>1</sup> H NMR spectrum of 319 in C <sub>6</sub> D <sub>6</sub> . Traces of pentane present .....	84
<b>Figure III.24</b> <sup>31</sup> P{ <sup>1</sup> H} NMR spectrum of 319 in C <sub>6</sub> D <sub>6</sub> .....	85
<b>Figure III.25</b> <sup>1</sup> H NMR spectrum of attempted thermolysis of 319 with PhI in C <sub>6</sub> D <sub>6</sub> after 30 h. ....	85

<b>Figure III.26</b> $^1\text{H}$ NMR spectrum of thermolysis of (POCOP)Co(Ph)(SPh) (316) with PPh <sub>3</sub> in C <sub>6</sub> D <sub>6</sub> after 6 h. Trace pentane present. ....	86
<b>Figure III.27</b> $^{31}\text{P}$ { $^1\text{H}$ } NMR spectrum of thermolysis of (POCOP)Co(Ph)(SPh) (316) with PPh <sub>3</sub> in C <sub>6</sub> D <sub>6</sub> after 6 h. ....	86
<b>Figure III.28</b> $^1\text{H}$ NMR spectrum of 319 in CDCl <sub>3</sub> . Trace pentane present .....	87
<b>Figure III.29</b> $^{13}\text{C}$ { $^1\text{H}$ } NMR spectrum of 319 in CDCl <sub>3</sub> . Trace pentane present. ....	88
<b>Figure III.30</b> ESI-MS of a solution of 319 in CDCl <sub>3</sub> . $M/Z^+ = 186$ corresponds to 2-phenylresorcinol .....	88
<b>Figure IV.1</b> Previously reported complexes of cobalt with PNP ligands .....	94
<b>Figure IV.2</b> Synthesis of ( <sup>Me</sup> PNP <sup>iPr</sup> )Co <sup>II</sup> complexes .....	95
<b>Figure IV.3</b> Synthesis of ( <sup>Me</sup> PNP <sup>iPr</sup> )Co(Ph)(X) complexes.....	96
<b>Figure IV.4</b> (a) Attempt at synthesis of ( <sup>Me</sup> PNP <sup>iPr</sup> )Co(Ph)(Ph) (b) Synthesis of ( <sup>Me</sup> PNP <sup>iPr</sup> )Co(Ph)(SAr) .....	97
<b>Figure IV.5</b> ORTEP drawing (50% probability ellipsoids) of ( <sup>Me</sup> PNP <sup>iPr</sup> )Co(Ph)(OAc) (406). Select atom labeling. Hydrogen atoms are omitted for clarity. Selected bond distances (Å) and angles (deg) for 406 follow: Co1-P1, 2.2619(7); Co1-P2, 2.2353(6); Co1-O1, 1.990(1); Co1-O2, 2.117(1); Co1-N1, 1.933(1); Co1-C29, 1.940(1); P1-Co1-P2, 165.63(3); N1-Co1-C29, 97.59(5); O2-Co1-N1, 101.59(5); O1-Co1-N1, 165.17(5).....	98
<b>Figure IV.6</b> Thermolysis of ( <sup>Me</sup> PNP <sup>iPr</sup> )Co(Ph)(SPh) (410).....	98
<b>Figure IV.7</b> Thermolysis of ( <sup>Me</sup> PNP <sup>Et,iPr</sup> )Co(Ph)(SPh) (418).....	99
<b>Figure IV.8</b> Possibilities during thermolysis of ( <sup>Me</sup> PNP <sup>iPr</sup> )Co(Ph)(SPh) (410) .....	100
<b>Figure IV.9</b> Thermolysis of 410 and 418 (a) without BHT and (b) with BHT as a radical trap .....	101
<b>Figure IV.10</b> Thermolysis of 411, (a), (b) possibilities (c) observation from experiment .....	102
<b>Figure IV.11</b> $^1\text{H}$ NMR of ( <sup>Me</sup> PNP <sup>iPr</sup> )Co(Ph)(OAc) (406) in C <sub>6</sub> D <sub>6</sub> .....	106
<b>Figure IV.12</b> $^{13}\text{C}$ { $^1\text{H}$ } NMR of ( <sup>Me</sup> PNP <sup>iPr</sup> )Co(Ph)(OAc) (406) in C <sub>6</sub> D <sub>6</sub> .....	107
<b>Figure IV.13</b> $^1\text{H}$ NMR of ( <sup>Me</sup> PNP <sup>iPr</sup> )Co(Ph)(Cl) (407) in C <sub>6</sub> D <sub>6</sub> .....	108



<b>Figure IV.14</b> $^{13}\text{C}\{^1\text{H}\}$ NMR of $(^{\text{Me}}\text{PNP}^{\text{iPr}})\text{Co}(\text{Ph})(\text{Cl})$ (407) in $\text{C}_6\text{D}_6$ .....	108
<b>Figure IV.15</b> $^1\text{H}$ NMR of $(^{\text{Me}}\text{PNP}^{\text{iPr}})\text{Co}(\text{Ph})(\text{I})$ (408) in $\text{C}_6\text{D}_6$ .....	109
<b>Figure IV.16</b> $^{13}\text{C}\{^1\text{H}\}$ NMR of $(^{\text{Me}}\text{PNP}^{\text{iPr}})\text{Co}(\text{Ph})(\text{I})$ (408) in $\text{C}_6\text{D}_6$ .....	110
<b>Figure IV.17</b> $^1\text{H}$ NMR of $(^{\text{Me}}\text{PNP}^{\text{iPr}})\text{Co}(\text{Ph})(\text{SPh})$ (410) in $\text{C}_6\text{D}_6$ .....	111
<b>Figure IV.18</b> $^1\text{H}$ NMR of $(^{\text{Me}}\text{PNP}^{\text{iPr}})\text{Co}(\text{Ph})(\text{SAr}^{\text{F}})$ (411) in $\text{C}_6\text{D}_6$ .....	112
<b>Figure IV.19</b> $^1\text{H}$ NMR of $^{\text{Me}}\text{PN}(\text{Li})\text{P}^{\text{iPr},\text{Et}}$ (413) in $\text{C}_6\text{D}_6$ .....	113
<b>Figure IV.20</b> $^{13}\text{C}\{^1\text{H}\}$ NMR of $^{\text{Me}}\text{PN}(\text{Li})\text{P}^{\text{iPr},\text{Et}}$ (413) in $\text{C}_6\text{D}_6$ .....	114
<b>Figure IV.21</b> $^{31}\text{P}\{^1\text{H}\}$ NMR of $^{\text{Me}}\text{PN}(\text{Li})\text{P}^{\text{iPr},\text{Et}}$ (413) in $\text{C}_6\text{D}_6$ .....	114
<b>Figure IV.22</b> $^1\text{H}$ NMR of $(^{\text{Me}}\text{PNP}^{\text{iPr},\text{Et}})\text{Co}(\text{Ph})(\text{I})$ (417) in $\text{C}_6\text{D}_6$ .....	116
<b>Figure IV.23</b> $^1\text{H}$ NMR of $(^{\text{Me}}\text{PNP}^{\text{iPr},\text{Et}})\text{Co}(\text{Ph})(\text{SPh})$ (418) in $\text{C}_6\text{D}_6$ .....	117
<b>Figure IV.24</b> $^{31}\text{P}\{^1\text{H}\}$ NMR of $(^{\text{Me}}\text{PNP}^{\text{iPr},\text{Et}})\text{Co}(\text{Ph})(\text{SPh})$ (418) in $\text{C}_6\text{D}_6$ .....	117
<b>Figure IV.25</b> $^{19}\text{F}$ NMR of thermolysis $(^{\text{Me}}\text{PNP}^{\text{iPr}})\text{Co}(\text{Ph})(\text{SAr}^{\text{F}})$ (411) in $\text{C}_6\text{D}_6$ after 3 h.....	120
<b>Figure V.1</b> Previously reported poly-pincer complexes with rigid ligands.....	122
<b>Figure V.2</b> (a) Previously reported pincer with flexible linkers (b) PCN and PNN complexes of Pd reported by our group.....	123
<b>Figure V.3</b> (a) Synthesis of $^{\text{R}}\text{PCN}-\text{C}_n$ ligands(b) Synthesis of $(^{\text{R}}\text{PCN})\text{NiCl}$ complexes (c) Synthesis of $(^{\text{tBu}}\text{PCN})\text{PdCl}$ complexes (d) Synthesis of $(^{\text{R}}\text{PCN})\text{MOTf}$ complexes.....	124
<b>Figure V.4</b> Synthesis of binuclear (PCN) Ni complex with a pendant amine linker ....	126
<b>Figure V.5</b> Synthesis of (PNN)NiX complexes.....	127
<b>Figure V.6</b> ORTEP drawing (50% probability ellipsoids) of $(^{\text{iPr}}\text{PCN}-\text{C}_2)\text{NiCl}$ (501a-NiCl)(left) Selected bond distances (Å) and angles (deg) for 501a-NiCl follow: Ni1-C6, 1.846(2); N1-Cl1, 2.199(1); Ni1-N1, 1.965(2); Ni1-P1, 2.114(1); N1-Ni1-P1, 163.39(5); N1-Ni1-Cl1, 98.69(5); P1-Ni1-Cl1, 97.82(2); C6-Ni1-P1, 80.95(7); C6-Ni1-N1, 82.44(8) (b) $(^{\text{iPr}}\text{PCN}-\text{C}_4)\text{NiCl}$ (501b-NiCl) (right) Select atom labeling. Hydrogen atoms are omitted for clarity. Selected bond distances (Å) and angles (deg) for 501b-NiCl follow: Ni1-Cl1, 2.199(3); Ni1-N1, 1.978(4); Ni1-P1, 2.128(3); Ni1-C6 1.847(4);	

C6-Ni1-N1, 82.7(1); C6-Ni1-P1, 80.9(1); C6-Ni1-Cl1, 175.3(1); P1-Ni1-Cl1, 97.84(4).....	128
<b>Figure V.7</b> ORTEP drawing (50% probability ellipsoids) of ( <sup>t</sup> BuPCN-C <sub>2</sub> )PdCl (502a-PdCl) (left) Selected bond distances (Å) and angles (deg) for 502a-PdCl follow: Pd1-Cl1, 2.391(1); Pd1-N1, 2.125(3); Pd1-P1, 2.220(1); Pd1-C1 1.952(3); P1-Pd1-C1, 79.6(1); C1-Pd1-N1, 79.3(1); Cl1-Pd1-C1, 174.2(1); P1-Pd1-Cl1, 105.24(3) and ( <sup>t</sup> BuPCN-C <sub>4</sub> )PdCl (502b-PdCl) (right) Selected bond distances (Å) and angles (deg) for 502b-PdCl follow: Pd1-Cl1, 2.395(2); Pd1-N2, 2.142(4); Pd1-P1, 2.224(2); Pd1-C1 1.953(6); C1-Pd1-P1, 79.3(2); C1-Pd1-N2, 78.9(2); Cl1-Pd1-N2, 97.6(1); Cl1-Pd1-P1, 104.27(6).....	129
<b>Figure V.8</b> ORTEP drawing (50% probability ellipsoids) of ( <sup>i</sup> PrPNN-C <sub>2</sub> )NiOAc (503a-NiOAc) Select atom labeling. Hydrogen atoms are omitted for clarity. Selected bond distances (Å) and angles (deg) for 503a-NiOAc follow: Ni1-N2, 1.882(3); N1-O3, 1.874(2); Ni1-N1, 1.941(2); Ni1-P2, 2.158(1); N1-Ni1-P2, 174.37(8); N2-Ni1-O3, 178.0(1); N2-Ni1-P2, 85.40(8).....	129
<b>Figure V.9</b> <sup>1</sup> H NMR spectrum of ( <sup>i</sup> PrPCN-C <sub>2</sub> )NiCl (1a-NiCl) in CD <sub>2</sub> Cl <sub>2</sub> . Minor residual diethylether and dichloromethane present .....	132
<b>Figure V.10</b> <sup>13</sup> C{ <sup>1</sup> H} NMR spectrum of ( <sup>i</sup> PrPCN-C <sub>2</sub> )NiCl (501a-NiCl)in CD <sub>2</sub> Cl <sub>2</sub> . Minor residual diethylether and dichloromethane present. ....	132
<b>Figure V.11</b> <sup>31</sup> P{ <sup>1</sup> H} NMR spectrum of ( <sup>i</sup> PrPCN-C <sub>2</sub> )NiCl (501a-NiCl)in CD <sub>2</sub> Cl <sub>2</sub> . .....	133
<b>Figure V.12</b> <sup>1</sup> H NMR spectrum of ( <sup>i</sup> PrPCN-C <sub>4</sub> )NiCl (501b-NiCl) in CD <sub>2</sub> Cl <sub>2</sub> . Residual diethylether present.....	134
<b>Figure V.13</b> <sup>13</sup> C{ <sup>1</sup> H} NMR spectrum of ( <sup>i</sup> PrPCN-C <sub>4</sub> )NiCl (501b-NiCl)in CD <sub>2</sub> Cl <sub>2</sub> . Residual diethylether present.....	134
<b>Figure V.14</b> <sup>31</sup> P{ <sup>1</sup> H} NMR spectrum of ( <sup>i</sup> PrPCN-C <sub>4</sub> )NiCl (501b-NiCl)in CD <sub>2</sub> Cl <sub>2</sub> . .....	135
<b>Figure V.15</b> <sup>1</sup> H NMR spectrum of ( <sup>i</sup> PrPCN-C <sub>2</sub> )NiOTf (501a-NiOTf) in CD <sub>2</sub> Cl <sub>2</sub> . .....	136
<b>Figure V.16</b> <sup>13</sup> C{ <sup>1</sup> H} NMR spectrum of ( <sup>i</sup> PrPCN-C <sub>2</sub> )NiOTf (501a-NiOTf) in CD <sub>2</sub> Cl <sub>2</sub> . .....	136
<b>Figure V.17</b> <sup>31</sup> P{ <sup>1</sup> H} NMR spectrum of ( <sup>i</sup> PrPCN-C <sub>2</sub> )NiOTf (501a-NiOTf) in CD <sub>2</sub> Cl <sub>2</sub> . .....	136
<b>Figure V.18</b> <sup>19</sup> F NMR spectrum of ( <sup>i</sup> PrPCN-C <sub>2</sub> )NiOTf (501a-NiOTf) in CD <sub>2</sub> Cl <sub>2</sub> .....	137

<b>Figure V.19</b> $^1\text{H}$ NMR spectrum of ( $^{i\text{Pr}}\text{PCN-C}_4$ )NiOTf (501b-NiOTf) in $\text{CD}_2\text{Cl}_2$ . Minor diethylether present.....	138
<b>Figure V.20</b> $^{13}\text{C}\{^1\text{H}\}$ NMR spectrum of ( $^{i\text{Pr}}\text{PCN-C}_4$ )NiOTf (501b-NiOTf) in $\text{CD}_2\text{Cl}_2$ . Minor diethylether present.....	138
<b>Figure V.21</b> $^{31}\text{P}\{^1\text{H}\}$ NMR spectrum of ( $^{i\text{Pr}}\text{PCN-C}_4$ )NiOTf (501b-NiOTf) in $\text{CD}_2\text{Cl}_2$ .	138
<b>Figure V.22</b> $^{19}\text{F}$ NMR spectrum of ( $^{i\text{Pr}}\text{PCN-C}_4$ )NiOTf (501b-NiOTf) in $\text{CD}_2\text{Cl}_2$ .....	139
<b>Figure V.23</b> $^1\text{H}$ NMR spectrum of ( $^{t\text{Bu}}\text{PCN-C}_2$ ) (502a) in $\text{CDCl}_3$ .....	140
<b>Figure V.24</b> $^{13}\text{C}\{^1\text{H}\}$ NMR spectrum of ( $^{t\text{Bu}}\text{PCN-C}_2$ ) (502a) in $\text{CDCl}_3$ .....	140
<b>Figure V.25</b> $^{31}\text{P}\{^1\text{H}\}$ NMR spectrum of ( $^{t\text{Bu}}\text{PCN-C}_2$ ) (502a) in $\text{CDCl}_3$ .....	140
<b>Figure V.26</b> $^1\text{H}$ NMR spectrum of ( $^{t\text{Bu}}\text{PCN-C}_4$ ) (502b) in $\text{CDCl}_3$ .....	142
<b>Figure V.27</b> $^{13}\text{C}\{^1\text{H}\}$ NMR spectrum of ( $^{t\text{Bu}}\text{PCN-C}_4$ ) (502b) in $\text{CDCl}_3$ .....	142
<b>Figure V.28</b> $^{31}\text{P}\{^1\text{H}\}$ NMR spectrum of ( $^{t\text{Bu}}\text{PCN-C}_4$ ) (502b) in $\text{CDCl}_3$ .....	142
<b>Figure V.29</b> $^1\text{H}$ NMR spectrum of ( $^{t\text{Bu}}\text{PCN-C}_2$ )NiCl (502a-NiCl) in $\text{CD}_2\text{Cl}_2$ .....	143
<b>Figure V.30</b> $^{13}\text{C}\{^1\text{H}\}$ NMR spectrum of ( $^{t\text{Bu}}\text{PCN-C}_2$ )NiCl (502a-NiCl) in $\text{CD}_2\text{Cl}_2$ ....	144
<b>Figure V.31</b> $^{31}\text{P}\{^1\text{H}\}$ NMR spectrum of ( $^{t\text{Bu}}\text{PCN-C}_2$ )NiCl (502a-NiCl) in $\text{CD}_2\text{Cl}_2$ ....	144
<b>Figure V.32</b> $^1\text{H}$ NMR spectrum of ( $^{t\text{Bu}}\text{PCN-C}_4$ )NiCl (502b-NiCl) in $\text{C}_6\text{D}_6$ .....	145
<b>Figure V.33</b> $^{31}\text{P}\{^1\text{H}\}$ NMR spectrum of ( $^{t\text{Bu}}\text{PCN-C}_4$ )NiCl (502b-NiCl) in $\text{C}_6\text{D}_6$ .....	145
<b>Figure V.34</b> $^1\text{H}$ NMR spectrum of ( $^{t\text{Bu}}\text{PCN-C}_2$ )NiOTf (502a-NiOTf) in $\text{CD}_2\text{Cl}_2$ .....	146
<b>Figure V.35</b> $^{13}\text{C}\{^1\text{H}\}$ NMR spectrum of ( $^{t\text{Bu}}\text{PCN-C}_2$ )NiOTf (502a-NiOTf) in $\text{CD}_2\text{Cl}_2$	147
<b>Figure V.36</b> $^{31}\text{P}\{^1\text{H}\}$ NMR spectrum of ( $^{t\text{Bu}}\text{PCN-C}_2$ )NiOTf (502a-NiOTf) in $\text{CD}_2\text{Cl}_2$	147
<b>Figure V.37</b> $^{19}\text{F}$ NMR spectrum of ( $^{t\text{Bu}}\text{PCN-C}_2$ )NiOTf (502a-NiOTf) in $\text{CD}_2\text{Cl}_2$ .....	147
<b>Figure V.38</b> $^1\text{H}$ NMR spectrum of ( $^{t\text{Bu}}\text{PCN-C}_4$ )NiOTf (502b-NiOTf) in $\text{CD}_2\text{Cl}_2$ .....	148
<b>Figure V.39</b> $^{31}\text{P}\{^1\text{H}\}$ NMR spectrum of ( $^{t\text{Bu}}\text{PCN-C}_4$ )NiOTf (502b-NiOTf) in $\text{CD}_2\text{Cl}_2$	148
<b>Figure V.40</b> $^{19}\text{F}$ NMR spectrum of ( $^{t\text{Bu}}\text{PCN-C}_4$ )NiOTf (502b-NiOTf) in $\text{CD}_2\text{Cl}_2$ .....	149
<b>Figure V.41</b> $^1\text{H}$ NMR spectrum of ( $^{t\text{Bu}}\text{PCN-C}_2$ )PdCl (502a-PdCl) in $\text{CD}_2\text{Cl}_2$ .....	150

<b>Figure V.42</b>	$^{13}\text{C}\{^1\text{H}\}$ NMR spectrum of ( $^{\text{tBu}}\text{PCN-C}_2$ )PdCl (502a-PdCl) in $\text{CD}_2\text{Cl}_2$ .....	150
<b>Figure V.43</b>	$^{31}\text{P}\{^1\text{H}\}$ NMR spectrum of ( $^{\text{tBu}}\text{PCN-C}_2$ )PdCl (502a-PdCl) in $\text{CD}_2\text{Cl}_2$ .....	151
<b>Figure V.44</b>	$^1\text{H}$ NMR spectrum of ( $^{\text{tBu}}\text{PCN-C}_4$ )PdCl (502b-PdCl) in $\text{CD}_2\text{Cl}_2$ .....	152
<b>Figure V.45</b>	$^{31}\text{P}\{^1\text{H}\}$ NMR spectrum of ( $^{\text{tBu}}\text{PCN-C}_4$ )PdCl (502b-PdCl) in $\text{CD}_2\text{Cl}_2$ .....	152
<b>Figure V.46</b>	$^1\text{H}$ NMR spectrum of ( $^{\text{tBu}}\text{PCN-C}_2$ )PdOTf (502a-PdOTf) in $\text{CD}_2\text{Cl}_2$ .....	153
<b>Figure V.47</b>	$^{13}\text{C}\{^1\text{H}\}$ NMR spectrum of ( $^{\text{tBu}}\text{PCN-C}_2$ )PdOTf (502a-PdOTf) in $\text{CD}_2\text{Cl}_2$ .....	153
<b>Figure V.48</b>	$^1\text{H}$ NMR spectrum of ( $^{\text{tBu}}\text{PCN-C}_4$ )PdOTf (502b-PdOTf) in $\text{CD}_2\text{Cl}_2$ .....	154
<b>Figure V.49</b>	$^{13}\text{C}\{^1\text{H}\}$ NMR spectrum of ( $^{\text{tBu}}\text{PCN-C}_4$ )PdOTf (502b-PdOTf) in $\text{CD}_2\text{Cl}_2$ .....	154
<b>Figure V.50</b>	$^{31}\text{P}\{^1\text{H}\}$ NMR spectrum of ( $^{\text{tBu}}\text{PCN-C}_4$ )PdOTf (502b-PdOTf) in $\text{CD}_2\text{Cl}_2$	155
<b>Figure V.51</b>	$^{19}\text{F}$ NMR spectrum of ( $^{\text{tBu}}\text{PCN-C}_4$ )PdOTf (502b-PdOTf) in $\text{CD}_2\text{Cl}_2$ .....	155
<b>Figure V.52</b>	$^1\text{H}$ NMR spectrum of ( $^{\text{iPr}}\text{PNN-C}_2$ )NiCl (503a-NiCl) in $\text{CD}_2\text{Cl}_2$ .....	156
<b>Figure V.53</b>	$^{31}\text{P}\{^1\text{H}\}$ NMR spectrum of ( $^{\text{iPr}}\text{PNN-C}_2$ )NiCl (503a-NiCl) in $\text{CD}_2\text{Cl}_2$ .....	156
<b>Figure V.54</b>	$^1\text{H}$ NMR spectrum of ( $^{\text{iPr}}\text{PNN-C}_2$ )NiOAc (503a-NiOAc) in $\text{C}_6\text{D}_6$ .....	157
<b>Figure V.55</b>	$^{31}\text{P}\{^1\text{H}\}$ NMR spectrum of ( $^{\text{iPr}}\text{PNN-C}_2$ )NiOAc (503a-NiOAc) in $\text{C}_6\text{D}_6$ ..	158
<b>Figure V.56</b>	$^1\text{H}$ NMR spectrum of 504a' in $((\text{CD}_3)_2\text{SO})$ .....	159
<b>Figure V.57</b>	$^1\text{H}$ NMR spectrum of 504a in $\text{C}_6\text{D}_6$ .....	160
<b>Figure V.58</b>	$^{31}\text{P}\{^1\text{H}\}$ NMR spectrum of 504a in $\text{C}_6\text{D}_6$ .....	160
<b>Figure V.59</b>	$^1\text{H}$ NMR spectrum of ( $^{\text{tBu}}\text{PCN-C}_2\text{NC}_2$ )NiCl (504a-NiCl) in $\text{CD}_2\text{Cl}_2$ .....	161
<b>Figure V.60</b>	$^{31}\text{P}\{^1\text{H}\}$ NMR spectrum of ( $^{\text{tBu}}\text{PCN-C}_2\text{NC}_2$ )NiCl (504a-NiCl) in $\text{CD}_2\text{Cl}_2$ .....	161

## LIST OF TABLES

	Page
<b>Table I.1</b> Thermodynamic and kinetic parameters calculated by Goldman and coworkers <sup>113</sup> .....	11
<b>Table II.1</b> <sup>31</sup> P{ <sup>1</sup> H} and <sup>19</sup> F NMR chemical shifts of compounds referred to frequently in this chapter.....	26
<b>Table III.1</b> <sup>31</sup> P{ <sup>1</sup> H} chemical shifts of known (POCOP) species .....	65

## CHAPTER I

### INTRODUCTION AND LITERATURE REVIEW

#### 1.1. General introduction to pincer ligands

Development of pincer ligands is one of the monumental steps in the evolution of multidentate ligands geared towards imparting interesting reactivity to a metal center by altering the electronics and the sterics at the metal.<sup>1</sup> Pincer ligands are tridentate ligand systems that are designed to be easily modifiable in order to control the environment around the metal center and tune the same for desired reactivity (**Figure I.1**). Another useful attribute of these ligands is the unprecedented stability and robustness of their metal complexes due to the chelating effect of the side arms. They usually bind in meridional fashion and follow a nomenclature with the ligand abbreviated as  $E_1XE_2$  (side arm donors  $E_1, E_2$ ; central donor X) and their metal complexes are named as  $(E_1XE_2)M$  (metal M). Some commonly encountered pincer ligands relevant to our research can be broadly classified into types: (a) anionic such as PNP,<sup>2-6</sup> PCP,<sup>7-11</sup> POCOP,<sup>12-14</sup> Fryzuk type PNP (FryPNP)<sup>15-17</sup> or (b) neutral pincer ligands based on pyridine.<sup>18-21</sup> (**Figure I.2**)

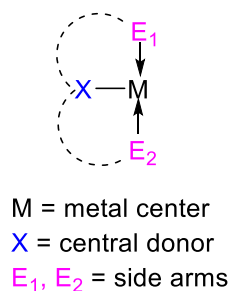
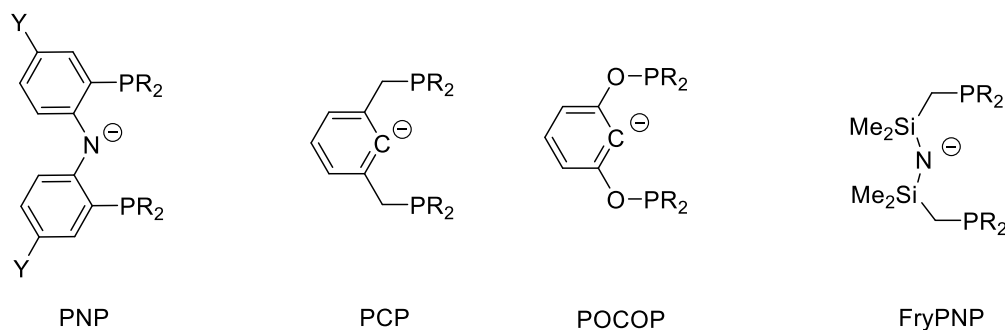


**Figure I.1** A typical pincer complex

Our efforts in this report are mainly focused on utilization of the PNP and POCOP type pincer ligands. POCOP pincers are usually synthesized from resorcinol and its derivatives. The first examples of POCOP ligands and complexes were reported by Morales-Morales<sup>12</sup> and have since found uses in a multitude of catalytic organic transformations.<sup>22,23</sup> Diarylamido based PNP pincer ligands were reported first by our group<sup>2,24</sup> and others.<sup>6,25</sup> The rigid nature of the scaffold and the easy modifications of electron density and steric stress on the metal by changes in the aryl backbone and the phosphine side arms<sup>26,27</sup> respectively, have enabled a variety of chemistry to be carried out by PNP complexes of Ir,<sup>28</sup> Rh,<sup>29,30</sup> Pd,<sup>27,31,32</sup> and Ni.<sup>27,33,34</sup>

#### Anionic Pincer Ligands



#### Neutral Pincer Ligands

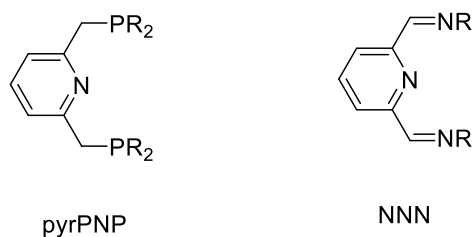


**Figure I.2** Some typical pincer ligands with the acronyms used for them

## 1.2. Coupling catalyzed by transition metals

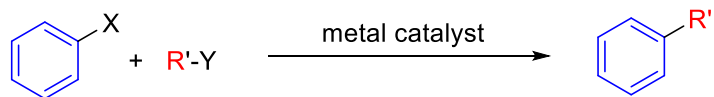
### 1.2.1 History of transition metal catalyzed coupling reactions

A coupling reaction is a reaction where two organic fragments are coupled with the aid of a metal catalyst. The most common coupling reactions involve coupling of an aryl halide with another organic molecule. Palladium catalyzed cross-coupling reactions of aryl halides are one of the most versatile and important tools in a chemists repertoire with uses in the fields of pharmaceuticals<sup>35</sup>, agro chemicals and development of new materials.<sup>36</sup>

First examples of C-C coupling reactions using palladium catalysts were the coupling of aryl halides and alkenes, discovered concurrently by Mizoroki<sup>37,38</sup> and Heck<sup>39-41</sup>. Following these, several examples of C-C coupling reactions of other types were reported by Suzuki,<sup>42-44</sup> Negishi,<sup>45,46</sup> and Sonogashira<sup>47</sup> amongst others. Further advancements have been made to include copulings other than C-C coupling such as C-N, C-O and C-S couplings.<sup>48-51</sup> The importance of these coupling reactions has been recognized universally, most notably by the 2010 Nobel Prize in chemistry to acknowledge the work of Heck, Negishi, and Suzuki “for palladium catalyzed cross-coupling in organic synthesis”.<sup>52</sup> These reactions are typically characterized by diverse substrate scopes, high functional group tolerance and ambient reaction conditions.<sup>53</sup>



**A general coupling reaction**



**Pd catalyzed cross-coupling of aryl halides**

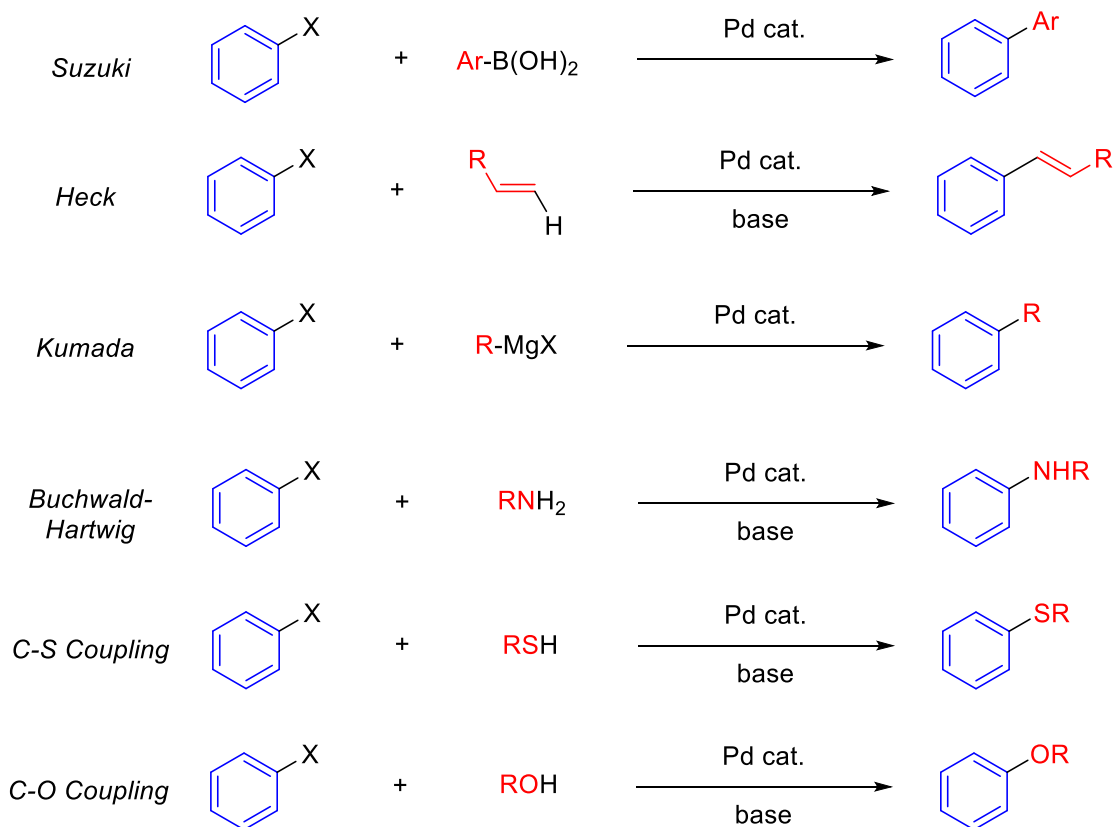
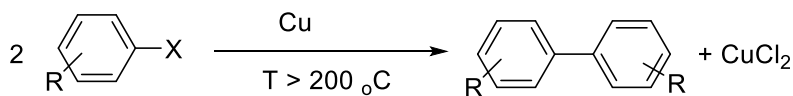


**Figure I.3** Pd catalyzed C-C and C-heteroatom cross coupling reactions

Ni is a cheaper and more abundant alternative to Pd and use of Ni catalysts has been explored for Suzuki, Negishi and Kumada-Corriu Coupling.<sup>54-60</sup> Although these reactions are interesting, the superior efficiency and specificity of Pd catalysts make them more desirable for applications where there are strict regulations for product purity.

**Ullman 1901**



**Further developments**

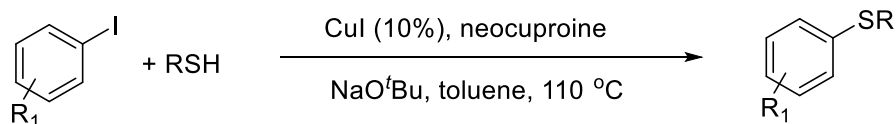
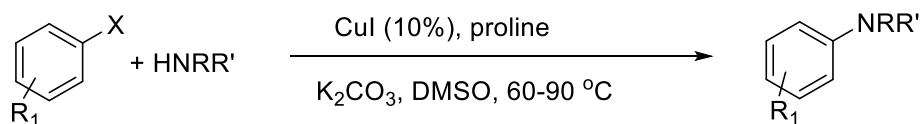
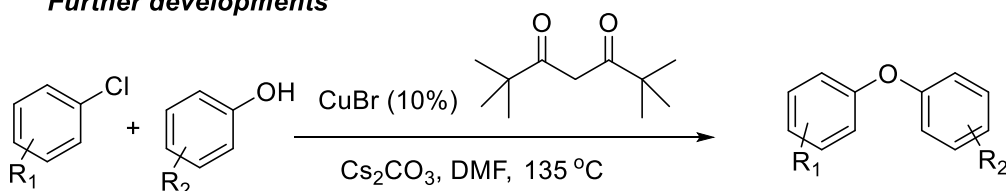


**Figure I.4** Copper catalyzed coupling reactions

Copper catalysts were reported to catalyze coupling reactions for the first time by Ullman<sup>61–63</sup> in the early 1900s and shortly thereafter another report was published by Goldberg.<sup>64</sup> The first Ullman type reactions needed extreme conditions such as temperatures over 200 °C, but a lot of advancement has been made since then to diversify their applications and make the reaction conditions milder.<sup>65–68</sup> (**Figure I.4**)

Rh complexes have also been used for cross coupling reactions with aryl halides. Initial examples<sup>69–80</sup> of such reactivity had sparse mechanistic details except for reports by Bergman and Ellman.<sup>79,81</sup> Our group has also published a series of reports describing coupling reactions and investigations into the mechanisms involved.<sup>82–85</sup> Coupling

reactions with Co, being from the same group as Rh and much cheaper and more abundant, are highly desirable and have also been recently explored with successful efforts describing C-C,<sup>86,87</sup> and C-S<sup>88</sup> couplings. Unfortunately, the understanding of mechanistic details is sparse in these reports. However, deeper insight into the mechanism of these coupling reactions will benefit future efforts towards development of more Co catalysts. Due to this, mechanistic understanding and isolation of intermediates will be one of our primary goals in our cobalt chemistry described in chapters 3 and 4.

### 1.2.2. Mechanism of transition metal catalyzed coupling reactions

Most transition metal catalyzed coupling reactions involve the interchange between the  $M^n$  and  $M^{n+2}$  oxidation states of the metal involved, through three basic steps (1) oxidative addition (OA) (2) transmetalation, and (3) reductive elimination (RE) as illustrated in **Figure I.5**.<sup>89</sup>

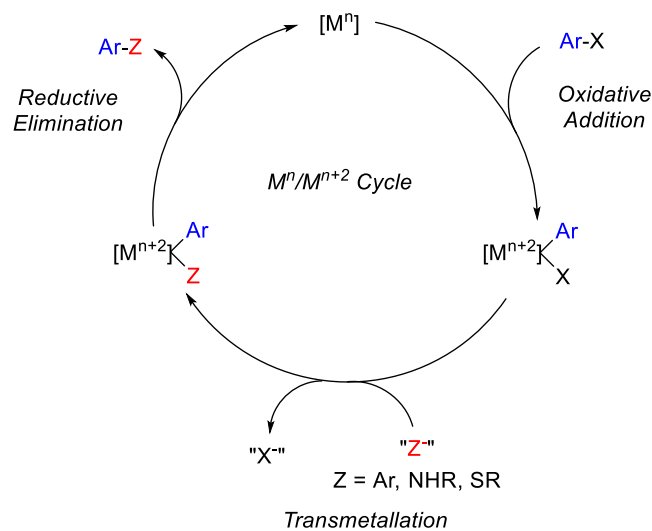


**Figure I.5** Generalized mechanism for coupling reactions using a  $M^n/M^{n+2}$  cycle

### 1.2.2.1 Classical mechanism of coupling reactions with palladium

Oxidative addition of a C-X bond to a metal center involves the formal oxidation of  $M^n$  to  $M^{n+2}$  and the cleavage of the C-X bond and formation of two new C-R and C-X bonds. This step usually occurs in a concerted fashion with the C-X bond being broken and the M-X and M-C bonds being formed simultaneously.<sup>90</sup> The OA of aryl halides to Pd(0) complexes occurs fastest with highly unsaturated metal centers such as those in 12- and 14-electron  $L_2Pd$  and  $LPd$  species.<sup>89,91,92</sup> Based on a number of kinetic studies conducted on the oxidative addition of aryl halides to Pd(0) complexes a lot of insight into the process has been achieved. Typically the OA occurs to 14-electron  $L_2Pd(0)$  complex. Oxidative addition to  $(PPh_3)_3Pd$  (which in turn is generated upon dissolution of  $(PPh_3)_4Pd$ ) occurs by initial reversible dissociation of a phosphine ligand to generate  $(PPh_3)_2Pd$ .<sup>92-94</sup> **(Figure I.6 (a))** Complexes with sterically bulky phosphine ligands such as tri(*o*-tolyl)phosphine and tri-*tert*-butylphosphine, can be isolated as  $L_2Pd(0)$  species<sup>95,96</sup> and undergo elimination of one phosphine ligand prior to coordination and subsequent OA of Ar-X.<sup>91,97</sup> **(Figure I.6 (b))**

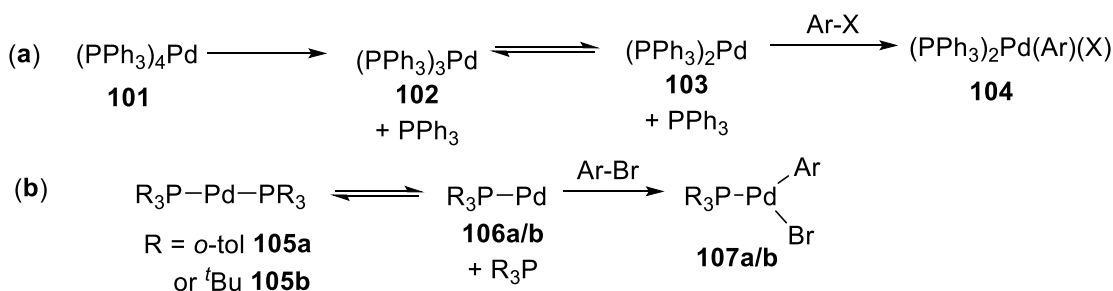


**Figure I.6** (a) OA of aryl halides to  $(PPh_3)_4Pd$  (b) OA of aryl halides to Pd(0) complexes with bulky phosphines

RE is the microscopic reverse of OA and hence involves the formal reduction of  $M^{n+2}$  to  $M^n$ , with the cleavage of M-C and M-C'/heteroatom bond and formation of C-C'/heteroatom bonds. For  $d^8$  transition metal complexes, RE was observed to be fastest from three coordinate complexes.<sup>89,98,99</sup> However, RE from four coordinate complexes has also been observed with chelating bidentate ligands.<sup>89</sup>

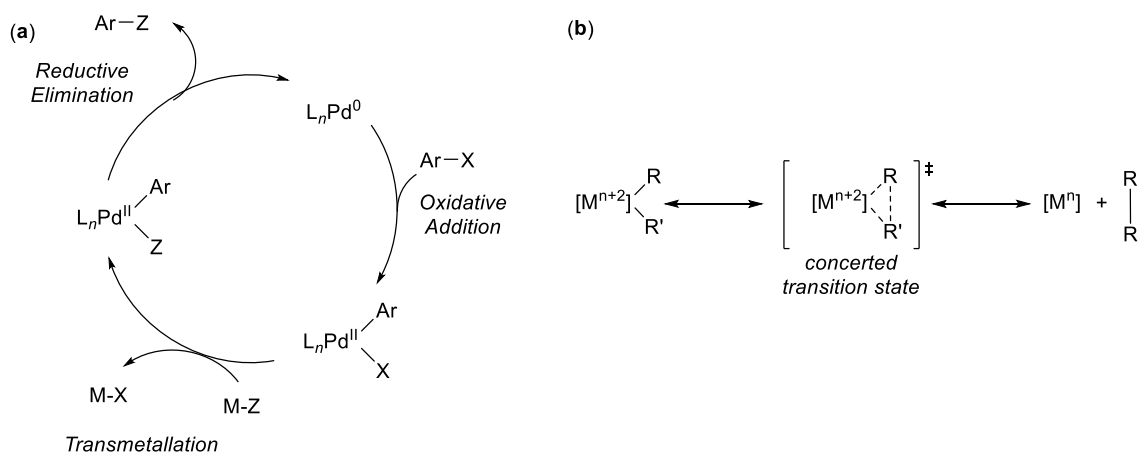


**Figure 1.7** (a) Catalytic cycle for Pd catalyzed coupling reactions (b) RE/OA via a concerted transition state

The electronics and sterics of the auxiliary ligands are also very important in enhancing the propensity of a metal center for OA/RE. An electronic rich metal center is better for OA due to its ability to stabilize the higher oxidation states attained upon OA. On the same note, RE is favored from electron poor metal centers.<sup>89,90,100,101</sup> So, in order for the same system to be suitable for both OA and RE as would be desirable for a catalytic cycle, the ancillary ligands have to be fine-tuned. Due to this, ligand design has played a pivotal role in the development of Pd catalyzed reactions.<sup>102</sup>

Since our research efforts are focused on utilization of cobalt for cross coupling reactions, mechanism of cross coupling reactions from Rh will be discussed next as they

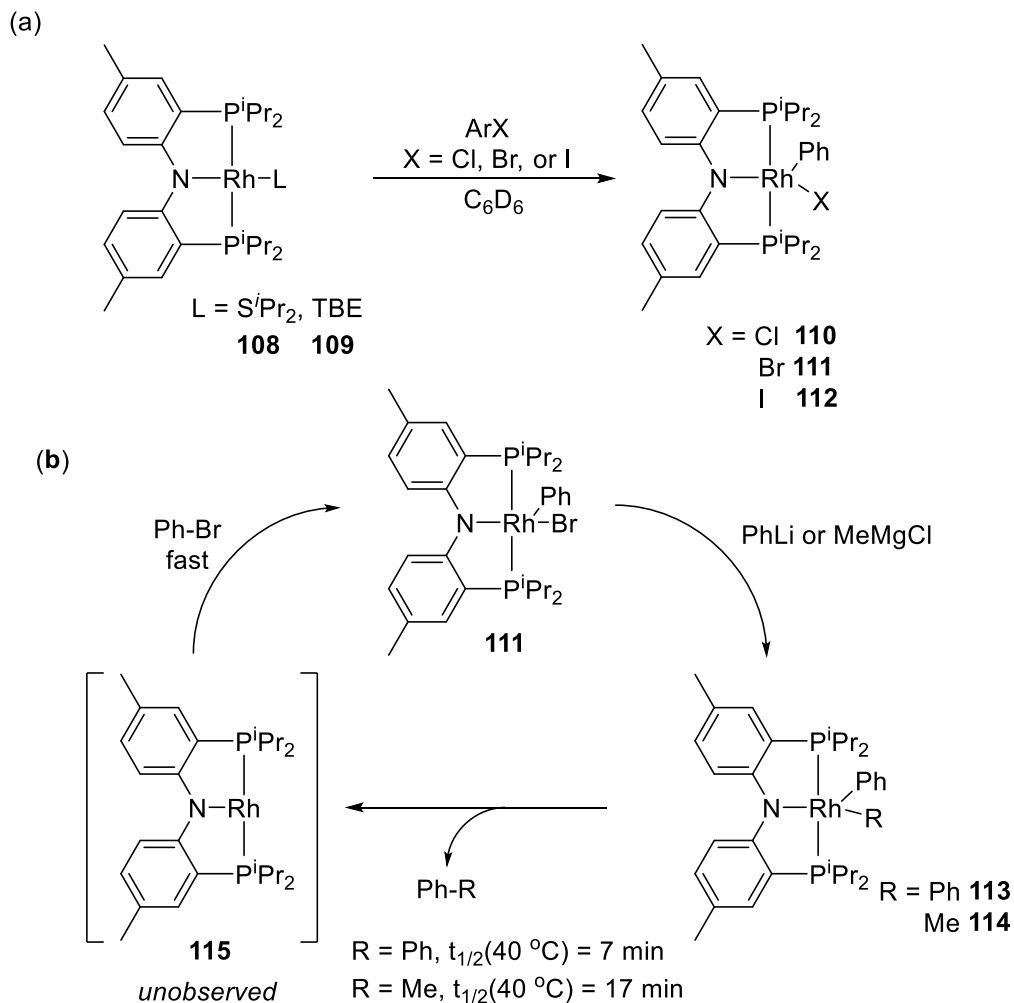
involve a Rh<sup>I</sup>/Rh<sup>III</sup> couple and involve OA to a d<sup>8</sup> center and RE from d<sup>6</sup> metal centers. Understanding of such mechanism is important as our research discussed in subsequent chapters explores possibility of a similar mechanism with OA to d<sup>8</sup> Co<sup>I</sup> and RE from d<sup>6</sup> Co<sup>III</sup>.

### 1.2.2.2 Mechanism of coupling reactions with Rh

OA of aryl halides to Rh(I) has been reported in some instances<sup>103-106</sup> and has been observed to be faster at low coordinate Rh(I) complexes. OA of both aryl chlorides and bromides to low coordinate Rh(I) supported by  $\beta$ -diiminate ligands was reported by Budzelaar and coworkers.<sup>107,108</sup> Another example of OA of aryl-chlorides to low coordinate Rh(I) generated by loss of H<sub>2</sub> from [(P<sup>*i*</sup>Bu<sub>3</sub>)<sub>2</sub>Rh(H)<sub>2</sub>]<sup>+</sup> was reported by Weller.<sup>109</sup> RE from Rh(III) involving aryl ligands had not been examined in great detail until a recent study by our group.<sup>110</sup>

The work from our group using (PNP)Rh fragments<sup>110-112</sup> is one of the few examples where both OA of aryl halide and RE of C-C bonds have been observed and studied in detail. RhI compounds of the type (PNP)Rh(L) (L = S<sup>*i*</sup>Pr<sub>2</sub>, TBE) were synthesized. Three coordinate Rh<sup>I</sup> species were obtained *in-situ* by loss of L and presence of such coordinatively unsaturated Rh<sup>I</sup> facilitated the OA of aryl halides. (**Figure I.8**) OA of aryl bromides was observed to be more favored over the corresponding aryl-chloride in competition studies with 10 eq. each of Ph-Br and Ph-Cl.<sup>112</sup> RE and transmetalation steps were also observed using species of the type (PNP)Rh(Ph)<sub>2</sub> and (PNP)Rh(Ph)(Br) respectively.<sup>110</sup> Upon looking at each of the steps, RE of Ph-Ph and Ph-Me to produce (PNP)Rh<sup>I</sup> were found to be the rate limiting steps in the synthetic cycles emulating the

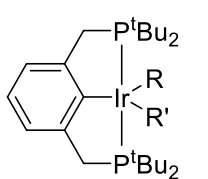
mechanism for catalytic coupling with Rh, as both the transmetalation and OA steps were found to proceed much quicker than RE (**Figure I.8**)



**Figure I.8** (a) OA of aryl halides to a (PNP)Rh<sup>I</sup> fragment (b) synthetic cycle for catalytic intermediates involving (PNP)Rh

Another important step towards better elucidation of the mechanism of catalytic coupling using Rh/Ir was obtained by the studies of C-C RE from five coordinate d<sup>6</sup> Ir complexes supported by PCP pincer ligands performed by Goldman and coworkers.<sup>113</sup> The observations made in this report are beneficial to similar pincer supported d<sup>6</sup> Rh and

Co complexes. It was observed that the thermodynamic favorability of RE increased with the bulk of eliminating groups as observed for RE from  $d^8$  Pd. This is justified by relief of the steric stress on the metal center upon RE. However, interestingly the rate of RE from  $d^6$  compounds was negatively affected by increase in the bulk of the participating groups. (**Table I.1**) This observation can be explained by the face-on orientation of the aryl groups that is necessary during the transition state for RE to occur. Such an orientation can be obtained by rotation of the Rh-C<sub>Ar</sub> bond from the ground state side-on orientation that minimizes the steric repulsion between the aryl group and the phosphine side arms. The rotational barrier is higher for bulkier eliminating groups leading to slower RE. Comparing it to RE from  $d^8$  complexes of Pd, it was observed that the ground state of the analogous species of  $d^8$ , Pd the eliminating ligands are already pre-arranged in a face on orientation thus removing the need for any rotation before RE. (**Figure I.9**)

 <p><b>116</b> (PCP<sup>tBu</sup>)Ir(R)(R')</p>	<i>R</i>	<i>R</i> '	$\Delta G^\ddagger$ (kcal/mol)	$\Delta G$ (kcal/mol)
	Ph	Me	27.1	-24.1
	Ph	Ph	32.4	-25.9
	Ph	Vinyl	20.7	-23.1
	Vinyl	Me	17.7	-15.7
	Vinyl	CCPh	18.1	-0.5
	CCPh	CCPh	7.0	-10.2

**Table I.1** Thermodynamic and kinetic parameters calculated by Goldman and coworkers<sup>113</sup>



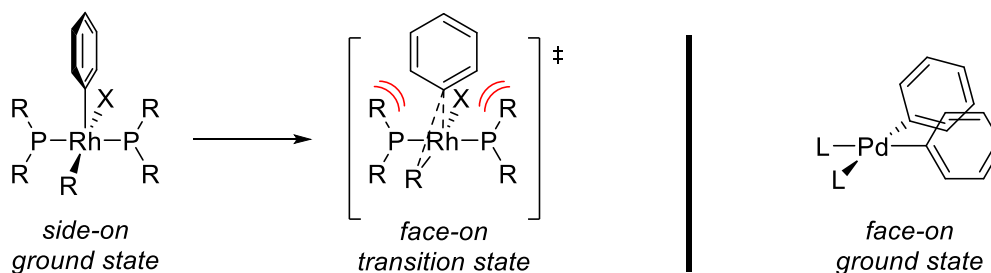


**Figure I.9** Comparison of ground state structures of  $d^6$  Rh and  $d^8$  Pd complexes prior to RE.

Most recently, our group reported the utility of (POCOP)Rh catalysts in Kumada-Corriu and C-S couplings.<sup>83,114</sup> The mechanistic details were also investigated by the isolation of the proposed intermediates and studying their interchange. (**Figure I.10**) To our knowledge, this system represents one of the few examples<sup>73,76,81,114</sup> where Rh based catalysis has been observed and the mechanistic details have been successfully probed.

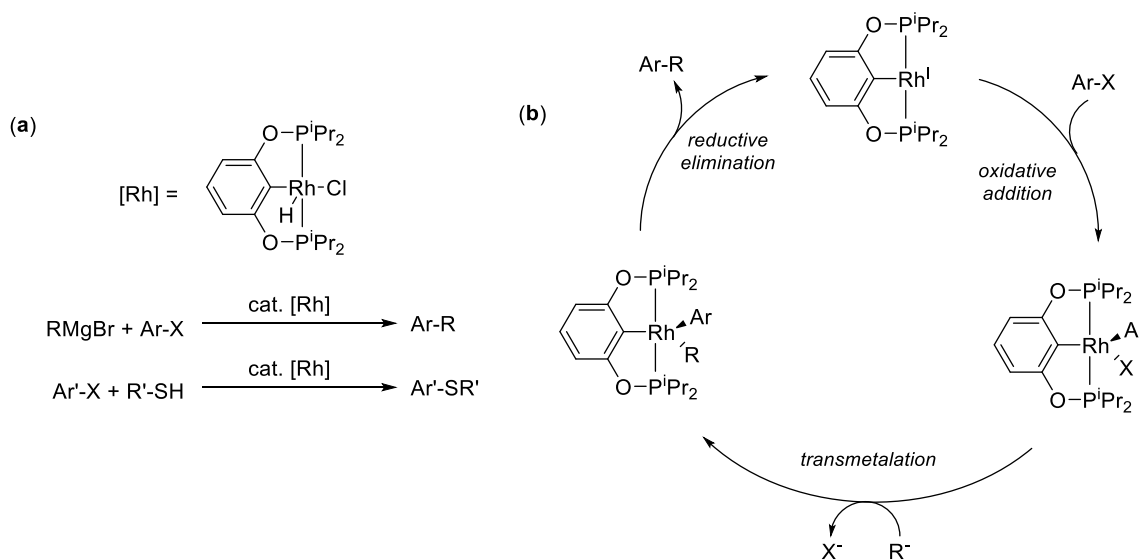


**Figure I.10** (a) Catalytic reactions with (POCOP)Rh(H)(Cl) (b) Mechanism for catalytic coupling using (POCOP)Rh catalysts

In general, it seems that the catalysis proceeds through OA of aryl halide to three coordinate  $\text{Rh}^{\text{I}}$  and RE from a five coordinate  $\text{Rh}^{\text{III}}$ . Pincer ligands such as PNP and

POCOP have allowed for the successful isolation of these Rh<sup>I</sup> and Rh<sup>III</sup> species and studying their interchange. These ligands therefore, should serve as good starting points for our investigations into analogous chemistry with cobalt.

## CHAPTER II

### REDUCTION OF CO<sub>2</sub> TO FREE CO BY A Pd<sup>I</sup>-Pd<sup>I</sup> DIMER\*

#### 2.1. Introduction

Carbon dioxide, due to its strong bonds and overall non polar nature is a very unreactive molecule when it comes to transformation to organic compounds. Processes for conversion of CO<sub>2</sub> into chemicals are worth investigating due to the high abundance of CO<sub>2</sub> in our atmosphere and challenges presented by its low reactivity. One such reaction is the reduction of CO<sub>2</sub> to CO. Carbon monoxide is a versatile C1-feedstock as demonstrated by its utilization in making specialty chemicals by processes such as the Monsanto process or the hydroformylation reactions.<sup>115</sup>

A major source of CO in industry is by passing air over a bed of coke in an oven where CO<sub>2</sub> is produced initially which then reacts with more hot carbon to give CO via the Boudouard reaction.<sup>116</sup> Another process of making CO is by reacting steam with hot coke to produce a mixture of CO and H<sub>2</sub>.<sup>117</sup> Steam reforming of natural gas is another prominent way of producing CO by reacting alkane with steam.<sup>117,118</sup> Combustion of coal in insufficient supply of air also produces CO.<sup>117</sup> In addition to these methods CO can also be produced by photochemical and electrochemical reduction of CO<sub>2</sub>.<sup>119</sup> The reduction of CO<sub>2</sub> to CO is already prominent in biology where it is catalyzed efficiently and reversibly by the carbon monoxide dehydrogenase enzyme.<sup>120</sup>

---

\* Parts of this chapter reproduced by permission of The Royal Society of Chemistry from: Palit, C. M.; Graham, D. J.; Chen, C.-H.; Foxman, B. M.; Ozerov, O. V. *Chem. Commun.* **2014**, 50, 12840, Copyright 2014 by Royal Society of Chemistry

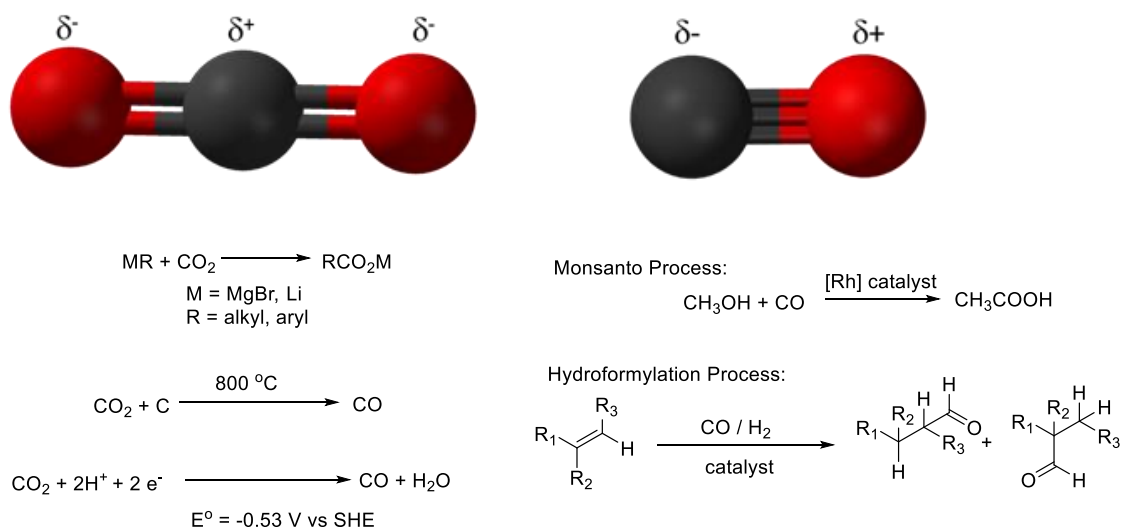


**Figure II.1** Comparison of the polarity and reactivity of CO<sub>2</sub> and CO.

In the domain of chemistry, some notable catalysts for reduction of CO<sub>2</sub> to CO have been developed with Re<sup>121</sup>, Ni<sup>122</sup>, Pd<sup>123–126</sup> and Ru<sup>127</sup>. There have been several examples of stoichiometric chemical reduction of CO<sub>2</sub> to CO using a variety of transition metal complexes<sup>128–132</sup>, uranium<sup>133</sup>, and main group elements.<sup>134–137</sup> The success of these examples was dependent on trapping of the formal oxide (O<sup>2-</sup>) generated in the reduction of CO<sub>2</sub>, by making strong bonds to highly oxophilic elements such as metal-oxos or Si-O and Al-O. In addition, the evolution of free CO required the transition metals involved to have low affinity to bind CO as a ligand. An example where all these different parts have been put together is the catalytic reduction of CO<sub>2</sub> to CO by a Cu(I) catalyst utilizing pinB-Bpin to consume the oxide equivalent reported by Sadighi et. al.<sup>138</sup> (**Figure II.2**)

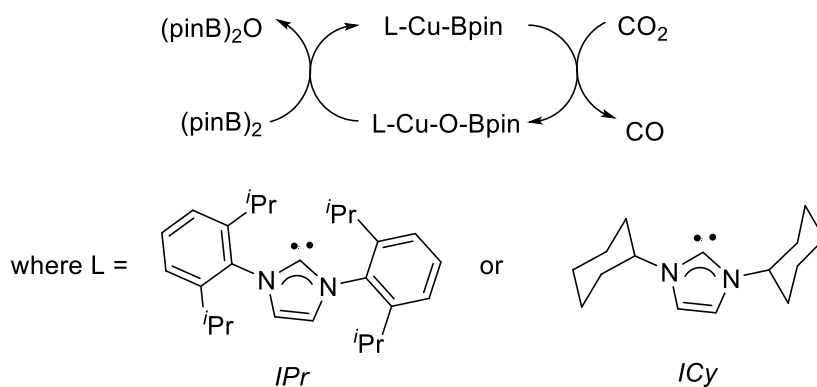


**Figure II.2** Catalytic reduction of CO<sub>2</sub> to CO by a Cu(I)NHC catalyst using (Bpin)<sub>2</sub>

Of particular interest to us, were the reports by Dubois et. al.<sup>123–126</sup> on the polyphosphine-supported Pd<sup>II</sup> electrocatalysts for the reduction of CO<sub>2</sub> to CO (**Figure II.3**), in light of recent work undertaken in our group with the Pd<sup>I</sup>-Pd<sup>I</sup> dimer [(<sup>F</sup>PNP)Pd]<sub>2</sub> (**201**).<sup>31,139,140</sup> Dubois et. al. arrived at the conclusion that Pd<sup>I</sup>-Pd<sup>I</sup> dimers were the undesirable decomposition products in their system but in some cases, bimetallic bis-Pd systems displayed enhanced catalytic rates. Due to the ability of **201** to activate other small molecules, we were encouraged to investigate its reactivity with CO<sub>2</sub>.

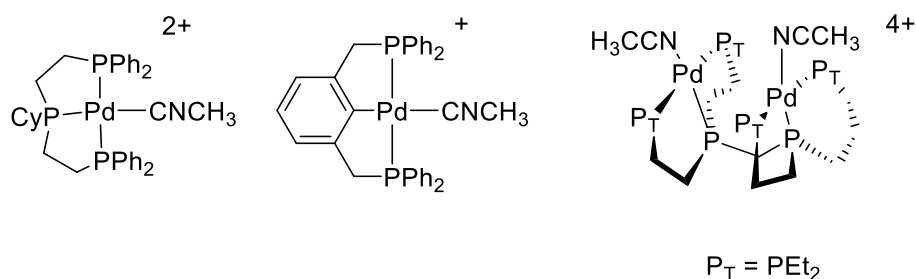


**Figure II.3** Pd catalysts for the reduction of CO<sub>2</sub> to CO reported by Dubois

## 2.2. Results and discussions

### 2.2.1. Overview of (<sup>F</sup>PNP<sup>iPr</sup>) ligand and past reactivity of [(<sup>F</sup>PNP)Pd-]<sub>2</sub>

A series of diarylamido based PNP ligands have been synthesized and the activity of their complexes with metals such as Pd, Ni, Ir, Rh studied by our group and several others. The <sup>F</sup>PNP ligand combines all the attributes of a normal PNP ligand with the presence of a convenient <sup>19</sup>F NMR tag on the aryl backbone. This tag proves valuable in as the <sup>19</sup>F NMR chemical shifts are diagnostic of the reactivity/substituents at the metal center.<sup>141</sup>

A series of (<sup>F</sup>PNP)Pd<sup>II</sup> compounds relevant to the chemistry described in this chapter can be synthesized by simple procedures as described in our previous publications. [(<sup>F</sup>PNP)Pd-]<sub>2</sub> (**201**) has proven especially effective at activation of small molecules where the Pd<sup>I</sup>-Pd<sup>I</sup> bond serves as a two electron donor to small molecules and forms two Pd<sup>II</sup> fragments. The reactivity of **201** with several small molecules such as H<sub>2</sub>, H<sub>2</sub>O, NH<sub>3</sub> and O<sub>2</sub> have been explored by past researchers in the Ozerov group and the observations have been summarized in **Figure II.4**.

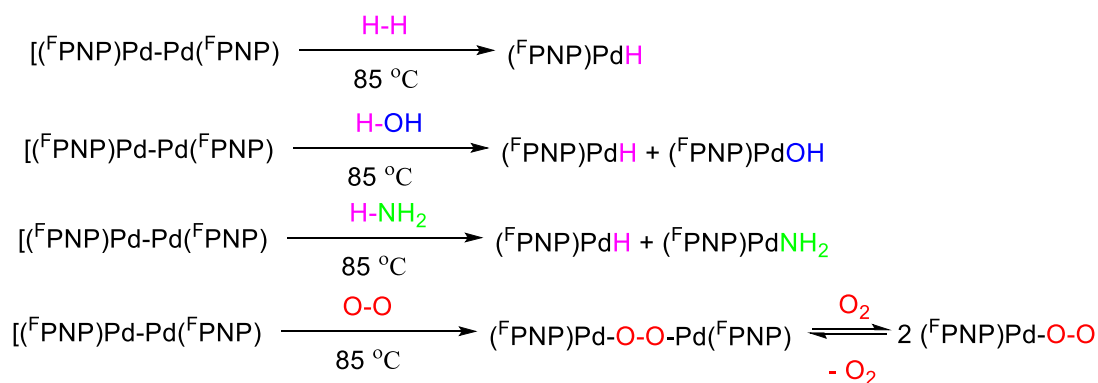
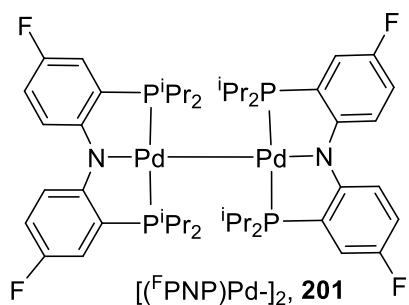


**Figure II.4** Previously reported reactivity of  $[(^{\text{F}}\text{PNP})\text{Pd-}]_2$  (**201**) with small molecules

### 2.2.2. Preliminary reactions of **201** with $\text{CO}_2$ and $\text{CS}_2$

Our first experiments at reacting  $\text{C}_6\text{D}_6$  solutions of **201** with 1 atm of  $\text{CO}_2$  led to no observable reaction by NMR spectroscopy even at 80 °C and under illumination. Reactions with analogous  $\text{CS}_2$  however, yielded clean insertion of  $\text{CS}_2$  into the Pd-Pd bond to give the  $\text{CS}_2$  bridged Pd dimer **203**; with the reaction proceeding rapidly (10 min) upon illumination and much more slowly (12 h) at 80 °C in the dark. Solution NMR of **203** shows two distinct Pd centers each with local  $\text{C}_{2v}$  symmetry.  $^{19}\text{F}$  NMR chemical shifts further helped establish that one Pd was bound to a carbon while the other was bound to a much more electronegative heteroatom.<sup>141</sup>

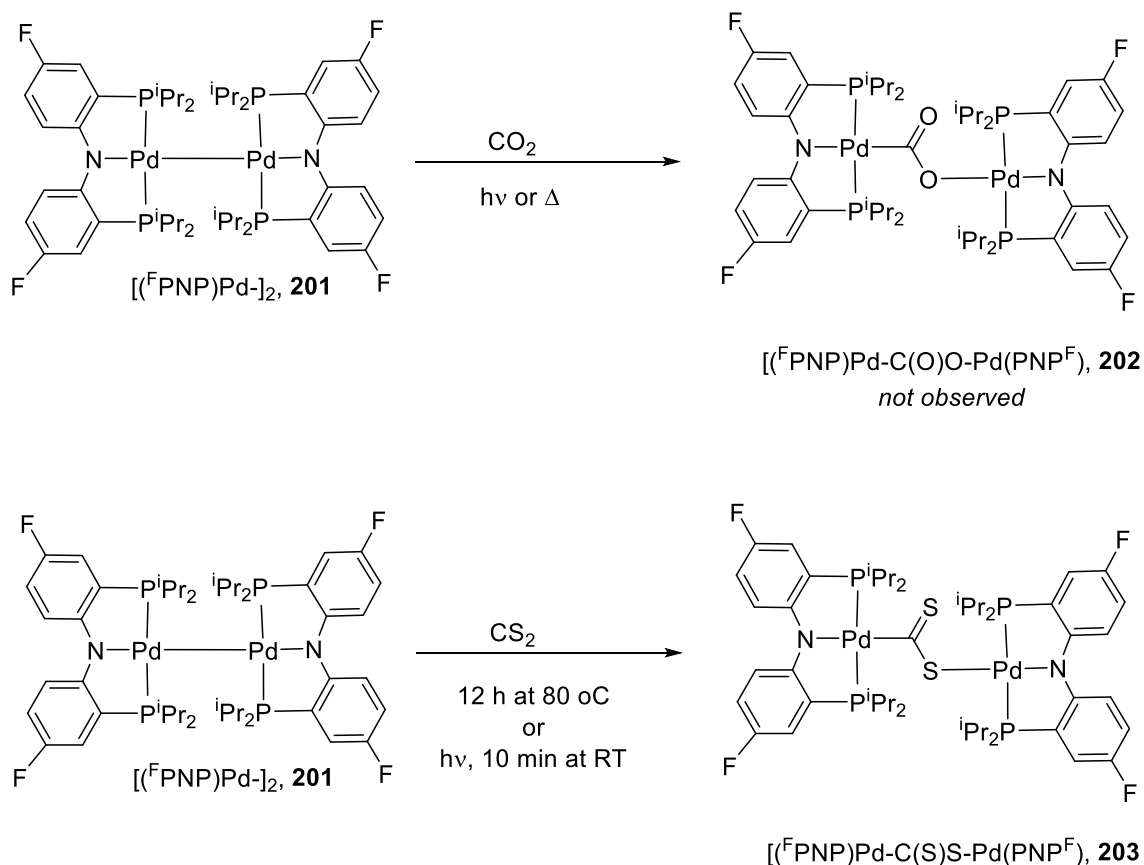


**Figure II.5** Reactivity of **201** with  $\text{CO}_2$  and  $\text{CS}_2$

Such an insertion is not unique as insertion of  $\text{CS}_2$  into  $\text{Pd}^{\text{I}}-\text{Pd}^{\text{I}}$  single bonds<sup>142</sup> and analogous  $\text{Pt}^{\text{I}}-\text{Pt}^{\text{I}}$  has been previously reported.<sup>142,143</sup> Based on the observed difference in reactivity of **201** with  $\text{CO}_2$  and  $\text{CS}_2$ , we hypothesized that a  $\text{CO}_2$  insertion product **202** analogous to **203** might be kinetically accessible but not thermodynamically favorable. This hypothesis was based on the previously reported related complexes with  $\text{Pd}^{\text{II}}-\text{C}(\text{=O})\text{O}-\text{Pd}^{\text{II}}$  and  $\text{Pt}^{\text{II}}-\text{C}(\text{=O})\text{O}-\text{Pt}^{\text{II}}$  subunits obtained via condensation of metalcarboxylic acids ( $\text{M}^{\text{II}}-\text{COOH}$ ) with  $\text{M}^{\text{II}}-\text{OH}$ .<sup>144,145</sup> A  $\text{Rh}^{\text{I}}-\text{CO}_2-\text{Rh}^{\text{I}}$  complex synthesized via insertion of  $\text{CO}_2$  into a  $\text{Rh}^0-\text{Rh}^0$  bond has also been reported in the past.<sup>146</sup> We further identified that a possible equilibrium between **201** and **202** can be driven



forward by reaction of the Pd-O bond in **202** with an oxophilic reagent such as Me<sub>3</sub>SiX, hence leading to the conversion of 1 equivalent of CO<sub>2</sub>.

### 2.2.3. Reactions of **201** with CO<sub>2</sub> and Me<sub>3</sub>SiX reagents

Thermolysis of a C<sub>6</sub>D<sub>6</sub> solution of **201** in the presence of Me<sub>3</sub>SiX (X = Cl, OTf) under 1 atm of CO<sub>2</sub> for 18h, resulted in complete consumption of **201** and formation of (<sup>F</sup>PNP)PdCl (**204**) and (<sup>F</sup>PNP)PdOTf (**205**) as the dominant Pd products in 70% and 90% yields respectively (by NMR vs (<sup>F</sup>PNP)Me as an internal standard). The other Pd product observed in the reaction with Me<sub>3</sub>SiCl was (<sup>F</sup>PNP)PdH (30%). (Me<sub>3</sub>Si)<sub>2</sub>O was observed by <sup>1</sup>H NMR spectroscopy confirming the abstraction of the formal O<sup>2-</sup> by two Me<sub>3</sub>Si<sup>+</sup> fragments. Observation of **204**, **205** and (Me<sub>3</sub>Si)<sub>2</sub>O by NMR spectroscopy suggested that the other product based on stoichiometry might be CO (**Figure II.6**). In order to confirm the formation of CO and quantify the amount produced we envisioned trapping of the evolved CO with a transition metal complex.

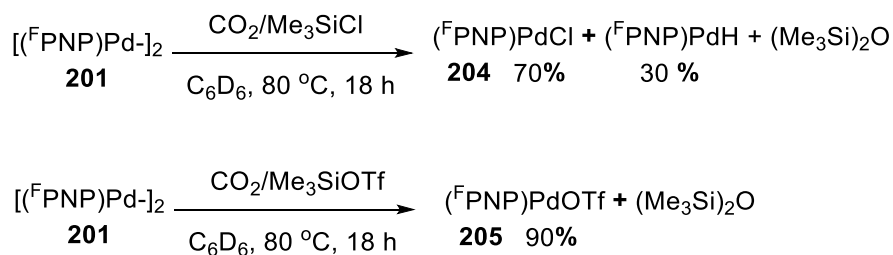


**Figure II.6** Reactivity of **201** with CO<sub>2</sub> in the presence of Me<sub>3</sub>SiX

### 2.2.4. Trapping of evolved CO with (<sup>Me</sup>PNP)Ir(D)(C<sub>6</sub>D<sub>5</sub>)

(<sup>Me</sup>PNP)Ir(D)(C<sub>6</sub>D<sub>5</sub>) (**207D**) was selected as an in-situ trap for free CO in order to quantify the production of CO from the reactions of **201** with CO<sub>2</sub> and Me<sub>3</sub>SiX. **207D** can be quantitatively prepared by thermolysis of **206**<sup>147</sup> in C<sub>6</sub>D<sub>6</sub>. Thermolysis of **201** in C<sub>6</sub>D<sub>6</sub>

under 1 atm of CO<sub>2</sub> in the presence of Me<sub>3</sub>SiOTf and **207D** produced 85% yield of **205** and 65% yield of (<sup>Me</sup>PNP)Ir(D)(C<sub>6</sub>D<sub>5</sub>)(CO) (**208D**). The analogous reaction with Me<sub>3</sub>SiCl yielded 70% yield of **205**, 30% yield of (<sup>F</sup>PNP)PdH<sup>148</sup> and 45% yield of **208D**. In order to establish that the amount of CO observed through **208D** is indeed the CO being produced the reaction of **201** with CO<sub>2</sub> and Me<sub>3</sub>SiX, several control reactions were performed and have been discussed in the next section.

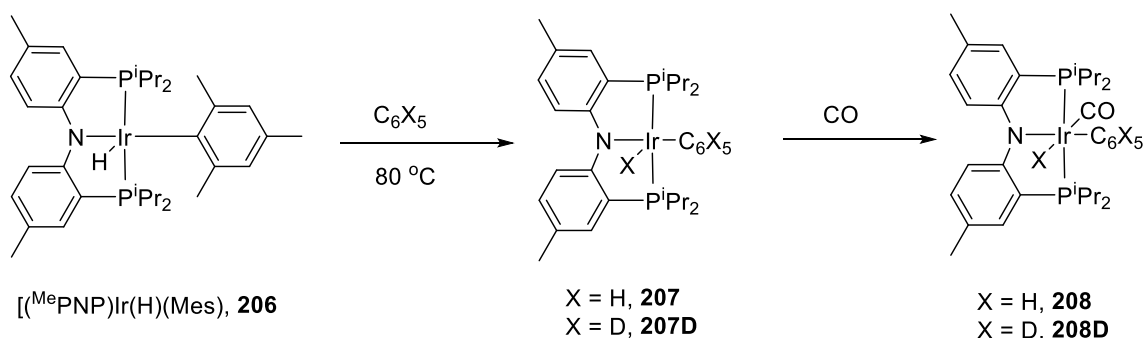


**Figure II.7** Synthesis of the in-situ trap **207D** and its reaction with CO

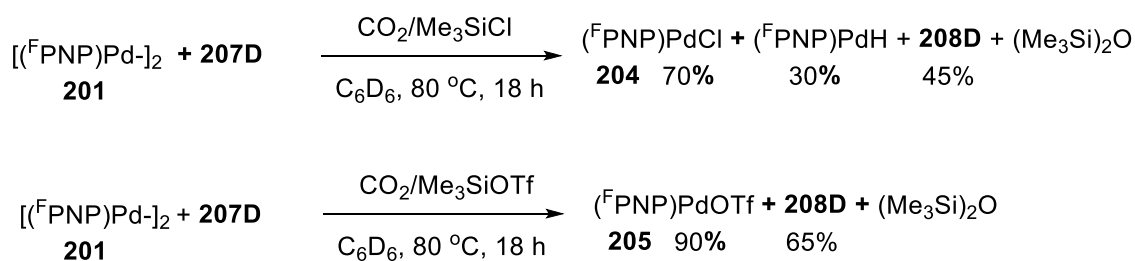


**Figure II.8** Reactions of **201** with CO<sub>2</sub>/Me<sub>3</sub>SiX in the presence of **207D** as a trap for CO

### 2.2.5. Control reactions

The Ir complex **207D** showed no reaction with CO<sub>2</sub> with or without Me<sub>3</sub>SiOTf and Me<sub>3</sub>SiCl. Thermolysis of **207D** at 80 °C for 24 h under 1 atm of CO<sub>2</sub> in the presence of Me<sub>3</sub>SiOTf resulted in 60% consumption of **207D**, but **208D** was not observed as a product.

Thermolysis of **207D** at 80 °C for 18 h under 1 atm of CO<sub>2</sub> in the presence of Me<sub>3</sub>SiCl resulted in complete consumption of **207D** and a mixture of products that did not contain **208D**. Treatment of **207D** with Me<sub>3</sub>SiCl (or Me<sub>3</sub>SiOTf) and CO, followed by thermolysis resulted only in the formation of **208D**.

For Pd control reactions, we determined that **201** does react with CO upon thermolysis, with or without Me<sub>3</sub>SiCl or Me<sub>3</sub>SiOTf. However, **204** was only a minor product (10%) from the Me<sub>3</sub>SiCl/CO reaction, and **205** was not observed at all in the Me<sub>3</sub>SiOTf/CO reaction. The dimer **201** did not react with either Me<sub>3</sub>SiCl or Me<sub>3</sub>SiOTf alone after 18 h at 80 °C in C<sub>6</sub>D<sub>6</sub>. (<sup>F</sup>PNP)PdH was also unaffected when thermolyzed under CO<sub>2</sub> atmosphere and thus is unlikely to be involved as an intermediate. Closely related (PNP)PdH compounds have been shown not to react with CO<sub>2</sub>.<sup>149</sup>

The exact nature of the products in the control reactions was not established but the combination of our control reactions indicates that **208D** is indeed produced by trapping of CO generated by **201**/CO<sub>2</sub>/Me<sub>3</sub>SiOTf and not via the reduction of CO<sub>2</sub> in the coordination sphere of Ir. In addition, **205** is indeed primarily produced in the same CO<sub>2</sub> reduction by **201**. With Me<sub>3</sub>SiCl, although (<sup>F</sup>PNP)PdH is observed as a side product, but most of **208D** observed in the **201**/CO<sub>2</sub>/Me<sub>3</sub>SiCl reactions does originate from the trapping of free CO.

#### 2.2.6. Mechanistic insight

The observation that the reaction of **201** with CO<sub>2</sub> proceeds to completion in the presence of Me<sub>3</sub>SiX reagents gave more credence to our hypothesis that the reaction of **201** with CO<sub>2</sub> is an equilibrium which is driven forward by the abstraction of a formal O<sup>2-</sup>

by two  $\text{Me}_3\text{Si}^+$  fragments. We propose the formation of a probable  $\text{CO}_2$  bridged complex **202** followed by metathesis of Pd-O with Si-X bonds to give **204/205** and **211**. (**Figure II.9**) The possible next step is the decarbonylation of **211** before or after reacting with a second equivalent of  $\text{Me}_3\text{SiX}$ . Similar decarbonylations of  $(\text{PCP})\text{PdC}(=\text{O})\text{OH}$  and of  $(\text{PCP})\text{Pd}-\text{C}(=\text{O})\text{O}-\text{Pd}(\text{PCP})$  have been reported by Campora et. al., where PCP is  $\kappa^3$ -2,6( $^i\text{Pr}_2\text{PCH}_2$ ) $_2\text{C}_6\text{H}_3$ .

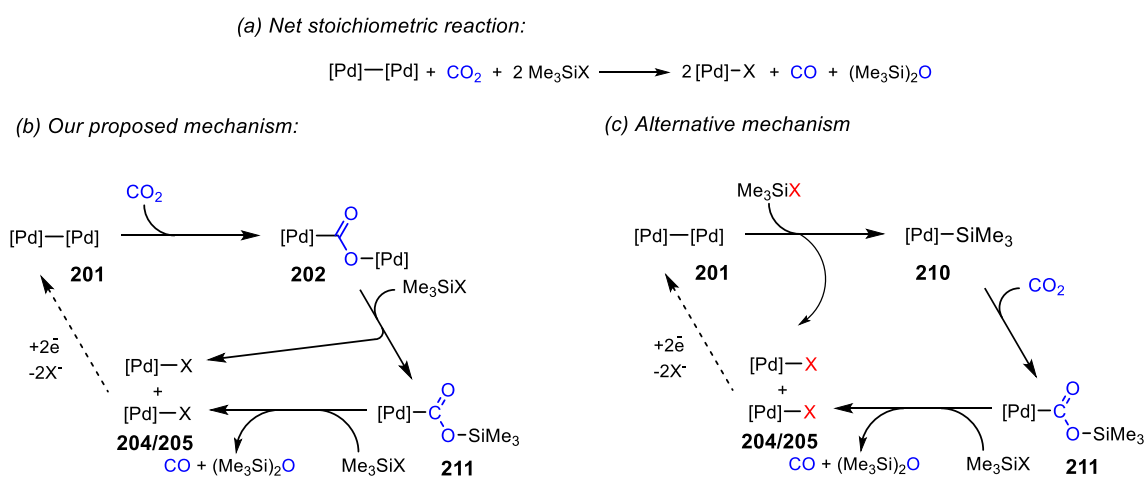


**Figure II.9** Overall stoichiometry of the reaction and possible mechanisms

Another possible mechanism is the reaction of **201** with  $\text{Me}_3\text{SiX}$  to give  $(^{\text{F}}\text{PNP})\text{Pd}-\text{SiMe}_3$  (**210**) and **204/205**. **210** can further react with  $\text{CO}_2$  and  $\text{Me}_3\text{SiX}$  to give another equivalent of **204/205**,  $\text{CO}$  and  $(\text{Me}_3\text{Si})_2\text{O}$ . To explore the possibility of such a mechanism  $(^{\text{F}}\text{PNP})\text{Pd}-\text{SiMe}_3$  (**210**) was synthesized separately as described in **Figure II.10** and upon exposing a solution of **210** to  $\text{CO}_2$ , no reaction was observed. This led us to believe that **Figure II.9** (b) illustrates the most possible mechanism for our observed reactivity.

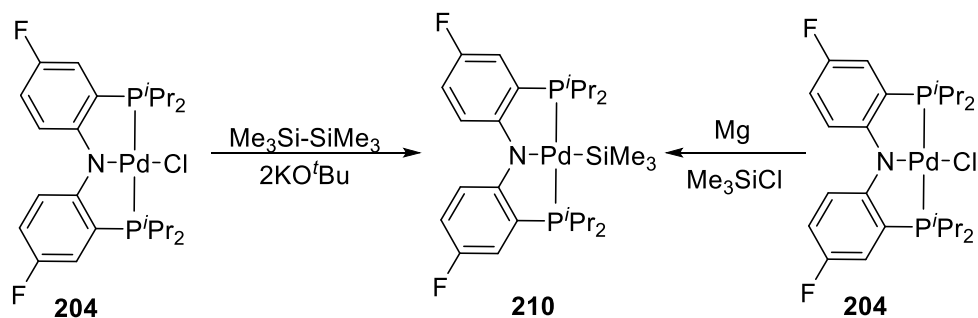


**Figure II.10** Synthesis of <sup>F</sup>PNP)Pd(SiMe<sub>3</sub>) (**210**) from of <sup>F</sup>PNP)PdCl (**204**)

### 2.3. Conclusion

In summary, we have demonstrated that the Pd<sup>I</sup>-Pd<sup>I</sup> dimer **201** can reduce CO<sub>2</sub> to free CO with the help of Me<sub>3</sub>SiOTf, or less efficiently with Me<sub>3</sub>SiCl. Release of free CO mediated by a late transition metal catalyst is a challenge because of the generally high affinity of late metal complexes in reduced oxidation states for binding CO. In our system, this problem is circumvented by the pincer ligation of Pd and by the relatively low affinity of either Pd<sup>I</sup> or Pd<sup>II</sup> oxidation states for CO as a ligand.

### 2.4. Experimental details

#### 2.4.1. General considerations

Unless specified otherwise, all manipulations were performed under an argon atmosphere using standard Schlenk line or glove box techniques. Toluene, ethyl ether, and pentane were dried and deoxygenated (by purging) using a PureSolv solvent purification system by Innovative Technologies Inc. and stored over molecular sieves in an Ar-filled glove box. C<sub>6</sub>D<sub>6</sub> and THF were dried over and distilled from NaK/Ph<sub>2</sub>CO/18-crown-6 and stored over molecular sieves in an Ar-filled glove box. <sup>F</sup>PNP)PdH, [(<sup>F</sup>PNP)Pd]<sub>2</sub> (**201**), <sup>F</sup>PNP)Me and (<sup>Me</sup>PNP)Ir(H)(Mes) (**206**) were prepared according to the published

procedures.<sup>24,32,147,148</sup> All other chemicals were used as received from commercial vendors. The halogen lamp used for some of the reactions used 250 W tungsten halogen bulbs manufactured by Plusrite. NMR spectra were recorded on a Varian iNova 300 MHz, Varian iNova 400 MHz or a Varian iNova 500 MHz instrument. For  $^1\text{H}$  and  $^{13}\text{C}$  NMR spectra, the residual solvent peak was used as an internal reference.  $^{31}\text{P}$  NMR spectra were referenced externally using 85%  $\text{H}_3\text{PO}_4$  at 0 ppm,  $^{19}\text{F}$  NMR spectra were referenced externally using trifluoroacetic acid at -78.5 ppm and  $^{29}\text{Si}$  NMR spectra were referenced externally using tetramethylsilane at 0 ppm. Addition of 10 mg of  $\text{Cr}(\text{acac})_3$  to the sample dramatically increased the signal to noise ratio for  $^{29}\text{Si}$  NMR.<sup>150</sup> Elemental analyses were performed by CALI, Inc. (Parsippany, NJ).

#### *2.4.2. Estimation of number of moles of gases in J. Young NMR tube headspace*

A typical J. Young NMR tube of 7 inch length has a usable volume of approximately 2.4 mL. The amount of solvent used in all of the experiments described below is a maximum of 1 mL. This leaves 1.4 mL of headspace for any gases being added after 3 freeze-pump-thaw cycles which corresponds to at least 60  $\mu\text{mol}$  at ambient temperature by ideal gas law. Hence, any gas being used in the experiments listed below is always in a large excess as compared to the metal complexes and  $\text{Me}_3\text{SiCl}$  or  $\text{Me}_3\text{SiOTf}$ .

#### *2.4.3. General procedure for preparation of a stock solution of (FNP)Me*

The oily  $(^{\text{F}}\text{PNP})\text{Me}$  was synthesized using previously published procedures. The purity was confirmed by analysis of the sample by  $^{31}\text{P}$ ,  $^{19}\text{F}$  and  $^1\text{H}$  NMR spectroscopy. The amount obtained was dissolved in 10 mL of  $\text{C}_6\text{D}_6$  in a volumetric flask. A 0.5 mL aliquot was taken from this stock solution and a known amount of fluorobenzene was added using

a micro syringe as an internal standard. The concentration of the stock solution was then determined using  $^{19}\text{F}$  NMR with fluorobenzene as an internal standard.

*2.4.4. In-situ generation of  $(^{\text{Me}}\text{PNP})\text{Ir}(\text{D})(\text{C}_6\text{D}_5)$  (**207D**) from  $(^{\text{Me}}\text{PNP})\text{Ir}(\text{H})(\text{Mes})$  (**206**).*

For all the experiments listed below, wherever required,  $(^{\text{Me}}\text{PNP})\text{Ir}(\text{D})(\text{C}_6\text{D}_5)$  was generated in-situ, according to previously published procedure, by heating an equivalent amount of  $(^{\text{Me}}\text{PNP})\text{Ir}(\text{H})(\text{Mes})$  in  $\text{C}_6\text{D}_6$  at  $80\text{ }^\circ\text{C}$  for 1 h. Complete conversion to  $(^{\text{Me}}\text{PNP})\text{Ir}(\text{D})(\text{C}_6\text{D}_5)$  takes place upon this thermolysis, as established by analysis of the samples by  $^{31}\text{P}$  NMR spectroscopy.

*2.4.5. Spectral details for some previously reported compounds.*

The characteristic peaks in the  $^{19}\text{F}$  and  $^{31}\text{P}\{^1\text{H}\}$  NMR spectra of the compounds published earlier which are observed as products in the reactions in this manuscript, have been listed below for easy reference:

<b>Compound</b>	$(^{\text{F}}\text{PNP})$ Me	$(^{\text{F}}\text{PNP})\text{PdH}$	$(^{\text{F}}\text{PNP})\text{PdCl}$ <b>(204)</b>	$(^{\text{F}}\text{PNP})\text{PdOTf}$ <b>(205)</b>	$(^{\text{Me}}\text{PNP})\text{Ir}(\text{D})$ $(\text{C}_6\text{D}_5)$ <b>(208D)</b>
<b><math>^{31}\text{P}\{^1\text{H}\}</math></b>	<b>-6.2</b>	<b>59.2</b>	<b>47.4</b>	<b>52.9</b>	<b>45.8</b>
<b><math>^{19}\text{F}</math></b>	<b>-121.7</b>	<b>-131.5</b>	-128.8	<b>-77.5, -126.9</b>	<b>N/A</b>

**Table II.1**  $^{31}\text{P}\{^1\text{H}\}$  and  $^{19}\text{F}$  NMR chemical shifts of compounds referred to frequently in this chapter

#### 2.4.6. Reactions of $[(^F\text{PNP})\text{Pd}]_2$ (**201**) with $\text{CO}_2$

**Reaction of  $[(^F\text{PNP})\text{Pd}]_2$  (**201**) with  $\text{CO}_2$ .**  $[(^F\text{PNP})\text{Pd}]_2$  (**201**) (13.4 mg, 12.1  $\mu\text{mol}$ ) was dissolved in  $\text{C}_6\text{D}_6$  ca. 2 mL in a J. Young NMR tube. The solution was then degassed using 3 freeze-pump-thaw cycles and  $\text{CO}_2$  was then added through a flushed gas line. The J. Young tube was then left in an oil bath at 80 °C. The reaction was monitored by analysis of the sample by  $^{31}\text{P}$ ,  $^1\text{H}$  and  $^{19}\text{F}$  NMR spectroscopy and no changes were detected after 24 h.

**Reaction of  $[(^F\text{PNP})\text{Pd}]_2$  (**201**) with  $\text{CO}_2$  with hv.**  $[(^F\text{PNP})\text{Pd}]_2$  (**201**) (13.4 mg, 12.1  $\mu\text{mol}$ ) was dissolved in  $\text{C}_6\text{D}_6$  ca. 2 mL in a J. Young NMR tube. The solution was degassed using 3 freeze-pump-thaw cycles and  $\text{CO}_2$  was then added through a flushed gas line. The J. Young tube was then left in an oil bath at 80 °C and was irradiated using a halogen lamp. The reaction was monitored by  $^{31}\text{P}$  and  $^{19}\text{F}$  NMR spectroscopy and no changes were observed after 24 h.

**Reaction of  $[(^F\text{PNP})\text{Pd}]_2$  (**201**) with  $\text{CO}_2$  and  $\text{Me}_3\text{SiOTf}$ .**  $[(^F\text{PNP})\text{Pd}]_2$  (**201**) (10 mg, 9.1  $\mu\text{mol}$ ) was dissolved in  $\text{C}_6\text{D}_6$  ca. 0.8 mL in a J. Young NMR tube.  $\text{Me}_3\text{SiOTf}$  (3.5  $\mu\text{L}$ , 4.3 mg, 20  $\mu\text{mol}$ ) was added to this solution using a syringe, followed by addition of  $(^F\text{PNP})\text{Me}$  (200  $\mu\text{L}$  of 0.09 M stock solution in  $\text{C}_6\text{D}_6$ , 18  $\mu\text{mol}$ ) as an internal standard. The solution was then degassed using three freeze-pump-thaw cycles and  $\text{CO}_2$  was then added through a flushed gas line. The J. Young tube was then placed in an oil bath at 80 °C. The reaction was monitored by  $^{31}\text{P}$  and  $^{19}\text{F}$  NMR spectroscopy and proceeded to completion after heating for 18 h. Complete conversion of  $[(^F\text{PNP})\text{Pd}]_2$  into  $(^F\text{PNP})\text{PdOTf}$  (**205**) (90%) and an unidentified product (10%) was observed by the



analysis of the sample by  $^{31}\text{P}\{^1\text{H}\}$  and  $^{19}\text{F}$  NMR spectroscopy (**Figure II.11** and **Figure II.12**). The resonances for the unidentified product were observed at 56.9 ppm (10%) in the  $^{31}\text{P}\{^1\text{H}\}$  and -124.4 and -125.6 ppm (5% each) and another resonance at -78.7 ppm in the  $^{19}\text{F}$  NMR spectra of the sample. Comparing the  $^1\text{H}$  NMR spectra of the starting sample and sample after completion shows complete consumption of  $\text{Me}_3\text{SiOTf}$  and conversion into  $(\text{Me}_3\text{Si})_2\text{O}$  (**Figure II.13**).

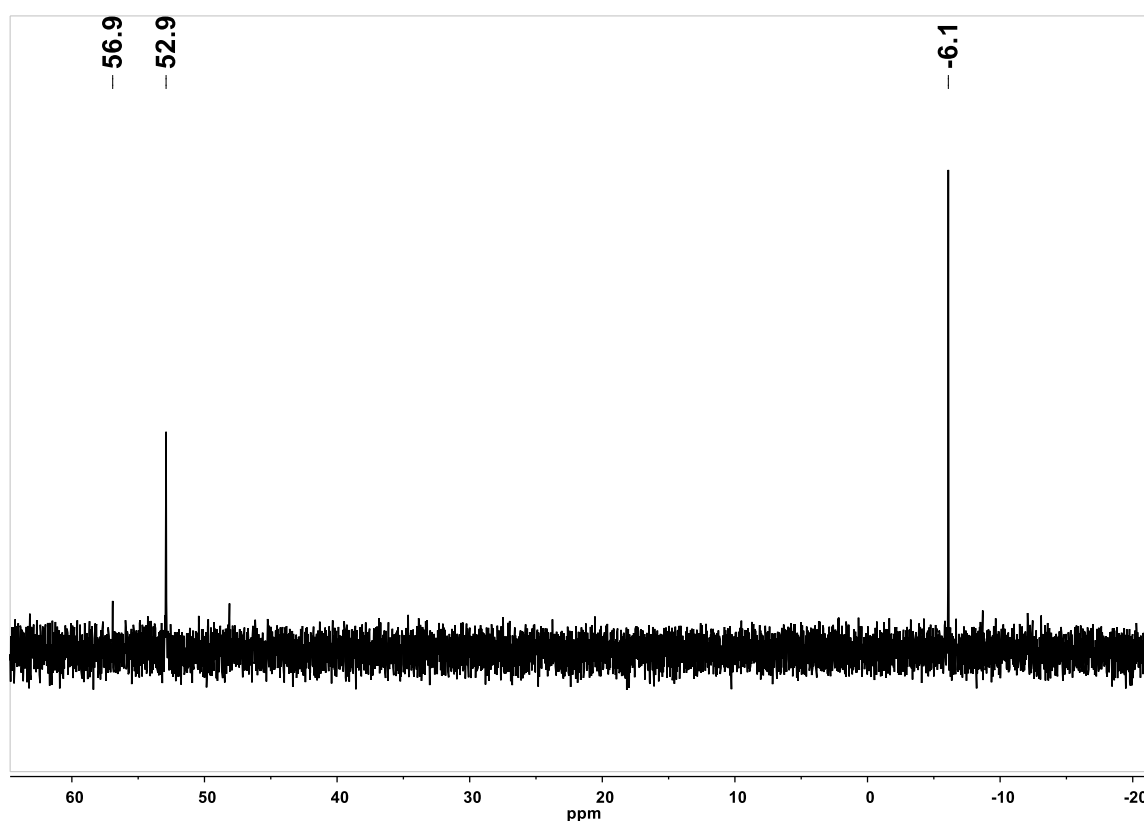


**Figure II.11**  $^{31}\text{P}\{^1\text{H}\}$  NMR (300 MHz,  $\text{C}_6\text{D}_6$ ) spectrum of the reaction of  $[(^{\text{F}}\text{PNP})\text{Pd}]_2$  (**201**) with  $\text{CO}_2$  and  $\text{Me}_3\text{SiOTf}$  after heating for 18 h

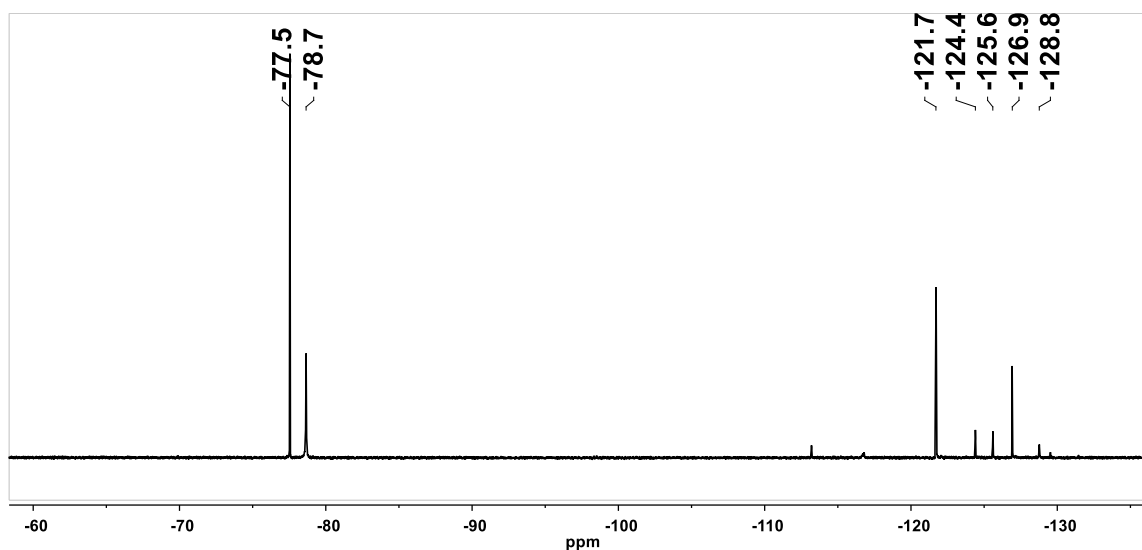


**Figure II.12**  $^{19}\text{F}$  NMR (300 MHz,  $\text{C}_6\text{D}_6$ ) spectrum of the reaction of  $[(^{\text{F}}\text{PNP})\text{Pd-}]_2$  (**201**) with  $\text{CO}_2$  and  $\text{Me}_3\text{SiOTf}$  after heating for 18 h

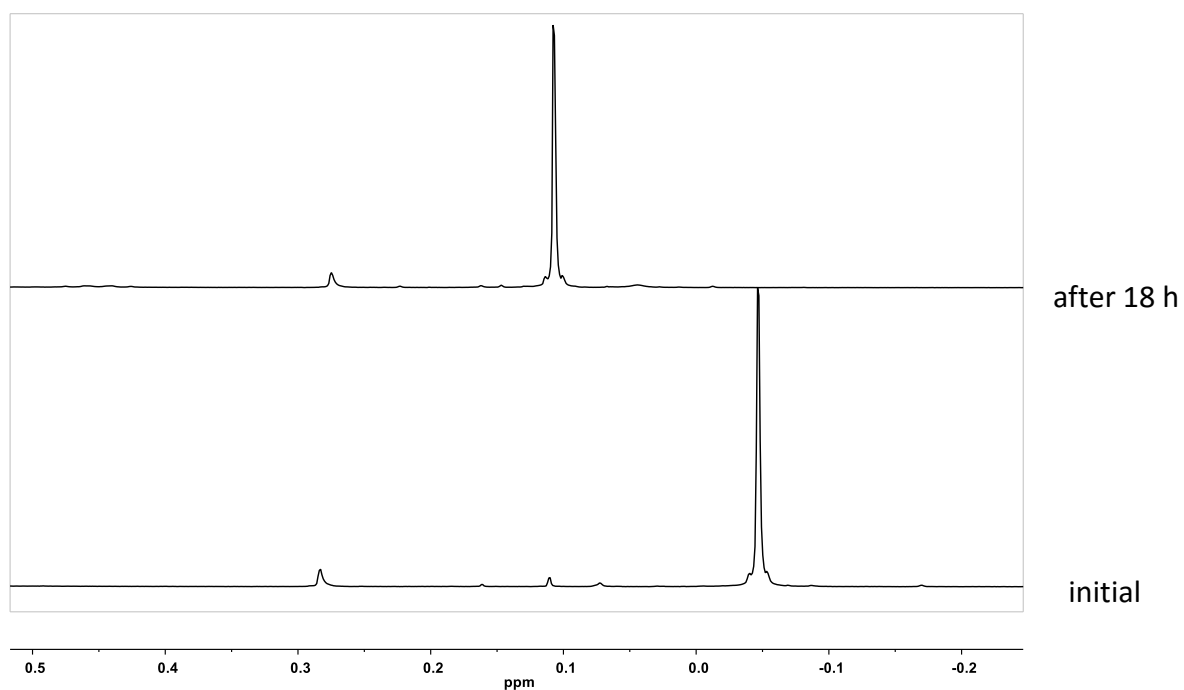


**Figure II.13** Silyl region of the  $^1\text{H}$  NMR (300 MHz,  $\text{C}_6\text{D}_6$ ) stacked spectra of the reaction of  $[(^{\text{F}}\text{PNP})\text{Pd-}]_2$  (**201**) with  $\text{CO}_2$  and  $\text{Me}_3\text{SiOTf}$  showing conversion of  $\text{Me}_3\text{SiOTf}$  (-0.05 ppm) into  $(\text{Me}_3\text{Si})_2\text{O}$  (0.11 ppm)

**Reaction with  $[(^F\text{PNP})\text{Pd}]_2$  (201) with  $\text{CO}_2$  and  $\text{Me}_3\text{SiCl}$ .**  $[(^F\text{PNP})\text{Pd}]_2$  (201) (10 mg, 9.1  $\mu\text{mol}$ ) was placed into a J. Young NMR tube. To it,  $(^F\text{PNP})\text{Me}$  (18.0  $\mu\text{mol}$ , 200  $\mu\text{L}$  of 0.09 M stock solution in  $\text{C}_6\text{D}_6$ ) was added using a syringe. The volume was made up to 800  $\mu\text{L}$  by adding 600  $\mu\text{L}$  of  $\text{C}_6\text{D}_6$  using a syringe.  $\text{Me}_3\text{SiCl}$  (2.7  $\mu\text{L}$ , 2.3 mg, 20  $\mu\text{mol}$ ) was added to this solution using another syringe. The solution was degassed using three freeze-pump-thaw cycles and  $\text{CO}_2$  was then added through a flushed gas line. The J. Young tube was then placed in an oil bath at 80  $^\circ\text{C}$ . The reaction was periodically monitored by  $^{31}\text{P}$  and  $^{19}\text{F}$  NMR spectroscopy and was noted to proceed to completion after 18 h. Complete conversion of  $[(^F\text{PNP})\text{Pd}]_2$  into  $(^F\text{PNP})\text{PdCl}$  (204) (70%) and  $(^F\text{PNP})\text{PdH}$  (30%) was observed by the analysis of the sample by  $^{31}\text{P}\{^1\text{H}\}$  and  $^{19}\text{F}$  NMR spectroscopy (**Figure II.14** and **Figure II.15**). Comparing the  $^1\text{H}$  NMR spectra of the starting sample and sample after completion shows unreacted  $\text{Me}_3\text{SiCl}$  and  $(\text{Me}_3\text{Si})_2\text{O}$  and an unidentified resonance at 0.19 ppm (**Figure II.16**)

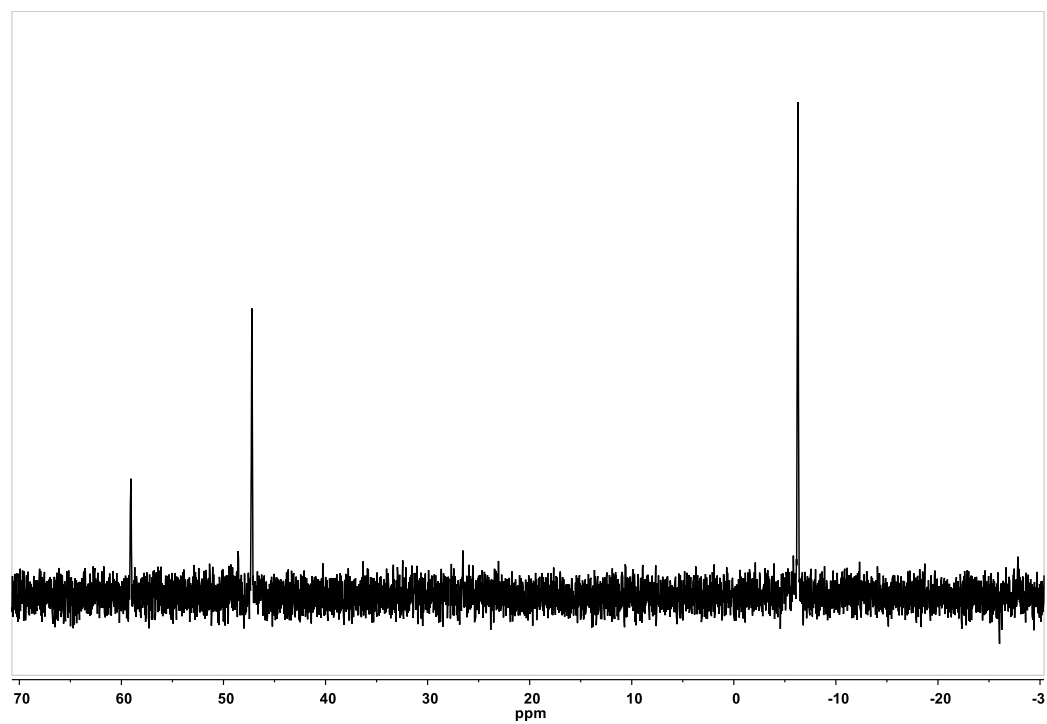


**Figure II.14**  $^{31}\text{P}\{^1\text{H}\}$  (300 MHz,  $\text{C}_6\text{D}_6$ ) NMR spectrum of the reaction of  $[(^{\text{F}}\text{PNP})\text{Pd-}]_2$  (**201**) with  $\text{CO}_2$  and  $\text{Me}_3\text{SiCl}$  after heating for 18 h

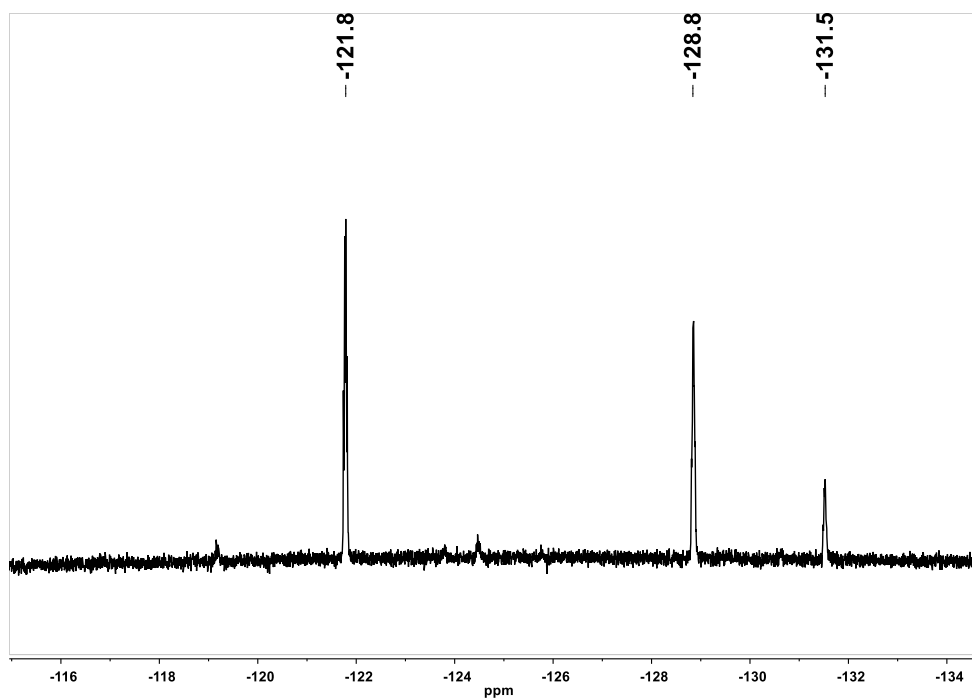


**Figure II.15**  $^{19}\text{F}$  NMR (300 MHz,  $\text{C}_6\text{D}_6$ ) spectrum of the reaction of  $[(^{\text{F}}\text{PNP})\text{Pd}]_2$  (**201**) with  $\text{CO}_2$  and  $\text{Me}_3\text{SiCl}$  after heating for 18 h

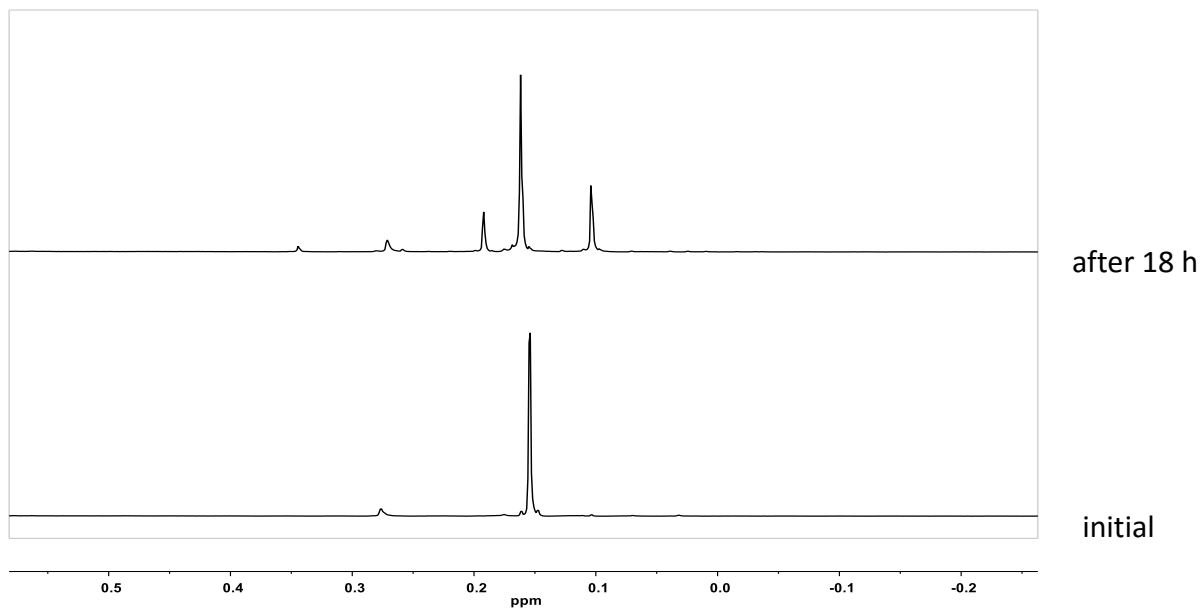


**Figure II.16** Silyl region of the  $^1\text{H}$  NMR (300 MHz,  $\text{C}_6\text{D}_6$ ) stacked spectra of the reaction of  $[(^{\text{F}}\text{PNP})\text{Pd}]_2$  (**201**) with  $\text{CO}_2$  and  $\text{Me}_3\text{SiCl}$  showing unreacted  $\text{Me}_3\text{SiCl}$  (0.17 ppm),  $(\text{Me}_3\text{Si})_2\text{O}$  (0.11 ppm) and unidentified resonance at 0.19 ppm

#### 2.4.7. Synthesis of $(^F\text{PNP})\text{Pd-C(S)S-Pd}(\text{PNP}^F)$ (**203**) and its reactions

**Reaction of  $[(^F\text{PNP})\text{Pd}]_2$  (**201**) with  $\text{CS}_2$  under irradiation.**  $[(^F\text{PNP})\text{Pd}]_2$  (**201**) (134 mg, 121  $\mu\text{mol}$ ) was dissolved in toluene ca. 20 mL in a PTFE lined screw capped flask. To this,  $\text{CS}_2$  (13.0  $\mu\text{L}$ , 16.6 mg, 218  $\mu\text{mol}$ ) was added using a syringe. The solution was then irradiated using a halogen lamp and the solution turned bright red in 10 minutes. The volatiles were removed under vacuum and the red solid obtained was re-dissolved in diethyl ether.  $(^F\text{PNP})\text{Pd-C(S)S-Pd}(\text{PNP}^F)$  (**203**) was obtained as red crystals when the solution was left to cool at  $-25\text{ }^\circ\text{C}$ . Yield: 120 mg (80%).  $^1\text{H NMR}$  ( $\text{C}_6\text{D}_6$ ) (**Figure II.17**):  $\delta$  7.49 (m, 2H, Ar-H), 7.32 (m, 2H, Ar-H), 6.92 (m, 2H, Ar-H), 6.82 (m, 2H, Ar-H), 6.73 (m, 2H, Ar-H), 6.66 (m, 2H, Ar-H), 2.80 (m, 4H,  $\text{PCH}(\text{CH}_3)_2$ ), 2.22 (m, 4H,  $\text{PCH}(\text{CH}_3)_2$ ), 1.36-1.28 (overlapping m, 24 H,  $\text{PCH}(\text{CH}_3)_2$ ), 1.09-1.03 (overlapping m, 24 H,  $\text{PCH}(\text{CH}_3)_2$ ).  $^{13}\text{C}\{^1\text{H}\}$  NMR ( $\text{C}_6\text{D}_6$ ) (**Figure II.20**):  $\delta$  285.3 (t,  $J_{\text{C-P}} = 8\text{ Hz}$ , Pd- $\text{CS}_2$ -Pd), 160.1 (t,  $J_{\text{C-P}} = 10\text{ Hz}$ , C-N), 159.9 (t,  $J_{\text{C-P}} = 10\text{ Hz}$ , C-N), 154.2 (dvt,  $J_{\text{C-F}} = 235\text{ Hz}$ ,  $J_{\text{C-P}} = 4\text{ Hz}$ , C-F), 154.0 (dvt,  $J_{\text{C-F}} = 235\text{ Hz}$ ,  $J_{\text{C-P}} = 4\text{ Hz}$ , C-F), 121.3 (td,  $J_{\text{C-P}} = 18\text{ Hz}$ ,  $J_{\text{C-F}} = 4\text{ Hz}$ , C-P), 120.5 (td,  $J_{\text{C-P}} = 18\text{ Hz}$ ,  $J_{\text{C-F}} = 4\text{ Hz}$ , C-P), 119.2 - 118.0 (overlapping peaks, C-Ar), 116.2 (m, C-Ar), 115.4 (m, C-Ar), 27.5 (vt,  $J_{\text{C-P}} = 11\text{ Hz}$ ,  $\text{PCHMe}_2$ ), 24.5 (vt,  $J_{\text{C-P}} = 11\text{ Hz}$ ,  $\text{PCHMe}_2$ ), 20.1 ( $\text{PCHMe}_2$ ), 18.9 ( $\text{PCHMe}_2$ ), 18.6 ( $\text{PCHMe}_2$ ), 17.4 ( $\text{PCHMe}_2$ ).  $^{19}\text{F}$  NMR ( $\text{C}_6\text{D}_6$ ) (**Figure II.19**):  $\delta$  -129.1 (2F), -130.5 (2F).  $^{31}\text{P}\{^1\text{H}\}$  NMR ( $\text{C}_6\text{D}_6$ ) (**Figure II.18**):  $\delta$  51.3 (2P), 33.8 (2P). Anal. Calcd. for  $\text{C}_{49}\text{H}_{68}\text{F}_4\text{N}_2\text{P}_4\text{Pd}_2\text{S}_2$ : C, 50.65; H, 5.90; N, 2.41. Found: C, 50.58; H, 5.80; N, 2.37.

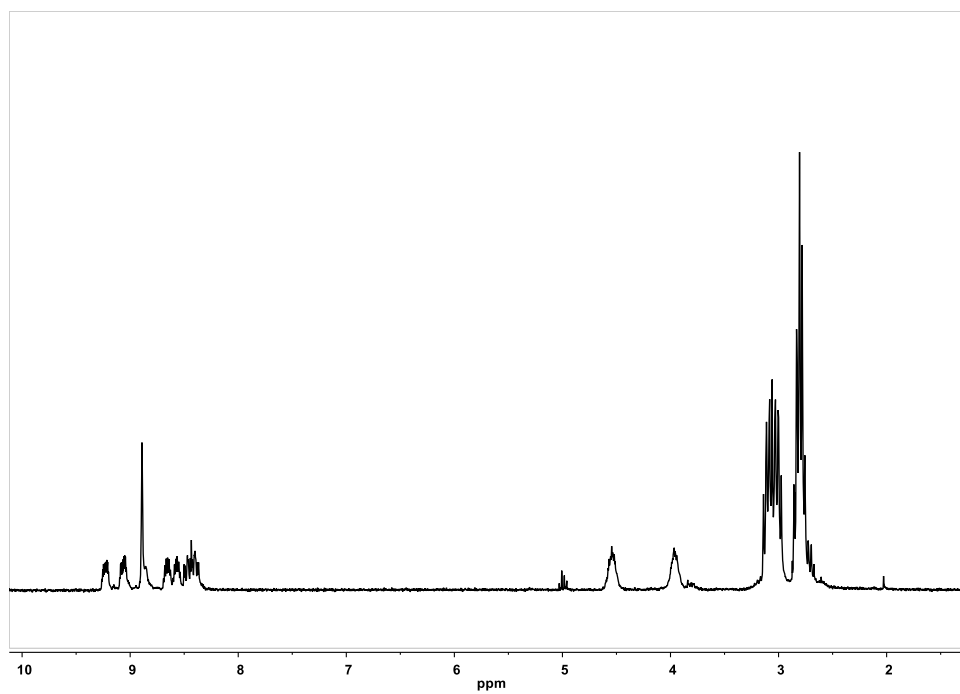


**Figure II.17** <sup>1</sup>H NMR (300 MHz, C<sub>6</sub>D<sub>6</sub>) spectrum of (F)PNP)Pd-C(S)S-Pd(PNP)F (**203**) (minute impurities of Et<sub>2</sub>O)

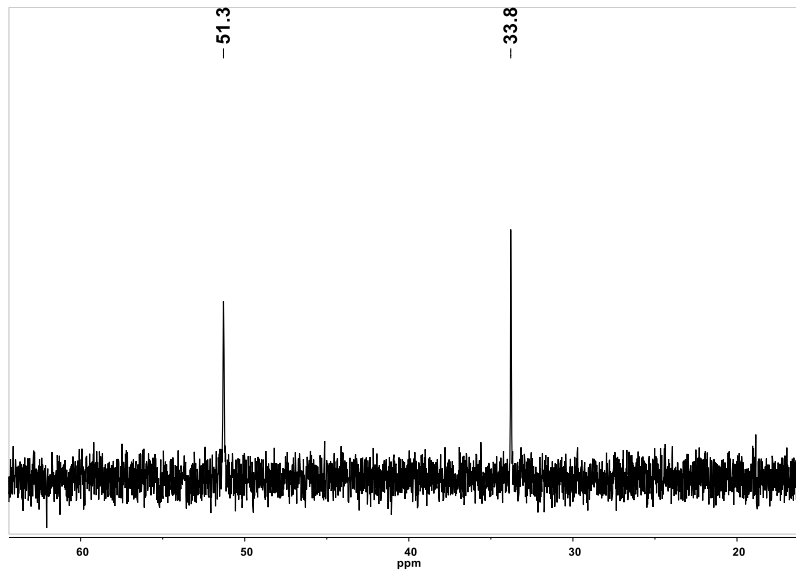


**Figure II.18** <sup>31</sup>P{<sup>1</sup>H} (300 MHz, C<sub>6</sub>D<sub>6</sub>) NMR spectrum of (F)PNP)Pd-C(S)S-Pd(PNP)F (**203**)

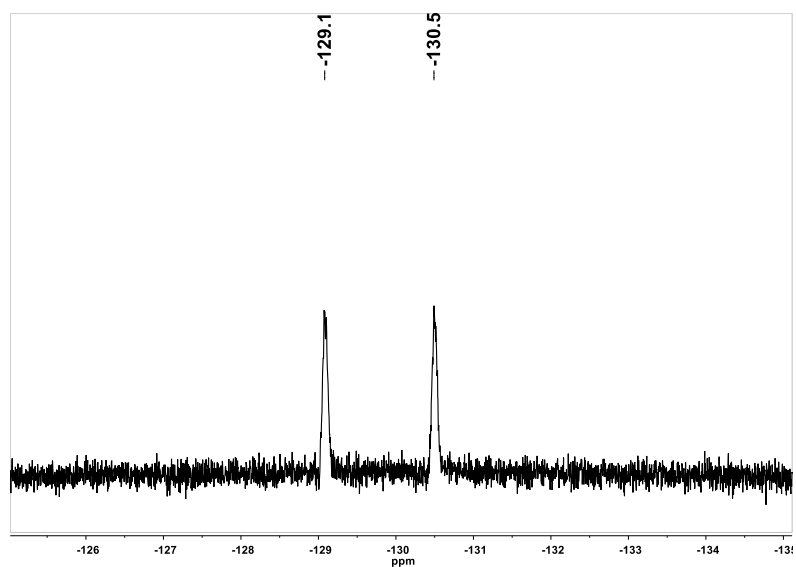


**Figure II.19**  $^{19}\text{F}$  NMR (300 MHz,  $\text{C}_6\text{D}_6$ ) spectrum of  $(^{\text{F}}\text{PNP})\text{Pd-C(S)S-Pd(PNP}^{\text{F}})$  (**203**)

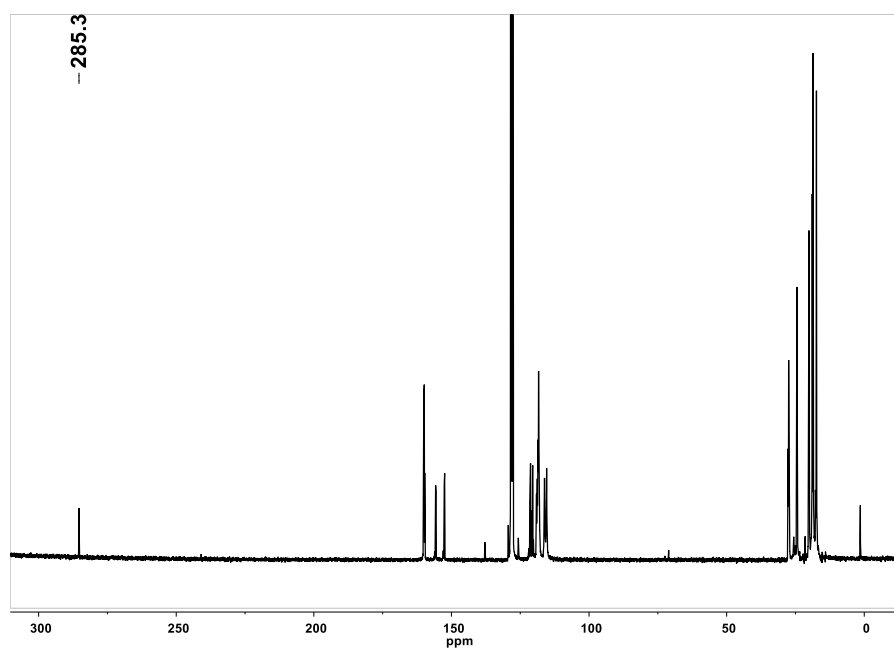


**Figure II.20**  $^{13}\text{C}\{^1\text{H}\}$  (300 MHz,  $\text{C}_6\text{D}_6$ ) NMR spectrum of  $(^{\text{F}}\text{PNP})\text{Pd-C(S)S-Pd(PNP}^{\text{F}})$  (**203**) (Pd- $\text{CS}_2$ -Pd resonates at 285.3 ppm)

**Reaction of  $[(^{\text{F}}\text{PNP})\text{Pd}]_2$  (**201**) with  $\text{CS}_2$  at RT in the absence of light.**  $[(^{\text{F}}\text{PNP})\text{Pd}]_2$  (**201**) (13.4 mg, 12.1  $\mu\text{mol}$ ) was dissolved in  $\text{C}_6\text{D}_6$  ca. 2 mL in a J. Young NMR tube. To



this, CS<sub>2</sub> (1.3 μL, 1.7 mg, 22 μmol) was added using a syringe. The NMR tube was then left at room temperature covered by aluminum foil to prevent interaction with light. 75% conversion into the CS<sub>2</sub> bridged dimer, (<sup>F</sup>PNP)Pd-C(S)S-Pd(PNP<sup>F</sup>) (**203**) was observed after 2 days on analysis of the sample by <sup>31</sup>P and <sup>19</sup>F NMR spectroscopy. No further conversion was observed even after 7 days.

**Reaction of [(<sup>F</sup>PNP)Pd]<sub>2</sub> (**201**) with CS<sub>2</sub> at 80 °C in the absence of light.**

[(<sup>F</sup>PNP)Pd]<sub>2</sub> (**201**) (13.4 mg, 12.1 μmol) was dissolved in C<sub>6</sub>D<sub>6</sub> ca. 2 mL in a J. Young NMR tube. To this, CS<sub>2</sub> (1.3 μL, 1.7 mg, 22 μmol) was added using a syringe. The NMR tube was then placed in an oil bath at 80 °C and covered by aluminum foil to prevent interaction with light. Complete conversion into the CS<sub>2</sub> bridged dimer was observed after 12 h by analysis of the reaction mixture <sup>31</sup>P and <sup>19</sup>F NMR spectroscopy.

**Reaction of (<sup>F</sup>PNP)Pd-C(S)S-Pd(PNP<sup>F</sup>) (**203**) with Me<sub>3</sub>SiOTf.** (<sup>F</sup>PNP)Pd-C(S)S-Pd(PNP<sup>F</sup>) (**203**) (20 mg, 17 μmol) was placed in a J. Young NMR tube and dissolved in ca. 600 μL of C<sub>6</sub>D<sub>6</sub>. To this Me<sub>3</sub>SiOTf (6.2 μL, 7.6 mg, 34 μmol) was added using a syringe. The J. Young tube was then placed in an oil bath at 80 °C and the reaction was monitored by <sup>31</sup>P and <sup>19</sup>F NMR spectroscopy. No changes were observed after 18 h by analysis of the sample by <sup>31</sup>P and <sup>19</sup>F NMR spectroscopy.

**Reaction of (<sup>F</sup>PNP)Pd-C(S)S-Pd(PNP<sup>F</sup>) (**203**) with Me<sub>3</sub>SiCl.** (<sup>F</sup>PNP)Pd-C(S)S-Pd(PNP<sup>F</sup>) (**203**) (20 mg, 17 μmol) was placed in a J. Young NMR tube and dissolved in ca. 600 μL of C<sub>6</sub>D<sub>6</sub>. To this, Me<sub>3</sub>SiCl (4.5 μL, 3.8 mg, 34 μmol) was added using a syringe. The J. Young tube was then placed in an oil bath at 80 °C and the reaction was monitored

by  $^{31}\text{P}$  and  $^{19}\text{F}$  NMR spectroscopy. No changes were observed after 18 h by analysis of the sample by  $^{31}\text{P}$  and  $^{19}\text{F}$  NMR spectroscopy.

#### 2.4.8. Characterization of $(^{\text{Me}}\text{PNP})\text{Ir}(\text{H})(\text{Ph})\text{CO}$ (**208**)

**Synthesis of  $(^{\text{Me}}\text{PNP})\text{Ir}(\text{H})(\text{Ph})\text{CO}$  (**208**)**.  $(^{\text{Me}}\text{PNP})\text{Ir}(\text{H})(\text{Mes})$  (**206**) (100 mg, 134  $\mu\text{mol}$ ) was dissolved in benzene ca. 5 mL in a PTFE lined screw capped flask and heated at 50  $^{\circ}\text{C}$  for an hour and converted to  $(^{\text{Me}}\text{PNP})\text{Ir}(\text{H})(\text{Ph})$  (**207**) by following previously published procedures.<sup>3</sup> The solution was then degassed using three freeze-pump-thaw cycles and CO was then added through a flushed gas line which immediately turned the solution bright yellow. The volatiles were then removed under vacuum yielding a bright yellow powder. Yield: 90 mg (91%)  $^1\text{H}$  NMR ( $\text{C}_6\text{D}_6$ ):  $\delta$  7.96 (br, 2H,  $-\text{C}_6\text{H}_5$ ), 7.68 (dt,  $J = 8$  Hz, 2 Hz, 2H, PNP-aryl  $H$ ), 7.05-6.93 (m, 3H,  $-\text{C}_6\text{H}_5$ ), 6.83 (br, 2H, PNP-aryl  $H$ ), 6.75 (dd,  $J = 8$  Hz, 2 Hz, 2H, PNP-aryl  $H$ ), 2.34-2.17 (m, 4H,  $-\text{CH}(\text{CH}_3)_2$ ), 2.17 (s, 6H, Ar- $\text{CH}_3$ ), 1.10-0.80 (m, 24H,  $-\text{CH}(\text{CH}_3)_2$ ), -6.99 (t,  $^3J_{\text{P-H}} = 18$  Hz, 1H, Ir-H).  $^{13}\text{C}\{^1\text{H}\}$  NMR ( $\text{C}_6\text{D}_6$ ):  $\delta$  180.8 (m, Ir-CO), 161.2 (t,  $J = 8$  Hz), 131.8, 131.0, 128.4, 128.2, 128.0, 124.4 (t,  $J = 5$  Hz), 124.1 (t,  $J = 25$  Hz), 121.5, 115.7 (t,  $J = 5$  Hz), 26.3 (t,  $J = 15$  Hz), 25.7 (t,  $J = 18$  Hz), 20.5, 18.7, 17.7, 17.6, 17.2.  $^{31}\text{P}\{^1\text{H}\}$  NMR ( $\text{C}_6\text{D}_6$ ):  $\delta$  28.0 (s). IR ( $\text{C}_6\text{D}_6$ ,  $\text{cm}^{-1}$ )  $\nu(\text{CO})$ : 2000.

**Synthesis of  $(^{\text{Me}}\text{PNP})\text{Ir}(\text{D})(\text{C}_6\text{D}_5)\text{CO}$  (**208D**)**.  $(^{\text{Me}}\text{PNP})\text{Ir}(\text{H})(\text{Mes})$  (**206**) (10 mg, 13.4  $\mu\text{mol}$ ) was dissolved in  $\text{C}_6\text{D}_6$  ca. 0.5 mL in a J. Young NMR tube and heated at 50  $^{\circ}\text{C}$  for an hour and converted to  $(^{\text{Me}}\text{PNP})\text{Ir}(\text{D})(\text{C}_6\text{D}_5)$  (**207D**) by following previously published procedures.<sup>3</sup> The volatiles were then removed and the obtained solid was re-dissolved in ca. 0.5 mL of  $\text{C}_6\text{D}_6$ . This solution was then degassed using three freeze-pump-

thaw cycles and CO was then added through a flushed gas line. The solution immediately turned yellow.  $^{31}\text{P}$  NMR analysis of the sample confirmed complete conversion to  $(^{\text{Me}}\text{PNP})\text{Ir}(\text{D})(\text{C}_6\text{D}_5)\text{CO}$  (**208D**).  $^1\text{H}$  NMR ( $\text{C}_6\text{D}_6$ ):  $\delta$  7.68 (dt,  $J = 8$  Hz, 2 Hz, 2H, PNP-aryl  $H$ ), 6.83 (br, 2H, PNP-aryl  $H$ ), 6.75 (dd,  $J = 8$  Hz, 2 Hz, 2H, PNP-aryl  $H$ ), 2.34-2.17 (m, 4H,  $-\text{CH}(\text{CH}_3)_2$ ), 2.17 (s, 6H, Ar- $\text{CH}_3$ ), 1.10-0.80 (m, 24H,  $-\text{CH}(\text{CH}_3)_2$ ).  $^{31}\text{P}\{^1\text{H}\}$  NMR ( $\text{C}_6\text{D}_6$ ):  $\delta$  28.0 (s). IR ( $\text{C}_6\text{D}_6$ ,  $\text{cm}^{-1}$ )  $\nu(\text{CO})$ : 2000.

#### 2.4.9. CO trapping experiments

**Reaction of  $[(^{\text{F}}\text{PNP})\text{Pd}]_2$  (**201**) with  $\text{Me}_3\text{SiOTf}$  and  $\text{CO}_2$  and  $(^{\text{Me}}\text{PNP})\text{Ir}(\text{D})(\text{C}_6\text{D}_5)$  (**207D**) as CO trap.**  $(^{\text{Me}}\text{PNP})\text{Ir}(\text{H})(\text{Mes})$  (**206**) (7.0 mg, 9.0  $\mu\text{mol}$ ) was dissolved in ca. 0.4 mL of  $\text{C}_6\text{D}_6$  in a J. Young NMR tube and converted into an equivalent amount of  $(^{\text{Me}}\text{PNP})\text{Ir}(\text{D})(\text{C}_6\text{D}_5)$  (**207D**) upon thermolysis. To this,  $[(^{\text{F}}\text{PNP})\text{Pd}]_2$  (**201**) (10 mg, 9.0  $\mu\text{mol}$ ) and  $(^{\text{F}}\text{PNP})\text{Me}$  (18.0  $\mu\text{mol}$ , 200  $\mu\text{L}$  of 0.09 M stock solution in  $\text{C}_6\text{D}_6$ ) were added.  $\text{Me}_3\text{SiOTf}$  (3.8  $\mu\text{L}$ , 4.7 mg, 21  $\mu\text{mol}$ ) was added to this solution using a syringe. The solution was degassed using three freeze-pump-thaw cycles and  $\text{CO}_2$  was then added through a flushed gas line. The J. Young tube was then placed in an oil bath at 80  $^\circ\text{C}$ . The reaction was periodically monitored by  $^{31}\text{P}$  and  $^{19}\text{F}$  NMR spectroscopy; complete consumption of  $[(^{\text{F}}\text{PNP})\text{Pd}]_2$  was noted after 18 h. 65% trapping of CO was observed by the formation of  $(^{\text{Me}}\text{PNP})\text{Ir}(\text{D})(\text{C}_6\text{D}_5)(\text{CO})$  (**208D**) measured against the internal standard resonance at -6.2 ppm. Other products in the reaction mixture, from the analysis using  $^{31}\text{P}$  and  $^{19}\text{F}$  NMR spectroscopy, corresponded to  $(^{\text{F}}\text{PNP})\text{PdOTf}$  (**205**) (yield = 85%) and unidentified products with resonances at 39.6 ppm and 57.4 ppm in  $^{31}\text{P}$  NMR (**Figure II.21**) and -78.4 ppm in  $^{19}\text{F}$  NMR spectra of the sample. Comparing the  $^1\text{H}$  NMR spectra

of the starting sample and sample after completion shows complete consumption of  $\text{Me}_3\text{SiOTf}$  and conversion into  $(\text{Me}_3\text{Si})_2\text{O}$ .

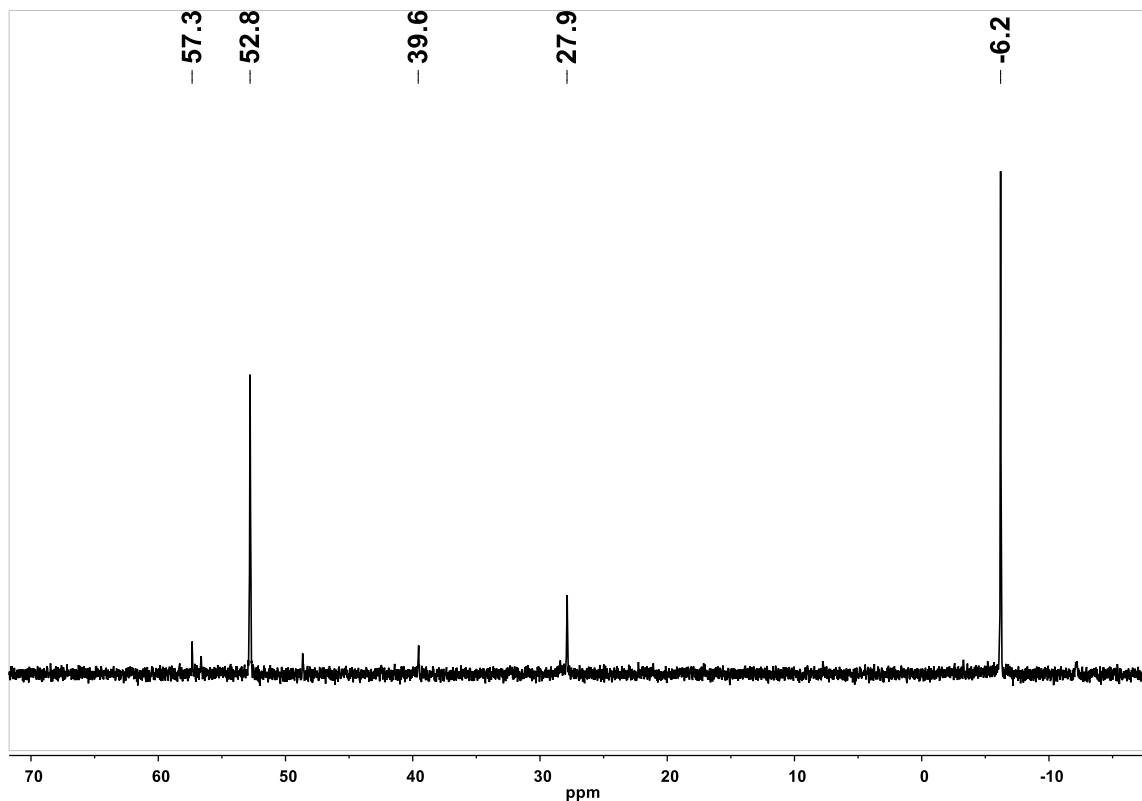


**Figure II.21**  $^{31}\text{P}\{^1\text{H}\}$  (300 MHz,  $\text{C}_6\text{D}_6$ ) NMR spectrum of the reaction of  $[(^{\text{F}}\text{PNP})\text{Pd}]_2$  (**201**) with  $\text{CO}_2$  and  $\text{Me}_3\text{SiOTf}$  and  $(^{\text{Me}}\text{PNP})\text{Ir}(\text{D})(\text{C}_6\text{D}_5)$  (**207D**) as in-situ CO trap after heating for 18 h

**Reaction of  $[(^{\text{F}}\text{PNP})\text{Pd}]_2$  (**201**) with  $\text{Me}_3\text{SiCl}$  and  $\text{CO}_2$  and  $(^{\text{Me}}\text{PNP})\text{Ir}(\text{D})(\text{C}_6\text{D}_5)$  (**207D**) as CO trap.**  $(^{\text{Me}}\text{PNP})\text{Ir}(\text{H})(\text{Mes})$  (**206**) (7.0 mg, 9.0  $\mu\text{mol}$ ) was taken in a J. Young NMR tube in 600  $\mu\text{L}$  of  $\text{C}_6\text{D}_6$ . This NMR tube was placed in an oil bath at 80  $^\circ\text{C}$  and complete conversion of  $(^{\text{Me}}\text{PNP})\text{Ir}(\text{H})(\text{Mes})$  (**206**) to  $(^{\text{Me}}\text{PNP})\text{Ir}(\text{D})(\text{C}_6\text{D}_5)$  (**207D**) was confirmed by the  $^{31}\text{P}\{^1\text{H}\}$  and  $^1\text{H}$  NMR spectrum of the reaction mixture. To this  $(^{\text{F}}\text{PNP})\text{Me}$  (18.0  $\mu\text{mol}$ , 200  $\mu\text{L}$  of 0.09 M stock solution in  $\text{C}_6\text{D}_6$ ) was added using a syringe and separately  $[(^{\text{F}}\text{PNP})\text{Pd}]_2$  (**201**) (10 mg, 9.0  $\mu\text{mol}$ ) was weighed and added.

Me<sub>3</sub>SiCl (2.7 μL, 2.3 mg, 21 μmol) was added to this solution using another syringe. The solution was degassed using three freeze-pump-thaw cycles and CO<sub>2</sub> was then added through a flushed gas line. The J. Young tube was then placed in an oil bath at 80 °C. The reaction was monitored by <sup>31</sup>P{<sup>1</sup>H} and <sup>19</sup>F NMR spectroscopy and complete consumption of [(<sup>F</sup>PNP)Pd-]<sub>2</sub> was observed after heating for 18 h. 45% trapping of CO was observed in <sup>31</sup>P NMR by the formation of (<sup>Me</sup>PNP)Ir(D)(C<sub>6</sub>D<sub>5</sub>)(CO) (**208D**) as measured against the internal standard. Other products in the reaction mixture, from the analysis using <sup>31</sup>P{<sup>1</sup>H} and <sup>19</sup>F NMR spectroscopy, corresponded to (<sup>F</sup>PNP)PdCl (**204**) (70%), (<sup>F</sup>PNP)PdH (30%), unreacted (<sup>Me</sup>PNP)Ir(D)(C<sub>6</sub>D<sub>5</sub>) (**207D**) (50% of the original Ir concentration against the internal standard) (45.7 ppm). Unidentified products (<5% total) were also obtained corresponding to resonances at 59.1, 62.5 and 63.3 ppm in the <sup>31</sup>P{<sup>1</sup>H} (**Figure II.22**) and -119.4 and -124.8 in the <sup>19</sup>F NMR of the reaction mixture. Comparing the <sup>1</sup>H NMR spectra of the starting sample and sample after completion shows unreacted Me<sub>3</sub>SiCl and (Me<sub>3</sub>Si)<sub>2</sub>O and an unidentified resonance at 0.19 ppm).

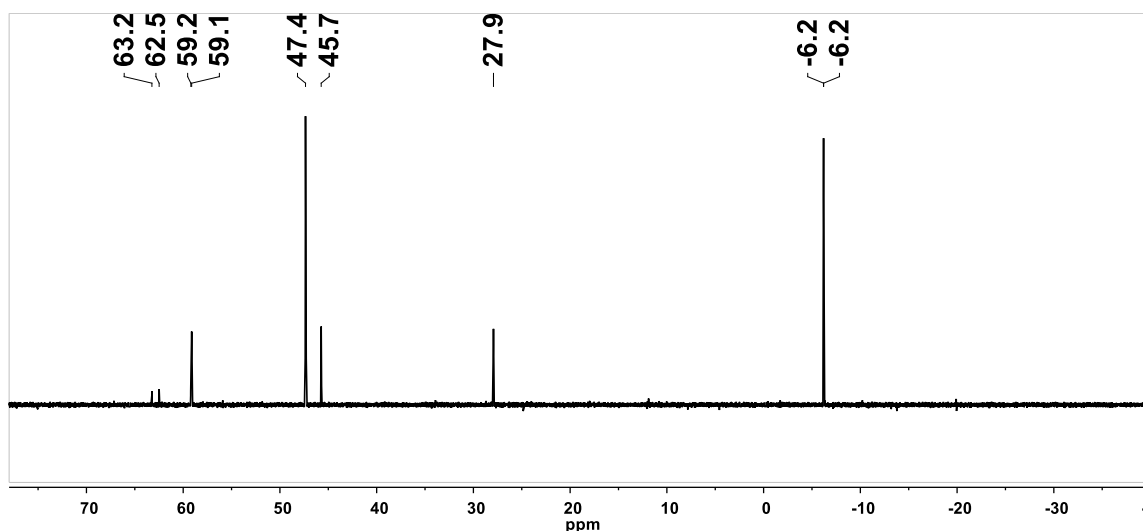


**Figure II.22**  $^{31}\text{P}\{^1\text{H}\}$  (300 MHz,  $\text{C}_6\text{D}_6$ ) NMR spectrum of the reaction of  $[(^{\text{F}}\text{PNP})\text{Pd-}]_2$  (**201**) with  $\text{CO}_2$  and  $\text{Me}_3\text{SiCl}$  and  $(^{\text{Me}}\text{PNP})\text{Ir}(\text{D})(\text{C}_6\text{D}_5)$  (**207D**) as in-situ CO trap after heating for 18 h

**Reaction of  $[(^{\text{F}}\text{PNP})\text{Pd-}]_2$  (**201**) with  $\text{Me}_3\text{SiOTf}$  and  $\text{CO}_2$   $(^{\text{Me}}\text{PNP})\text{Ir}(\text{D})(\text{C}_6\text{D}_5)$  (**207D**) as CO trap without  $(^{\text{F}}\text{PNP})\text{Me}$  as internal standard.**  $(^{\text{Me}}\text{PNP})\text{Ir}(\text{H})(\text{Mes})$  (**206**) (9.0 mg, 12.1  $\mu\text{mol}$ ) was dissolved in ca. 0.6 mL of  $\text{C}_6\text{D}_6$  in a J. Young NMR tube and converted into an equivalent amount of  $(^{\text{Me}}\text{PNP})\text{Ir}(\text{D})(\text{C}_6\text{D}_5)$  (**207D**) upon thermolysis. To this,  $[(^{\text{F}}\text{PNP})\text{Pd-}]_2$  (**201**) (13.4 mg, 12.1  $\mu\text{mol}$ ) was added.  $\text{Me}_3\text{SiOTf}$  (4.8  $\mu\text{L}$ , 6.0 mg, 26.7  $\mu\text{mol}$ ) was added to this solution using a syringe. The solution was degassed using three freeze-pump-thaw cycles and  $\text{CO}_2$  was then added through a flushed gas line. The J. Young tube was then placed in an oil bath at 80  $^\circ\text{C}$ . The reaction was periodically monitored by  $^{31}\text{P}$  and  $^{19}\text{F}$  NMR spectroscopy; complete consumption of  $[(^{\text{F}}\text{PNP})\text{Pd-}]_2$  was noted after 18 h. 50% trapping of CO was observed by the formation of  $(^{\text{Me}}\text{PNP})\text{Ir}(\text{D})(\text{C}_6\text{D}_5)(\text{CO})$  (**208D**). Other products in the reaction mixture, from the analysis using  $^{31}\text{P}$  and  $^{19}\text{F}$  NMR spectroscopy, corresponded to  $(^{\text{F}}\text{PNP})\text{PdOTf}$  (**205**) (yield

= 90%) and an unidentified product with resonances at 57.4 ppm in  $^{31}\text{P}$  NMR and -78.5 ppm in  $^{19}\text{F}$  NMR spectra of the sample.

#### 2.4.10. Control reactions

**Reaction of  $[(^{\text{F}}\text{PNP})\text{Pd}]_2$  (201) with CO.**  $[(^{\text{F}}\text{PNP})\text{Pd}]_2$  (201) (13.4 mg, 12.1  $\mu\text{mol}$ ) was dissolved in  $\text{C}_6\text{D}_6$  ca. 2 mL in a J. Young NMR tube. To this,  $(^{\text{F}}\text{PNP})\text{Me}$  (26.6  $\mu\text{L}$  of 0.453M stock solution in  $\text{C}_6\text{D}_6$ , 12.1  $\mu\text{mol}$ ) was added as an internal standard. The solution was degassed using 3 freeze-pump-thaw cycles, and CO was added to it through a flushed gas line. The J. Young tube was then placed in an oil bath at 70  $^{\circ}\text{C}$ . Two resonances apart from the internal standard were observed after 24 h in both  $^{19}\text{F}$  NMR (2:3, -123.6 ppm: -130.1 ppm) and  $^{31}\text{P}\{^1\text{H}\}$  NMR (2:3, 12.3 ppm (s) : 33.5 ppm (br))

**Reaction of  $[(^{\text{F}}\text{PNP})\text{Pd}]_2$  (201) with  $\text{Me}_3\text{SiOTf}$ .**  $[(^{\text{F}}\text{PNP})\text{Pd}]_2$  (201) (13.4 mg, 12.1  $\mu\text{mol}$ ) was dissolved in  $\text{C}_6\text{D}_6$  ca. 2 mL in a J. Young NMR tube. To this,  $(^{\text{F}}\text{PNP})\text{Me}$  (26.6  $\mu\text{L}$  of 0.453M stock solution in  $\text{C}_6\text{D}_6$ , 12.1  $\mu\text{mol}$ ) was added as an internal standard.  $\text{Me}_3\text{SiOTf}$  (4.6  $\mu\text{L}$ , 5.6 mg, 25.4  $\mu\text{mol}$ ) was then added to this solution using a syringe. The NMR tube was then placed in an oil bath at 80  $^{\circ}\text{C}$ . No reaction was observed after 18 h of heating.

**Reaction of  $[(^{\text{F}}\text{PNP})\text{Pd}]_2$  (201) with  $\text{Me}_3\text{SiCl}$ .**  $[(^{\text{F}}\text{PNP})\text{Pd}]_2$  (201) (13.4 mg, 12.1  $\mu\text{mol}$ ) was dissolved in  $\text{C}_6\text{D}_6$  ca. 2 mL in a J. Young NMR tube. To this,  $(^{\text{F}}\text{PNP})\text{Me}$  (26.6  $\mu\text{L}$  of 0.453M stock solution in  $\text{C}_6\text{D}_6$ , 12.1  $\mu\text{mol}$ ) was added as an internal standard.  $\text{Me}_3\text{SiCl}$  (4.0  $\mu\text{L}$ , 3.5 mg, 31.5  $\mu\text{mol}$ ) was then added to this solution using a syringe. The NMR tube was then placed in an oil bath at 80  $^{\circ}\text{C}$ . No reaction was observed after 24 h of heating.

**Reaction of [(<sup>F</sup>PNP)Pd-]<sub>2</sub> (201) with Me<sub>3</sub>SiOTf and CO.** [(<sup>F</sup>PNP)Pd-]<sub>2</sub> (**201**) (13.4 mg, 12.1 μmol) was dissolved in C<sub>6</sub>D<sub>6</sub> ca. 2 mL in a J. Young NMR tube. To this, (<sup>F</sup>PNP)Me (26.6 μL of 0.453M stock solution in C<sub>6</sub>D<sub>6</sub>, 12.1 μmol) was added as an internal standard. Me<sub>3</sub>SiOTf (4.6 μL, 5.6 mg, 25.4 μmol) was then added to this solution using a syringe. The solution was degassed using 3 freeze-pump-thaw cycles, and CO was added to it through a flushed gas line. The J. Young tube was then placed in an oil bath at 80 °C. Analysis of the reaction mixture by <sup>31</sup>P NMR spectroscopy after 12 h showed conversion to (<sup>F</sup>PNP)PdH (6%) and unidentified compounds which resonated at 14.6 ppm (12%), 33.2 ppm (60%), 59.1 ppm, 75.4 ppm (6%). <sup>19</sup>F NMR analysis of the same sample shows unidentified resonances at -123.6 ppm, -125.5 and -130.1 ppm in addition to the internal standard signal the resonance for (<sup>F</sup>PNP)PdH and the resonance for Me<sub>3</sub>SiOTf at -78.7 ppm. None of these unidentified resonances are observed in the analogous reaction of [(<sup>F</sup>PNP)Pd-]<sub>2</sub> with Me<sub>3</sub>SiOTf and CO<sub>2</sub>.

**Reaction of [(<sup>F</sup>PNP)Pd-]<sub>2</sub> (201) with Me<sub>3</sub>SiCl and CO.** [(<sup>F</sup>PNP)Pd-]<sub>2</sub> (**201**) (13.4 mg, 12.1 μmol) was dissolved in C<sub>6</sub>D<sub>6</sub> ca. 2 mL in a J. Young NMR tube. To this, (<sup>F</sup>PNP)Me (26.6 μL of 0.453M stock solution in C<sub>6</sub>D<sub>6</sub>, 12.1 μmol) was added as an internal standard. Me<sub>3</sub>SiCl (3.2 μL, 2.7 mg, 25.4 μmol) was then added to this solution using a syringe. The solution was degassed using 3 freeze-pump-thaw cycles, and CO was added to it through a flushed gas line. The J. Young tube was then placed in an oil bath at 80 °C. Analysis of the reaction mixture by <sup>31</sup>P NMR spectroscopy after 12 h showed conversion to an unidentified compound which resonated at 33.5 ppm (90%) and (<sup>F</sup>PNP)PdCl (**204**) (10%) . <sup>19</sup>F NMR analysis of the same sample shows an unidentified product



corresponding to the resonance at -130.1 ppm in addition to the internal standard signal and the resonance for (<sup>F</sup>PNP)PdCl (**204**) (-128.6 ppm). None of the unidentified resonances are observed in the analogous reaction of [(<sup>F</sup>PNP)Pd-]<sub>2</sub> with Me<sub>3</sub>SiCl and CO<sub>2</sub>.

**Preparation of a solution of (<sup>Me</sup>PNP)Ir(D)(C<sub>6</sub>D<sub>5</sub>) (**207D**) and (<sup>F</sup>PNP)Me in C<sub>6</sub>D<sub>6</sub>.**

For the control reactions with (<sup>Me</sup>PNP)Ir(D)(C<sub>6</sub>D<sub>5</sub>) listed below, a solution of (<sup>Me</sup>PNP)Ir(D)(C<sub>6</sub>D<sub>5</sub>) (**207D**) and (<sup>F</sup>PNP)Me in C<sub>6</sub>D<sub>6</sub> was prepared by dissolving (<sup>Me</sup>PNP)Ir(H)(Mes) (**206**) (9 mg, 12.1 μmol) in ca. 800 μL of C<sub>6</sub>D<sub>6</sub> in a J. Young NMR tube and adding to this (<sup>F</sup>PNP)Me (26.6 μL of 0.453M stock solution in C<sub>6</sub>D<sub>6</sub>, 12.1 μmol) using a syringe. The NMR tube was then placed in an oil bath at 80 °C to convert the (<sup>Me</sup>PNP)Ir(H)(Mes) into (<sup>Me</sup>PNP)Ir(D)(C<sub>6</sub>D<sub>5</sub>) according to previously published procedures.<sup>3</sup> Conversion to (<sup>Me</sup>PNP)Ir(D)(C<sub>6</sub>D<sub>5</sub>) was confirmed by <sup>31</sup>P and <sup>1</sup>H NMR spectroscopy before doing any subsequent reactions.

**Reaction of (<sup>Me</sup>PNP)Ir(D)(C<sub>6</sub>D<sub>5</sub>) (**207D**) with Me<sub>3</sub>SiOTf .** Me<sub>3</sub>SiOTf (4.6 μL, 5.6 mg, 25.4 μmol) was added using a syringe to a solution of (<sup>Me</sup>PNP)Ir(D)(C<sub>6</sub>D<sub>5</sub>) (**207D**) and (<sup>F</sup>PNP)Me in C<sub>6</sub>D<sub>6</sub> which was prepared as mentioned above. The J. Young tube was then placed in an oil bath at 80 °C. Analysis of the reaction mixture by <sup>31</sup>P NMR spectroscopy after 24 h showed no reaction.

**Reaction of (<sup>Me</sup>PNP)Ir(D)(C<sub>6</sub>D<sub>5</sub>) (**207D**) with Me<sub>3</sub>SiCl.** Me<sub>3</sub>SiCl (3.2 μL, 2.7 mg, 25.4 μmol) was added using a syringe to a solution of (<sup>Me</sup>PNP)Ir(D)(C<sub>6</sub>D<sub>5</sub>) (**207D**) and (<sup>F</sup>PNP)Me in C<sub>6</sub>D<sub>6</sub>, which was prepared as mentioned above. The J. Young tube was then placed in an oil bath at 80 °C. Analysis of the reaction mixture by <sup>31</sup>P NMR spectroscopy after 24 h showed no reaction.

**Reaction of  $(^{\text{Me}}\text{PNP})\text{Ir}(\text{D})(\text{C}_6\text{D}_5)$  (207D) with  $\text{Me}_3\text{SiOTf}$  and CO.**  $\text{Me}_3\text{SiOTf}$  (4.6  $\mu\text{L}$ , 5.6 mg, 25.4  $\mu\text{mol}$ ) was added using a syringe to a solution of  $(^{\text{Me}}\text{PNP})\text{Ir}(\text{D})(\text{C}_6\text{D}_5)$  and  $(^{\text{F}}\text{PNP})\text{Me}$  in  $\text{C}_6\text{D}_6$  which was prepared as mentioned above. The solution was degassed using 3 freeze-pump-thaw cycles, and CO was added to it through a flushed gas line. The J. Young tube was then placed in an oil bath at 80 °C.  $^{31}\text{P}$  NMR spectrum of the reaction mixture after 24 h showed only a resonance at  $\delta$  28.0 ppm corresponding to  $(^{\text{Me}}\text{PNP})\text{Ir}(\text{D})(\text{C}_6\text{D}_5)(\text{CO})$  (208D) in addition to the internal standard signal.

**Reaction of  $(^{\text{Me}}\text{PNP})\text{Ir}(\text{D})(\text{C}_6\text{D}_5)$  (207D) with  $\text{Me}_3\text{SiCl}$  and CO.**  $\text{Me}_3\text{SiCl}$  (6.4  $\mu\text{L}$ , 5.4 mg, 50.8  $\mu\text{mol}$ ) was added using a syringe to a solution of  $(^{\text{Me}}\text{PNP})\text{Ir}(\text{D})(\text{C}_6\text{D}_5)$  (207D) and  $(^{\text{F}}\text{PNP})\text{Me}$  in  $\text{C}_6\text{D}_6$  which was prepared as mentioned above.. The solution was degassed using 3 freeze-pump-thaw cycles and CO was added through a flushed gas line. The J. Young tube was then placed in an oil bath at 80 °C.  $^{31}\text{P}$  NMR spectrum of the reaction mixture after 24 h showed only a resonance at  $\delta$  27.9 ppm corresponding to  $(^{\text{Me}}\text{PNP})\text{Ir}(\text{D})(\text{C}_6\text{D}_5)\text{CO}$  (208D) in addition to the internal standard signal.

**Reaction of  $(^{\text{Me}}\text{PNP})\text{Ir}(\text{D})(\text{C}_6\text{D}_5)$  (207D) with  $\text{Me}_3\text{SiOTf}$  and  $\text{CO}_2$ .**  $\text{Me}_3\text{SiOTf}$  (4.6  $\mu\text{L}$ , 5.4 mg, 25.4  $\mu\text{mol}$ ) was added using a syringe to a solution of  $(^{\text{Me}}\text{PNP})\text{Ir}(\text{D})(\text{C}_6\text{D}_5)$  (207D) and  $(^{\text{F}}\text{PNP})\text{Me}$  in  $\text{C}_6\text{D}_6$  which was prepared as mentioned above.. The solution was degassed using 3 freeze-pump-thaw cycles and  $\text{CO}_2$  was added through a flushed gas line. The J. Young tube was then placed in an oil bath at 80 °C.  $^{31}\text{P}$  NMR spectrum of the reaction mixture after 24 h shows only one discernible resonance corresponding to  $(^{\text{Me}}\text{PNP})\text{Ir}(\text{D})(\text{C}_6\text{D}_5)$  with intensity corresponding to 40% of the original with some solid observed to be crashing out.

**Reaction of  $(^{\text{Me}}\text{PNP})\text{Ir}(\text{D})(\text{C}_6\text{D}_5)$  (**207D**) with  $\text{Me}_3\text{SiCl}$  and  $\text{CO}_2$ .**  $\text{Me}_3\text{SiCl}$  (3.2  $\mu\text{L}$ , 2.7 mg, 25.4  $\mu\text{mol}$ ) was added using a syringe to a solution of  $(^{\text{Me}}\text{PNP})\text{Ir}(\text{D})(\text{C}_6\text{D}_5)$  (**207D**) and  $(^{\text{F}}\text{PNP})\text{Me}$  in  $\text{C}_6\text{D}_6$  which was prepared as mentioned above. The solution was degassed using 3 freeze-pump-thaw cycles and  $\text{CO}_2$  was added through a flushed gas line. The J. Young tube was then placed in an oil bath at 80  $^\circ\text{C}$ . The solution slowly turned green from the original dark blue. Analysis of the reaction mixture by  $^{31}\text{P}$  NMR spectroscopy after 1 h shows 50% conversion to an unknown compound which resonated at 22.9 ppm. On letting the reaction continue, a  $^{31}\text{P}$  NMR spectrum of the reaction mixture after 18 h showed unidentified resonances at 45.1 ppm, 26.8 ppm and 22.9 ppm (4:3:1) in addition to the internal standard signal.

**Reaction of  $(^{\text{F}}\text{PNP})\text{PdH}$  with  $\text{CO}_2$ .**  $(^{\text{F}}\text{PNP})\text{PdH}$  (14.0 mg, 25.1  $\mu\text{mol}$ ) was dissolved in  $\text{C}_6\text{D}_6$  ca. 2 mL in a J. Young NMR tube. The solution was then degassed using 3 freeze-pump-thaw cycles and  $\text{CO}_2$  was then added through a flushed gas line. The J. Young tube was then left in an oil bath at 80  $^\circ\text{C}$ . The reaction was monitored by  $^{31}\text{P}$  NMR spectroscopy and no reaction was observed after 24 h.

#### *2.4.11. Synthesis of $(^{\text{F}}\text{PNP})\text{Pd-SiMe}_3$ (**210**) and its reactions*

**Reaction of  $(^{\text{F}}\text{PNP})\text{PdCl}$  (**204**) with  $\text{Me}_3\text{Si-SiMe}_3$  and  $\text{KO}^t\text{Bu}$ .**  $(^{\text{F}}\text{PNP})\text{PdCl}$  (**204**) (130 mg, 225  $\mu\text{mol}$ ) and  $\text{KO}^t\text{Bu}$  (30 mg, 267  $\mu\text{mol}$ ) were dissolved in 1,4-dioxane ca. 1 mL in a J. Young NMR tube. To this,  $\text{Me}_3\text{Si-SiMe}_3$  (100  $\mu\text{L}$ , 71.5 mg, 490  $\mu\text{mol}$ ) was added using a syringe and the J. Young tube was then placed in an oil bath at 80  $^\circ\text{C}$ . The reaction was monitored by  $^{31}\text{P}$  NMR spectroscopy. 50% conversion of  $(^{\text{F}}\text{PNP})\text{PdCl}$  (**204**) to a mixture of products was observed after 45 mins with the reaction not proceeding any

further even on extended heating. A further equivalent of KO<sup>t</sup>Bu (30 mg, 267 μmol) was added and the NMR tube was replaced in the oil bath. Complete conversion of (<sup>F</sup>PNP)PdCl (**204**) was observed after 45 mins of further heating. The volatiles were removed under vacuum and the solid mixture was redissolved in pentane ca. 10 mL and filtered through a pad of celite. The filtrate was collected and a red solid (50 mg) was obtained on removing the volatiles. The product was a mixture of (<sup>F</sup>PNP)Pd-SiMe<sub>3</sub> (**210**) (63%), (<sup>F</sup>PNP)PdH (20%) and the rest was unknown compounds. <sup>1</sup>H NMR (C<sub>6</sub>D<sub>6</sub>) (only peaks corresponding to (<sup>F</sup>PNP)Pd-SiMe<sub>3</sub> (**210**) are being reported) <sup>1</sup>H NMR (C<sub>6</sub>D<sub>6</sub>) δ 7.54-7.48 (m, 2H, Ar-*H*), 6.92-6.70 (m, 4H, Ar-*H*, overlapping with peaks from impurities), 2.18 (m, 4H, PCH(CH<sub>3</sub>)<sub>2</sub>, overlapping with peaks from impurities), 1.10-0.90 (m, 24 H, PCH(CH<sub>3</sub>)<sub>2</sub>, overlapping with peaks from impurities), 0.52 (s, 9 H, Si(CH<sub>3</sub>)<sub>3</sub>). <sup>19</sup>F NMR (C<sub>6</sub>D<sub>6</sub>): δ -131.4. <sup>31</sup>P{<sup>1</sup>H}NMR (C<sub>6</sub>D<sub>6</sub>): δ 46.2. <sup>29</sup>Si{<sup>1</sup>H}NMR (C<sub>6</sub>D<sub>6</sub>): δ 3.77 (t, <sup>2</sup>J<sub>Si-P</sub> = 6 Hz, Pd-Si).

**Reaction of (<sup>F</sup>PNP)PdCl (**204**) with Mg and Me<sub>3</sub>SiCl.** (<sup>F</sup>PNP)PdCl (**204**) (50.2 mg, 87.1 μmol), Mg powder (10.1 mg, 417 μmol) were taken in a 25 mL schlenck flask and ca. 5 mL of THF were added to dissolve the solids. To this rapidly stirring solution, Me<sub>3</sub>SiCl (76.0 μL, 65.1 mg, 599 μmol) was added using a syringe. An aliquot of this solution was taken after an hour and analyzed using <sup>31</sup>P and <sup>19</sup>F NMR spectroscopy and complete conversion of (<sup>F</sup>PNP)PdCl (**204**) was observed after 1 h. The <sup>31</sup>P NMR spectrum of the reaction mixture showed (<sup>F</sup>PNP)PdH (7%) at 60.2 ppm, [(<sup>F</sup>PNP)Pd-]<sub>2</sub> (**201**) (33%) at 47.3 ppm and (<sup>F</sup>PNP)Pd-SiMe<sub>3</sub> (**210**) (60%) was observed at 47.0 ppm. The <sup>19</sup>F NMR spectrum of the reaction mixture showed only 2 peaks, one corresponding to overlapping

peaks for  $(^F\text{PNP})\text{PdH}$  (7%) and  $[(^F\text{PNP})\text{Pd}]_2$  (**201**) (33%) at -132.0 ppm and another one for  $(^F\text{PNP})\text{Pd-SiMe}_3$  (**210**) (60%) was observed at -132.1 ppm.

**Reaction of  $(^F\text{PNP})\text{PdCl}$  (**204**) with  $\text{KO}^t\text{Bu}$ .**  $(^F\text{PNP})\text{PdCl}$  (**204**) (57.1 mg, 100  $\mu\text{mol}$ ) and  $\text{KO}^t\text{Bu}$  (23 mg, 205  $\mu\text{mol}$ ) were dissolved in 1,4-dioxane ca. 500  $\mu\text{L}$  in a J. Young NMR tube and the tube was then placed in an oil bath at 80  $^\circ\text{C}$ . The reaction was monitored by  $^{31}\text{P}$  NMR spectroscopy. Complete conversion of  $(^F\text{PNP})\text{PdCl}$  (**204**) to  $(^F\text{PNP})\text{PdH}$  (24%) at 60.2 ppm,  $[(^F\text{PNP})\text{Pd}]_2$  (**201**) (58%) at 47.5 ppm and an unknown compounds (11% and 7%) at 46.4 ppm and 40.7 ppm respectively, was observed after 1 h with no observation of  $(^F\text{PNP})\text{Pd-SiMe}_3$  (**210**) being produced.

**Reaction of  $(^F\text{PNP})\text{Pd-SiMe}_3$  (**210**) with  $(^F\text{PNP})\text{PdCl}$  (**204**).**  $(^F\text{PNP})\text{PdCl}$  (**204**) (10 mg, 17.3  $\mu\text{mol}$ ) and the mixture of products obtained in the synthesis of  $(^F\text{PNP})\text{Pd-SiMe}_3$  (**210**) (13.1 mg, 17.3  $\mu\text{mol}$  in Si) were taken in a J. Young tube and dissolved in ca. 600  $\mu\text{L}$  of  $\text{C}_6\text{D}_6$ . The NMR tube was then placed in an oil bath at 80  $^\circ\text{C}$  and the reaction was monitored by  $^{31}\text{P}$  and  $^{19}\text{F}$  NMR spectroscopy. No changes were observed after 18 h by  $^{31}\text{P}$  and  $^{19}\text{F}$  NMR spectroscopy of the sample.

**Reaction of  $(^F\text{PNP})\text{Pd-SiMe}_3$  (**210**) with  $\text{CO}_2$ .** The mixture of products obtained in the synthesis of  $(^F\text{PNP})\text{Pd-SiMe}_3$  (**210**) (13.1 mg, 17.3  $\mu\text{mol}$  in Si) was taken in a J. Young tube and dissolved in ca. 600  $\mu\text{L}$  of  $\text{C}_6\text{D}_6$ . The solution was degassed using 3 freeze-pump-thaw cycles and  $\text{CO}_2$  was added through a flushed gas line. The NMR tube was then placed in an oil bath at 80  $^\circ\text{C}$  and the reaction was monitored by  $^{31}\text{P}$  and  $^{19}\text{F}$  NMR spectroscopy. No changes were observed after 18 h by  $^{31}\text{P}$  and  $^{19}\text{F}$  NMR spectroscopy of the sample.

## CHAPTER III

### POCOP COBALT COMPLEXES RELEVANT TO CATALYTIC COUPLING AND REDUCTIVE ELIMINATION STUDIES

#### 3.1. Introduction

Transition metal mediated coupling reactions have become an irreplaceable part of a chemist's repertoire due to their ever increasing scope and applicability. However, it is an interesting issue how majority of these coupling reactions use palladium<sup>48,53,151-153</sup>. Expansion of this chemistry to include other cheaper and more abundant metals is a task that deserves to be undertaken.<sup>154-160</sup> Although transition metal mediated catalysis involving one-electron transformations in some catalytic steps have been observed,<sup>161,162</sup> majority of the most versatile and popular catalytic reactions involve two electron reactivity at the metal centre. From the mechanisms of such metal catalyzed coupling reactions, two electron activity is vital for the bond-breaking (cleavage of bonds of the type R-X (X = halide) and formation of M-R and M-X bonds) (oxidative addition) and bond-making (cleavage of bonds of the type M-R and M-R' and formation of R-R' bonds) (reductive elimination) steps in the catalytic cycle (**Figure III.1**).

We have recently highlighted the ability of (POCOP)Rh complexes to catalyze coupling reactions.<sup>83,114</sup> As discussed previously in chapter I, catalysis using Rh involves interconversion between Rh(I) and Rh(III) during the catalytic cycle. An analogous cycle can also be imagined for cobalt where it switches between Co(I) and Co(III) through OA and RE steps. If such a cycle is proved to be feasible and robust, cobalt is an important and viable alternative due to it being more abundant and cheap as compared to Rh. So our

steps will be focused towards isolating the proposed intermediates with Co(I) and Co(III) and investigate the viability of a catalytic cycle involving these intermediates. Coupling reactions with a Co<sup>I</sup>/Co<sup>III</sup> type cycle similar to Rh however, might be hindered by the proclivity of cobalt to undergo one-electron transformations. To prevent such undesired one-electron side reactions, the choice of ancillary ligands might play an important role in stabilizing the Co(I) and Co(III) oxidation states, so we expect ligand optimization to prevent one-electron transformations as another important undertaking.

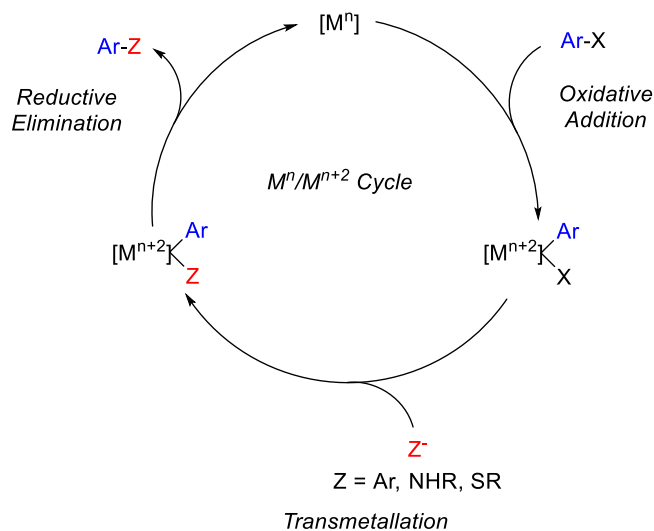


**Figure III.1** General  $M^n/M^{n+2}$  for transition metal catalyzed coupling reactions between aryl halides with nucleophiles.

Looking into the history of cobalt based catalytic cross-coupling, there have been a few reports of cobalt(II) halides (along with stoichiometric amounts of phosphine ligands) catalyzing coupling reactions including C-C and C-S coupling reactions.<sup>86,88,163</sup> (**Figure III.2**) Although these catalysts have shown good versatility in term of substrate scope, no mechanistic details were discussed in these reports.

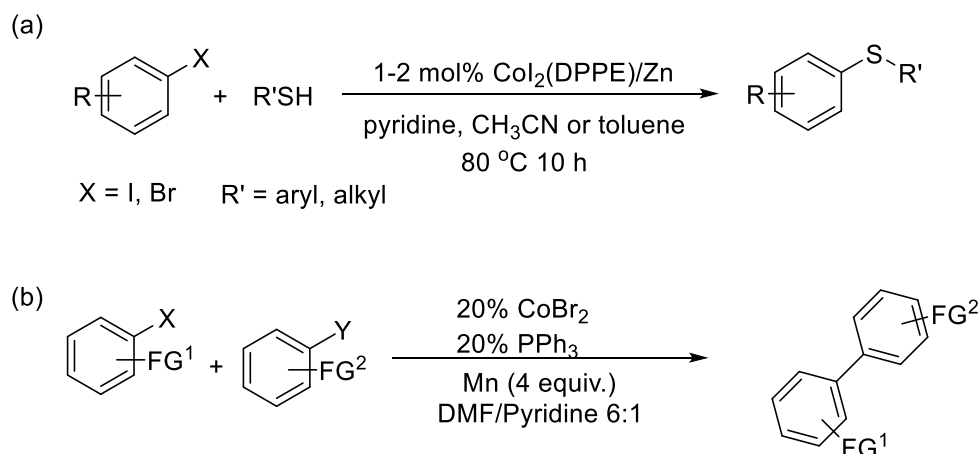


**Figure III.2** Examples of coupling reactions catalyzed by Co<sup>II</sup> halides

More recently, the Chirik group<sup>87,164–167</sup> and others<sup>168,169</sup> have demonstrated the applicability of pincer cobalt systems in catalysis such as C-H borylation and hydroboration of alkenes. Separately, mechanistic investigations into steps such as RE and OA have also been reported by the groups of Fout,<sup>170</sup> Bernskoetter<sup>171</sup> and Tonzetich.<sup>172</sup> Chirik and coworkers have elucidated the mechanism of C-H borylation using (pyrPNP)Co complexes and have been successful in showing OA to Co<sup>I</sup> and RE from Co<sup>III</sup> species. Although very interesting in their own right, one key difference between such reports and our efforts is that the proposed mechanisms for the Chirik systems involve OA of a B-H bond to a Co<sup>I</sup> center followed by loss of H<sub>2</sub> and OA of a C-H bond and finally elimination of a C-B bond. As illustrated in **Figure III.3**, this involves a neutral pincer ligand which leads to OA to four coordinate Co<sup>I</sup> species and reductive elimination from six coordinate Co<sup>III</sup> species whereas our efforts will involve OA of aryl halide bonds to a Co<sup>I</sup> center and RE of C-X (X = C, N, O, S) from Co<sup>III</sup>. We expect our systems to work differently from those described by Chirik since the nature of bonds being activated during



OA (C-X vs C-H) and the bonds being formed during RE (C-C/C-S vs C-B) are different and require different pathways. In addition our systems are designed to involve OA to 3 coordinate  $\text{Co}^{\text{I}}$  and RE from 5 coordinate  $\text{Co}^{\text{III}}$  complexes.

More analogous to our proposed research is our recent reports of Rh catalysts for C-S and C-C Kumada-Corriu coupling.<sup>84,114,173</sup> As illustrated in our reports, these catalyses' proceed via OA to three coordinate  $\text{Rh}^{\text{I}}$  and RE from five coordinate  $\text{Rh}^{\text{III}}$  centers (**Figure III.3**). Due to Co being from the same group and  $\text{Co}^{\text{I}}$  and  $\text{Co}^{\text{III}}$  complexes having the same number of d electrons as  $\text{Rh}^{\text{I}}$  and  $\text{Rh}^{\text{III}}$  respectively, a similar mechanism can be hypothesized for our pincer Co catalysts with anionic pincer ligands. Such a mechanism is beneficial for catalytic cross coupling of aryl halides since OA to three coordinate species is much more favored over OA to four coordinate species for OA of R-X bonds to  $d^8 \text{Rh}^{\text{I}}$ , similarly RE from five coordinate species is more facile than from six coordinate species for  $d^6 \text{Rh}^{\text{III}}$ .<sup>89</sup> The validity of our hypothesis will be investigated in this and the subsequent chapter through synthetic isolation of the proposed intermediates and studying the elementary steps of the catalytic cycle.

So, in this study we have strived to potentially identify and isolate the intermediates involved in C-X (X = C, N, S) coupling with (POCOP)Co systems analogous to our previously published (POCOP)Rh catalysts<sup>83,114</sup> and study their interchange and their utility in catalytic coupling reactions. Studying their interchange via an analogous synthetic cycle would allow for direct observation of the two-electron reactions that are important for the catalytic cyclic involving a  $\text{Co}^{\text{I}}/\text{Co}^{\text{III}}$  cycle.

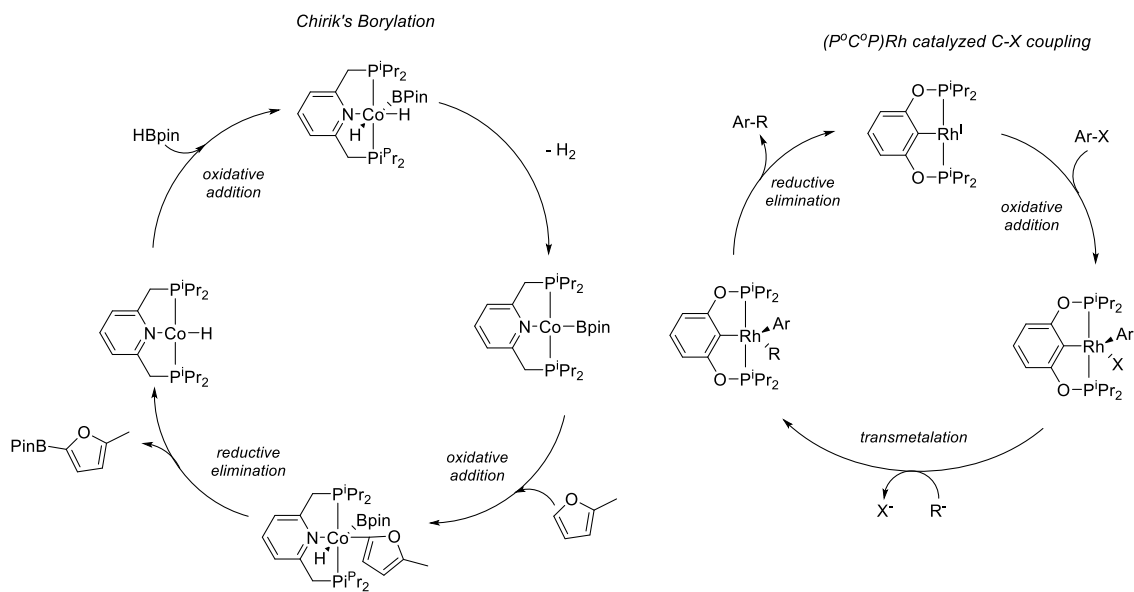


**Figure III.3** Comparison of proposed mechanisms for Chirik's system and our Rh catalysts

## 3.2. Results and discussion

### 3.2.1. Synthesis of $Co^{II}$ complexes

The introduction of the POCOP ligand into the coordination sphere of Co was accomplished by reaction of (POCOP)H with anhydrous  $CoCl_2$  in the presence of dimethylaminopyridine (DMAP), producing (POCOP)Co(Cl) (**301**) as a bright yellow solid in a 35% yield upon workup. The  $^1H$  NMR spectrum of **301** displayed four broad, strongly contact-shifted signals with integral ratios of 24:4:2:1, consistent with formation of a paramagnetic  $Co^{II}$  complex. The signals of relative intensity 24 (two overlapping resonances of 12H each) and 4 intensities correspond to the methyl and methine protons of the isopropyl groups, respectively; the resonances of intensity 2 and 1 correspond to the aromatic protons of the aryl backbone. The separation and matching integrations of peaks for different types of protons in the structure of the paramagnetic spectra of (POCOP)Co<sup>II</sup>

complexes is similar to  $\text{Co}^{\text{II}}$  complexes described by the groups of Chirik<sup>164</sup> and Fryzuk<sup>15</sup>. An Evans method measurement of the magnetic moment in solution yielded  $2.18 \mu\text{B}$ , consistent with a single unpaired electron, as would be expected for an approximately square-planar, low-spin  $\text{Co}(\text{II})$  complex. **301** readily served as a starting material for the synthesis of analogous  $(\text{POCOP})\text{CoX}$  complexes. Treatment of solutions of **301** with  $\text{Me}_3\text{Si-X}$  ( $\text{X} = \text{Br}, \text{I}, \text{OTf}$ ) resulted in rapid and clean formation of  $(\text{POCOP})\text{Co}(\text{Br})$  (**302**),  $(\text{POCOP})\text{Co}(\text{I})$  (**303**), and  $(\text{POCOP})\text{Co}(\text{OTf})$  (**304**).  $(\text{POCOP})\text{Co}(\text{F})$  (**305**) was synthesized by the reaction of **304** with  $\text{CsF}$  at RT. (**Figure III.4**)

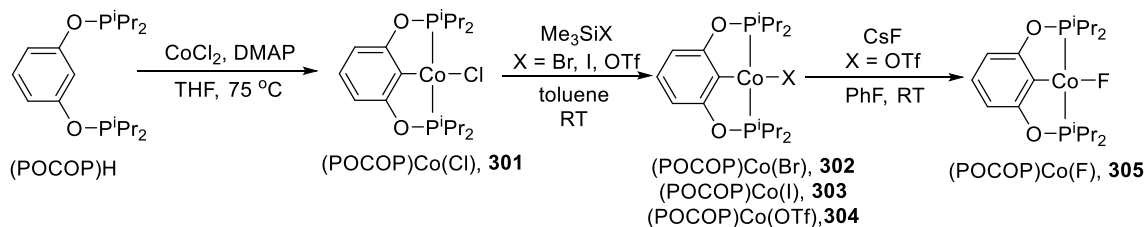


**Figure III.4** Synthesis of  $(\text{POCOP})\text{Co}$  halide complexes

Reaction of **301** with  $\text{NaOBU}^t$ ,  $\text{MeLi}$  or  $\text{PhLi}$ , respectively, resulted in the formation of  $(\text{POCOP})\text{Co}(\text{OBU}^t)$  (**306**),  $(\text{POCOP})\text{Co}(\text{Me})$  (**307**), and  $(\text{POCOP})\text{Co}(\text{Ph})$  (**308**). The synthesis of  $(\text{POCOP})\text{Co-SPh}$  (**309**) was readily accomplished in 77% isolated yield by treatment of **301** with thiophenol, surprisingly not requiring addition of a base. (**Figure III.5**) All of the  $\text{Co}^{\text{II}}$  complexes (**301** to **309**) displayed clearly analogous patterns in their  $^1\text{H}$  NMR spectra, corresponding to the same 12:12:4:2:1 set of resonances noted for **301**. These data are indicative of all these compounds being low-spin  $\text{Co}(\text{II})$  complexes possessing  $\text{C}_{2v}$  symmetry on the NMR time scale in solution.

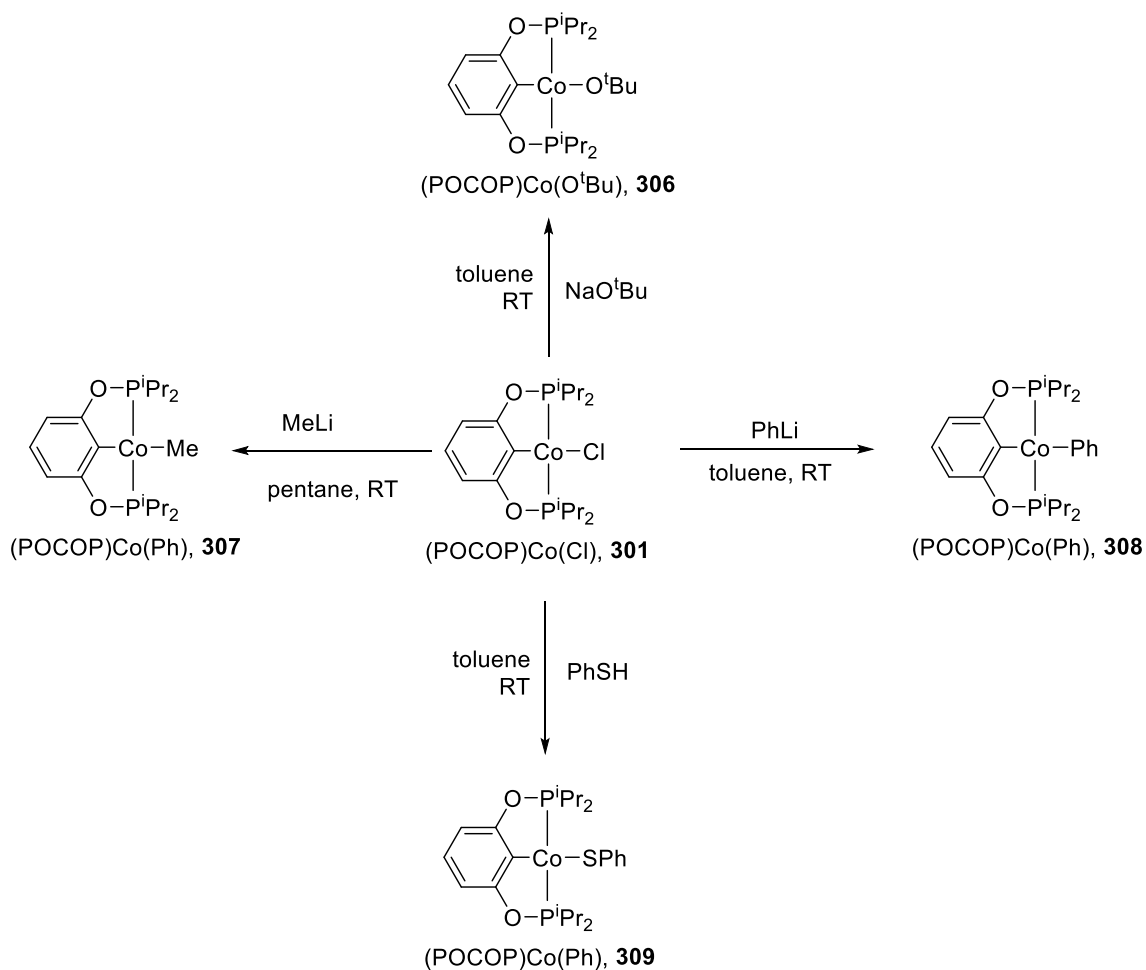


**Figure III.5** Synthesis of (POCOP)Co(R) compounds

### 3.2.2. Synthesis of $\text{Co}^{\text{III}}$ complexes

Oxidation of **301** with *N*-chlorosuccinimide (NCS) resulted in an immediate color change to dark brown and formation of a new product. It also exhibited broad and contact-shifted, yet well-resolved signals in the  $^1\text{H}$  NMR spectrum in integral ratios appropriate for the POCOP ligand. The identity of the product was determined to be (POCOP)CoCl<sub>2</sub> (**311**) by an X-ray study on a single X-ray quality crystal. The effective magnetic moment ( $\mu_{\text{eff}}$ ) of **311** was determined to be 2.44 and 2.46 by the Evans method and a magnetic

susceptibility balance, respectively. Although this is somewhat smaller than the theoretical  $2.83 \mu\text{B}$  value; the overall formulation is consistent with an intermediate spin Co(III) compound. This was particularly interesting as examples of five coordinate Co(III) complexes with intermediate spin are very scarce.<sup>174</sup> Treatment of **311** with 1 equiv. of  $\text{PMe}_3$  resulted in an immediate color change from brown to green and formation of diamagnetic  $(\text{POCOP})\text{Co}(\text{Cl})_2(\text{PMe}_3)$  (**312**). (**Figure III.6**) **312** displayed characteristic diamagnetic resonances in the  $^1\text{H}$  NMR spectrum, and broad singlets at 178.0 ppm and  $-16.7$  ppm in the  $^{31}\text{P}$  NMR spectrum in a 2:1 ratio. Single X-ray quality crystals were grown and the obtained structure shows an octahedral structure with chloride groups *trans* to each other and the phosphine *trans* to the central carbon of the pincer ligand.

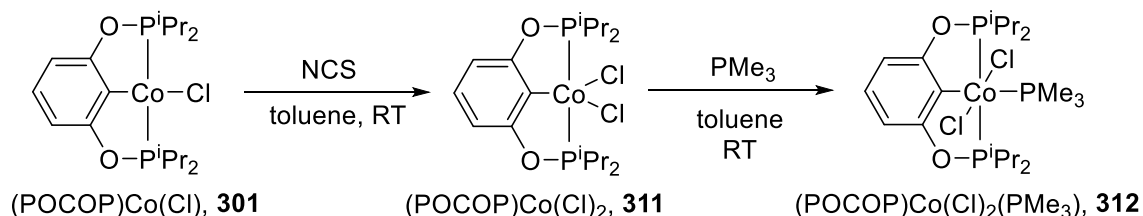


**Figure III.6** Synthesis of  $(\text{POCOP})\text{Co}(\text{Cl})_2$  (**311**) and  $(\text{POCOP})\text{Co}(\text{Cl})_2(\text{PMe}_3)$  (**312**)

Oxidation of  $(\text{POCOP})\text{Co-Ph}$  (**308**) with NCS at RT for 12h in pentane resulted in a mixture of  $(\text{POCOP})\text{CoCl}$  (**301**) and a new compound identified as  $(\text{POCOP})\text{Co}(\text{Ph})(\text{Cl})$  (**313**), along with some biphenyl. The **313** in these mixtures decayed over time into biphenyl and  $(\text{POCOP})\text{CoCl}$ . Pure samples of **313** could be isolated in minute yield by recrystallization; however, solutions of **313** obtained in this fashion inevitably degraded into  $(\text{POCOP})\text{CoCl}$  (**301**) and biphenyl, as well. In contrast, oxidation of  $(\text{POCOP})\text{Co-Ph}$  (**308**) with 0.55 equiv. of  $\text{PhI}(\text{OAc})_2$  overnight in toluene led to clean isolation of  $(\text{POCOP})\text{Co}(\text{Ph})(\text{OAc})$  (**314**) in 80% yield without any detectable amounts of

paramagnetic impurities or biphenyl. **314** was found to be stable at RT in a solution in  $C_6D_6$  and no detectable decomposition was observed after heating the same solution at  $80^\circ C$  for 90 mins. **314** offered an alternative synthetic route to  $Co^{III}$  aryl halide complexes. Metathetic reactions of **314** with  $Me_3SiCl$  and  $Me_3SiI$  in  $C_6D_6$  cleanly yielded  $(POCOP)Co(Ph)(Cl)$  (**313**) and  $(POCOP)Co(Ph)(I)$  (**315**), after 18 h and 10 mins respectively. (**Figure III.7 (a), (b)**)

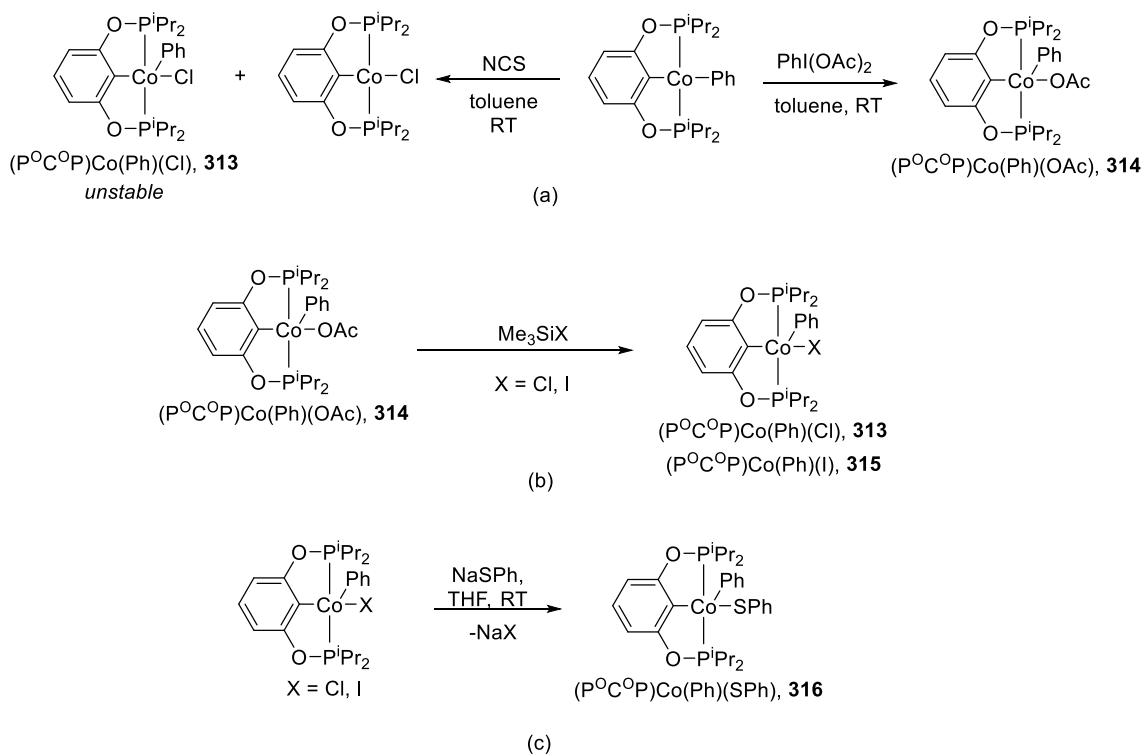


**Figure III.7** (a) Synthesis of  $(POCOP)Co^{III}$  compounds by 1 e- oxidation of  $(POCOP)Co(Ph)$  (b) Alternative synthesis of  $(POCOP)Co(Ph)(X)$  (c) Synthesis of  $(POCOP)Co(Ph)(SPh)$

Interestingly, **313** synthesized by this route was much less prone to decomposition (<5% after 2 d at RT in  $C_6D_6$ ) than the material obtained from **308** and NCS. No decomposition was evident by NMR upon aging solutions of **315** for 5 d at RT. It is

possible that decomposition of **313** is catalyzed by traces of NCS or some other NCS-derived impurities. **315** readily reacted with sodium thiophenolate to furnish (POCOP)Co(Ph)(SPh) (**316**). (**Figure III.7 (c)**) In contrast, our attempts to produce analogous (POCOP)Co(Ph)(Me) (**317**) and (POCOP)CoPh<sub>2</sub> (**318**) complexes were not successful. Reactions of **314**, **313** and **315** with MeLi or PhLi provided no spectroscopic evidence of **317** or **318** in situ and the major product in all cases was (POCOP)Co-Ph with (POCOP)Co-Me being observed as a minor product in the reaction with MeLi. The reaction of (POCOP)Co(Ph)(I) with PhMgBr showed quantitative conversion to (POCOP)Co(Ph) and Ph-Ph. Interestingly, the reaction of (POCOP)Co(Ph)(I) with MeMgCl showed quantitative conversion to equal amounts of (POCOP)Co-Ph (45% of initial (POCOP)Co(Ph)(I)), (POCOP)Co-Me (45% of initial (POCOP)Co(Ph)(I)) and Ph-Me (40% of initial (POCOP)Co(Ph)(I)) with no observation of Me-Me. This indicates the possibility of RE of Ph-Me followed by comproportionation of (POCOP)Co<sup>I</sup> with (POCOP)Co(Ph)(Me).

### 3.2.3. X-ray structural studies<sup>†</sup>

The structures of several (POCOP)Co complexes were unambiguously determined from crystals grown from pentane solutions at -35 °C. (POCOP)Co(SPh) (**309**) was observed to crystallize in the monoclinic system with the P<sub>21/c</sub> space group yielding yellow crystals. The ligands attain a slightly distorted square planar geometry around the Co center, with the P1-Co1-P2 and C7-Co1-S1 angles being lower than 180 degrees at

---

<sup>†</sup>Single Crystal X-Ray Structures for **309** and **311** were solved by Dr. Samuel Timpa while the rest were solved by C. M. Palit

161.86(2) and 163.15(6) degrees respectively (**Figure III.8**). (POCOP)Co(Cl)<sub>2</sub> (**311**) yielded green crystals in the orthorhombic system with the space group  $P_{bca}$  with the geometry around the Co center (POCOP)Co(Cl)<sub>2</sub> (**311**) observed to have an interesting geometry which appears to be square pyramidal based just upon the geometry index proposed by Addison and coworkers,<sup>175</sup> with  $\tau = 0.245$ . However, a closer look at the C<sub>ligand</sub>-Co-Cl bond angles gives us values of C1-Co1-Cl2, 144.4(1) and C1-Co1-Cl1, 110.3(1) leading us to believe that the structure is more likely a distorted trigonal bipyramidal structure where both the Cl atoms moving away from their ideal positions in a TBP structure (C<sub>ligand</sub>-Co-Cl value of 120°) (**Figure III.9(a)**). The crystals of (POCOP)Co(Cl)<sub>2</sub>(PMe<sub>3</sub>) (**312**) show an octahedral geometry around the Co center (**Figure III.9(b)**) with very similar Co-Cl bond lengths of 2.285(2) Å and 2.238(2) Å in **311** and 2.258(1) Å and 2.253(1) Å in **312**.

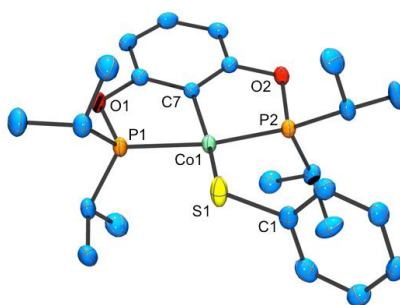


**Figure III.8** ORTEP drawing (50% probability ellipsoids) of (POCOP)Co(SPh) (**309**). Select atom labeling. Hydrogen atoms are omitted for clarity. Selected bond distances (Å) and angles (deg) for **309** follow: Co1-P1, 2.1816(8); Co1-P2, 2.1719(9); Co1-S1, 2.1706(8); S1-C1, 1.773(2); P1-Co1-P2, 161.86(2); C7-Co1-S1, 163.15(6); Co1-S1-C1, 119.89(7).



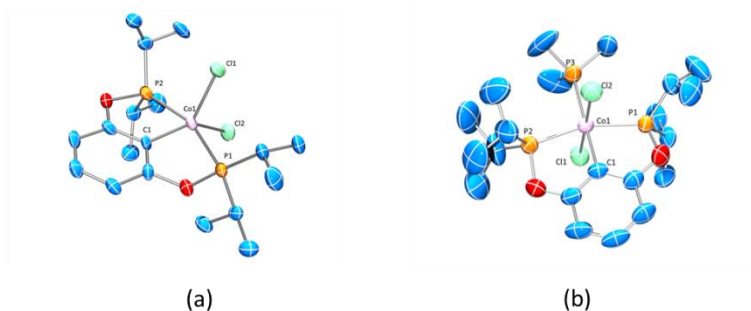


**Figure III.9** ORTEP drawing (50% probability ellipsoids) of (a) (POCOP)Co(Cl)<sub>2</sub> (**311**). Select atom labeling. Hydrogen atoms are omitted for clarity. Selected bond distances (Å) and angles (deg) for **311** follow: Co1-Cl1, 2.285(2); Co1-Cl2, 2.238(2); Co1-C1, 1.934(4), C1-Co1-C1, 110.3(1); C1-Co1-Cl2, 144.4(1); P1-Co1-P2, 159.10(3). (b) (POCOP)Co(Cl)<sub>2</sub>(PMe<sub>3</sub>) (**312**). Select atom labeling. Hydrogen atoms are omitted for clarity. Selected bond distances (Å) and angles (deg) for **312** follow: Co1-P1, 2.263(1); Co1-P2, 2.270(1); Co1-P3, 2.303(1); Co1-C1, 1.969(5); Co1-Cl1, 2.258(1); Co1-Cl2, 2.253(1); P1-Co1-P2, 159.04(5); Cl1-Co1-Cl2, 179.21(5); Cl1-Co1-P1, 94.16(5); Cl1-Co1-P3, 91.52(5); P3-Co1-P1, 99.76(5).

(POCOP)Co<sup>III</sup> compounds of the type (POCOP)Co(Ph)(X) where X = I, SPh) crystallize in the triclinic system with (POCOP)Co(Ph)(I) and (POCOP)Co(Ph)(SPh) attaining the  $P_{21/n}$  and  $P_{21/c}$  space groups respectively. The geometry around the Co centers is distorted square pyramidal with the Ph ligand occupying the apical position putting the strongly *trans* influence ligands (Ph<sup>-</sup> and central C<sup>-</sup> of POCOP) cis to each other with the I and S atoms distorted slightly out of plane from their ideal positions in a square pyramidal structure. Comparison of (POCOP)Co(Ph)(I) (**315**) (**Figure III.10**) and (POCOP)Co(Ph)(SPh) (**316**) (**Figure III.11**) with analogous Rh structures published by our group earlier<sup>83,114</sup> show very similar structure.

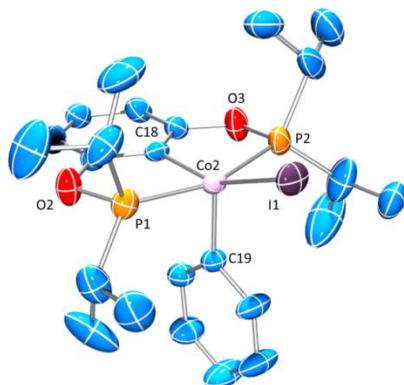


**Figure III.10** ORTEP drawing (50% probability ellipsoids) of (POCOP)Co(Ph)(I) (**315**). Select atom labeling. Hydrogen atoms are omitted for clarity. Selected bond distances (Å) and angles (deg) for **315** follow: Co2-P1, 2.210(2); Co2-P2, 2.204(2); Co2-I1, 2.601(2); Co2-C18, 1.907(3); Co2-C19, 1.940(3); P1-Co2-P2, 161.83(4); C18-Co2-I1, 155.19(9); C19-Co2-I1, 115.86(9); C18-Co2-C19, 88.9(1)

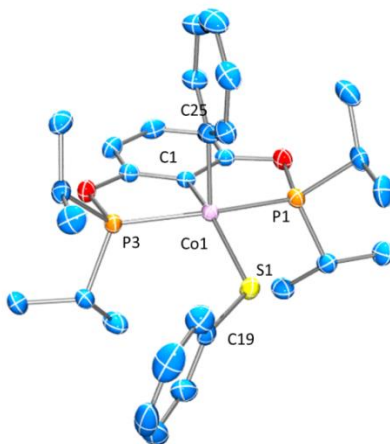


**Figure III.11** ORTEP drawing (50% probability ellipsoids) of (POCOP)Co(Ph)(SPh) (**316**). Select atom labeling. Hydrogen atoms are omitted for clarity. Selected bond distances (Å) and angles (deg) for **316** follow: Co1-C25, 1.947(2); Co1-P3, 2.222(1); Co1-P1, 2.223(1); Co1-S1, 2.215(1); Co1-C1, 1.933(2); C1-Co1-C25, 89.54(8); C1-Co1-P3, 81.80(5); C1-Co1-P1, 80.24(5); C1-Co1-S1, 148.98(6); C25-Co1-S1, 119.96(6)

### 3.2.4. Discussion of spin states of (POCOP)Co compounds

For (POCOP)Co<sup>III</sup> compounds the spin-state (diamagnetic/ low spin, S=0 vs paramagnetic/intermediate spin, S = 1) was observed to vary with the geometry and the nature of the ligands around the Co center. (POCOP)Co(Cl)<sub>2</sub> (**311**) appears to be a mix of different spin states as the observed  $\mu_{\text{eff}} = 2.44$  gives a  $S < 1$ . This is also reflected in the observed geometry of the molecule where it appears to be an intermediate between square pyramidal and trigonal bipyramidal structures. These observations warrant more investigations into **311** to better understand its electronic structure. Adding another ligand PMe<sub>3</sub> to **311** yields octahedral (POCOP)Co(Cl)<sub>2</sub>(PMe<sub>3</sub>) (**312**) where Co<sup>III</sup> obtains the low spin state leading to the compound being diamagnetic. (POCOP)Co(Ph)(I) (**315**) obtains a square pyramidal geometry because the presence of a strong field ligand such as Ph<sup>-</sup> changes the splitting pattern of the orbitals causing filling of the dxz, dyz and dxy orbitals to be filled with the 6 d electrons from Co<sup>III</sup>, hence attaining a low spin state of S = 0 and be diamagnetic. (**Figure III.12 (a)**)

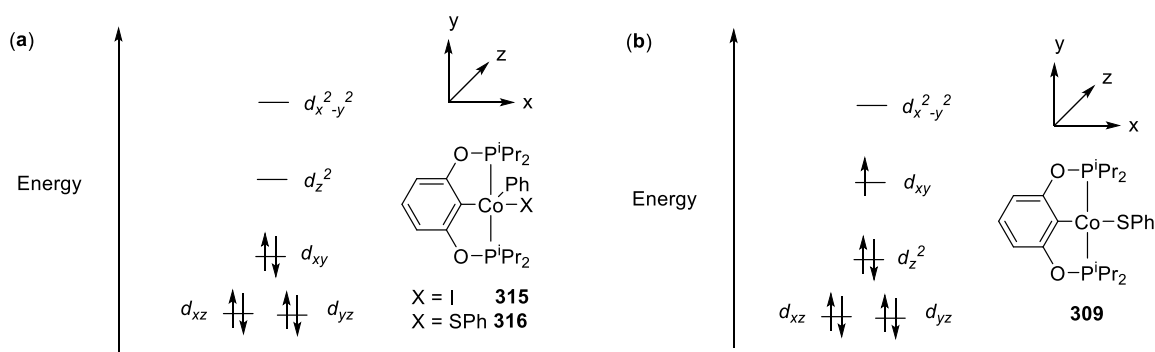


**Figure III.12** (a) Expected electronic structure for **315** and **316** in square pyramidal geometry (b) Expected electronic structure for **309** in square planar geometry

The effect of geometry change on the spin state can also be seen in Co<sup>II</sup> complexes where our (POCOP)Co<sup>II</sup> complexes are low-spin ( $S = 1/2$ ) due to the square planar geometry as observed in **309** and strong field ligands enforced by the POCOP pincer ligand. (**Figure III.12 (b)**) A low spin state and square planar geometry is also observed in Co<sup>II</sup> complexes with other rigid pincer ligands reported by Mindiola<sup>176</sup> and Chirik<sup>167</sup>. Four coordinate complexes of Co<sup>II</sup> supported by non-rigid ligands can however attain tetrahedral geometry and high spin states easily as demonstrated by Drulis<sup>177</sup> and Travnicek.<sup>178</sup>

### 3.2.5. Thermolysis and observation of *C*<sub>ligand</sub>-*C*<sub>Ph</sub> reductive elimination from **316**

In analogous (POCOP)Rh system reported by our group<sup>114</sup>, thermolysis of (POCOP)Rh(Ph)(SPh) (**322**) yielded (POCOP)Rh(SPh<sub>2</sub>) (**323**). Thermolysis of (POCOP)Co(Ph)(SPh) (**316**) in C<sub>6</sub>D<sub>6</sub> however, proceeds to give **319** as the sole product observable by NMR spectroscopy with a single peak which resonates at 148.7 ppm in its <sup>31</sup>P NMR spectrum and only diamagnetic resonances in the <sup>1</sup>H spectrum. This product does not however show any further reaction with PPh<sub>3</sub> or PhI as would be expected from (POCOP)Co(SPh<sub>2</sub>), if the thermolysis proceeded as with the analogous Rh system. (**Figure III.13**) These observations suggest that **319** is not a (POCOP)Co<sup>I</sup> species.

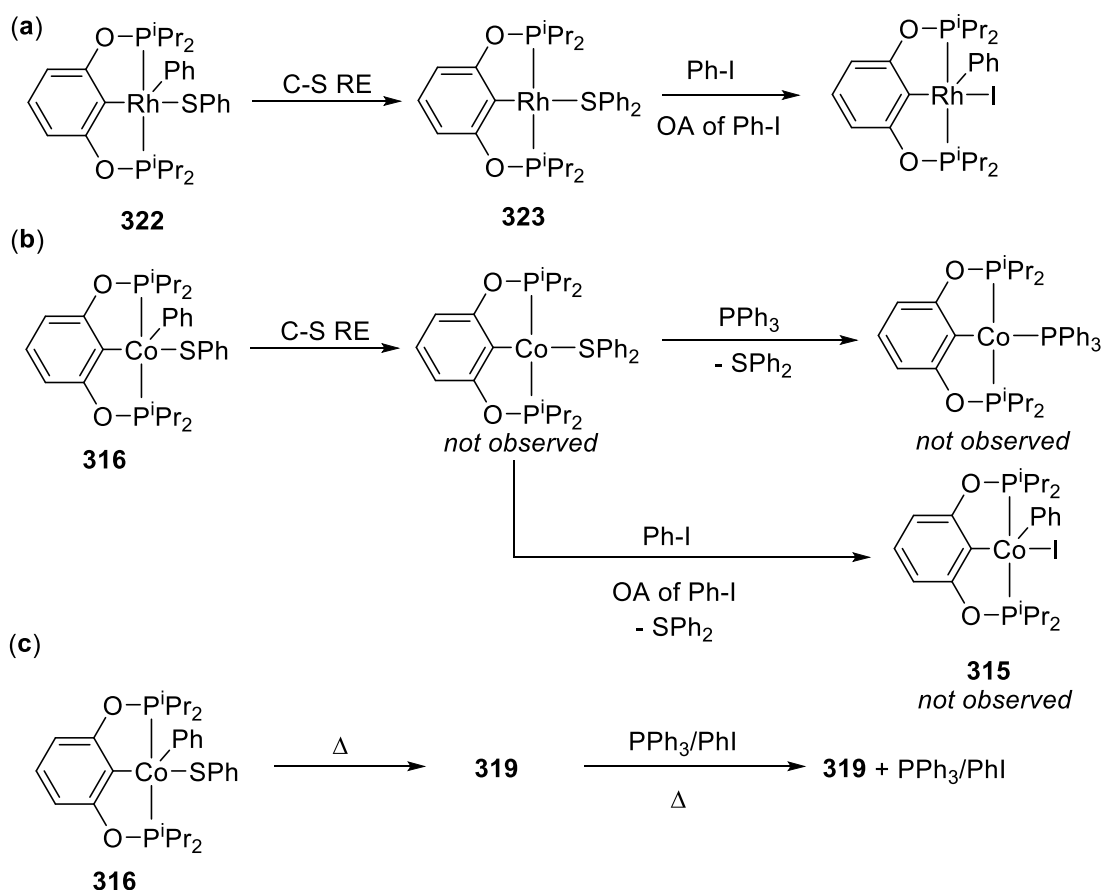


**Figure III.13** (a) Previously reported observations upon thermolysis of (POCOP)Rh(Ph)(SPh) (b) Expected observations for thermolysis of (POCOP)Co(Ph)(SPh) (c) Actual observations

Upon comparison of the <sup>1</sup>H, <sup>13</sup>C and <sup>31</sup>P spectra of **319** with the library of POCOP ligands and (POCOP)Co compounds available to us (**Table III.1**), the spectra of **319** match closely to that of the free ligand suggesting a possible RE of Ph or SPh with the central carbon of the POCOP ligand. Hydrolysis of the thermolysis product **319** with aq. HCl followed by extraction with dichloromethane and filtration through silica gives 2-phenylresorcinol<sup>179</sup> (**320**) in near quantitative yields confirming the RE of C<sub>Ph</sub> with central carbon of the POCOP ligand. This led us to conclude that the RE of C<sub>Ph</sub> with C<sub>ligand</sub> rules

out other possibilities upon thermolysis of **316** such as (a) the desired C-S RE of C<sub>Ph</sub> with SPh and (b) C-S RE of SPh with the central carbon donor of the pincer ligand (**Figure III.14**).

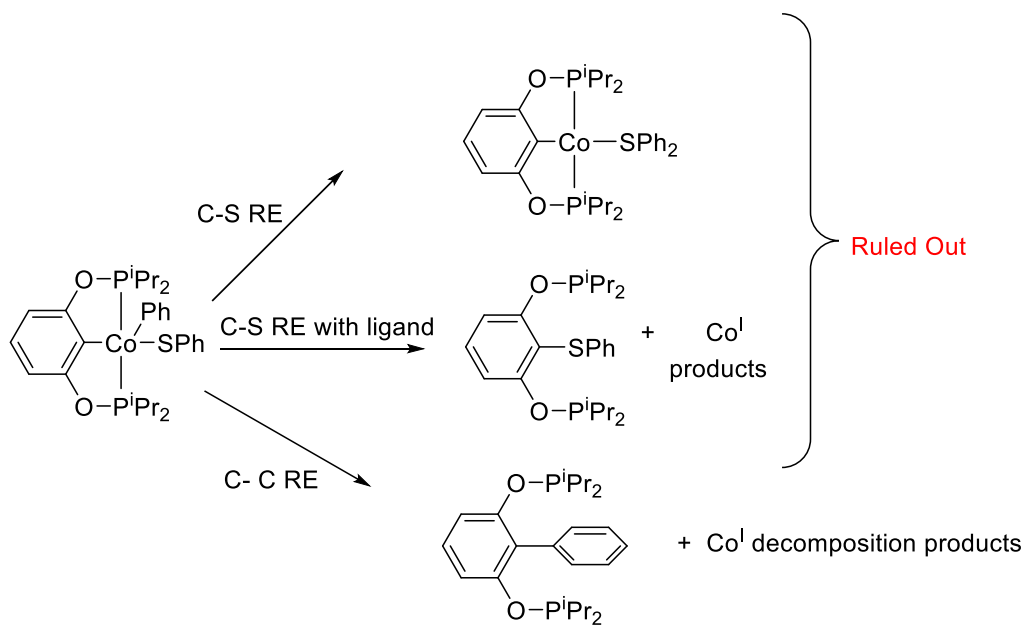


**Figure III.14** Possibilities upon thermolysis of (POCOP)Co(Ph)(SPh)

<sup>31</sup> P for Known (POCOP)Co	<sup>31</sup> P NMR shifts
(POCOP)Co(Ph)(I)	184.5 ppm
(POCOP)Co(Ph)(SPh)	183.3 ppm
(POCOP)H (ligand) <sup>12</sup>	147.2 ppm
<b>319</b>	148.5 ppm
(POCOP <sup>t</sup> Bu)Co(H <sub>2</sub> ) <sup>180</sup>	233 ppm

**Table III.1** <sup>31</sup>P{<sup>1</sup>H} chemical shifts of known (POCOP) species

### 3.3. Conclusion

In this effort, we have isolated a series of (POCOP)Co<sup>II</sup> complexes as precursors to their Co<sup>III</sup> analogs. Through 1 e<sup>-</sup> oxidation of these compounds, we were successful in isolating previously unreported cobalt complexes of the type (POCOP)Co(Ar)(X) and (POCOP)Co(Ar)(SPh) pertinent to a catalytic cycle for C-S coupling involving Co<sup>I</sup>/Co<sup>III</sup>, and study their spectroscopic and structural properties. RE of C-S was however unsuccessful with C<sub>Ar</sub>-C<sub>ligand</sub> being observed instead. In order to facilitate C-S RE a move to pincer ligands where C<sub>Ar</sub>-C<sub>ligand</sub> is either not possible or more difficult, is warranted. Our future efforts will be directed towards exploring other pincers to facilitate C-S RE and subsequent catalytic activity.

### 3.4. Experimental details

#### 3.4.1 General considerations

Unless otherwise specified, all manipulations were performed under an argon atmosphere using standard Schlenk line or glove box techniques. Toluene, THF, pentane, and isooctane were dried and deoxygenated (by purging) using a solvent purification system and stored over molecular sieves in an Ar-filled glove box. C<sub>6</sub>D<sub>6</sub> and hexanes were dried over and distilled from NaK/Ph<sub>2</sub>CO/18-crown-6 and stored over molecular sieves in an Ar-filled glove box. Fluorobenzene was dried with and then distilled or vacuum transferred from CaH<sub>2</sub>. (POCOP)H<sup>12</sup> was synthesized according to published procedures. NaSPh was prepared by reacting PhSH with 1 eq. of NaH in THF followed by pumping down and washing with Et<sub>2</sub>O. All other chemicals were used as received from commercial vendors. NMR spectra were recorded on a Varian NMRS 500 (<sup>1</sup>H NMR, 499.686 MHz;

$^{13}\text{C}$  NMR, 125.659 MHz,  $^{31}\text{P}$  NMR, 202.298 MHz,  $^{19}\text{F}$  NMR, 470.111 MHz) spectrometer. For  $^1\text{H}$  and  $^{13}\text{C}$  NMR spectra, the residual solvent peak was used as an internal reference.  $^{31}\text{P}$  NMR spectra were referenced externally using 85%  $\text{H}_3\text{PO}_4$  at  $\delta$  0 ppm.  $^{19}\text{F}$  NMR spectra were referenced externally using 1.0 M  $\text{CF}_3\text{CO}_2\text{H}$  in  $\text{CDCl}_3$  at -78.5 ppm. Elemental analyses were performed by CALI Labs, Inc. (Parsippany, NJ).

#### 3.4.2. Synthesis of (POCOP)Co<sup>II</sup> compounds<sup>‡</sup>

**Synthesis of (POCOP)CoCl (301).** (POCOP)H (1.54 g, 4.52 mmol) was combined with  $\text{CoCl}_2$  (586 mg, 4.51 mmol) and DMAP (552 mg, 4.52 mmol) in a Teflon capped flask and partially dissolved in dioxane. The flask was heated at 80 °C for 20 h producing a green solution. The solution was passed through a pad of Celite and volatiles were removed by vacuum. The product was extracted with pentane and dried under vacuum to give a bright yellow-green solid. The product was recrystallized from pentane at -35 °C to give yellow crystalline solid (689 mg, 35% yield). The compound displayed broad signals outside of the standard diamagnetic range in  $^1\text{H}$  NMR spectrum, indicative of a paramagnetic complex.  $^1\text{H}$  NMR ( $\text{C}_6\text{D}_6$ ):  $\delta$  43.72 (bs, 4H), 12.11 (bs, 24 H), -14.71 (bs, 2H), -53.02 (bs, 1H). (**Figure III.15**) Elem. Anal. Calc. for  $\text{C}_{18}\text{H}_{31}\text{ClCoO}_2\text{P}_2$ : C, 49.61; H, 7.17. Found: C, 49.54; H, 7.08. The magnetic moment for **301** was determined to be 2.18  $\mu_{\text{B}}$  by Evans Method.

---

<sup>‡</sup> (POCOP)Co<sup>II</sup> compounds except (POCOP)Co(SPh) and (POCOP)Co(Me) first isolated by Dr. Samuel Timpa



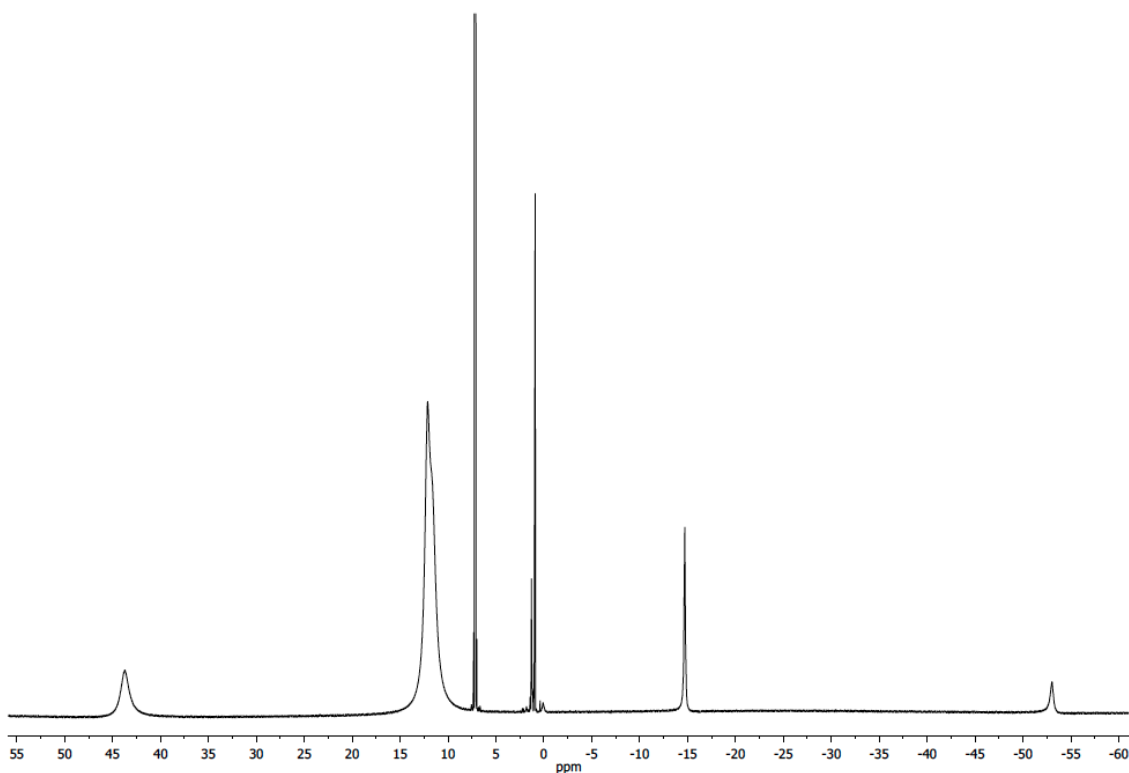


**Figure III.15**  $^1\text{H}$  NMR of (POCOP)CoCl (**301**) in  $\text{C}_6\text{D}_6$

**Synthesis of (POCOP)CoBr (302).** (POCOP)CoCl (**301**) (28 mg, 0.064 mmol) was added to a J. Young tube and dissolved in  $\text{C}_6\text{D}_6$ .  $\text{Me}_3\text{SiBr}$  (10  $\mu\text{L}$ , 0.076 mmol) was added to the sample, resulting in a color change to slightly yellow-green. The reaction was complete after 10 min at RT indicated by complete conversion to a new paramagnetic product and the presence of  $\text{Me}_3\text{SiCl}$  in the  $^1\text{H}$  NMR spectrum. The volatiles were removed by vacuum to give a yellow powder. The product was recrystallized from a saturated pentane solution at  $-35\text{ }^\circ\text{C}$  to give an orange crystalline solid (22 mg, 72%).  $^1\text{H}$  NMR ( $\text{C}_6\text{D}_6$ ):  $\delta$  45.16 (bs, 4H), 12.75 (bs, 12H), 12.00 (bs, 12H),  $-17.91$  (bs, 2H),  $-41.58$  (bs, 1H). Elem. Anal. Calc. for  $\text{C}_{18}\text{H}_{31}\text{BrCoO}_2\text{P}_2$ : C, 45.02; H, 6.51. Found: C, 44.95; H, 6.63.

**Synthesis of (POCOP)CoI (303).** (POCOP)CoCl (**301**) (30 mg, 0.069 mmol) was added to a J. Young tube and dissolved in C<sub>6</sub>D<sub>6</sub>. Me<sub>3</sub>SiI (11 μL, 0.078 mmol) was added to the sample, resulting in a color change to yellow-green. The color was slightly darker than that observed with (POCOP)CoBr. The reaction was complete after 10 min at RT indicated by complete conversion to a new paramagnetic product and the presence of Me<sub>3</sub>SiCl in the <sup>1</sup>H NMR spectrum. The volatiles were removed by vacuum to give a yellow powder. The product was recrystallized from a saturated pentane solution at -35 °C to give a dark orange crystalline solid (15 mg, 43%). <sup>1</sup>H NMR (C<sub>6</sub>D<sub>6</sub>): δ 40.35 (bs, 4H), 12.81 (bs, 12H), 12.01 (bs, 12H), -20.18 (bs, 2H), -27.73 (bs, 1H).

**Synthesis of (POCOP)CoOTf (304).** (POCOP)CoCl (**301**) (712 mg, 1.64 mmol) was added to a Schlenk flask and dissolved in C<sub>6</sub>D<sub>6</sub>. The solution was treated with Me<sub>3</sub>SiOTf (592 μL, 3.27 mmol). This led to no noticeable color change; however, the <sup>1</sup>H NMR spectrum of this reaction showed conversion to a new product along with the signal for Me<sub>3</sub>SiCl. The volatiles were removed from the reaction by vacuum to give a yellow-orange solid (850 mg, 94%). <sup>1</sup>H NMR (C<sub>6</sub>D<sub>6</sub>): δ 39.06 (bs, 4H, CHMe<sub>2</sub>), 11.26 (bs, 12H, CHMe<sub>2</sub>), 9.99 (bs, 12H, CHMe<sub>2</sub>), -24.72 (bs, 1H, Ar-H), -26.33 (bs, 2H, Ar-H). Elem. Anal. Calc. for C<sub>19</sub>H<sub>31</sub>CoF<sub>3</sub>O<sub>5</sub>P<sub>2</sub>S: C, 41.54; H, 5.69. Found: C, 41.37; H, 5.58.

**Synthesis of (POCOP)CoF (305).** (POCOP)CoOTf (**304**) (840 mg, 1.53 mmol) was added to a Schlenk flask and dissolved in C<sub>6</sub>H<sub>5</sub>F. The solution was treated with CsF (735 mg, 4.83 mmol) and allowed to stir at RT overnight. The solution became a slightly darker orange color. Volatiles were removed by vacuum. The product was extracted with pentane and passed through a pad of Celite to remove CsOTf and excess CsF. The compound was

recrystallized from a minimum of pentane at  $-35\text{ }^{\circ}\text{C}$ . This gave primarily orange solid with some dark black solid. The recrystallized was washed with cold pentane, which removed the dark solid and left the light orange product. The solid was dried under vacuum to give a light orange solid (399 mg, 63%).  $^1\text{H NMR}$  ( $\text{C}_6\text{D}_6$ ):  $-23.38$  (bs, 4H,  $\text{CHMe}_2$ ),  $8.37$  (bs, 12H,  $\text{CHMe}_2$ ),  $6.77$  (bs, 12H,  $\text{CHMe}_2$ ),  $0.38$  (bs, 1H, Ar-H),  $0.12$  (bs, 2H, Ar-H). Elem. Anal. Calc. for  $\text{C}_{18}\text{H}_{31}\text{CoFO}_2\text{P}_2$ : C, 51.56; H, 7.45. Found: C, 51.39; H, 7.56.

**Synthesis of (POCOP)CoO<sup>t</sup>Bu (306).** (POCOP)CoCl (**301**) (185 mg, 0.42 mmol) was added to a Schlenk flask and dissolved in toluene. NaO<sup>t</sup>Bu (41 mg, 0.43 mmol) was added to the solution, resulting in an immediate color change to orange. The reaction was stirred at RT for 1 h. The volatiles were removed under vacuum. The product was extracted with pentane, passed through a pad of Celite, and dried under vacuum. The product was recrystallized from a concentrated toluene solution layered with pentane at  $-35\text{ }^{\circ}\text{C}$  to give a brown solid (127 mg, 63%).  $^1\text{H NMR}$  ( $\text{C}_6\text{D}_6$ ):  $\delta$   $14.93$  (bs, 4H),  $4.36$  (bs, 26H),  $-9.88$  (bs, 9H),  $-79.53$  (bs, 1H). Elem. Anal. Calc. for  $\text{C}_{22}\text{H}_{40}\text{CoO}_3\text{P}_2$ : C, 55.81; H, 8.52. Found: C, 55.71; H, 8.36.

**Synthesis of (POCOP)Co(Me) (307).** (POCOP)Co(Cl) (**301**) (170 mg, 0.391 mmol) was added to a Schlenk flask and dissolved in pentane. The solution was treated with MeLi (293  $\mu\text{L}$ , 1.6 M in OEt<sub>2</sub>, 0.25 mmol) leading to an immediate color change from light yellow to dark green. After stirring for 30 min at RT, the solution was passed through a pad of Celite and the volatiles were removed by vacuum to give a green solid. The solid was recrystallized from toluene layered with pentane at  $-35\text{ }^{\circ}\text{C}$  to give a dark green crystalline solid (120 mg, 74% yield). The compound displayed broad signals outside of

the standard diamagnetic range in the  $^1\text{H}$  NMR spectrum, indicative of a paramagnetic complex.  $^1\text{H}$  NMR ( $\text{C}_6\text{D}_6$ ):  $\delta$  53.26 (bs, 4H), 13.14 (bs, 12H), 11.71 (bs, 12H), -9.08 (bs, 5H), -45.83 (bs, 1H). Elem. Anal. Calc. for  $\text{C}_{19}\text{H}_{34}\text{CoO}_2\text{P}_2$ : C, 54.94; H, 8.25. Found: C, 54.85; H, 8.50.

**Synthesis of (POCOP)Co(Ph) (308).** (POCOP)CoCl (**301**) (91 mg, 0.21 mmol) was added to a Schlenk flask and dissolved in pentane. The solution was treated with PhLi (140  $\mu\text{L}$ , 1.8 M in  $^n\text{Bu}_2\text{O}$ , 0.25 mmol) leading to an immediate color change from light yellow to dark green. After stirring for 30 min at RT, the solution was passed through a pad of Celite and the volatiles were removed by vacuum to give a green solid. The solid was recrystallized from toluene layered with pentane at  $-35\text{ }^\circ\text{C}$  to give a dark green crystalline solid (81 mg, 81% yield). The compound displayed broad signals outside of the standard diamagnetic range in the  $^1\text{H}$  NMR spectrum, indicative of a paramagnetic complex.  $^1\text{H}$  NMR ( $\text{C}_6\text{D}_6$ ):  $\delta$  35.99 (bs, 4H), 13.78 (bs, 1H), 11.95 (bs, 12H), 7.31 (bs, 12H), -7.43 (bs, 1H), -15.76 (bs, 2H), -20.04 (bs, 2H), -40.32 (bs, 2H). (**Figure III.16**) Elem. Anal. Calc. for  $\text{C}_{24}\text{H}_{36}\text{CoO}_2\text{P}_2$ : C, 60.38; H, 7.60. Found: C, 60.22; H, 7.69.

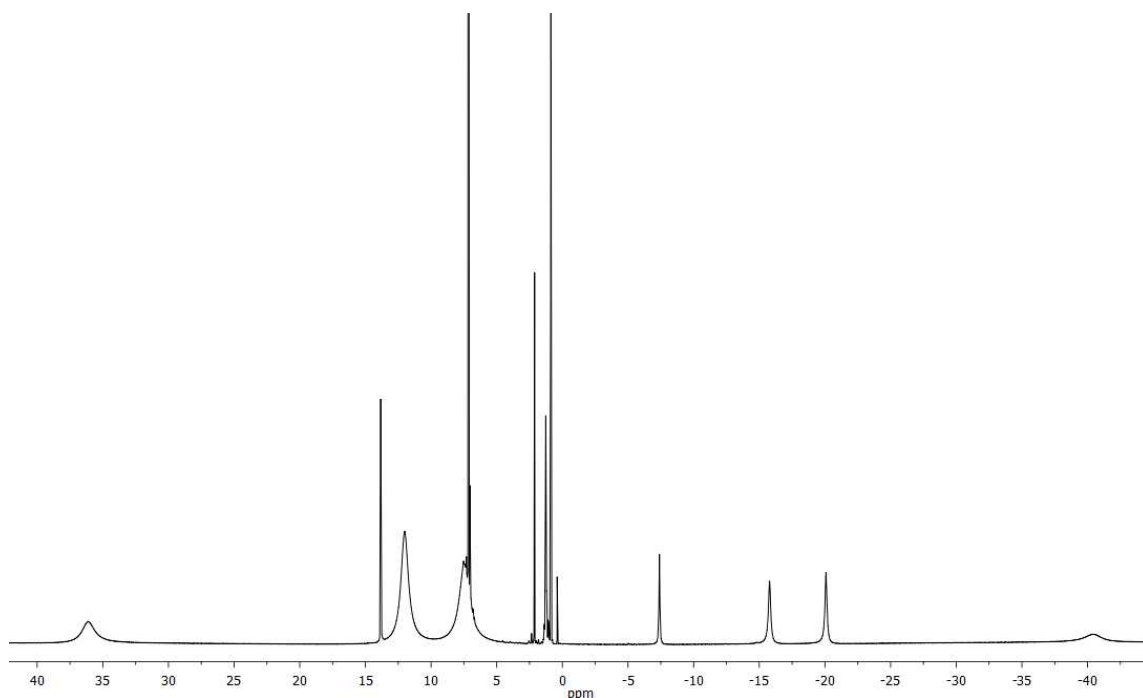


**Figure III.16**  $^1\text{H}$  NMR of (POCOP)Co(Ph) (**308**) in  $\text{C}_6\text{D}_6$ . Minor residual pentane, toluene, and grease present.

**Synthesis of (POCOP)Co(SPh) (309).** (POCOP)CoCl (**301**) (100 mg, 0.229 mmol) was added to a Schlenk flask and dissolved in ca. 10 mL of toluene. To this, PhSH (24.6  $\mu\text{L}$ , 26.5 mg, 0.240 mmol) was added using a syringe. The reaction was stirred at RT for 4 h. The volatiles were removed under vacuum. The product was extracted with pentane, passed through a pad of Celite, and dried under vacuum. The product was recrystallized from a concentrated pentane solution at  $-35\text{ }^\circ\text{C}$  to give yellow crystals (90 mg, 77%).  $^1\text{H}$  NMR ( $\text{C}_6\text{D}_6$ ) :  $\delta$  35.78 (br, 4H), 8.58 (br, 24H), 6.20 (br, 2H), 4.08 (br, 1H), -2.84 (br, 2H), -20.89 (br, 2H), -67.93 (br, 1H). (**Figure III.17**) Elem. Anal. Calc. for  $\text{C}_{24}\text{H}_{36}\text{CoO}_2\text{P}_2\text{S}$ : C, 56.58; H, 7.12. Found: C, 56.48; H, 7.04.

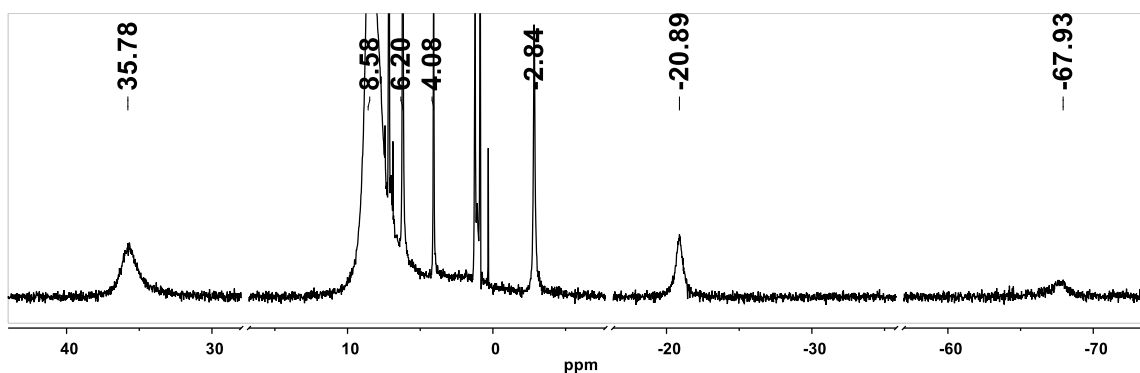


**Figure III.17**  $^1\text{H}$  NMR spectrum of  $(\text{POCOP})\text{Co}(\text{SPh})$  (**309**) in  $\text{C}_6\text{D}_6$ . Minor residual pentane present.

### 3.4.3. Synthesis of $(\text{POCOP})\text{Co}^{\text{III}}$ compounds<sup>§</sup>

**Synthesis of  $(\text{POCOP})\text{Co}(\text{Cl})_2$  (**311**).**  $(\text{POCOP})\text{CoCl}$  (**301**) (320 mg, 0.74 mmol) and NCS (98 mg, 0.735 mmol) were combined in a Schlenk flask and dissolved in toluene. The reaction underwent an immediate color change to brown and was stirred at RT for 2 h. The volatiles were removed by vacuum. The product was extracted with pentane and passed through a pad a Celite. The volatiles were removed to yield a brown solid. The solid was recrystallized from a saturated pentane solution at  $-35\text{ }^\circ\text{C}$  to give a crystalline brown solid (250 mg, 72%). X-ray quality crystals of the product were grown from a saturated toluene solution layered with pentane at  $-35\text{ }^\circ\text{C}$ . The compound displayed broad signals outside of the standard diamagnetic range in  $^1\text{H}$  NMR spectrum, indicative of a paramagnetic complex.  $^1\text{H}$  NMR ( $\text{C}_6\text{D}_6$ ):  $\delta$  45.77 (bs, 2H),  $-5.85$  (bs, 12H),  $-7.99$  (bs, 12H),  $-63.22$  (bs, 4H). (**Figure III.18**) The resonance corresponding to the central proton on the ligand backbone could not be identified and is likely overlapping with one of the

---

<sup>§</sup>  $(\text{POCOP})(\text{Cl})_2$ ,  $(\text{POCOP})\text{Co}(\text{Ph})(\text{OAc})$  and  $(\text{POCOP})\text{Co}(\text{Ph})(\text{Cl})$  (via NCS) isolated by Dr. Samuel Timpa

other broad signals. Elem. Anal. Calc. for  $C_{18}H_{31}Cl_2CoO_2P_2$ : C, 45.88; H, 6.63. Found: C, 46.26; H, 6.35. The effective magnetic moment was determined to be  $2.44 \mu_B$  by Evans method and 2.46 by magnetic susceptibility balance.

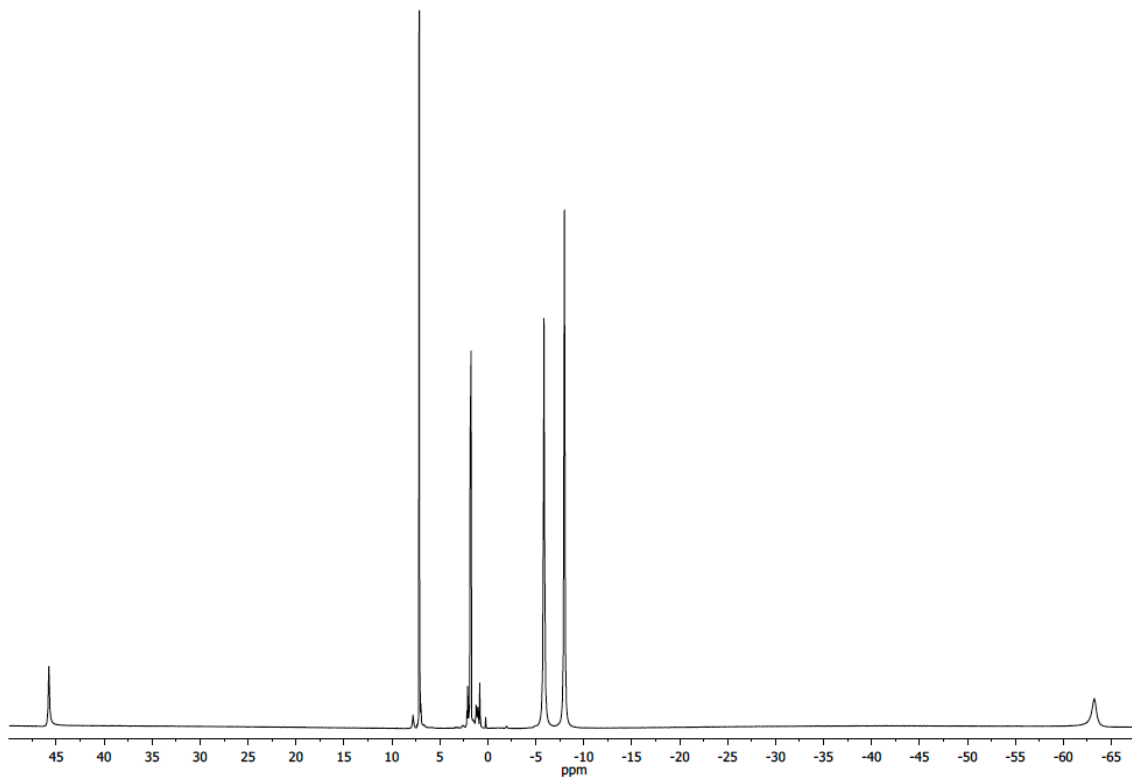


**Figure III.18**  $^1H$  NMR spectrum of  $(POCOP)Co(Cl)_2$  (**311**) in  $C_6D_6$ . Minor residual pentane and toluene present.

**Synthesis of  $(POCOP)Co(Cl)_2(PMe_3)$  (**312**).**  $(POCOP)Co(Cl)_2$  (**311**) (35 mg, 0.075 mmol) was added to J. Young tube and dissolved in toluene.  $PMe_3$  (7.7  $\mu L$ , 0.075 mmol) was added to the sample, resulting in an immediate color change from brown to green. After 1 h at RT, the reaction was passed through a pad of Celite and the volatiles were removed by vacuum to give a green solid. The solid was redissolved in  $C_6D_6$  for NMR analysis.  $^1H$  NMR ( $C_6D_6$ ) (**Figure III.19**):  $\delta$  7.02 (t, 7.5 Hz, 1H, *Ar*), 6.92 (d, 7.5 Hz, 2H, *Ar*), 3.08 (m, 4H,  $CHMe_2$ ), 1.42 (d, 7.5 Hz, 9H,  $PMe_3$ ), 1.32 (q, 7.5 Hz, 12H,  $CHMe_2$ ),

1.21 (q, 5.5 Hz, 12H, CHMe<sub>2</sub>). <sup>13</sup>C{<sup>1</sup>H} NMR (C<sub>6</sub>D<sub>6</sub>) δ 165.6 (td, J<sub>C-P</sub> = 7.1 Hz, 1.2 Hz, C-Co), 106.9 (td, J<sub>C-P</sub> = 5.4 Hz, 1.9 Hz C-O), 29.5 (t, J<sub>C-P</sub> = 7.9 Hz CHMe<sub>2</sub>), 19.2 (s, CHMe<sub>2</sub>), 18.8 (s, CHMe<sub>2</sub>), 17.8 (dt, J<sub>C-P</sub> = 22.5 Hz, 2.2 Hz, PMe<sub>3</sub>). <sup>31</sup>P{<sup>1</sup>H} NMR (C<sub>6</sub>D<sub>6</sub>) δ 178.0 (s), -16.7 (s) (2:1 ratio, respectively). Elem. Anal. Calc. for C<sub>21</sub>H<sub>40</sub>Cl<sub>2</sub>CoO<sub>2</sub>P<sub>3</sub>: C, 46.09; H, 7.37. Found: C, 46.29; H, 7.24.

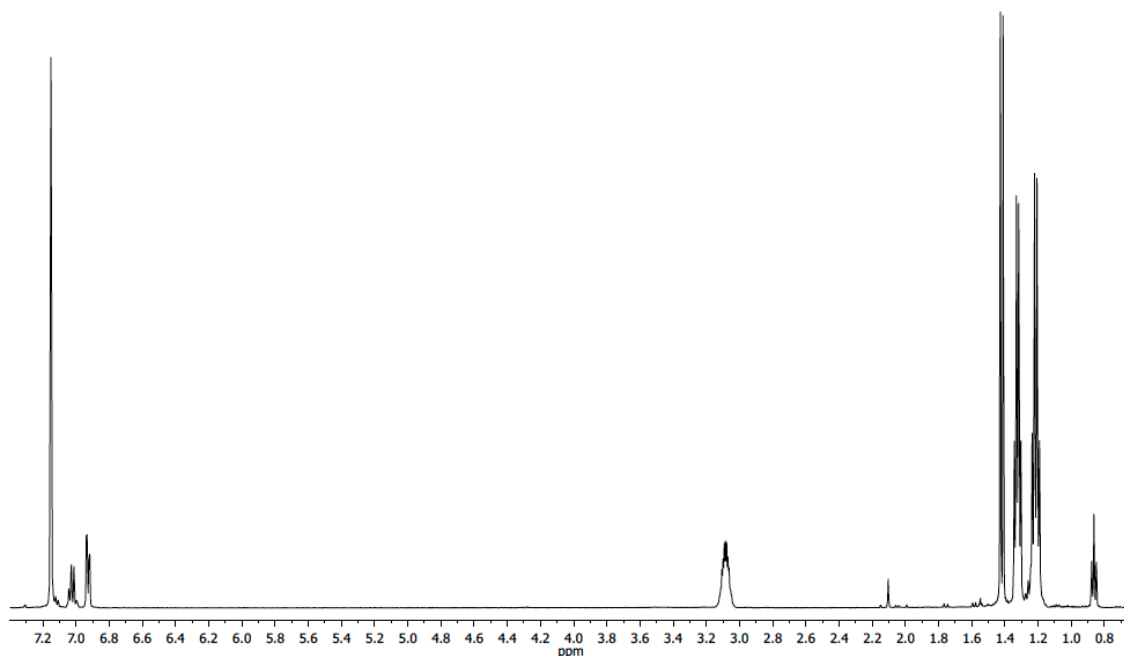


**Figure III.19** <sup>1</sup>H NMR of (POCOP)Co(Cl)<sub>2</sub>(PMe<sub>3</sub>) (**312**) in C<sub>6</sub>D<sub>6</sub>. Minor residual pentane and toluene present.

**Synthesis of (POCOP)Co(Ph)(Cl) (313).** (POCOP)Co(Ph) (**308**) (194 mg, 0.41 mmol) was added to a Schlenk flask and dissolved in pentane. The solution was treated with NCS (58 mg, 0.44 mmol) and stirred at RT for 12 h producing a green-yellow solution. A blue insoluble solid crashed out of the pentane solution and was removed by filtration. The volatiles were removed under vacuum to give a green-yellow solid. The <sup>1</sup>H NMR spectrum of this solid shows paramagnetic signals corresponding to (POCOP)CoCl



(**301**) as well as diamagnetic signals corresponding to (POCOP)Co(Ph)(Cl) (**313**). The solid was dissolved in pentane and crystallized at -35 °C. The recrystallization produced a green crystalline solid and yellow crystalline solid. The yellow solid was determined to be (POCOP)CoCl (**301**) and the green solid was determined to be (POCOP)Co(Ph)(Cl) (**313**). Dissolution of the green solid in C<sub>6</sub>D<sub>6</sub> showed clean **313** in the <sup>1</sup>H NMR spectrum. After several hours at RT, the same sample showed formation of (POCOP)Co(Cl) (**301**) and biphenyl in addition to (POCOP)Co(Ph)(Cl) (**313**) in the <sup>1</sup>H NMR spectrum.

**Alternate synthesis of (POCOP)Co(Ph)(Cl) (313) . (POCOP)Co(Ph)(OAc) (314)** (12 mg, 0.022 mmol) was dissolved in C<sub>6</sub>D<sub>6</sub> ca. 800 μl in a J. Young NMR tube with a PTFE screw cap. To this, Me<sub>3</sub>SiCl (3.40 μl, 2.91 mg, 0.27 mmol) was added using a syringe. The mixed solution was left to stir at RT for 18h and complete conversion to (POCOP)Co(Ph)(Cl) (**313**) was observed using NMR spectroscopy. The volatiles were removed and pure (POCOP)Co(Ph)(Cl) (**313**) was observed as a green solid. The green solid was dissolved in minimal pentane and put in the freezer at -35 °C. Much less decomposition (< 5% over two days) to (POCOP)Co(Cl) observed as compared to (POCOP)Co(Ph)(Cl) (**313**) obtained from (POCOP)Co(Ph) (**308**) and NCS. <sup>1</sup>H NMR (C<sub>6</sub>D<sub>6</sub>): δ 8.04 (bs, 1H, Ph-*H*), 7.01 (t, 8.5 Hz, 1H, Ar-*H*), 6.69 (d, 8.0 Hz, 2H, Ar-*H*), 6.53 (t, 7.0 Hz, 1H, Ph-*H*), 6.47 (bs, 1H, Ph-*H*), 6.21 (bs, 1H, Ph-*H*), 5.17 (bs, 1H, Ph-*H*), 2.81 (m, 2H, CHMe<sub>2</sub>), 2.16 (m, 2H, CHMe<sub>2</sub>), 1.21 (q, 7.5 Hz, 6H, CHMe<sub>2</sub>), 1.09 (m, 12H CHMe<sub>2</sub>), 0.83 (q, 7.5 Hz, 6H, CHMe<sub>2</sub>); (**Figure III.20**) <sup>13</sup>C{<sup>1</sup>H} NMR (C<sub>6</sub>D<sub>6</sub>): δ 171.0 (t, 8 Hz, C-Co), 140.9 (br), 137.5 (br), 128.9 (br), 127.6 (br), 125.0 (br), 123.7 (s), 106.8 (t,

5.4 Hz, C-O), 29.9 (t, 9.2 Hz, CHMe<sub>2</sub>), 27.9 (t, 11.7 Hz, CHMe<sub>2</sub>), 18.6 (s, CHMe<sub>2</sub>), 17.5 (s, CHMe<sub>2</sub>), 16.0 (s, CHMe<sub>2</sub>), 15.7 (s, CHMe<sub>2</sub>). <sup>31</sup>P{<sup>1</sup>H} NMR (C<sub>6</sub>D<sub>6</sub>): δ 176.7 (bs).

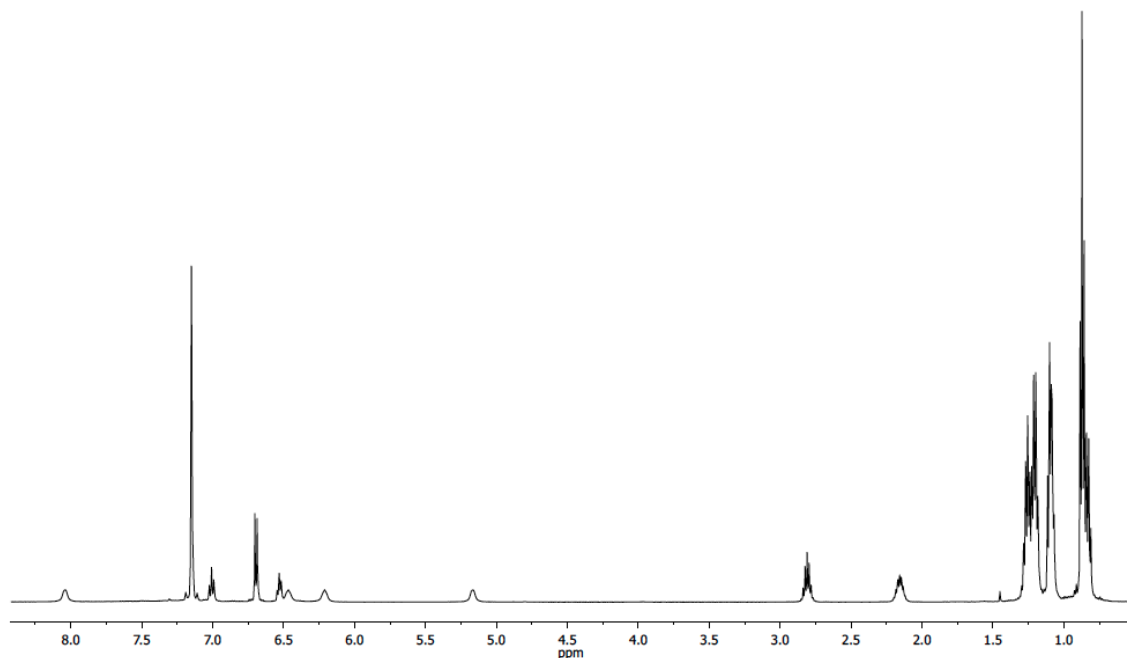


**Figure III.20** <sup>1</sup>H NMR spectrum of (POCOP)Co(Ph)(Cl) (**313**) in C<sub>6</sub>D<sub>6</sub>. Large amount of residual pentane present.

**Synthesis of (POCOP)Co(Ph)(OAc) (314).** (POCOP)Co(Ph) (**308**) (300 mg, 0.629 mmol) was added to Schlenk flask and dissolved in toluene to give a dark green solution. PhI(OAc)<sub>2</sub> (101 mg, 0.314 mmol) was added to the reaction. The solution quickly became light yellow in color. After stirring overnight at RT, the solution became red in color. The volatiles were removed by vacuum. The product was extracted with pentane and passed through a pad of Celite. The volatiles were removed to give a red-orange solid. The solid was dissolved in a minimum of pentane and left overnight at -35 °C to yield a red crystalline solid (270 mg, 80%). <sup>1</sup>H NMR (C<sub>6</sub>D<sub>6</sub>): δ 8.07 (d, 9.5 Hz, 1H, Ph), 6.99 (t, 6.5 Hz, 1H, Ar), 6.96 (t, 6.5 Hz, 1H, Ph), 6.81 (t, 6.5 Hz, 1H, Ph), 6.68 (d, 6.0 Hz, 2H, Ar),

6.63 (t, 9.5 Hz, 1H, Ph), 5.79 (d, 9.5 Hz, 1H, Ph), 2.58 (bm, 2H, CHMe<sub>2</sub>), 1.94 (m, 2H, CHMe<sub>2</sub>), 1.75 (s, 3H, CO<sub>2</sub>Me), 1.29 (q, 6.5 Hz, 6H, CHMe<sub>2</sub>), 1.17 (q, 6.5 Hz, 6H, CHMe<sub>2</sub>), 1.02 (q, 6.5 Hz, 6H, CHMe<sub>2</sub>), 0.88 (q, 6.5 Hz, 6H, CHMe<sub>2</sub>) (**Figure III.21**). <sup>13</sup>C{<sup>1</sup>H} NMR (C<sub>6</sub>D<sub>6</sub>): δ 182.6 (s, CO<sub>2</sub>Me), 168.5 (t, 8.4 Hz, C-Co), 141.8 (s), 141.2 (s), 134.9 (s), 129.1 (s), 127.6 (s), 125.4 (s), 123.4(s), 106.3 (t, 5.0 Hz, C-O), 28.6 (t, 6.7 Hz, CHMe<sub>2</sub>), 28.2 (t, 11 Hz, CHMe<sub>2</sub>), 23.7 (s, CO<sub>2</sub>Me), 17.8 (s, CHMe<sub>2</sub>), 17.2 (s, CHMe<sub>2</sub>), 16.4 (s, CHMe<sub>2</sub>), 15.8 (s, CHMe<sub>2</sub>). <sup>31</sup>P{<sup>1</sup>H} NMR (C<sub>6</sub>D<sub>6</sub>): δ 179.3 (bs).

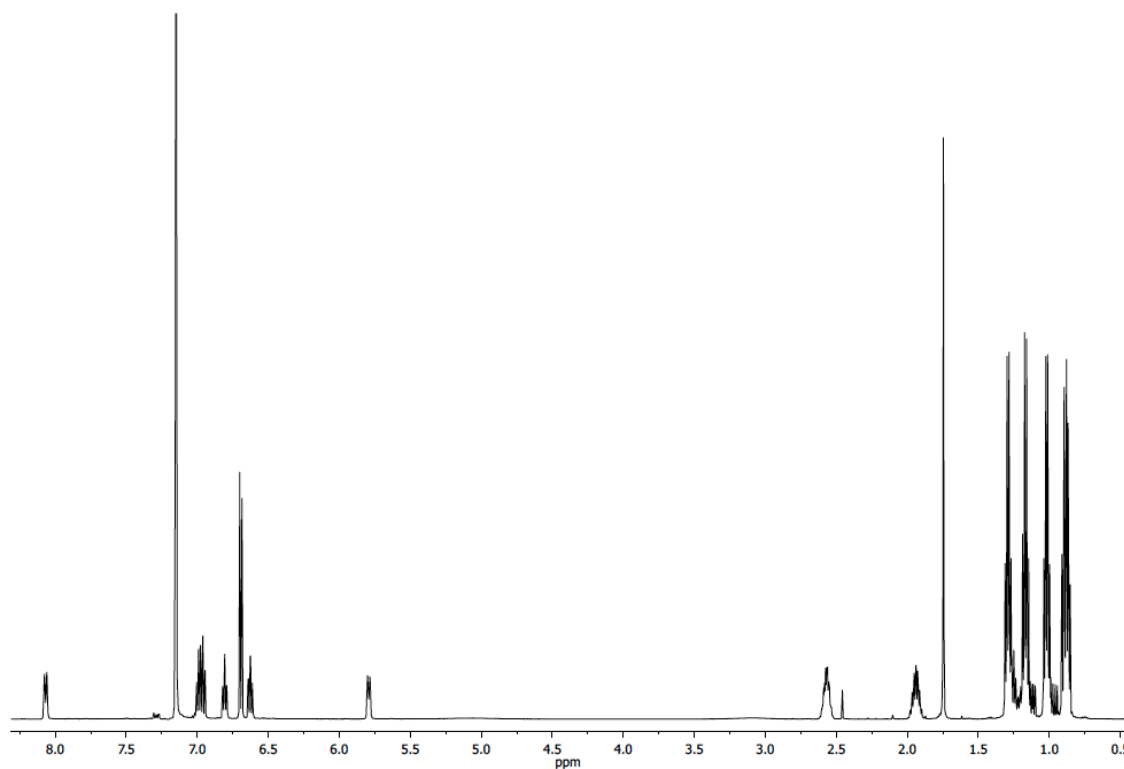


**Figure III.21** <sup>1</sup>H NMR spectrum of (POCOP)Co(Ph)(OAc) (**314**) in C<sub>6</sub>D<sub>6</sub>. Minor residual pentane and toluene present.

**Synthesis of (POCOP)Co(Ph)(I) (315).** (POCOP)Co(Ph)(OAc) (**314**) (54 mg, 0.099 mmol) was dissolved in C<sub>6</sub>D<sub>6</sub> ca. 800 μl in a J. Young NMR tube with a PTFE screw cap. To this, Me<sub>3</sub>SiI (16 μl, 22 mg, 0.110 mmol) was added using a syringe. Complete

conversion to (POCOP)Co(Ph)(I) was observed using NMR spectroscopy after 10 mins. The volatiles were removed and pure (POCOP)Co(Ph)(I) was observed as a green solid (40 mg, 67% yield).  $^1\text{H}$  NMR ( $\text{C}_6\text{D}_6$ ):  $\delta$  7.43 (bs, 1H, Ph-*H*), 7.05 (t, 8.5 Hz, 1H, Ar-*H*), 6.67 (d, 8.0 Hz, 2H, Ar-*H*), 6.42-6.35 (overlapping m, , 2H, Ph-*H*), 6.09 (bs, 1H, Ph-*H*), 5.16 (bs, 1H, Ph-*H*), 3.22 (m, 2H, CHMe<sub>2</sub>), 2.31 (m, 2H, CHMe<sub>2</sub>), 1.34 (q, 7.5 Hz, 6H, CHMe<sub>2</sub>), 1.12 (q, 7.5 Hz, 6H, CHMe<sub>2</sub>), 0.83 (m, 12H CHMe<sub>2</sub>).  $^{13}\text{C}\{^1\text{H}\}$  NMR ( $\text{C}_6\text{D}_6$ ):  $\delta$  170.2 (t, 8 Hz, C-Co), 140.5 (s), 138.2 (s), 131.1 (br), 129.0 (s), 124.3 (s), 124.0 (s), 106.9 (t, 5.4 Hz, C-O), 31.8 (t, 9.2 Hz, CHMe<sub>2</sub>), 28.5 (t, 11.7 Hz, CHMe<sub>2</sub>), 18.8 (s, CHMe<sub>2</sub>), 17.6 (s, CHMe<sub>2</sub>), 17.0 (s, CHMe<sub>2</sub>), 16.6 (s, CHMe<sub>2</sub>).  $^{31}\text{P}\{^1\text{H}\}$  NMR ( $\text{C}_6\text{D}_6$ )  $\delta$  184.5 (bs). Elem. Anal. Calc. for  $\text{C}_{24}\text{H}_{36}\text{CoIO}_2\text{P}_2$ : C, 47.70; H, 6.00. Found: C, 47.62 ; H, 5.81. No significant decomposition to (POCOP)Co(I) observed over a period of 5 days.

**Synthesis of (POCOP)Co(Ph)(SPh) (316) :** (POCOP)Co(Ph)(I) (**315**) (40 mg, 0.067 mmol) was dissolved in ca. 5 mL of THF in a schlenk flask and the solution was cooled to  $-35\text{ }^\circ\text{C}$ . . To this, Sodium thiophenolate (10 mg, 0.069 mmol) was added while stirring. The reaction was left to stir at RT for 1 h. The volatiles were pumped off and the products were extracted by pentane and filtered through a pad of celite on a glass frit. The volatiles were pumped off obtaining a brownish yellow powder. The product was extracted with cold  $\text{Me}_3\text{Si}_2\text{O}$  ca. 3mL and put in the freezer for recrystallization at  $-35\text{ }^\circ\text{C}$ . Overnight recrystallization yielded (POCOP)Co(Ph)(SPh) (**316**) as a brown powder (30 mg, 84% yield).  $^1\text{H}$  NMR ( $\text{C}_6\text{D}_6$ ):  $\delta$  8.30 (bs, 1H, Ph-*H*), 7.77-7.72 (m, 2H, Ar-*H*), 7.07-6.91 (overlapping m, 4H, Ar-*H*), 6.74 (d,  $J=9\text{ Hz}$ , 2H, Ar-*H*), 6.61 (t,  $J=5.8\text{ Hz}$ , 2H, Ar-*H*), 6.34 (bs, 1H, Ph-*H*), 5.38 (bs, 1H, Ph-*H*), 2.50-2.20 (overlapping m, 4H, CHMe<sub>2</sub>), 1.17-

1.02 (overlapping m, 18H,  $\text{CHMe}_2$ ), 0.72 (q, 7.2 Hz, 6H,  $\text{CHMe}_2$ ). (**Figure III.22**)  $^{13}\text{C}\{^1\text{H}\}$  NMR ( $\text{C}_6\text{D}_6$ ) :  $\delta$  169.0 (t,  $J = 9$  Hz, C-Co), 141.7 (s), 137.2 (s), 133.5 (s), 124.6 (br), 123.6 (s), 106.2 (t,  $J = 5.5$  Hz, C-O), 29.8 (t,  $J = 8.5$  Hz,  $\text{CHMe}_2$ ), 29.1 (t, 11.7 Hz,  $\text{CHMe}_2$ ), 19.6 (t,  $J = 1.6$  Hz,  $\text{CHMe}_2$ ), 17.1 (t,  $J = 2.2$  Hz,  $\text{CHMe}_2$ ), 16.5 (s,  $\text{CHMe}_2$ ), 16.2 (s,  $\text{CHMe}_2$ ).  $^{31}\text{P}\{^1\text{H}\}$  NMR ( $\text{C}_6\text{D}_6$ ) :  $\delta$  183.3 (bs). Elem. Anal. Calc. for  $\text{C}_{30}\text{H}_{41}\text{CoO}_2\text{P}_2\text{S}$ : C, 61.43; H, 7.05. Found: C, 61.61; H, 6.91.

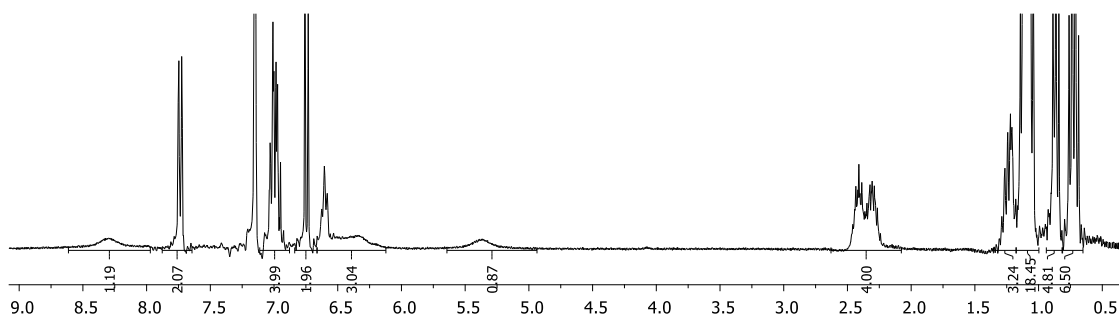


**Figure III.22**  $^1\text{H}$  NMR spectrum of  $(\text{POCOP})\text{Co}(\text{Ph})(\text{SPh})$  (**316**) in  $\text{C}_6\text{D}_6$ . Minor residual pentane present.

#### 3.4.4. Reactions of $(\text{POCOP})\text{Co}(\text{Ph})(X)$ complexes with alkyl reagents

**Reaction of  $(\text{POCOP})\text{Co}(\text{Ph})(\text{OAc})$  (**314**) with  $\text{PhLi}$ .**  $(\text{POCOP})\text{Co}(\text{Ph})(\text{OAc})$  (24 mg, 0.044 mmol) was dissolved in ca. 600  $\mu\text{L}$  of  $\text{C}_6\text{D}_6$  in a PTFE capped J. Young NMR tube. To this,  $\text{PhLi}$  (28  $\mu\text{L}$  of 1.8 M in  $^n\text{Bu}_2\text{O}$ , 0.05 mmol) was added using a syringe. The solution immediately turned green. Analysis of the reaction mixture by  $^1\text{H}$  NMR after 5 mins showed complete conversion to  $(\text{POCOP})\text{Co}(\text{Ph})$  with resonances for Ph-Ph also observed.

**Reaction of  $(\text{POCOP})\text{Co}(\text{Ph})(\text{OAc})$  (**314**) with  $\text{MeLi}$ .**  $(\text{POCOP})\text{Co}(\text{Ph})(\text{OAc})$  (12 mg, 0.022 mmol) was dissolved in ca. 600  $\mu\text{L}$  of  $\text{C}_6\text{D}_6$  in a PTFE capped J. Young NMR tube. To this,  $\text{MeLi}$  (20  $\mu\text{L}$  of 1.6 M in  $\text{Et}_2\text{O}$ , 0.032 mmol) was added using a syringe. The

solution immediately turned green. Analysis of the reaction mixture by  $^1\text{H}$  NMR after 5 mins showed complete conversion to (POCOP)Co(Ph).

**Reaction of (POCOP)Co(Ph)(Cl) (313) with PhLi.** (POCOP)Co(Ph)(Cl) (9 mg, 0.018 mmol) was dissolved in ca. 600  $\mu\text{L}$  of  $\text{C}_6\text{D}_6$  in a PTFE capped J. Young NMR tube. 1,4-dioxane (2  $\mu\text{L}$ , 2.07 mg, 0.023 mmol) was added using a syringe to serve as an internal standard. To this, PhLi (10  $\mu\text{L}$  of 1.8 M in  $^n\text{Bu}_2\text{O}$ , 0.018 mmol) was added using a syringe. The solution immediately turned green. Analysis of the reaction mixture by  $^1\text{H}$  NMR after 5 mins showed complete (> 95%) conversion to (POCOP)Co(Ph) with corresponding resonances for Ph-Ph also observed.

**Reaction of (POCOP)Co(Ph)(Cl) (313) with MeLi.** (POCOP)Co(Ph)(Cl) (10 mg, 0.0194 mmol) was dissolved in ca. 600  $\mu\text{L}$  of  $\text{C}_6\text{D}_6$  in a PTFE capped J. Young NMR tube. 1,4-dioxane (2  $\mu\text{L}$ , 2.07 mg, 0.023 mmol) was added using a syringe to serve as an internal standard. To this, MeLi (13  $\mu\text{L}$  of 1.6 M in  $\text{Et}_2\text{O}$ , 0.0219 mmol) was added using a syringe. The solution immediately turned green. Analysis of the reaction mixture by  $^1\text{H}$  NMR after 5 min showed the following composition (a) Co containing compounds : Unreacted (POCOP)Co(Ph)(Cl) (21%), (POCOP)Co(Ph) (60%), (POCOP)Co(Me) (14%) (b) Organic compounds: Me-Me (17%), Ph-Me (12%). (All percentages reflect yield w.r.t the original amount of (POCOP)Co(Ph)(Cl).)

**Reaction of (POCOP)Co(Ph)(I) (315) with PhLi.** (POCOP)Co(Ph)(I) (10 mg, 0.016 mmol) was dissolved in ca. 600  $\mu\text{L}$  of  $\text{C}_6\text{D}_6$  in a PTFE capped J. Young NMR tube. 1,4-dioxane (2  $\mu\text{L}$ , 2.07 mg, 0.023 mmol) was added using a syringe to serve as an internal standard. To this, PhLi (9  $\mu\text{L}$  of 1.8 M in  $^n\text{Bu}_2\text{O}$ , 0.017 mmol) was added using a syringe.

The solution immediately turned green. Analysis of the reaction mixture by  $^1\text{H}$  NMR after 5 mins showed complete ( $> 95\%$ ) conversion to  $(\text{POCOP})\text{Co}(\text{Ph})$  with corresponding resonances for Ph-Ph also observed.

**Reaction of  $(\text{POCOP})\text{Co}(\text{Ph})(\text{I})$  (315) with  $\text{PhMgBr}$ .**  $(\text{POCOP})\text{Co}(\text{Ph})(\text{I})$  (10 mg, 0.016 mmol) was dissolved in ca. 600  $\mu\text{L}$  of  $\text{C}_6\text{D}_6$  in a PTFE capped J. Young NMR tube.  $(\text{Me}_3\text{Si})_2\text{O}$  (2  $\mu\text{L}$ , 1.53 mg, 0.938  $\mu\text{mol}$ ) was added using a syringe to serve as an internal standard. To this,  $\text{PhMgBr}$  (7  $\mu\text{L}$  of 2.5 M in THF, 0.018 mmol) was added using a syringe. The solution was monitored by  $^1\text{H}$  NMR spectroscopy. Analysis of the reaction mixture by  $^1\text{H}$  NMR after 24 h showed complete ( $> 95\%$ ) conversion to  $(\text{POCOP})\text{Co}(\text{Ph})$  with corresponding resonances for Ph-Ph also observed.

**Reaction of  $(\text{POCOP})\text{Co}(\text{Ph})(\text{I})$  (315) with  $\text{MeLi}$ .**  $(\text{POCOP})\text{Co}(\text{Ph})(\text{I})$  (10 mg, 0.0165 mmol) was dissolved in ca. 600  $\mu\text{L}$  of  $\text{C}_6\text{D}_6$  in a PTFE capped J. Young NMR tube. 1,4-dioxane (2  $\mu\text{L}$ , 2.07 mg, 0.023 mmol) was added using a syringe to serve as an internal standard. To this,  $\text{MeLi}$  (11  $\mu\text{L}$  of 1.6 M in  $\text{Et}_2\text{O}$ , 0.0176 mmol) was added using a syringe. The solution immediately turned green. Analysis of the reaction mixture by  $^1\text{H}$  NMR after 5 min showed the following composition (a) Co containing compounds: Unreacted  $(\text{POCOP})\text{Co}(\text{Ph})(\text{I})$  (21%),  $(\text{POCOP})\text{Co}(\text{Ph})$  (60%), unidentified paramagnetic Co (18%) (b) Organic compounds: Me-Me (17%), Ph-Me (12%). (All percentages reflect yield w.r.t the original amount of  $(\text{POCOP})\text{Co}(\text{Ph})(\text{I})$ .)

**Reaction of  $(\text{POCOP})\text{Co}(\text{Ph})(\text{I})$  (315) with  $\text{MeMgCl}$ .**  $(\text{POCOP})\text{Co}(\text{Ph})(\text{I})$  (8.1 mg, 0.013 mmol) was dissolved in ca. 600  $\mu\text{L}$  of  $\text{C}_6\text{D}_6$  in a PTFE capped J. Young NMR tube.  $(\text{Me}_3\text{Si})_2\text{O}$  (2  $\mu\text{L}$ , 1.53 mg, 0.938  $\mu\text{mol}$ ) was added using a syringe to serve as an internal

standard. To this, MeMgCl (5.1  $\mu$ L of 3.0 M in THF, 0.016 mmol) was added using a syringe. Analysis of the reaction mixture by  $^1\text{H}$  NMR after 5 min showed the following composition (a) Co containing compounds: (POCOP)Co(Ph) (45%), (POCOP)Co(Me) (45%) unidentified paramagnetic Co (6%) (b) Organic compounds: Ph-Me (40%). (All percentages reflect yield w.r.t the original amount of (POCOP)Co(Ph)(I).)

#### *3.4.5. Decomposition studies of (POCOP)Co(R)(X) complexes*

**Decomposition of (POCOP)Co(Ph)(Cl) (313) at RT.** (POCOP)Co(Ph)(Cl) (8 mg, 0.016 mmol) was dissolved in ca. 600  $\mu$ L of  $\text{C}_6\text{D}_6$  in a PTFE capped J. Young NMR tube. 1,4-dioxane (2  $\mu$ L, 2.07 mg, 0.023 mmol) was added using a syringe to serve as an internal standard. The NMR tube was left at RT for several days and the decomposition of (POCOP)Co(Ph)(Cl) was monitored by  $^1\text{H}$  NMR spectroscopy. After 4 days the composition of the reaction mixture as observed by  $^1\text{H}$  NMR was (POCOP)Co(Ph)(Cl) (70% of initial), (POCOP)Co(Cl) (28% of initial concentration of (POCOP)Co(Ph)(Cl)) and (POCOP)Co(Ph) (<2% of initial concentration of (POCOP)Co(Ph)(Cl)). Biphenyl (14% of initial concentration of (POCOP)Co(Ph)(Cl)) was also observed.

**Decomposition of (POCOP)Co(Ph)(Cl) at RT with BHT as radical inhibitor.** (POCOP)Co(Ph)(Cl) (8 mg, 0.016 mmol) was dissolved in ca. 600  $\mu$ L of  $\text{C}_6\text{D}_6$  in a PTFE capped J. Young NMR tube. 1,4-dioxane (2  $\mu$ L, 2.07 mg, 0.023 mmol) was added using a syringe to serve as an internal standard. Butylated hydroxytoluene (BHT) (3.5 mg, 0.016 mmol) was also added to this mixture. The NMR tube was left at RT for several days and the decomposition of (POCOP)Co(Ph)(Cl) was monitored by  $^1\text{H}$  NMR spectroscopy. After 4 days the composition of the reaction mixture as observed by  $^1\text{H}$  NMR was



(POCOP)Co(Ph)(Cl) (75% of initial), (POCOP)Co(Cl) (24% of initial concentration of (POCOP)Co(Ph)(Cl)) and (POCOP)Co(Ph) (<1% of initial concentration of (POCOP)Co(Ph)(Cl)). Biphenyl (12% of initial concentration of (POCOP)Co(Ph)(Cl)) was also observed.

#### 3.4.6. Thermolysis of (POCOP)Co(Ph)(SPh) and analysis of the product mixture

**Thermolysis of (POCOP)Co(Ph)(SPh).** (POCOP)Co(Ph)(SPh) (4 mg, 6.82  $\mu\text{mol}$ ) was dissolved in ca. 600  $\mu\text{L}$  of  $\text{C}_6\text{D}_6$  in a PTFE capped J. Young NMR tube. The NMR tube was then placed in an oil bath at 80  $^\circ\text{C}$  for 30 mins. Upon analysis of the sample by  $^1\text{H}$  and  $^{31}\text{P}$  NMR spectroscopy, complete conversion to **319** was observed which showed the following resonances:  $^1\text{H}$  NMR ( $\text{C}_6\text{D}_6$ ) (**Figure III.23**):  $\delta$  7.52-7.42 (m, 3H, Ar-H), 7.36-7.24 (overlapping m, 5H, Ar-H), 7.22-7.05 (m overlapping with solvent, 4H, Ar-H), 7.22-7.05 (overlapping m, 2H, Ar-H), 1.55 (m, 4 H,  $\text{CH}(\text{Me})_2$ ), 0.99 -0.81 ppm (m, 24H,  $\text{CHMe}_2$ ).  $^{31}\text{P}\{^1\text{H}\}$  NMR ( $\text{C}_6\text{D}_6$ )  $\delta$  148.7 ppm. (**Figure III.24**)

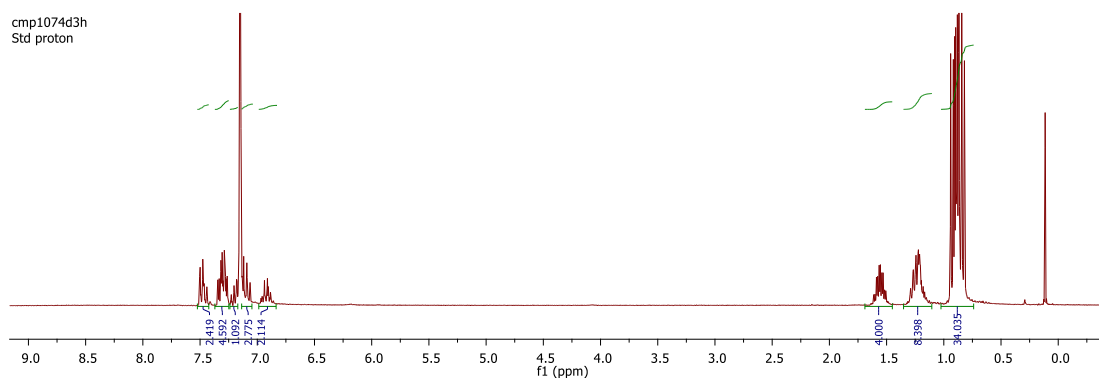


**Figure III.23**  $^1\text{H}$  NMR spectrum of **319** in  $\text{C}_6\text{D}_6$ . Traces of pentane present

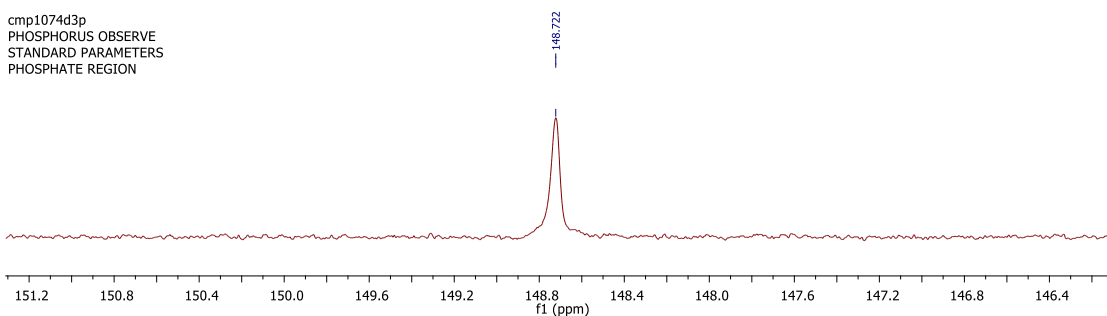


**Figure III.24**  $^{31}\text{P}\{^1\text{H}\}$  NMR spectrum of **319** in  $\text{C}_6\text{D}_6$

**Reaction of 319 with PhI.** (POCOP)Co(Ph)(SPh) (4 mg, 6.82  $\mu\text{mol}$ ) was dissolved in ca. 600  $\mu\text{L}$  of  $\text{C}_6\text{D}_6$  in a PTFE capped J. Young NMR tube. The NMR tube was then placed in an oil bath at 80  $^\circ\text{C}$  for 30 mins. Conversion to **319** was confirmed by  $^1\text{H}$  and  $^{31}\text{P}$  NMR spectroscopy. To this solution, PhI (0.8  $\mu\text{L}$ , 1.4 mg, 6.82  $\mu\text{mol}$ ) was added using a syringe and the tube was placed back in the oil bath. The reaction was monitored by  $^1\text{H}$  and  $^{31}\text{P}$  NMR spectroscopy and no changes were observed even after heating for 30 h. (**Figure III.25**)

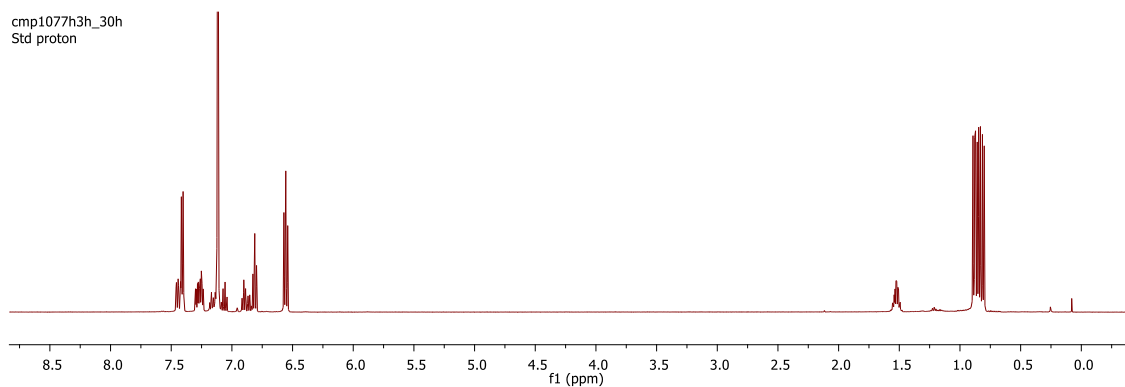


**Figure III.25**  $^1\text{H}$  NMR spectrum of attempted thermolysis of **319** with PhI in  $\text{C}_6\text{D}_6$  after 30 h.

**Thermolysis of (POCOP)Co(Ph)(SPh) (316) with  $\text{PPh}_3$ .** (POCOP)Co(Ph)(SPh) (10 mg, 17.1  $\mu\text{mol}$ ) and  $\text{PPh}_3$  (4.51 mg, 17.1  $\mu\text{mol}$ ) were dissolved in ca. 600  $\mu\text{L}$  of  $\text{C}_6\text{D}_6$  in a

PTFE capped J. Young NMR tube. The NMR tube was then placed in an oil bath and the reaction was monitored by  $^1\text{H}$  and  $^{31}\text{P}$  NMR spectroscopy. After 30 mins of heating, 319 and free  $\text{PPh}_3$  was observed. The composition of the mixture didn't change upon continued heating for 6 h. (**Figure III.26** and **Figure III.27**)

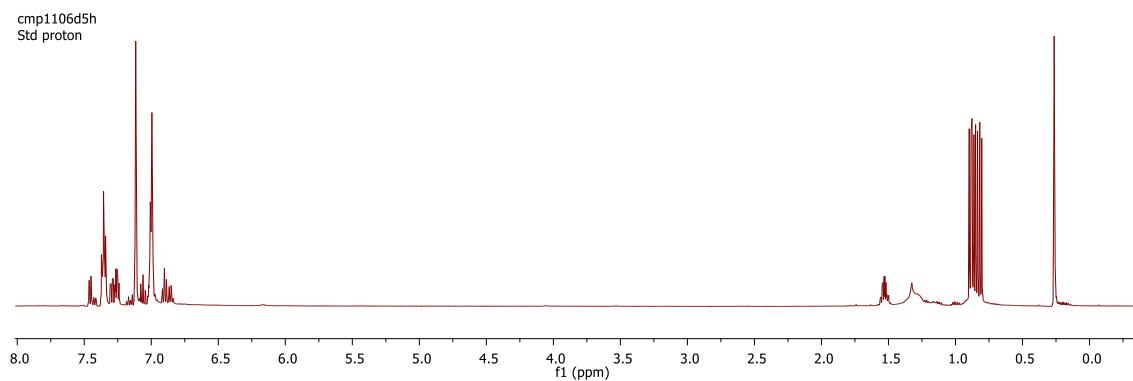


**Figure III.26**  $^1\text{H}$  NMR spectrum of thermolysis of  $(\text{POCOP})\text{Co}(\text{Ph})(\text{SPh})$  (**316**) with  $\text{PPh}_3$  in  $\text{C}_6\text{D}_6$  after 6 h. Trace pentane present.

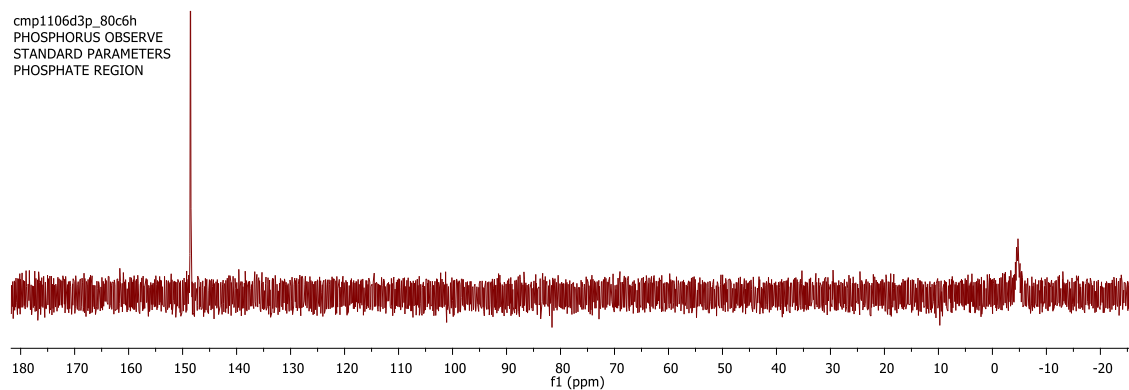


**Figure III.27**  $^{31}\text{P}$   $\{^1\text{H}\}$  NMR spectrum of thermolysis of  $(\text{POCOP})\text{Co}(\text{Ph})(\text{SPh})$  (**316**) with  $\text{PPh}_3$  in  $\text{C}_6\text{D}_6$  after 6 h.

**Hydrolysis of 319 and analysis of products.**  $(\text{POCOP})\text{Co}(\text{Ph})(\text{SPh})$  (18 mg, 30.9  $\mu\text{mol}$ ) and was dissolved in ca. 600  $\mu\text{L}$  of  $\text{C}_6\text{D}_6$  in a PTFE capped J. Young NMR tube. The NMR tube was then placed in an oil bath and the reaction was monitored by  $^1\text{H}$  and

$^{31}\text{P}$  NMR spectroscopy. After 30 mins of heating, **319** was confirmed as the only product. The volatiles were removed and the obtained brown solid was dissolved in ca. 2 mL of  $\text{CH}_2\text{Cl}_2$ . The solution was then washed 3x 2 mL of dilute HCl followed by washing with 3 x 2 mL of distilled water. The organic phase was separated and the volatiles were removed. The solids were dissolved in  $\text{CH}_2\text{Cl}_2$  and filtered through a plug of silica on a glass frit. A colorless solution was obtained from which volatiles were removed to give a waxy solid **320** (4 mg, 69% yield). **320** was determined to be 2-phenylresorcinol based on  $^1\text{H}$  and  $^{13}\text{C}$  NMR spectroscopy (**Figure III.28** and **Figure III.29**) and ESI-MS (**Figure III.30**).

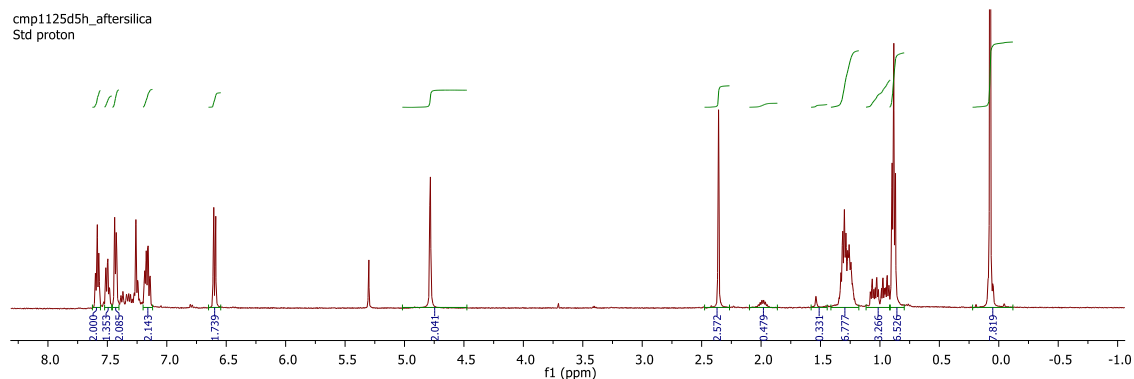


**Figure III.28**  $^1\text{H}$  NMR spectrum of **319** in  $\text{CDCl}_3$ . Trace pentane present

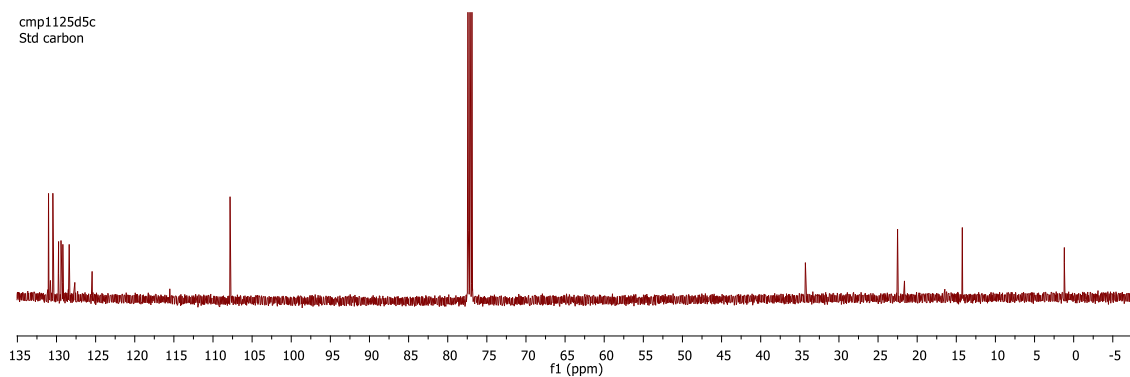


**Figure III.29**  $^{13}\text{C}\{^1\text{H}\}$  NMR spectrum of **319** in  $\text{CDCl}_3$ . Trace pentane present.

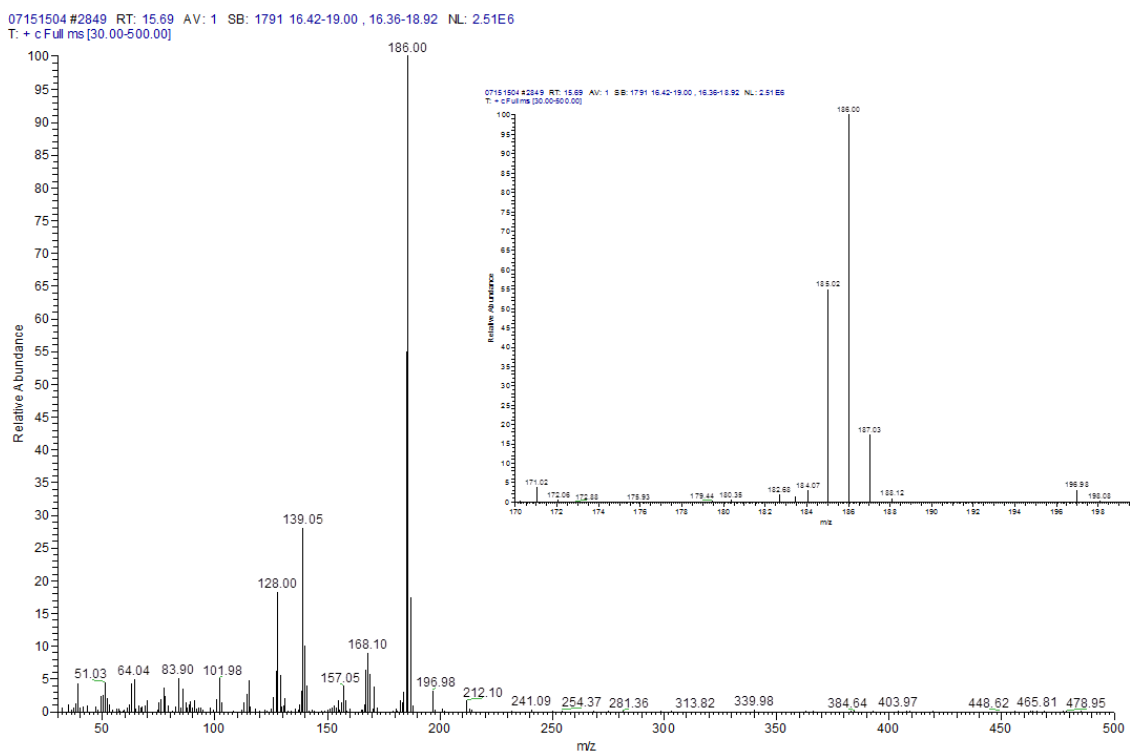


**Figure III.30** ESI-MS of a solution of **319** in  $\text{CDCl}_3$ .  $M/Z^+ = 186$  corresponds to 2-phenylresorcinol

### 3.4.7. X-ray crystallography

**X-Ray data collection, solution, and refinement for (POCOP)Co(SPh) (309).** A single orange crystal of suitable size and quality ( $0.06 \times 0.08 \times 0.10$  mm) was selected

from a representative sample of crystals of the same habit using an optical microscope, mounted onto a nylon loop and placed in a cold stream of nitrogen (110 K). Low-temperature X-ray data were obtained on a Bruker APEXII CCD based diffractometer (Mo sealed X-ray tube,  $K_{\alpha} = 0.71073 \text{ \AA}$ ). All diffractometer manipulations, including data collection, integration and scaling were carried out using the Bruker APEXII software.<sup>181</sup> An absorption correction was applied using SADABS.<sup>182</sup> The space group was determined on the basis of systematic absences and intensity statistics and the structure was solved by direct methods and refined by full-matrix least squares on  $F^2$ . The structure was solved in the monoclinic P 21/c space group using XS<sup>183</sup> (incorporated in X-Seed). This symmetry was confirmed by PLATON.<sup>184</sup> All non-hydrogen atoms were refined with anisotropic thermal parameters. Hydrogen atoms were placed in idealized positions and refined using riding model. The structure was refined (weighted least squares refinement on  $F^2$ ) to convergence.

**X-Ray data collection, solution, and refinement for (POCOP)Co(Cl)<sub>2</sub> (311).** A single green crystal of suitable size and quality ( $0.08 \times 0.05 \times 0.03 \text{ mm}$ ) was selected from a representative sample of crystals of the same habit using an optical microscope, mounted onto a nylon loop and placed in a cold stream of nitrogen (110 K). Low-temperature X-ray data were obtained on a Bruker APEXII CCD based diffractometer (Mo sealed X-ray tube,  $K_{\alpha} = 0.71073 \text{ \AA}$ ). All diffractometer manipulations, including data collection, integration and scaling were carried out using the Bruker APEXII software.<sup>181</sup> An absorption correction was applied using SADABS.<sup>182</sup> The space group was determined on the basis of systematic absences and intensity statistics and the structure was solved by

direct methods and refined by full-matrix least squares on  $F^2$ . The structure was solved in the orthorhombic  $P_{bca}$  space group using XS<sup>183</sup> (incorporated in X-Seed). This symmetry was confirmed by PLATON.<sup>184</sup> All non-hydrogen atoms were refined with anisotropic thermal parameters. Hydrogen atoms were placed in idealized positions and refined using riding model. The structure was refined (weighted least squares refinement on  $F^2$ ) to convergence. The check cif report indicates one Level B alert (RINTA01), which is most likely due to the quality of the data or the crystal.

**X-Ray data collection, solution, and refinement for (POCOP)Co(Cl)<sub>2</sub>(PMe<sub>3</sub>) (312).** A green, multi-faceted crystal of suitable size and quality (0.14 x 0.07 x 0.03 mm) was selected using an optical microscope and mounted onto a nylon loop. Low temperature (110 K) X-ray data were obtained on a Bruker APEXII CCD based diffractometer (Mo sealed X-ray tube,  $K_{\alpha} = 0.71073 \text{ \AA}$ ). All diffractometer manipulations, including data collection, integration and scaling were carried out using the Bruker APEXII software.<sup>181</sup> An absorption correction was applied using SADABS.<sup>182</sup> The structure was initially solved in the orthorhombic  $P_{212121}$  space group using XS<sup>183</sup> (incorporated in SHELXTL). The solution was refined by full-matrix least squares on  $F^2$ . No additional symmetry was found using ADDSYMM incorporated into the PLATON program.<sup>184</sup> All non-hydrogen atoms were refined with anisotropic thermal parameters. All hydrogen atoms on the main residue were placed in idealized positions and refined using a riding model. The structure was refined (weighted least squares refinement on  $F^2$ ) and the final least-squares refinement converged to  $R_1 = 0.0382$  ( $I > 2\sigma(I)$ , 5140 data) and  $wR_2 = 0.1012$  ( $F^2$ , 6087 data, 272 parameters).

### **X-Ray data collection, solution, and refinement for (POCOP)Co(Ph)(I) (315).**

A green, multi-faceted crystal of suitable size and quality (0.09 x 0.06 x 0.04 mm) was selected using an optical microscope and mounted onto a nylon loop. Low temperature (150 K) X-ray data were obtained on a Bruker APEXII CCD based diffractometer (Mo sealed X-ray tube,  $K_{\alpha} = 0.71073 \text{ \AA}$ ). All diffractometer manipulations, including data collection, integration and scaling were carried out using the Bruker APEXII software.<sup>181</sup> An absorption correction was applied using SADABS.<sup>182</sup> The structure was initially solved in the monoclinic  $P_{21/n}$  space group using XS<sup>183</sup> (incorporated in SHELXTL). The solution was refined by full-matrix least squares on  $F^2$ . No additional symmetry was found using ADDSYMM incorporated into the PLATON program.<sup>184</sup> All non-hydrogen atoms were refined with anisotropic thermal parameters. All hydrogen atoms on the main residue were placed in idealized positions and refined using a riding model. The structure was refined (weighted least squares refinement on  $F^2$ ) and the final least-squares refinement converged to  $R_1 = 0.0404$  ( $I > 2\sigma(I)$ , 5597 data) and  $wR_2 = 0.1062$  ( $F^2$ , 6849 data, 278 parameters).

### **X-Ray data collection, solution, and refinement for (POCOP)Co(Ph)(SPh) (316).**

A dark red, multi-faceted crystal of suitable size and quality (0.08 x 0.06 x 0.04 mm) was selected using an optical microscope and mounted onto a nylon loop. Low temperature (150 K) X-ray data were obtained on a Bruker APEXII CCD based diffractometer (Mo sealed X-ray tube,  $K_{\alpha} = 0.71073 \text{ \AA}$ ). All diffractometer manipulations, including data collection, integration and scaling were carried out using the Bruker APEXII software.<sup>181</sup> An absorption correction was applied using SADABS.<sup>182</sup> The structure was initially



solved in the monoclinic  $P_{21/c}$  space group using XS<sup>183</sup> (incorporated in SHELXTL). The solution was refined by full-matrix least squares on  $F^2$ . No additional symmetry was found using ADDSYMM incorporated into the PLATON program.<sup>184</sup> All non-hydrogen atoms were refined with anisotropic thermal parameters. The structure was refined (weighted least squares refinement on  $F^2$ ) and the final least-squares refinement converged to  $R_1 = 0.0348$  ( $I > 2\sigma(I)$ , 5592 data) and  $wR_2 = 0.0929$  ( $F^2$ , 7005 data, 333 parameters).

## CHAPTER IV

### COBALT COMPLEXES OF PNP LIGANDS AND OBSERVATION OF C-S COUPLING

#### 4.1. Introduction

In the previous chapter about the chemistry of (POCOP)Co complexes, we discussed the attempted C-S RE of the C<sub>Ph</sub> and S-Ph from (POCOP)Co(Ph)(SPh). Our observations in the POCOP systems suggest C<sub>Ph</sub>-C<sub>ligand</sub> RE to be the dominant outcome of the thermolysis of (POCOP)Co(Ph)(SPh). We hypothesize that this is due to the faster rate of C-C RE vs C-S RE.<sup>89</sup> In order to overcome this, we envision that the use of pincer ligands with a nitrogen central atom might prove beneficial, since the rates of C-S RE for aryl-thiolato complexes were found to be similar to, or faster than, those of the aryl-amido complexes of Pd<sup>II</sup> with the same ancillary DPPF ligands in a study by Hartwig.<sup>185</sup> First examples of cobalt complexes with (FryPNP) ligands were reported by Fryzuk and co-workers.<sup>15</sup> (<sup>Me</sup>PNP<sup>iPr</sup>)Cobalt complexes with diarylamido based PNP ligands, such as (<sup>Me</sup>PNP<sup>iPr</sup>)CoCl, (<sup>Me</sup>PNP<sup>iPr</sup>)CoO<sup>t</sup>Bu and (<sup>Me</sup>PNP<sup>iPr</sup>)Co(Bpin) have been previously reported by Mindiola et.al..<sup>186,176</sup> In addition, pyridine based (PNP)Co complexes have been reported by Chirik and coworkers<sup>187</sup> and have been used for C-H activation.<sup>188</sup> Additionally (aliPNP) ligands with aliphatic backbones have been used recently for hydrogenation,<sup>189,190</sup> dehydrogenation,<sup>191</sup> and N-alkylation.<sup>192</sup> (**Figure IV.1**) Due to our extensive expertise with the use of diarylamido based PNP ligands, and since their utility in catalytic reactions with Co has been scarcely explored, they were chosen over aliPNP or FryPNP, as the ligands of choice with central nitrogen donors for our experiments.

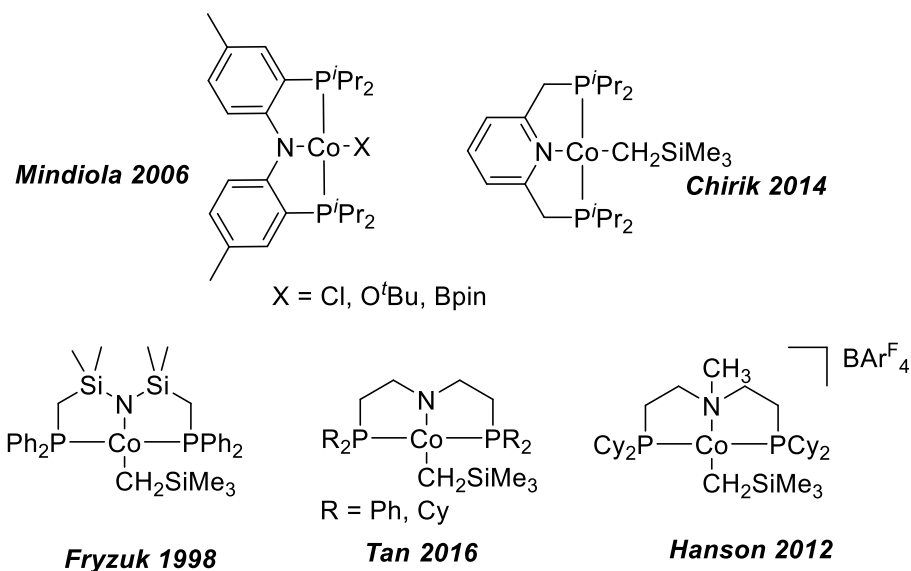


**Figure IV.1** Previously reported complexes of cobalt with PNP ligands

## 4.2. Results and discussions

### 4.2.1. Synthesis of PNP complexes of Co<sup>II</sup>

The diarylamido based PNP ligand and its lithium salt were prepared according to procedures previously published by our group.<sup>2,24,193</sup> (<sup>Me</sup>PNP<sup>iPr</sup>)CoCl (**401**) was synthesized by the procedure described by Mindiola and coworkers.<sup>176</sup> (<sup>Me</sup>PNP<sup>iPr</sup>)CoPh (**402**) was easily obtained by the reaction of **401** with an equivalent of PhLi. (**Figure IV.2 (a)**) (PNP)Co<sup>II</sup> thiolate compounds (<sup>Me</sup>PNP<sup>iPr</sup>)Co(SAr) (Ar = Ph (**404**), C<sub>6</sub>H<sub>4</sub>F-p (**405**)) were synthesized by the salt metathesis reactions of **401** with NaSAr. (**Figure IV.2 (b)**) In order to test the effect of sterics on the RE studies, a ligand with one of the diisopropylphosphino side arms replaced with diethylphosphino group was envisioned. The synthesis of the lithium salt of the asymmetric ligand (<sup>Me</sup>PN(Li)P<sup>Et,<sup>i</sup>Pr</sup>) (**413**) was carried out by Bryan Foley, a graduate student in the Ozerov group. Using **413**,

$(^{\text{Me}}\text{PNP}^{\text{Et},i\text{Pr}})\text{CoCl}$  (**414**),  $(^{\text{Me}}\text{PNP}^{\text{Et},i\text{Pr}})\text{Co}(\text{Ph})$  (**415**),  $(^{\text{Me}}\text{PNP}^{\text{Et},i\text{Pr}})\text{Co}(\text{SPh})$  (**416**) were synthesized with methods similar to that for the  $^{\text{Me}}\text{PNP}^{i\text{Pr}}$  ligand.

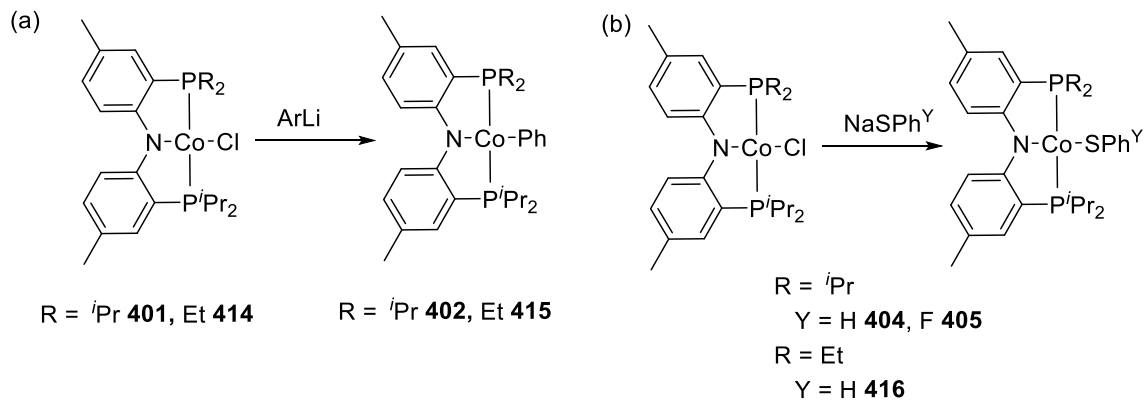


**Figure IV.2** Synthesis of  $(^{\text{Me}}\text{PNP}^{i\text{Pr}})\text{Co}^{\text{II}}$  complexes

#### 4.2.2. Synthesis of PNP complexes of Cobalt<sup>III</sup>

Cobalt<sup>III</sup> complexes with the PNP ligand were obtained in ways analogous to the ones described with our POCOP ligand in the previous chapter.  $(^{\text{Me}}\text{PNP}^{i\text{Pr}})\text{Co}(\text{Ph})(\text{OAc})$  (**406**) was obtained by the oxidation of **402** using 0.55 equivalents of the 2 e<sup>-</sup> oxidant  $\text{PhI}(\text{OAc})_2$ . Replacement of the acetate ion from **402** by oxophilic silyl reagents of the type  $\text{Me}_3\text{SiX}$  ( $\text{X} = \text{Cl}, \text{I}$ ) afforded catalytically relevant  $\text{Co}^{\text{III}}(\text{ary})(\text{halide})$  complexes  $(^{\text{Me}}\text{PNP}^{i\text{Pr}})\text{Co}(\text{Ph})(\text{X})$  ( $\text{X} = \text{Cl}$  (**407**), I (**408**)). (**Figure IV.3**) The asymmetric analogs  $(^{\text{Me}}\text{PNP}^{\text{Et},i\text{Pr}})\text{Co}(\text{Ph})(\text{I})$  (**417**), and  $(^{\text{Me}}\text{PNP}^{\text{Et},i\text{Pr}})\text{Co}(\text{Ph})(\text{SPh})$  (**418**) were also synthesized using similar procedures from **415**.

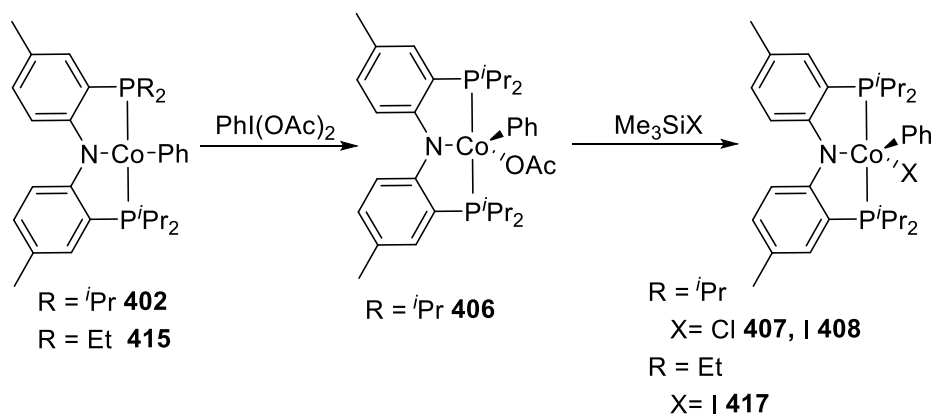


**Figure IV.3** Synthesis of  $(^{\text{Me}}\text{PNP}^i\text{Pr})\text{Co}(\text{Ph})(\text{X})$  complexes

Our attempt to isolate complexes of the type  $(^{\text{Me}}\text{PNP}^i\text{Pr})\text{Co}(\text{Ph})(\text{Ph})$  (**419**) by reaction of **406** with PhLi were unsuccessful, in a fashion similar to that for  $(\text{POCOP})\text{Co}$ , with the only products being  $(^{\text{Me}}\text{PNP}^i\text{Pr})\text{Co}(\text{Ph})$  (**402**) and biphenyl. (**Figure IV.4(a)**) The presence of biphenyl can be (a) due to spontaneous RE of Ph-Ph from **419** or (b) due to elimination of a  $\text{Ph}\cdot$  and subsequent attack of  $\text{Ph}\cdot$  on **419** to produce Ph-Ph and **402**. RE of Ph-Ph from **419** is an exciting prospect but more experiments need to be done to identify the mechanism of formation of Ph-Ph. Phenyl thiophenolato complexes of the type  $(^{\text{Me}}\text{PNP}^i\text{Pr})\text{Co}(\text{Ph})(\text{SAr})$  ( $\text{Ar} = \text{H}$  (**410**);  $\text{C}_6\text{H}_4\text{F}-p$  (**411**)) however, were easily synthesized by reaction of  $(^{\text{Me}}\text{PNP}^i\text{Pr})\text{Co}(\text{Ph})(\text{I})$  (**408**) with NaSAr. (**Figure IV.4 (b)**)

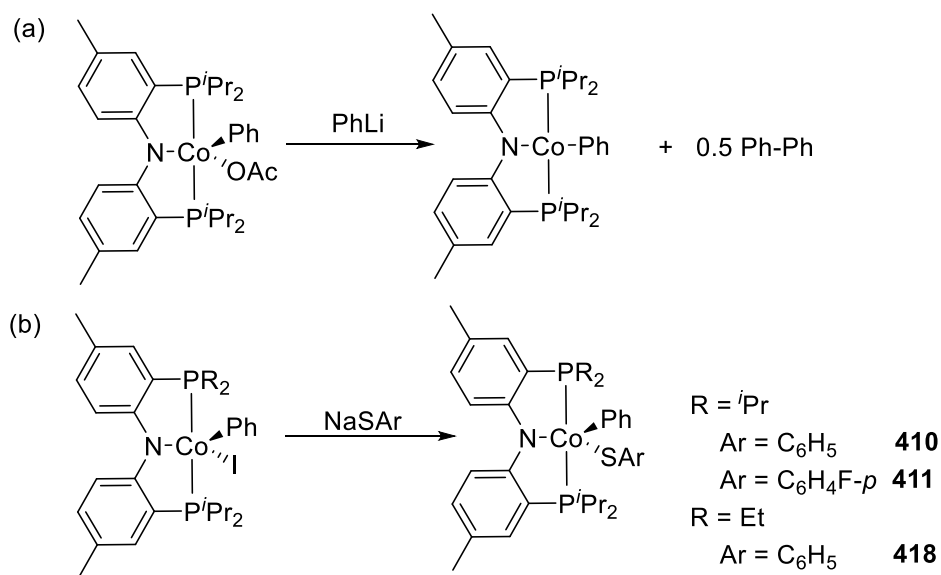


**Figure IV.4** (a) Attempt at synthesis of (<sup>Me</sup>PNP<sup>iPr</sup>)Co(Ph)(Ph) (b) Synthesis of (<sup>Me</sup>PNP<sup>iPr</sup>)Co(Ph)(SAr)

#### 4.2.3. Structure discussion

The structure of (<sup>Me</sup>PNP<sup>iPr</sup>)Co(Ph)(OAc) (**406**) was unambiguously determined from crystals grown from a pentane solution at -35 °C. **406** was observed to crystallize in the monoclinic system with the C<sub>2/c</sub> space group yielding light purple crystals. The ligands attain a distorted octahedral geometry around the Co center, with the acetate binding in a κ<sup>2</sup> fashion using both its oxygens to bind to Co. (**Figure IV.5**) The bond lengths to each O is slightly different with Co1-O1 being 1.990 Å and Co1-O2 was slightly longer at 2.117 Å. This aligns well with the fact that O2 is positioned *trans* to a more *trans* influencing aryl ligand where as O1 is *trans* to an amide ligand.

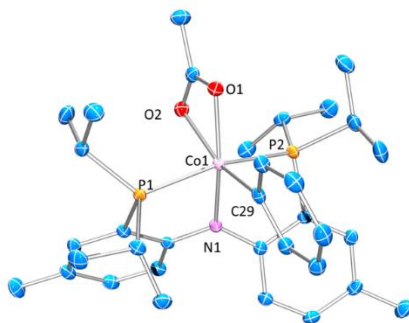


**Figure IV.5** ORTEP drawing (50% probability ellipsoids) of  $(^{\text{Me}}\text{PNP}^{\text{iPr}})\text{Co}(\text{Ph})(\text{OAc})$  (**406**). Select atom labeling. Hydrogen atoms are omitted for clarity. Selected bond distances (Å) and angles (deg) for **406** follow: Co1-P1, 2.2619(7); Co1-P2, 2.2353(6); Co1-O1, 1.990(1); Co1-O2, 2.117(1); Co1-N1, 1.933(1); Co1-C29, 1.940(1); P1-Co1-P2, 165.63(3); N1-Co1-C29, 97.59(5); O2-Co1-N1, 101.59(5); O1-Co1-N1, 165.17(5).

#### 4.2.4. Thermolysis experiments

Thermolysis of  $(^{\text{Me}}\text{PNP}^{\text{iPr}})\text{Co}(\text{Ph})(\text{SPh})$  (**410**) in  $\text{C}_6\text{D}_6$  at 80 °C, shows complete conversion of  $(^{\text{Me}}\text{PNP}^{\text{iPr}})\text{Co}(\text{Ph})$  (46% of initial  $(^{\text{Me}}\text{PNP}^{\text{iPr}})\text{Co}(\text{Ph})(\text{SPh})$ ),  $(^{\text{Me}}\text{PNP}^{\text{iPr}})\text{Co}(\text{SPh})$  (46% of initial  $(^{\text{Me}}\text{PNP}^{\text{iPr}})\text{Co}(\text{Ph})(\text{SPh})$ ) and  $\text{SPh}_2$  (48% of initial  $(^{\text{Me}}\text{PNP}^{\text{iPr}})\text{Co}(\text{Ph})(\text{SPh})$ ). (**Figure IV.6**) The stoichiometric ratio of the observed products suggests production of  $\frac{1}{2}$  equivalent of  $\text{PhSPh}$  per equivalent of **410**. Thermolysis of the asymmetric and sterically less bulky **418** yielded observations analogous to those for the thermolysis of **410**. (**Figure IV.7**)

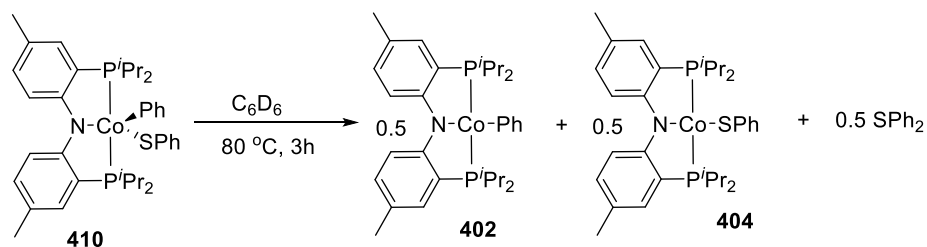


**Figure IV.6** Thermolysis of  $(^{\text{Me}}\text{PNP}^{\text{iPr}})\text{Co}(\text{Ph})(\text{SPh})$  (**410**)

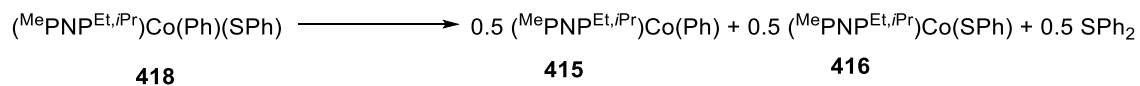


**Figure IV.7** Thermolysis of  $(\text{MePNP}^{\text{Et},i\text{Pr}})\text{Co}(\text{Ph})(\text{SPh})$  (**418**)

#### 4.2.5. Mechanistic studies

We hypothesize, that the production of 0.5 eq. of Ph-S-Ph per 1 eq. of  $(\text{MePNP}^{i\text{Pr}})\text{Co}(\text{Ph})(\text{SPh})$  can occur via one of two pathways (1) C-S RE from 1 equivalent of  $(\text{MePNP}^{i\text{Pr}})\text{Co}(\text{Ph})(\text{SPh})$  (**410**) to give  $(\text{MePNP}^{i\text{Pr}})\text{Co}^{\text{I}}$  and  $\text{SPh}_2$  and then the comproportionation of reactive  $\text{Co}^{\text{I}}$  with another equivalent of  $(\text{MePNP}^{i\text{Pr}})\text{Co}(\text{Ph})(\text{SPh})$  (**410**) to give 1 equivalent each of  $(\text{MePNP}^{i\text{Pr}})\text{Co}(\text{Ph})$  (**402**) and  $(\text{MePNP}^{i\text{Pr}})\text{Co}(\text{SPh})$  (**404**) (**Figure IV.8 (a)**) or (2) Two step formation of Ph-S-Ph from **410** via spontaneous reduction of  $\text{Co}^{\text{III}}$  to  $\text{Co}^{\text{II}}$  accompanied by the formation of either  $\text{PhS}\cdot$  or  $\text{Ph}\cdot$  followed by the reaction of these radicals with another equivalent of **410** to produce  $\text{SPh}_2$ . (**Figure IV.8 (b)**)



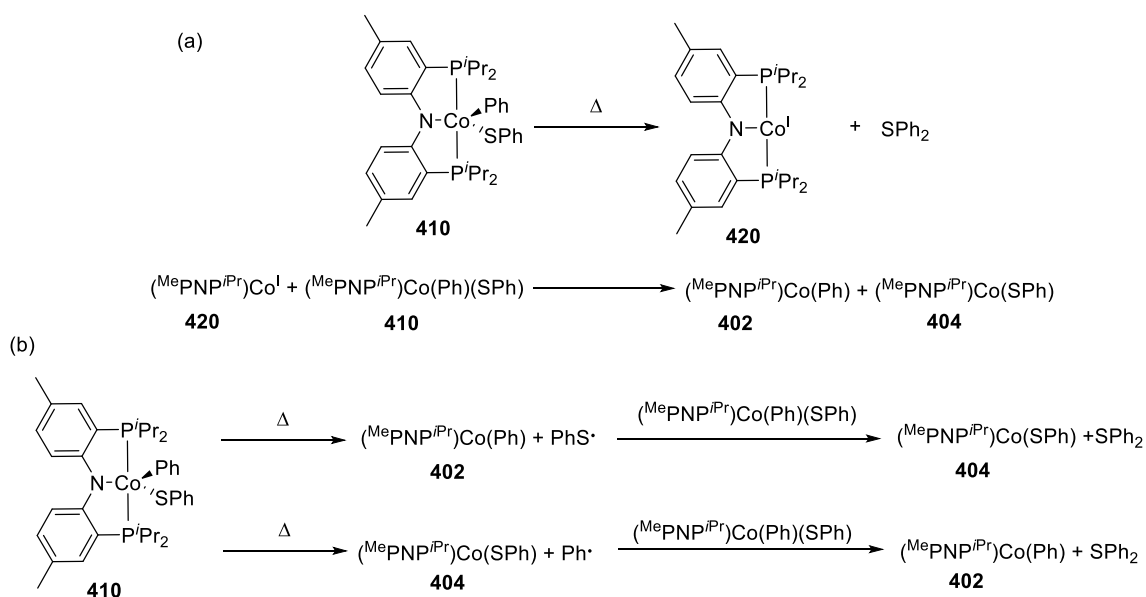


**Figure IV.8** Possibilities during thermolysis of  $(\text{MePNP}^{i\text{Pr}})\text{Co}(\text{Ph})(\text{SPh})$  (**410**)

Some evidence against a radical based mechanism was obtained by performing the thermolysis of **410** and **418** in the presence of an excess of the radical inhibitor, butylated hydroxytoluene (BHT), when the ratio of products obtained was almost identical to that of the thermolysis of **410** and **418** without any BHT, with the specific product ratios described in **Figure IV.9**.

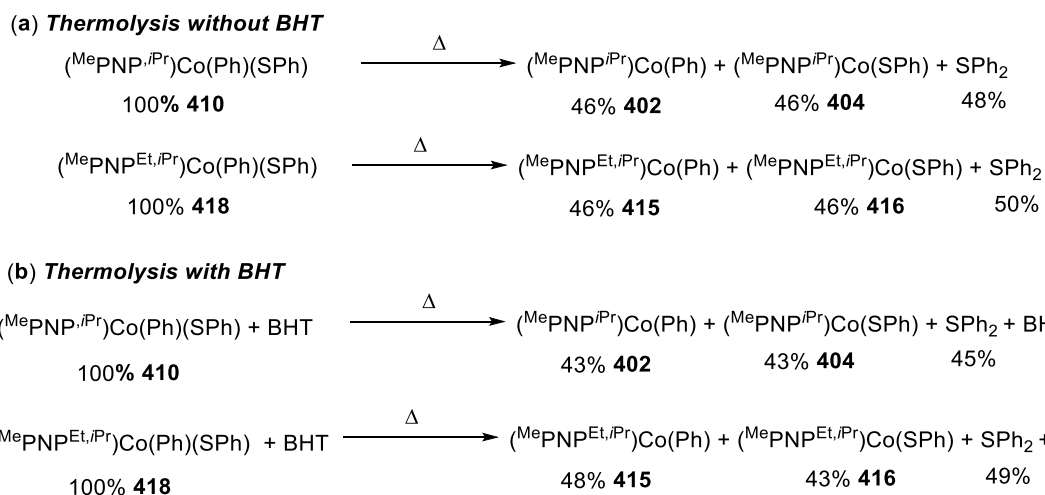


**Figure IV.9** Thermolysis of **410** and **418** (a) without BHT and (b) with BHT as a radical trap

Another experiment beneficial to eliminating the possibility of radical based mechanisms that was performed was the thermolysis of  $(\text{MePNP}^{i\text{Pr}})\text{Co}(\text{Ph})(\text{SC}_6\text{H}_4\text{F}-p)$  (**411**). We envision the possibility of reversible RE/OA of C-S bonds from **411** leading to the possible formation of the differently substituted  $(\text{MePNP}^{i\text{Pr}})\text{Co}(\text{Ar})(\text{SPh})$  as shown in **Figure IV.10 (a)**, This molecule can then interact with a molecule of  $(\text{MePNP}^{i\text{Pr}})\text{Co}(\text{Ph})(\text{SC}_6\text{H}_4\text{F}-p)$  leading to the formation of a combination of scrambling products possible in a radical based mechanism (**Figure IV.10 (b)**) However, upon thermolysis of  $(\text{MePNP}^{i\text{Pr}})\text{Co}(\text{Ph})(\text{SC}_6\text{H}_4\text{F}-p)$  (**411**), only  $(\text{MePNP}^{i\text{Pr}})\text{Co}(\text{Ph})$  (**402**),  $(\text{MePNP}^{i\text{Pr}})\text{Co}(\text{SC}_6\text{H}_4\text{F}-p)$  (**405**), and Ph-S-(C<sub>6</sub>H<sub>4</sub>F-*p*) are observed by <sup>1</sup>H and <sup>19</sup>F NMR spectroscopy (**Figure IV.10 (c)**). In order to further rule out radical based scrambling, a experiment such as the one described in **Figure IV.10 (b)** needs to be performed, formation of only Ph-S-Ar<sup>F</sup> as the only organic product being the desired observation.

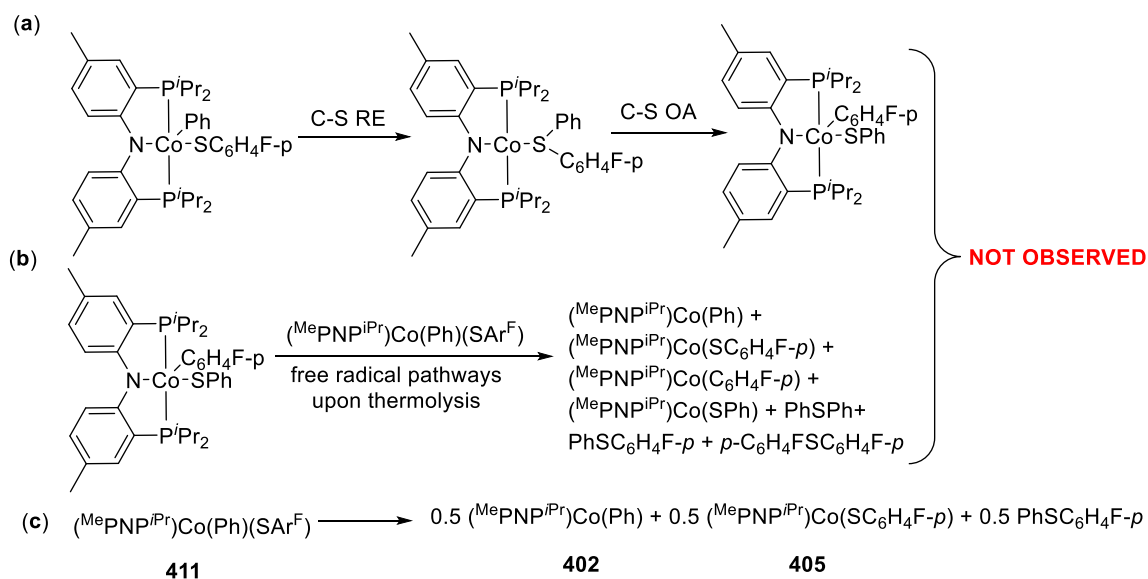


**Figure IV.10** Thermolysis of **411**, (a), (b) possibilities (c) observation from experiment

Another indication of the involvement of a  $(^{\text{Me}}\text{PNP}^{i\text{Pr}})\text{Co}^{\text{I}}$  intermediate (**420**) formed by C-S RE from  $(^{\text{Me}}\text{PNP}^{i\text{Pr}})\text{Co(Ph)(SPh)}$  (**410**) is that upon carrying the thermolysis of **410** with 100 eq of iodobenzene, 35% conversion to  $(^{\text{Me}}\text{PNP}^{i\text{Pr}})\text{Co(Ph)(I)}$  (**408**) was observed which indicates the possibility that the formation of  $(^{\text{Me}}\text{PNP}^{i\text{Pr}})\text{Co}^{\text{I}}$  is followed by two competing reactions namely, (a) the OA of PhI to give **408** and (b) comproportionation with **410** to give **402** and **404**. However, further experiments with a different Ar-X are warranted to confirm that **408** is indeed obtained from the OA of Ph-I to  $(^{\text{Me}}\text{PNP}^{i\text{Pr}})\text{Co}^{\text{I}}$ .

### 4.3. Conclusion and future experiments

In this project, PNP ligands were tested as alternatives to POCOP ligands to facilitate C-S RE from a  $\text{Co}^{\text{III}}(\text{Ph})(\text{SAr})$ . Use of nitrogen central donors indeed proved beneficial due to the production of 0.5 eq of Ph-S-Ar per equivalent of  $(\text{PNP})\text{Co}_2(\text{Ph})(\text{SAr})$ . However, further experiments are needed to ascertain that the source of Ph-S-Ar is C-S RE from  $(\text{PNP})\text{Co(Ph)(SAr)}$ . In addition, the production of Ph-S-Ar is accompanied by formation

of an equivalent each of (PNP)Co(Ph) and (PNP)Co(SAr) which are not a part of the catalytic cycle proposed in chapter 3, and whose origin is hypothesized to be the comproportionation of (PNP)Co<sup>I</sup> with (PNP)Co(Ph)(SAr). This comproportionation competes with the OA of Ar-X to (PNP)Co<sup>I</sup> to an extent that only 35% conversion to (PNP)Co(Ph)(I) is seen even with 100 eq of PhI. In order to overcome this reactivity and make possible the use of (PNP)Co complexes as catalysts, further experiments geared towards stabilizing the putative (PNP)Co<sup>I</sup> against comproportionation or making the RE of Ar-X to (PNP)Co<sup>I</sup> more dominant are warranted.

#### **4.4. Experimental details**

##### *4.4.1. General considerations*

Unless specified otherwise, all manipulations were performed under an argon atmosphere using standard Schlenk line or glove box techniques. Toluene, ethyl ether, and pentane were dried and deoxygenated (by purging) using a PureSolv solvent purification system by Innovative Technologies Inc. and stored over molecular sieves in an Ar-filled glove box. C<sub>6</sub>D<sub>6</sub> and THF were dried over and distilled from NaK/Ph<sub>2</sub>CO/18-crown-6 and stored over molecular sieves in an Ar-filled glove box. (MePNP<sup>iPr</sup>)CoCl (**401**)<sup>176</sup> and PNB<sup>r</sup><sup>27</sup> were prepared according to the published procedures. Sodium salts of thiophenols such as NaSPh and NaS-(C<sub>6</sub>H<sub>4</sub>F-p) were prepared by reacting the corresponding thiophenols with 1 eq. of NaH in THF followed by pumping down and washing with Et<sub>2</sub>O. All other chemicals were used as received from commercial vendors. NMR spectra were recorded on a Varian iNova 300 MHz, Bruker AvanceIII 400 MHz or a Varian iNova 500 MHz instrument. For <sup>1</sup>H and <sup>13</sup>C NMR spectra, the residual solvent peak was used as an

internal reference.  $^{31}\text{P}$  NMR spectra were referenced externally using 85%  $\text{H}_3\text{PO}_4$  at 0 ppm,  $^{19}\text{F}$  NMR spectra were referenced externally using trifluoroacetic acid at -78.5 ppm. Elemental analyses were performed by CALI, Inc. (Parsippany, NJ).

#### 4.4.2. Synthesis of $(^{\text{Me}}\text{PNP}^{\text{iPr}})\text{Co}^{\text{II}}$ complexes

**Synthesis of  $(^{\text{Me}}\text{PNP}^{\text{iPr}})\text{Co}(\text{Ph})$  (402).**  $(^{\text{Me}}\text{PNP}^{\text{iPr}})\text{Co}(\text{Cl})$  (401) (901 mg, 1.72 mmol) was dissolved in ca. 30 mL of toluene. To this solution PhLi (0.910 mL of 1.8 M in  $^{\text{n}}\text{Bu}_2\text{O}$ , 1.72 mmol) was added using a syringe. The solution changed color from deep blue to dark green over 10 mins. The reaction was left to stir for 1 h after which the solution was filtered through a pad of celite on a glass frit. The volatiles were pumped down, the green solid was re-dissolved in ca. 5 mL of toluene, layered with 10 mL of pentane and put in the freezer at  $-35\text{ }^\circ\text{C}$  overnight. Dark green crystalline solid (810 mg, 83% yield) was obtained.  $^1\text{H}$  ( $\text{C}_6\text{D}_6$ , 500 MHz,  $22\text{ }^\circ\text{C}$ ):  $\delta$  38.7 (overlapping br, 8H), 23.4 (br s, 4H), 14.9 (br s, 12H), 0.39 (br s, 17H), -14.0 (br s, 2H), -29.2 (br s, 1H), -93.0 (br s, 1H).

**Synthesis of  $(^{\text{Me}}\text{PNP}^{\text{iPr}})\text{Co}(\text{SPh})$  (404).**  $(^{\text{Me}}\text{PNP}^{\text{iPr}})\text{Co}(\text{Cl})$  (401) (52.2 mg, 0.098 mmol) was dissolved in ca. 10 mL of THF. To this solution NaSPh (13.1 mg, 0.098 mmol) was added. The solution changed color from deep blue to dark green over 30 mins. The reaction was left to stir for 1 h after which the volatiles were pumped down. The product was extracted with ca. 10 mL of pentane and filtered through a pad of celite on a glass frit. The volatiles were pumped down, and a green solid was obtained. (43 mg, 74% yield) was obtained.  $^1\text{H}$  ( $\text{C}_6\text{D}_6$ , 500 MHz,  $22\text{ }^\circ\text{C}$ ):  $\delta$  25.0 (br s, 6H), 23.6 (br s, 2H), 10.8 (br s, 2H), 9.42 (br s, 2H), 6.75 (br s, 4H), 4.03 (overlapping signals, 25 h), -10.4 (s, 2H), -20.3 (br s, 2H).

**Synthesis of  $(^{\text{Me}}\text{PNP}^{\text{iPr}})\text{Co}(\text{SAr}^{\text{F}})$  (405).**  $(^{\text{Me}}\text{PNP}^{\text{iPr}})\text{Co}(\text{Cl})$  (401) (90.1 mg, .172 mmol) was dissolved in ca. 10 mL of THF. To this solution  $\text{NaSAr}^{\text{F}}$  (28 mg, 0.189 mmol) was added. The solution changed color from deep blue to dark green over 30 mins. The reaction was left to stir for 1 h after which the volatiles were pumped down. The product was extracted with ca. 10 mL of pentane and filtered through a pad of celite on a glass frit. The volatiles were pumped down, and a green solid was obtained. (85 mg, 80% yield) was obtained.  $^1\text{H}$  ( $\text{C}_6\text{D}_6$ , 500 MHz, 22 °C):  $\delta$  25.4 (br s, 6H), 23.6 (br s, 2H), 10.9 (br s, 2H), 8.63 (br s, 2H), 6.46 (br s, 4H), 4.03 (br s, 24 h), -9.18 (s, 2H), -20.6 (br s, 2H).  $^{19}\text{F}$  ( $\text{C}_6\text{D}_6$ , 470 MHz, 22 °C):  $\delta$  -117.4 (br s). Elem. Anal. Calc. for  $\text{C}_{32}\text{H}_{44}\text{CoFNP}_2\text{S}$ : C, 62.53; H, 7.22; N, 2.28. Found: C, 62.08; H, 7.19; N, 2.06.

#### 4.4.3. Synthesis of $(^{\text{Me}}\text{PNP}^{\text{iPr}})\text{Co}^{\text{III}}$ complexes

**Synthesis of  $(^{\text{Me}}\text{PNP}^{\text{iPr}})\text{Co}(\text{Ph})(\text{OAc})$  (406).**  $(^{\text{Me}}\text{PNP})\text{Co}(\text{Ph})$  (402) (120 mg, 0.212 mmol) was dissolved in ca. 10 mL of  $\text{C}_6\text{H}_6$ . To this solution  $\text{PhI}(\text{OAc})_2$  (37 mg, 0.110 mmol) was added and the reaction was left to stir for 20 h. The volatiles were then removed and the product was extracted with 30 mL of pentane and filtered through a pad of celite on a glass frit. The volatiles were removed and a tan solid was obtained (110 mg, 83%). The solid was then redissolved in minimal amount of pentane and put in the freezer at -35 °C overnight. Light purple crystals were obtained and a single crystal was selected for X-ray diffraction.  $^1\text{H}$  ( $\text{C}_6\text{D}_6$ , 500 MHz, 22 °C):  $\delta$  7.45 (d,  $J = 8.5$  Hz, 2 H, Ar-*H*), 7.04 (d,  $J = 8.0$  Hz, 1 H, Ph-*ortho-H*), 6.99 (m, 2 H, Ar-*H*), 6.92 (td,  $J = 7.5$  Hz, 2 Hz, 1H, Ph-*meta-H*), 6.92 (t,  $J = 7.0$  Hz, 1H, Ph-*para-H*), 6.78 (td,  $J = 7.0$  Hz, 2 Hz, 1H, Ph-*meta-H*), 6.65 (dd,  $J = 7.0$  Hz, 1.5 Hz, 2H, Ar-*H*), 6.61 (d,  $J = 8.5$  Hz, 1 H, Ph-*ortho-H*), 2.47 (m, 2H,

CHMe<sub>2</sub>), 2.14 (overlapped m, 8 H, CHMe<sub>2</sub> (2H) and Ar-CH<sub>3</sub> (6H)), 1.68 (s, 3H, OC(=O)CH<sub>3</sub>), 1.35 (q, J= 7.5 Hz, 6 H, CHMe<sub>2</sub>), 1.27 (q, J= 6.5 Hz, 6 H, CHMe<sub>2</sub>), 1.03 (q, J= 7.5 Hz, 6 H, CHMe<sub>2</sub>), 0.58 (q, J= 7.0 Hz, 6 H, CHMe<sub>2</sub>). **(Figure IV.11)** <sup>13</sup>C{<sup>1</sup>H} (C<sub>6</sub>D<sub>6</sub>, 126 MHz, 22 °C): δ 183.2 (t, J= 1.8 Hz, OC(=O)CH<sub>3</sub>), 159.3 (t, J= 10.8 Hz, Co-C<sub>Ph</sub>), 140.4 (Ar-C), 135.6 (Ar-C), 131.84 (Ar-C), 125.9 (Ph-*meta*-C), 124.7 (t, J= 3.0 Hz, Ph-*ortho*-C), 124.6 (Ph-*meta*-C), 123.2 (Ph-*para*-C), 123.0 (Ar-C), 122.9 (Ar-C), 122.7 (Ar-C), 119.8 (t, J= 4.5 Hz, Ph-*ortho*-C), 23.8 (t, J= 10.6 Hz, CHMe<sub>2</sub>), 23.0 (Ar-CH<sub>3</sub>), 22.6 (t, J= 7.6 Hz, CHMe<sub>2</sub>), 20.7 (OC(=O)CH<sub>3</sub>), 19.2 (t, J = 2.0 Hz, CHMe<sub>2</sub>), 18.6 (br s, CHMe<sub>2</sub>), 17.8 (br s, CHMe<sub>2</sub>). **(Figure IV.12)** <sup>31</sup>P{<sup>1</sup>H} (C<sub>6</sub>D<sub>6</sub>, 126 MHz, 22 °C): δ 40.0 (br s).

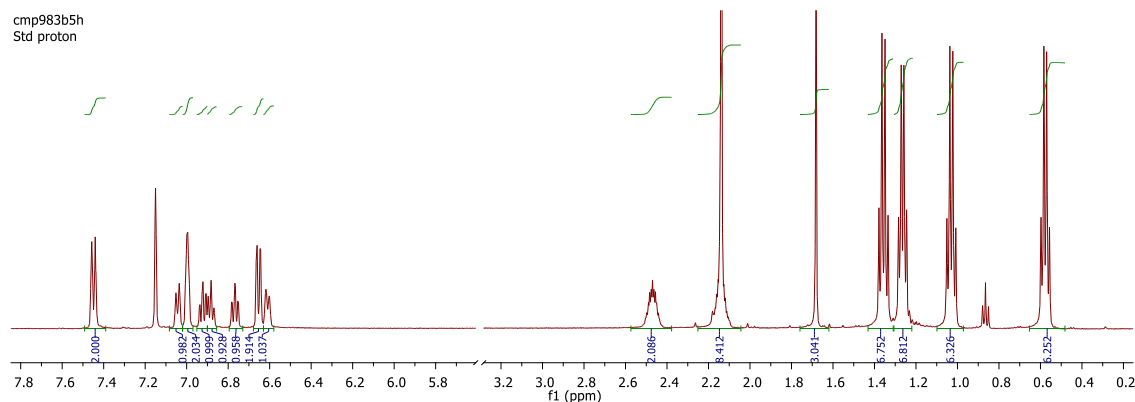


**Figure IV.11** <sup>1</sup>H NMR of (MePNP<sup>i</sup>Pr)Co(Ph)(OAc) (**406**) in C<sub>6</sub>D<sub>6</sub>

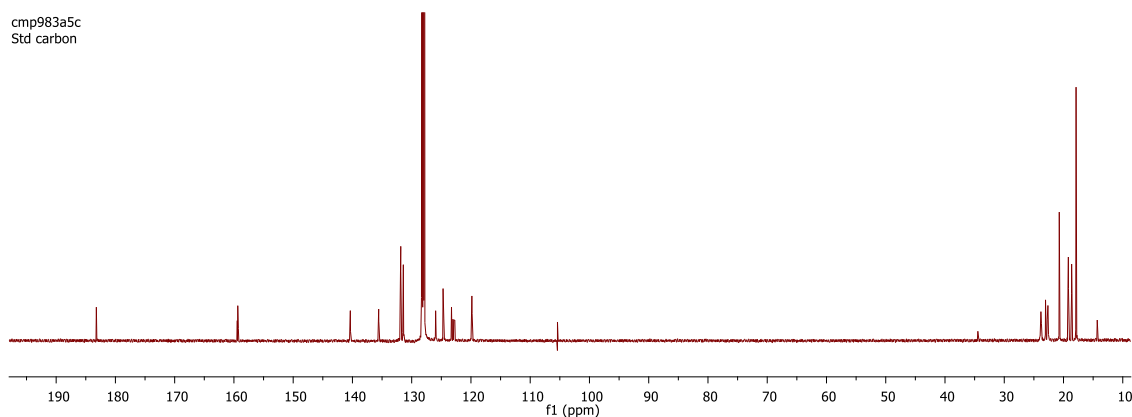


**Figure IV.12**  $^{13}\text{C}\{^1\text{H}\}$  NMR of  $(^{\text{Me}}\text{PNP}^{\text{iPr}})\text{Co}(\text{Ph})(\text{OAc})$  (**406**) in  $\text{C}_6\text{D}_6$

**Synthesis of  $(^{\text{Me}}\text{PNP}^{\text{iPr}})\text{Co}(\text{Ph})(\text{Cl})$  (**407**).**  $(^{\text{Me}}\text{PNP}^{\text{iPr}})\text{Co}(\text{Ph})(\text{OAc})$  (**406**) (14 mg, 0.022 mmol) was dissolved in ca. 5 mL of pentane. To this solution  $\text{Me}_3\text{SiCl}$  (3.1  $\mu\text{L}$ , 2.5 mg, 0.022 mmol) was added and the reaction was left to stir for 12 h. The volatiles were then removed and the product was extracted with ca. 5 mL of pentane and filtered through a pad of celite on a glass frit. The volatiles were removed and a blue-green solid was obtained (10 mg, 76%).  $^1\text{H}$  ( $\text{C}_6\text{D}_6$ , 500 MHz, 22  $^\circ\text{C}$ ):  $\delta$  7.77 (d,  $J = 8.5$  Hz, 2 H, Ar-*H*), 7.3 (d,  $J = 8.5$  Hz, 1 H, Ph-*ortho-H*), 7.12 (s, 2H, Ar-*H*), 6.71 (d,  $J = 8.5$  Hz, 2 H, Ar-*H*), 6.60 (t,  $J = 7.0$  Hz, 1H, Ph-*para-H*), 6.52 (td,  $J = 7.0$  Hz, 1.5 Hz, 1H, Ph-*meta-H*), 6.25 (td,  $J = 7.0$  Hz, 1.5 Hz, 1H, Ph-*meta-H*), 5.92 (d,  $J = 8.0$  Hz, 1H, Ph-*ortho-H*), 3.39 (m, 2H,  $\text{CHMe}_2$ ), 2.41 (m, 2 H,  $\text{CHMe}_2$ ), 2.15 (s, 6H, Ar- $\text{CH}_3$ ), 1.50 (m,  $J = 5.0$  Hz, 6 H,  $\text{CHMe}_2$ ), 1.16 (m,  $J = 6.0$  Hz, 6 H,  $\text{CHMe}_2$ ), 0.95 (m,  $J = 5.0$  Hz, 6 H,  $\text{CHMe}_2$ ), 0.39 (m,  $J = 5.0$  Hz, 6 H,  $\text{CHMe}_2$ ). **(Figure IV.13)**  $^{13}\text{C}\{^1\text{H}\}$  ( $\text{C}_6\text{D}_6$ , 126 MHz, 22  $^\circ\text{C}$ ):  $\delta$  161.8 (br, Co- $\text{C}_{\text{Ph}}$ ), 145.4 (Ar- $\text{C}$ ), 138.3 (Ar- $\text{C}$ ), 132.3 (Ar- $\text{C}$ ), 131.3 (overlapped Ar- $\text{C}$ , Ph-*ortho-C*), 125.7 (Ar- $\text{C}$ ), 124.9 (Ph- $\text{C}$ ), 123.9 (Ph- $\text{C}$ ), 122.4 (Ph- $\text{C}$ ), 122.2 (t,  $J = 4.5$  Hz, Ph-*ortho-C*), 24.8



(br, CHMe<sub>2</sub>), 24.3 (br, CHMe<sub>2</sub>), 20.4 (Ar-CH<sub>3</sub>), 19.2 (br s, CHMe<sub>2</sub>), 17.6 (br s, CHMe<sub>2</sub>), 17.2 (br s, CHMe<sub>2</sub>), 17.1 (br s, CHMe<sub>2</sub>). (**Figure IV.14**)

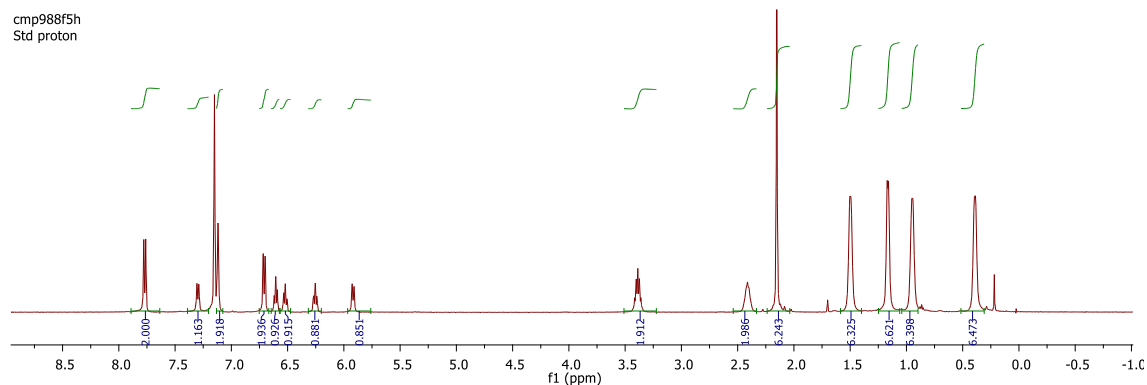


**Figure IV.13** <sup>1</sup>H NMR of (MePNP<sup>i</sup>Pr)Co(Ph)(Cl) (**407**) in C<sub>6</sub>D<sub>6</sub>

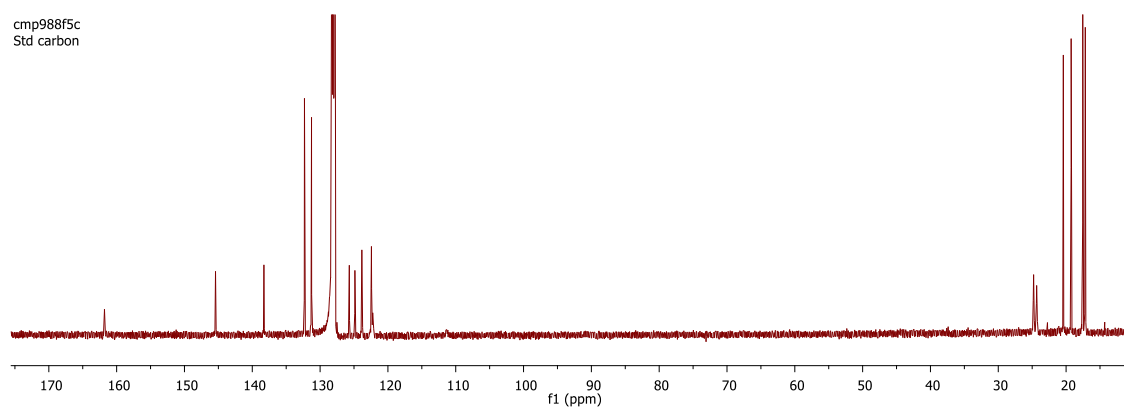


**Figure IV.14** <sup>13</sup>C{<sup>1</sup>H} NMR of (MePNP<sup>i</sup>Pr)Co(Ph)(Cl) (**407**) in C<sub>6</sub>D<sub>6</sub>

**Synthesis of (MePNP<sup>i</sup>Pr)Co(Ph)(I) (408).** (MePNP)Co(Ph)(OAc) (**406**) (100 mg, 0.161 mmol) was dissolved in ca. 10 mL of 1:1 mixture of toluene/C<sub>6</sub>H<sub>6</sub>. To this solution Me<sub>3</sub>SiI (23.1 μL, 32.2 mg, 0.161 mmol) was added and the reaction was left to stir for 1 h. The volatiles were then removed and the product was extracted with ca. 30 mL of pentane and filtered through a pad of celite on a glass frit. The volatiles were removed and a blue-green solid was obtained (101 mg, 90%). <sup>1</sup>H (C<sub>6</sub>D<sub>6</sub>, 500 MHz, 22 °C): δ 7.85 (d, J = 9.0 Hz, 2

H, Ar-H), 7.17 (overlapped m, 3 H, Ph-ortho-H and Ar-H), 6.71 (dd, J = 8.5 Hz, 1.0 Hz, 2 H, Ar-H), 6.51 (t, J = 7.5 Hz, 1H, Ph-para-H), 6.37 (td, J = 7.0 Hz, 1.0 Hz, 1H, Ph-meta-H), 6.13 (td, J = 7.0 Hz, 1.0 Hz, 1H, Ph-meta-H), 5.91 (d, J = 8.5 Hz, 1H, Ph-ortho-H), 4.05 (m, 2H, CHMe<sub>2</sub>), 2.67 (m, 2 H, CHMe<sub>2</sub>), 2.10 (s, 6H, Ar-CH<sub>3</sub>), 1.66 (m, J= 6.0 Hz, 6 H, CHMe<sub>2</sub>), 1.23 (m, J= 6.5 Hz, 6 H, CHMe<sub>2</sub>), 0.72 (m, J= 6.0 Hz, 6 H, CHMe<sub>2</sub>), 0.36 (m, J = 6.0 Hz, 6 H, CHMe<sub>2</sub>). **(Figure IV.15)** <sup>13</sup>C{<sup>1</sup>H} (C<sub>6</sub>D<sub>6</sub>, 126 MHz, 22 °C): δ 162.6 (br, Co-C<sub>Ph</sub>), 152.2 (Ar-C), 136.2 (Ar-C), 132.9 (Ar-C), 131.4 (Ph-C), 128.4 (Ar-C), 126.4 (Ph-C), 125.4 (Ph-C), 123.7 (Ar-C), 122.7 (Ph-C), 119.8 (t, J= 4.5 Hz, Ph-ortho-C), 27.0 (br, CHMe<sub>2</sub>), 24.8 (br, CHMe<sub>2</sub>), 20.6 (Ar-CH<sub>3</sub>), 18.7 (br s, CHMe<sub>2</sub>), 18.6 (br s, CHMe<sub>2</sub>) 17.6 (br s, CHMe<sub>2</sub>), 17.4 (br s, CHMe<sub>2</sub>). **(Figure IV.16)** <sup>31</sup>P{<sup>1</sup>H} (C<sub>6</sub>D<sub>6</sub>, 202 MHz, 22 °C): δ 37.5 (br s).

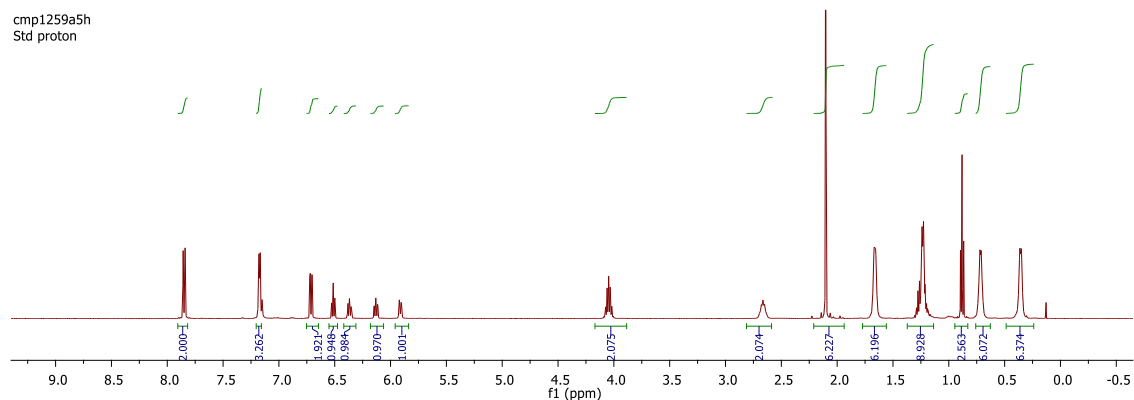


**Figure IV.15** <sup>1</sup>H NMR of (MePNP<sup>i</sup>Pr)Co(Ph)(I) (**408**) in C<sub>6</sub>D<sub>6</sub>

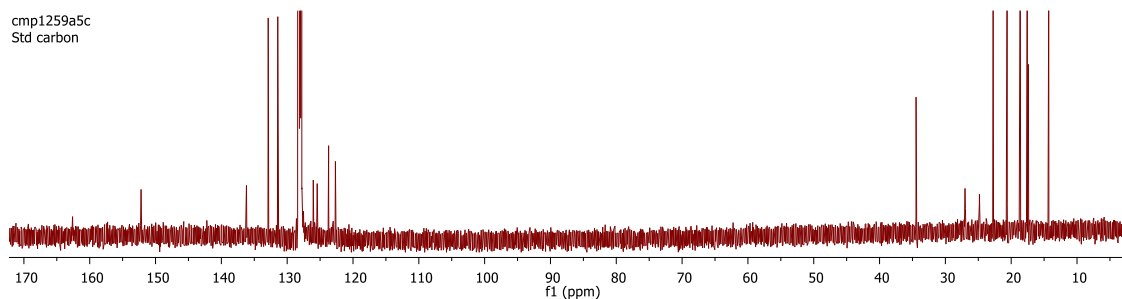


**Figure IV.16**  $^{13}\text{C}\{^1\text{H}\}$  NMR of  $(^{\text{Me}}\text{PNDiPr})\text{Co}(\text{Ph})(\text{I})$  (**408**) in  $\text{C}_6\text{D}_6$

**Synthesis of  $(^{\text{Me}}\text{PNDiPr})\text{Co}(\text{Ph})(\text{SPh})$  (**410**).**  $(^{\text{Me}}\text{PNDiPr})\text{Co}(\text{Ph})(\text{I})$  (**408**) (240 mg, 0.346 mmol) was dissolved in ca. 20 mL of THF. To this solution NaSPh (46 mg, 0.346 mmol) was added and the reaction was left to stir for 1 h. The volatiles were then removed and the product was extracted with ca. 20 mL of pentane and filtered through a pad of celite on a glass frit. The volatiles were removed and a deep blue solid was obtained (201 mg, 87%).  $^1\text{H}$  ( $\text{C}_6\text{D}_6$ , 500 MHz, 22 °C):  $\delta$  7.95–7.73 (overlapped m, 5 H, Ar-*H* (2H), Ph-*ortho-H* (1H), SPh-*H* (2H)), 7.09 (s, 2H, Ar-*H*), 7.03–6.93 (overlapped m, 3H, Ar-*H* (2H), SPh-*H* (1H)), 6.76 (dd,  $J = 8.0$  Hz, 1H, 2 H, SPh-*H*), 6.61 (t,  $J = 7.0$  Hz, 1H, Ph-*para-H*), 6.56 (br s, 1H, Ph-*meta-H*), 6.27 (br s, 1H, Ph-*meta-H*), 6.01 (br s, 1H, Ph-*ortho-H*), 2.88 (m, 2H,  $\text{CHMe}_2$ ), 2.48 (m, 2 H,  $\text{CHMe}_2$ ), 2.15 (s, 6H, Ar- $\text{CH}_3$ ), 1.25 (m,  $J = 6.0$  Hz, 6 H,  $\text{CHMe}_2$ ), 1.11 (m,  $J = 5.0$  Hz, 6 H,  $\text{CHMe}_2$ ), 0.95 (m,  $J = 5.0$  Hz, 6 H,  $\text{CHMe}_2$ ), 0.43 (m,  $J = 5.0$  Hz, 6 H,  $\text{CHMe}_2$ ). (**Figure IV.17**)  $^{31}\text{P}\{^1\text{H}\}$  ( $\text{C}_6\text{D}_6$ , 202 MHz, 22 °C):  $\delta$  31.1 (br s).

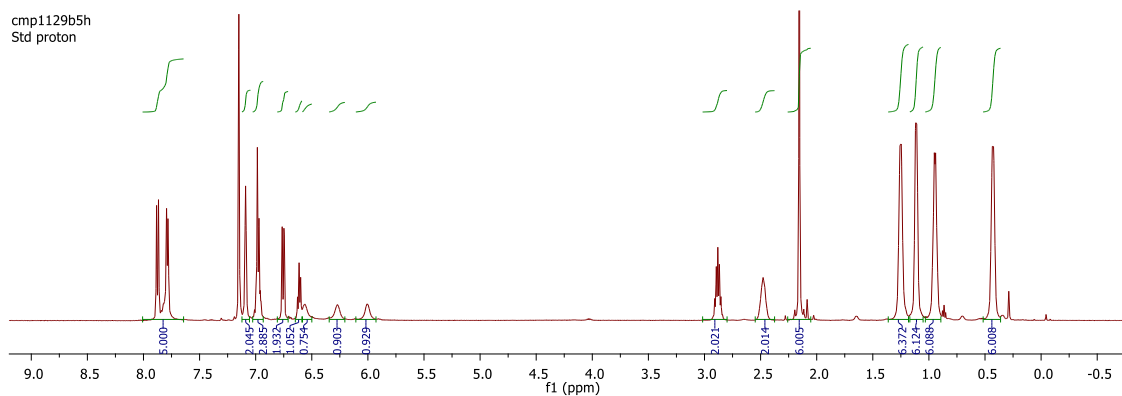


**Figure IV.17**  $^1\text{H}$  NMR of  $(^{\text{Me}}\text{PNP}^{\text{iPr}})\text{Co}(\text{Ph})(\text{SPh})$  (**410**) in  $\text{C}_6\text{D}_6$

**Synthesis of  $(^{\text{Me}}\text{PNP}^{\text{iPr}})\text{Co}(\text{Ph})(\text{SAr}^{\text{F}})$  (**411**).**  $(^{\text{Me}}\text{PNP}^{\text{iPr}})\text{Co}(\text{Ph})(\text{I})$  (**408**) (32 mg, 0.046 mmol) was dissolved in ca. 5 mL of THF. To this solution  $\text{NaSAr}^{\text{F}}$  (7.1 mg, 0.051 mmol) was added and the reaction was left to stir for 1 h. The volatiles were then removed and the product was extracted with ca. 10 mL of pentane and filtered through a pad of celite on a glass frit. The volatiles were removed and a blue gray solid was obtained (27 mg, 85%).  $^1\text{H}$  ( $\text{C}_6\text{D}_6$ , 500 MHz, 22 °C):  $\delta$  7.86 (d,  $J = 8.5$  Hz, 2 H, Ar-*H*), 7.69 (br, 1H, Ph-*ortho-H*), 7.61-7.52 (m, 2H,  $\text{SAr}^{\text{F}}$ -*H*), 7.09 (s, 2H, Ar-*H*), 6.76 (dd,  $J = 8.5$  Hz, 1.5 Hz, 2 H, Ar-*H*), 6.70-6.64 (m, 2H,  $\text{SAr}^{\text{F}}$ -*H*), 6.61 (t,  $J = 7.0$  Hz, 1H, Ph-*para-H*), 6.56 (br s, 1H, Ph-*meta-H*), 6.26 (br s, 1H, Ph-*meta-H*), 5.98 (br s, 1H, Ph-*ortho-H*), 2.82 (m, 2H,  $\text{CHMe}_2$ ), 2.44 (m, 2 H,  $\text{CHMe}_2$ ), 2.16 (s, 6H, Ar- $\text{CH}_3$ ), 1.20 (m,  $J = 6.5$  Hz, 6 H,  $\text{CHMe}_2$ ), 1.10 (m,  $J = 6.0$  Hz, 6 H,  $\text{CHMe}_2$ ), 0.90 (m,  $J = 5.5$  Hz, 6 H,  $\text{CHMe}_2$ ), 0.39 (m,  $J = 5.5$  Hz, 6 H,  $\text{CHMe}_2$ ). **(Figure IV.18)**  $^{31}\text{P}\{^1\text{H}\}$  ( $\text{C}_6\text{D}_6$ , 202 MHz, 22 °C):  $\delta$  30.6 (br s).  $^{19}\text{F}$  ( $\text{C}_6\text{D}_6$ , 470 MHz, 22 °C):  $\delta$  -119.2 (br s).

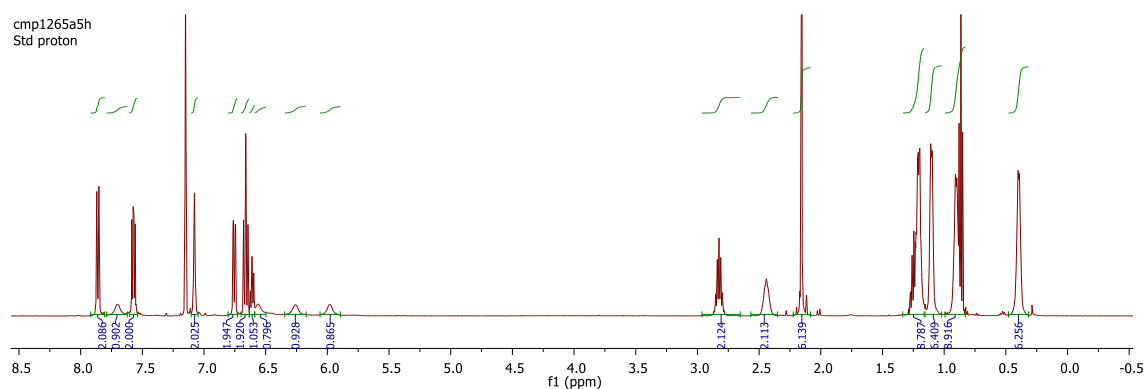


**Figure IV.18**  $^1\text{H}$  NMR of  $(^{\text{Me}}\text{PNP}^{\text{iPr}})\text{Co}(\text{Ph})(\text{SAr}^{\text{F}})$  (**411**) in  $\text{C}_6\text{D}_6$

#### 4.4.4. Synthesis of $(^{\text{Me}}\text{PNP}^{\text{iPr,Et}})$ ligand and its Co complexes

**Synthesis of  $^{\text{Me}}\text{PN}(\text{Li})\text{P}^{\text{iPr,Et}}$  (**413**).** PNB<sub>r</sub> (1.6081 g, 4.1 mmol) was combined with ~50 mL of diethyl ether in a 100 mL Schlenk flask. n-butyllithium (3.27 mL; 2.5 M in hexanes, 8.2 mmol) was added in two portions, the solution turned yellow upon addition. After three hours, diethylchlorophosphine (0.5344 g, 4.3 mmol) was added to the flask. The solution turned red upon addition, but quickly faded back to the previous yellow color. The solution was left to stir for 18h when ca. 1 mL of degassed 1:1 isopropanol:water was cannulated into the flask and the mixture was left to stir for 24 h. The volatiles were then removed *in vacuo* at 70° C. The solids were dissolved in pentane and filtered through a pad of celite on a glass frit and the volatiles were removed *in vacuo*. The oil which remained was transferred to a scintillation vial by reconstituting in a minimal amount of pentane. The pentane was removed *in vacuo* and the vial was allowed to sit overnight to evaporate any residual solvent. The vial contained 1.5208 g of oil which was assumed to be all product. The oil was dissolved in 10 mL of pentane and a stoichiometric amount of n-butyl lithium was added in one portion. Yellow solids immediately formed beneath a

brown supernatant. All solids were collected on a glass frit and washed with cold pentane (0.8954 g, 54%).  $^1\text{H}$  NMR ( $\text{C}_6\text{D}_6$ , 500 MHz):  $\delta$  7.20 (m, 1H, Ar-*H*), 6.98 (m, 4H, Ar-*H*), 6.89 (dd,  $J = 8.5$  Hz,  $J = 1.9$  Hz, 1H, Ar-*H*), 3.38 (s, 3H, N-*CH*<sub>3</sub>), 2.24 (s, 6H, Ar-*CH*<sub>3</sub>), 1.94 (m, 2H, P-*CH*-Me<sub>2</sub>), 1.57 (m, 2H, P-*CH*<sub>2</sub>-Me), 1.32 (m, 2 H, P-*CH*<sub>2</sub>-Me), 1.11 (dd,  $J = 14.0$  Hz,  $J = 7.06$  Hz), 0.7-1.0 (br, overlapping, 12H, P-*CH*-(*CH*<sub>3</sub>)<sub>2</sub> & both P-*CH*<sub>2</sub>-*CH*<sub>3</sub>). **(Figure IV.19)**  $^{13}\text{C}\{^1\text{H}\}$  NMR ( $\text{C}_6\text{D}_6$ , 125 MHz):  $\delta$  167.1 (d,  $J = 25$  Hz, Ar-P), 132.9, 132.2, 131.8, 131.5, 126.8, 125.5, 124.5, 124.2, 123.8, 23.2 (P-*CH*-Me<sub>2</sub>), 20.8 (Ar-Me), 20.7 (Ar-Me), 20.1 (P-*CH*-*CH*<sub>3</sub>), 10.38, 10.29. **(Figure IV.20)**  $^{31}\text{P}\{^1\text{H}\}$  NMR ( $\text{C}_6\text{D}_6$ , 202 MHz):  $\delta$  -1.94, -28.97. **(Figure IV.21)**

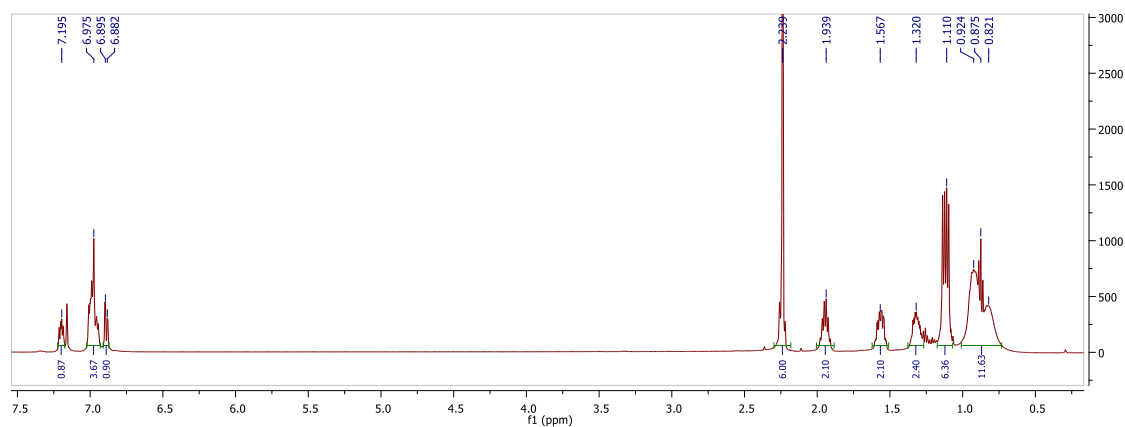


**Figure IV.19**  $^1\text{H}$  NMR of  $^{\text{Me}}\text{PN}(\text{Li})\text{P}^{\text{iPr,Et}}$  (**413**) in  $\text{C}_6\text{D}_6$

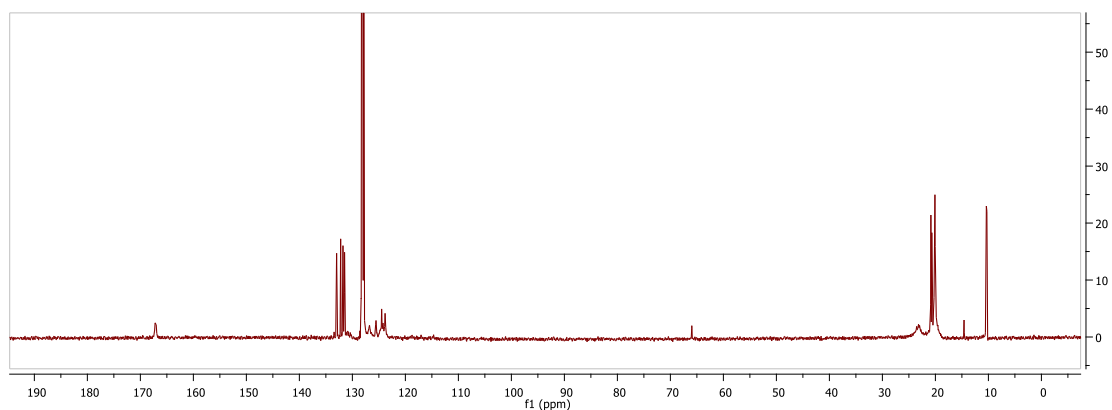


**Figure IV.20**  $^{13}\text{C}\{^1\text{H}\}$  NMR of  $\text{MePN}(\text{Li})\text{P}^{\text{iPr},\text{Et}}$  (**413**) in  $\text{C}_6\text{D}_6$

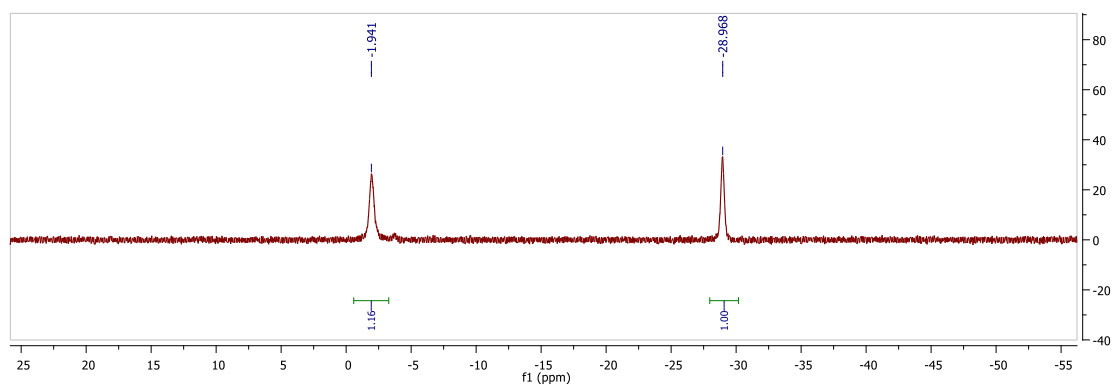


**Figure IV.21**  $^{31}\text{P}\{^1\text{H}\}$  NMR of  $\text{MePN}(\text{Li})\text{P}^{\text{iPr},\text{Et}}$  (**413**) in  $\text{C}_6\text{D}_6$

**Synthesis of  $(\text{MePNP}^{\text{iPr},\text{Et}})\text{CoCl}$  (**414**).**  $\text{MePN}(\text{Li})\text{P}^{\text{iPr},\text{Et}}$  (**413**) (430 mg, 1.05 mmol) was dissolved in ca. 20 mL of THF. To this solution,  $\text{CoCl}_2$  (140 mg, 1.05 mmol) was added and the solution was left to stir for 20 h. The volatiles were then removed and the product was extracted with ca. 20 mL of toluene and filtered through a pad of celite on a glass frit. The volatiles were pumped off and the blue green product was redissolved in ca. 10 mL of toluene and layered with ca. 20 mL of pentane and put in the freezer at  $-35\text{ }^\circ\text{C}$ . After overnight in the freezer, blue green crystalline product was obtained (306 mg, 59 %).  $^1\text{H}$

(C<sub>6</sub>D<sub>6</sub>, 500 MHz, 22 °C): δ 30.2 (br s), 29.4 (br s), 27.4 (br s), 24.8 (br s), 11.7 (br s), 5.85 (br s), 1.91 (br s), -11.1 (br s, 2H), - 25.5 (br s).

**Synthesis of (MePNP<sup>iPr,Et</sup>)Co(Ph) (415).** (MePNP<sup>iPr,Et</sup>)CoCl (**414**) (260 mg, 0.526 mmol) was dissolved in ca. 10 mL of C<sub>6</sub>H<sub>6</sub>. To this solution, PhLi (292 μL of 1.8 M in <sup>n</sup>Bu<sub>2</sub>O, 0.526 mmol) was added and the solution was left to stir for 1 h. After an hour the solution was filtered through a pad of celite on a glass frit. The volatiles were pumped off and the green product was redissolved in ca. 10 mL of pentane and put in the freezer at -35 °C. After overnight in the freezer, a green powder was obtained (254 mg, 90 %). <sup>1</sup>H (C<sub>6</sub>D<sub>6</sub>, 500 MHz, 22 °C): δ 51.1 (br s), 37.7 (br s), 36.2 (br s), 33.6 (br s), 24.6 (br s), 20.7 (br s), 13.9 (br s), 8.76 (br s), 8.21 (br s), -0.38 (br s), -11.7 (br s, 2H), - 28.3 (br s), -88.1 (br s).

**Synthesis of (MePNP<sup>iPr,Et</sup>)Co(Ph)(I) (417).** (MePNP<sup>iPr,Et</sup>)Co(Ph) (**415**) (269 mg, 0.501 mmol) was dissolved in ca. 10 mL of C<sub>6</sub>H<sub>6</sub>. To this solution, PhI(OAc)<sub>2</sub> (96 mg, 0.301 mmol) was added and the solution was left to stir for 20 h. The volatiles were pumped off and the product was redissolved in ca. 20 mL of pentane and filtered through a pad of celite on a glass frit. To the filtrate, Me<sub>3</sub>SiI (100 μL, 140 mg, 0.698 mmol) was added using a syringe and the solution was left to stir for 1 h. The volatiles were then pumped off to give a dark blue solid. The solids were extracted with pentane and put in a vial in the freezer at -35 °C. After overnight in the freezer, deep blue crystals were obtained (120 mg, 36%). <sup>1</sup>H (C<sub>6</sub>D<sub>6</sub>, 400 MHz, 22 °C): δ 7.70 (d, J = 8.8 Hz, 1 H, Ar-*H*), 7.54-7.41 (overlapping m, 2H, Ar-*H* (1H), Ph-*ortho-H* (1H)), 7.66 (d, J = 8.4 Hz, 1 H, Ar-*H*), 7.20-7.150 (m, 2H, Ar-*H* (1H), Ph-*H* (1H)) 6.79 (m, 2H, Ar-*H*), 6.79 (t, J = 6.8 Hz, 1H, Ph-



*para-H*), 6.52 – 6.03 (overlapped m, 2H, Ph-*H*), 3.87 (m, 1H, CHMe<sub>2</sub>), 3.06 (m, 1 H, CH<sub>2</sub>Me), 2.58 (m, 1H, CHMe<sub>2</sub>), 2.32 (s, 3H, Ar-CH<sub>3</sub>), 2.25 (s, 3H, Ar-CH<sub>3</sub>), 2.16 (m, 1H, CH<sub>2</sub>Me), 1.86-1.56 (overlapped m, 4H, CH<sub>2</sub>Me (1H), CHMe<sub>2</sub> (3H)), 1.26-1.15 (m, 4H, CHMe<sub>2</sub> (3H), CH<sub>2</sub>Me (1H) ), 1.04 (t, J = 7.2 Hz, 3H, CH<sub>2</sub>Me), 0.80 (t, J = 6.8 Hz, 3 H, CH<sub>2</sub>Me), 0.78-0.68 (m, 3H, CHMe<sub>2</sub>), ), 0.48-0.34 (m, 3H, CHMe<sub>2</sub>). (**Figure IV.22**)

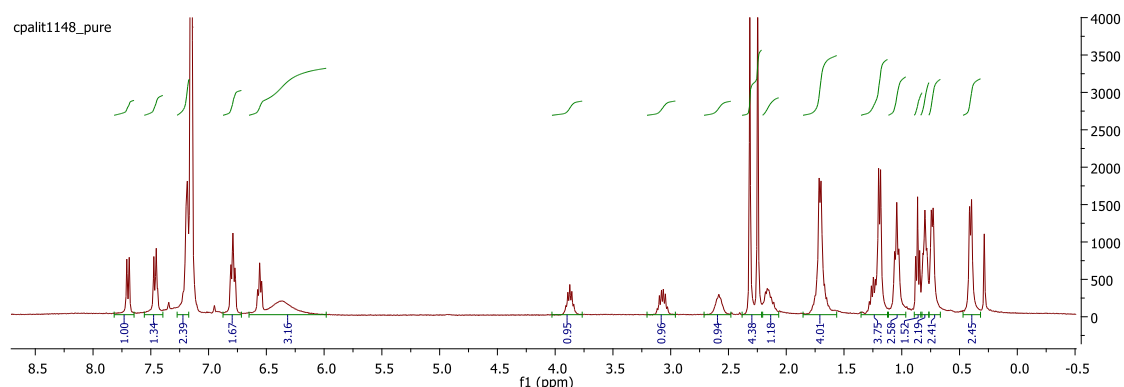


**Figure IV.22** <sup>1</sup>H NMR of (<sup>Me</sup>PNP<sup>iPr,Et</sup>)Co(Ph)(I) (**417**) in C<sub>6</sub>D<sub>6</sub>

**Synthesis of (<sup>Me</sup>PNP<sup>iPr,Et</sup>)Co(Ph)(SPh) (**418**).** (<sup>Me</sup>PNP<sup>iPr,Et</sup>)Co(Ph)(I) (**416**) (40 mg, 0.059 mmol) was dissolved in ca. 5 mL of THF. To this solution NaSPh (9.1 mg, 0.066 mmol) was added and the reaction was left to stir for 1 h. The volatiles were then removed and the product was extracted with ca. 10 mL of pentane and filtered through a pad of celite on a glass frit. The volatiles were removed the solid was extracted with ca. 2 mL of pentane and put in the freezer at -35 °C overnight. Deep blue crystals were obtained (12 mg, 32%). <sup>1</sup>H (C<sub>6</sub>D<sub>6</sub>, 400 MHz, 22 °C): δ 7.95 (d, J = 8.4 Hz, 1 H, Ph-ortho-*H*), 7.78-7.68 (m, 2H, Ar-*H*), 7.66 (d, J = 8.4 Hz, 1 H, Ar-*H*), 7.150 (overlapped with solvent, 2H, Ar-*H*), 7.09 (s, 1H, Ar-*H*), 7.03 (s, 1H, Ar-*H*), 6.99 – 6.90 (overlapped m, 3H, Ar-*H* (2H), SPh-*H* (1H)), 6.74 (t, J = 8.8 Hz, 2 H, SPh-*H*), 6.61 (t, J = 7.2 Hz, 1H, Ph-*para-H*),

6.44 (m, 2H, Ph-*ortho*-H), 3.05 (m, 1H, CHMe<sub>2</sub>), 2.57 (m, 1 H, CH<sub>2</sub>Me), 2.17 (s, 3H, Ar-CH<sub>3</sub>), 2.10 (s, 3H, Ar-CH<sub>3</sub>), 1.75 (m, 2 H, CH<sub>2</sub>Me), 1.61 (m, 3H, CHMe<sub>2</sub>), 1.40 (overlapping m, 2H, CH<sub>2</sub>Me (1H), CHMe<sub>2</sub> (1H)), 1.19 (m, 3 H, CH<sub>2</sub>Me), 1.05 (m, 3H, CHMe<sub>2</sub>), 0.77 (m, 3H, CH<sub>2</sub>Me), 0.69 (m, 3H, CHMe<sub>2</sub>), 0.45 (m, 3H, CHMe<sub>2</sub>). (**Figure IV.23**) <sup>31</sup>P{<sup>1</sup>H} (C<sub>6</sub>D<sub>6</sub>, 202 MHz, 22 °C): δ 34.4 (br d, J<sub>PP</sub>=249 Hz, 1P), 24.7 (br d, J<sub>PP</sub>=249 Hz). (**Figure IV.24**)

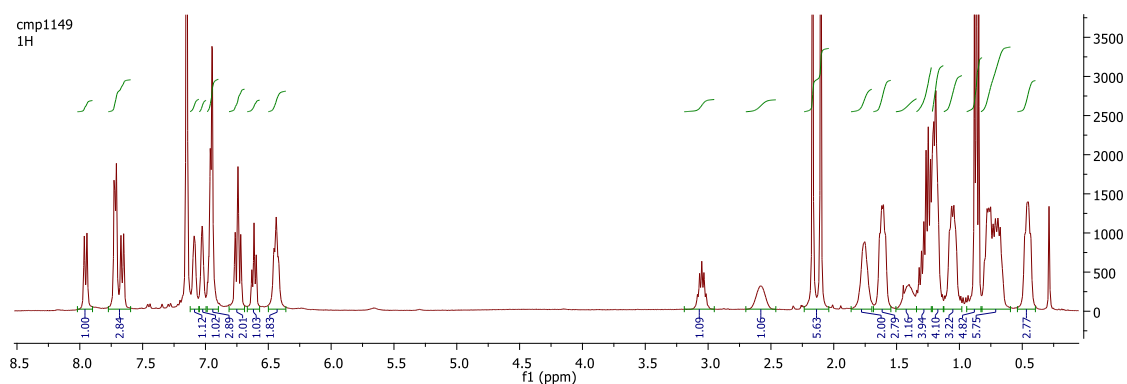


**Figure IV.23** <sup>1</sup>H NMR of (MePNP<sup>iPr,Et</sup>)Co(Ph)(SPh) (**418**) in C<sub>6</sub>D<sub>6</sub>

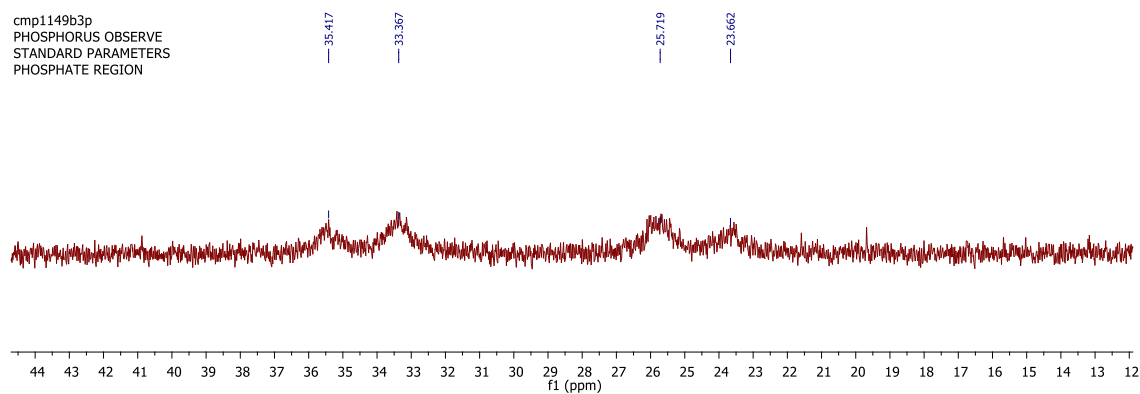


**Figure IV.24** <sup>31</sup>P{<sup>1</sup>H} NMR of (MePNP<sup>iPr,Et</sup>)Co(Ph)(SPh) (**418**) in C<sub>6</sub>D<sub>6</sub>

#### 4.4.5. Thermolysis experiments

**Thermolysis of  $(^{\text{Me}}\text{PNP}^{\text{iPr}})\text{Co}(\text{Ph})(\text{SPh})$  (410).**  $(^{\text{Me}}\text{PNP}^{\text{iPr}})\text{Co}(\text{Ph})(\text{SPh})$  (408) (4 mg, 0.006 mmol) was dissolved in ca. 600  $\mu\text{L}$  of  $\text{C}_6\text{D}_6$  in a PTFE capped J. Young NMR tube. To this, 1,4-dioxane (2  $\mu\text{L}$ , 2.07 mg, 0.023 mmol) was added using a syringe to serve as an internal standard. A  $^1\text{H}$  NMR spectra of the initial sampled was taken and then the NMR tube was placed in an oil bath at 80  $^\circ\text{C}$ . The reaction was monitored by  $^1\text{H}$  NMR spectroscopy and complete thermolysis was observed after 3 h. The final mixture was observed to contain  $(^{\text{Me}}\text{PNP}^{\text{iPr}})\text{Co}(\text{Ph})$  (46% of initial  $(^{\text{Me}}\text{PNP}^{\text{iPr}})\text{Co}(\text{Ph})(\text{SPh})$ ),  $(^{\text{Me}}\text{PNP}^{\text{iPr}})\text{Co}(\text{SPh})$  (46% of initial  $(^{\text{Me}}\text{PNP}^{\text{iPr}})\text{Co}(\text{Ph})(\text{SPh})$ ) and  $\text{SPh}_2$  (48% of initial  $(^{\text{Me}}\text{PNP}^{\text{iPr}})\text{Co}(\text{Ph})(\text{SPh})$ ) by  $^1\text{H}$  NMR spectroscopy .

**Thermolysis of  $(^{\text{Me}}\text{PNP}^{\text{iPr}})\text{Co}(\text{Ph})(\text{SPh})$  (410) with 100 eq. of PhI.**  $(^{\text{Me}}\text{PNP}^{\text{iPr}})\text{Co}(\text{Ph})(\text{SPh})$  (408) (4 mg, 0.006 mmol) was dissolved in ca. 600  $\mu\text{L}$  of  $\text{C}_6\text{D}_6$  in a PTFE capped J. Young NMR tube. PhI (74 mL, 134 mg, 0.657 mmol) was added using a syringe. To this, 1,4-dioxane (2  $\mu\text{L}$ , 2.07 mg, 0.023 mmol) was added using syringe to serve as an internal standard. A  $^1\text{H}$  NMR spectrum of the initial sample was taken and then the NMR tube was placed in an oil bath at 80  $^\circ\text{C}$ . The reaction was monitored by  $^1\text{H}$  NMR spectroscopy and complete thermolysis was observed after 3 h. 40% conversion of  $(^{\text{Me}}\text{PNP}^{\text{iPr}})\text{Co}(\text{Ph})(\text{SPh})$  to  $(^{\text{Me}}\text{PNP}^{\text{iPr}})\text{Co}(\text{Ph})(\text{I})$  was observed with the other thermolysis products as  $(^{\text{Me}}\text{PNP}^{\text{iPr}})\text{Co}(\text{Ph})$ ,  $(^{\text{Me}}\text{PNP}^{\text{iPr}})\text{Co}(\text{SPh})$  and  $\text{SPh}_2$  .

**Thermolysis of  $(^{\text{Me}}\text{PNP}^{\text{iPr}})\text{Co}(\text{Ph})(\text{SPh})$  (410) with BHT as a radical inhibitor.**  $(^{\text{Me}}\text{PNP}^{\text{iPr}})\text{Co}(\text{Ph})(\text{SPh})$  (408) (4 mg, 0.006 mmol) and dibutylhydroxytoluene (BHT) (2 mg, 0.009 mmol) was dissolved in ca. 600  $\mu\text{L}$  of  $\text{C}_6\text{D}_6$  in a PTFE capped J. Young NMR

tube. To this, 1,4-dioxane ( 2  $\mu$ L, 2.07 mg, 0.023 mmol) was added using a syringe to serve as an internal standard. A  $^1\text{H}$  NMR spectrum of the initial sample was taken and then the NMR tube was placed in an oil bath at 80  $^\circ\text{C}$ . The reaction was monitored by  $^1\text{H}$  NMR spectroscopy and complete thermolysis was observed after 3 h. The final mixture was observed to contain  $(^{\text{Me}}\text{PNP}^{i\text{Pr}})\text{Co}(\text{Ph})$  (43% of initial  $(^{\text{Me}}\text{PNP}^{i\text{Pr}})\text{Co}(\text{Ph})(\text{SPh})$ ),  $(^{\text{Me}}\text{PNP}^{i\text{Pr}})\text{Co}(\text{SPh})$  (43% of initial  $(^{\text{Me}}\text{PNP}^{i\text{Pr}})\text{Co}(\text{Ph})(\text{SPh})$ ) and PhSPh (45% of initial  $(^{\text{Me}}\text{PNP}^{i\text{Pr}})\text{Co}(\text{Ph})(\text{SPh})$ ) by  $^1\text{H}$  NMR spectroscopy .

**Thermolysis of  $(^{\text{Me}}\text{PNP}^{i\text{Pr}})\text{Co}(\text{Ph})(\text{SAr}^{\text{F}})$  (411).**  $(^{\text{Me}}\text{PNP}^{i\text{Pr}})\text{Co}(\text{Ph})(\text{SAr}^{\text{F}})$  (409) (12 mg, 0.006 mmol) was dissolved in ca. 600  $\mu$ L of  $\text{C}_6\text{D}_6$  in a PTFE capped J. Young NMR tube.  $^{19}\text{F}$  and  $^1\text{H}$  NMR spectrum of the initial sample was taken and then the NMR tube was placed in an oil bath at 80  $^\circ\text{C}$ . The reaction was monitored by  $^1\text{H}$  and  $^{19}\text{F}$  NMR spectroscopy and complete thermolysis was observed after 3 h. The final mixture was observed to contain a 1:1:1 ratio of  $(^{\text{Me}}\text{PNP}^{i\text{Pr}})\text{Co}(\text{Ph})$ ,  $(^{\text{Me}}\text{PNP}^{i\text{Pr}})\text{Co}(\text{SAr}^{\text{F}})$  and  $^{\text{F}}\text{Ar-S-Ph}$  and < 4% of unidentified paramagnetic compound by  $^1\text{H}$  NMR spectroscopy . The  $^{19}\text{F}$  NMR spectrum of the final mixture shows a 1:1 ratio of  $(^{\text{Me}}\text{PNP}^{i\text{Pr}})\text{Co}(\text{SAr}^{\text{F}})$  (-117.2 ppm) to  $^{\text{F}}\text{Ar-S-Ph}$  (-114.7 ppm) with minor signals at -113.4 ppm (< 1%) and 114.9 ppm (<5%).

**(Figure IV.25)**

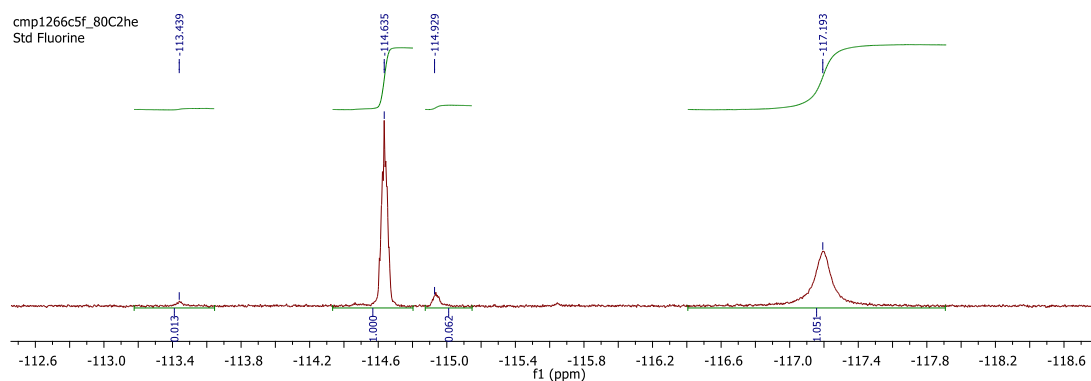


**Figure IV.25**  $^{19}\text{F}$  NMR of thermolysis ( $^{\text{Me}}\text{PNP}^{\text{iPr}}$ )Co(Ph)(SAr<sup>F</sup>) (**411**) in  $\text{C}_6\text{D}_6$  after 3 h

**Thermolysis of ( $^{\text{Me}}\text{PNP}^{\text{iPr,Et}}$ )Co(Ph)(SPh) (**418**).** ( $^{\text{Me}}\text{PNP}^{\text{iPr,Et}}$ )Co(Ph)(SPh) (**418**) (4 mg, 0.006 mmol) was dissolved in ca. 600  $\mu\text{L}$  of  $\text{C}_6\text{D}_6$  in a PTFE capped J. Young NMR tube. To this, 1,4-dioxane ( 2  $\mu\text{L}$ , 2.07 mg, 0.023 mmol) was added using a syringe to serve as an internal standard. A  $^1\text{H}$  NMR spectra of the initial sampled was taken and then the NMR tube was placed in an oil bath at 80  $^\circ\text{C}$ . The reaction was monitored by  $^1\text{H}$  NMR spectroscopy and complete thermolysis was observed after 3 h. The final mixture was observed to contain ( $^{\text{Me}}\text{PNP}^{\text{iPr,Et}}$ )Co(Ph) (46% of initial ( $^{\text{Me}}\text{PNP}^{\text{iPr,Et}}$ )Co(Ph)(SPh)), ( $^{\text{Me}}\text{PNP}^{\text{iPr,Et}}$ )Co(SPh) (46% of initial ( $^{\text{Me}}\text{PNP}^{\text{iPr,Et}}$ )Co(Ph)(SPh)) and  $\text{SPh}_2$  (50% of initial ( $^{\text{Me}}\text{PNP}^{\text{iPr}}$ )Co(Ph)(SPh)) by  $^1\text{H}$  NMR spectroscopy .

**Thermolysis of ( $^{\text{Me}}\text{PNP}^{\text{iPr,Et}}$ )Co(Ph)(SPh) (**418**) with BHT as a radical inhibitor.** ( $^{\text{Me}}\text{PNP}^{\text{iPr}}$ )Co(Ph)(SPh) (**408**) (5 mg, 0.008 mmol) and dibutylhydroxytoluene (BHT) (2 mg, 0.009 mmol) was dissolved in ca. 600  $\mu\text{L}$  of  $\text{C}_6\text{D}_6$  in a PTFE capped J. Young NMR tube. To this, 1,4-dioxane ( 2  $\mu\text{L}$ , 2.07 mg, 0.023 mmol) was added using a syringe to serve as an internal standard. A  $^1\text{H}$  NMR spectrum of the initial sample was taken and then the NMR tube was placed in an oil bath at 80  $^\circ\text{C}$ . The reaction was monitored by  $^1\text{H}$

NMR spectroscopy and complete thermolysis was observed after 3 h. The final mixture was observed to contain ( $^{\text{Me}}\text{PNP}^{\text{iPr,Et}}\text{Co(Ph)}$ ) (48% of initial ( $^{\text{Me}}\text{PNP}^{\text{iPr}}\text{Co(Ph)(SPh)}$ )), ( $^{\text{Me}}\text{PNP}^{\text{iPr,Et}}\text{Co(SPh)}$ ) (43% of initial ( $^{\text{Me}}\text{PNP}^{\text{iPr}}\text{Co(Ph)(SPh)}$ )) and PhSPh (49% of initial ( $^{\text{Me}}\text{PNP}^{\text{iPr,Et}}\text{Co(Ph)(SPh)}$ )) by  $^1\text{H}$  NMR spectroscopy .

#### 4.4.6. X-Ray crystallography

**X-Ray data collection, solution, and refinement for 406.** A dark purple, multi-faceted crystal of suitable size and quality (0.10 x 0.05 x 0.02 mm) was selected using an optical microscope and mounted onto a nylon loop. Low temperature (150 K) X-ray data were obtained on a Bruker APEXII CCD based diffractometer (Mo sealed X-ray tube,  $K_{\alpha}$  = 0.71073 Å). All diffractometer manipulations, including data collection, integration and scaling were carried out using the Bruker APEXII software.<sup>181</sup> An absorption correction was applied using SADABS.<sup>182</sup> The structure was initially solved in the monoclinic  $C_{2yc}$  space group using XS<sup>183</sup>(incorporated in SHELXTL). The solution was refined by full-matrix least squares on  $F^2$ . No additional symmetry was found using ADDSYMM incorporated into the PLATON program.<sup>184</sup> All non-hydrogen atoms were refined with anisotropic thermal parameters. The structure was refined (weighted least squares refinement on  $F^2$ ) and the final least-squares refinement converged to  $R_1 = 0.0299$  ( $I > 2\sigma(I)$ , 6839 data) and  $wR_2 = 0.0805$  ( $F^2$ , 7986 data, 383 parameters).

## CHAPTER V

### BINUCLEAR PCN AND PNN LIGANDS AND THEIR PD AND NI COMPLEXES

#### 5.1. Introduction

As mentioned previously in the introduction chapter, pincer ligands and their complexes find uses in a multitude of applications due to the variety of electronic and steric modifications available for a pincer ligand by changing the nature of the central donor and the side arms. However, one area which has been less explored is the possible cooperativity between metal centers using poly-nucleating pincers. The examples of poly pincers reported so far largely use rigid linkers<sup>194,195</sup> or are designed for electronic communication by putting two pincers on the same aromatic ring.<sup>196,197</sup> (**Figure V.1**)

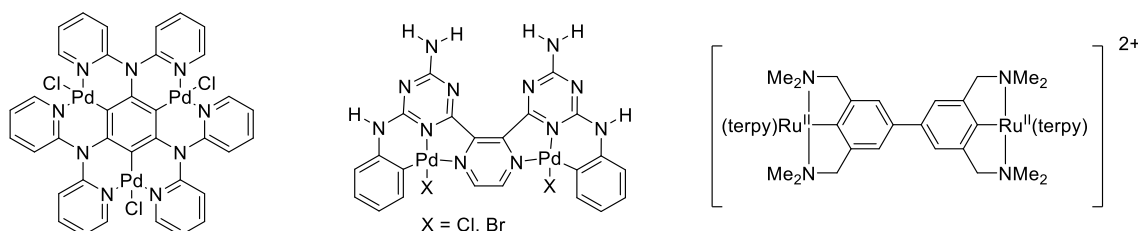


**Figure V.1** Previously reported poly-pincer complexes with rigid ligands

Although these are interesting examples, cooperation between metal centers for activating a substrate is highly improbable for such systems. In order to facilitate cooperativity of the metal centers, we envisioned the use of binuclear pincers where the two pincer sites are linked by flexible alkyl linkers. The flexibility of the linkers should allow the pincer nucleated metal sites to attain different distances and orientations with respect to each other, which could make these complexes useful for novel transformations of small molecules mediated by two metals interacting with the same molecule of substrate. Such complexes of Pd<sup>II</sup> have previously been reported with binucleating CNS<sup>198</sup> and NCN<sup>199</sup>

type pincers connected by flexible alkyl linkers. (**Figure V.2 (a)**) Drawing inspiration from such reports and building on the well-known mononuclear POCOP<sup>200,201</sup> and PNP<sup>6,24</sup> ligands, our group recently published binuclear PCN and PNN complexes of Pd.<sup>202</sup> (**Figure V.2 (b)**) In this effort, we strive to expand the library of such compounds to complexes of Ni and also to incorporate different steric bulk into the phosphine side arms and functionality in the linker.

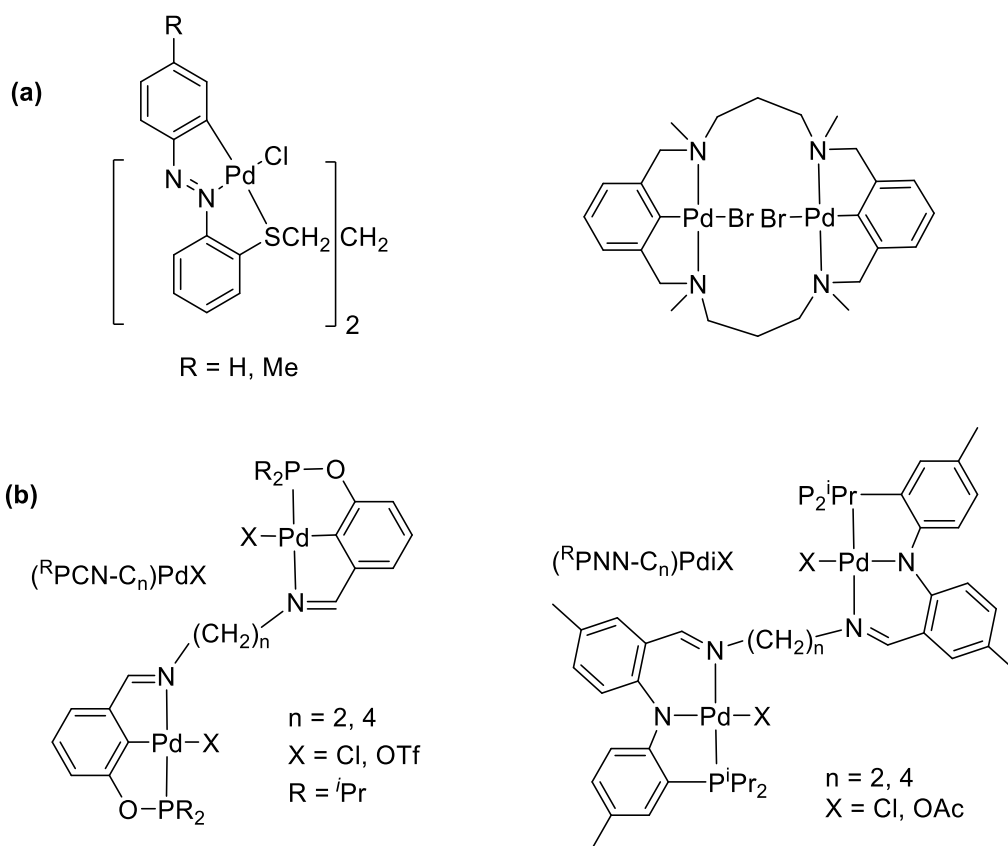


**Figure V.2** (a) Previously reported pincer with flexible linkers (b) PCN and PNN complexes of Pd reported by our group



## 5.2. Results and discussion

### 5.2.1. Synthetic details for PCN complexes

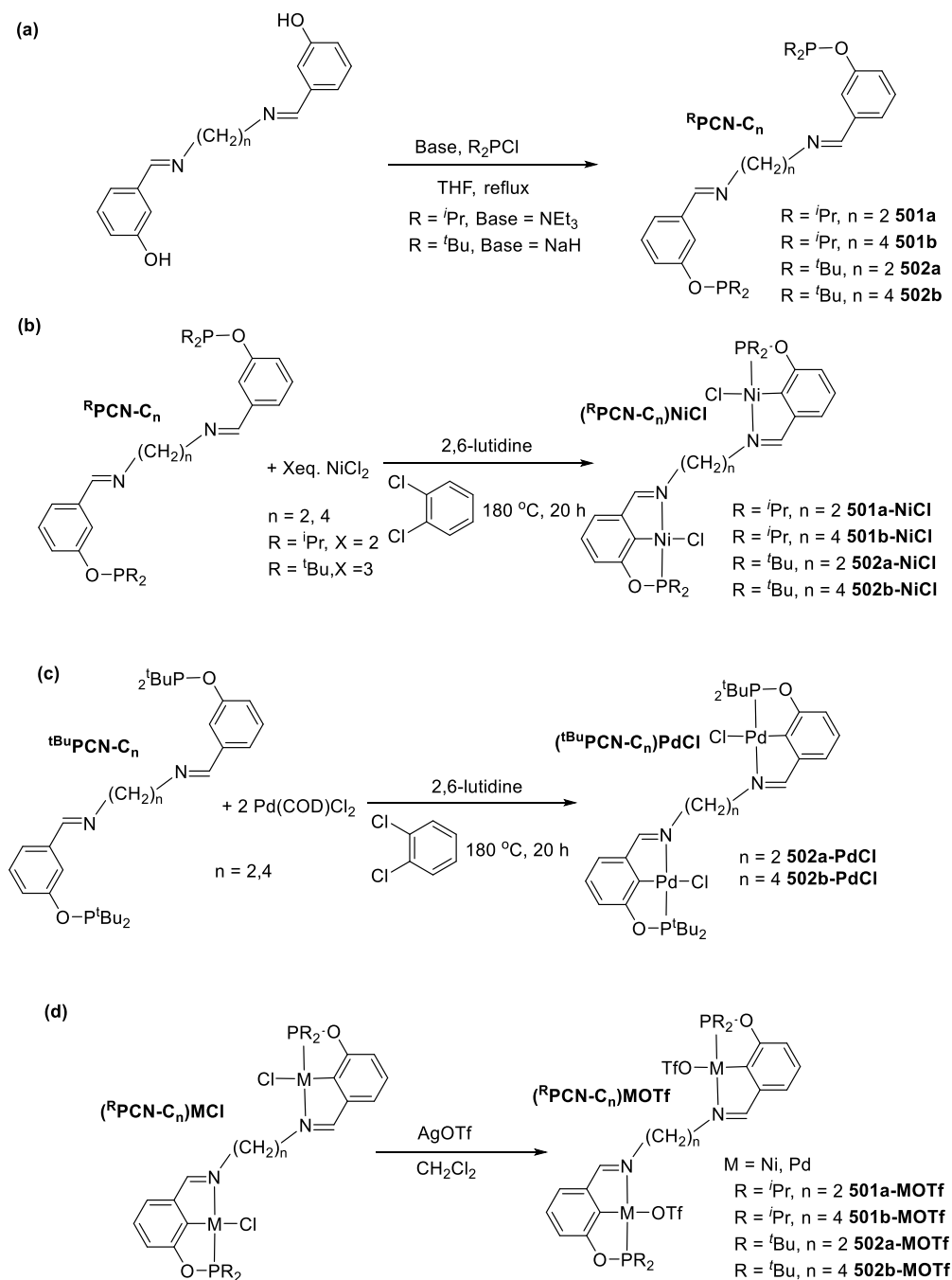


**Figure V.3** (a) Synthesis of  $R_2\text{PCN}-\text{C}_n$  ligands (b) Synthesis of  $(R_2\text{PCN})\text{NiCl}$  complexes (c) Synthesis of  $(^t\text{BuPCN})\text{PdCl}$  complexes (d) Synthesis of  $(R_2\text{PCN})\text{MOTf}$  complexes

Binuclear nickel complexes of the type ( $i^{\text{Pr}}\text{PCN-C}_n$ )NiX ( $n = 2,4$  X = Cl, OTf) were prepared by procedures similar to that of analogous Pd complexes previously reported by our group.<sup>202</sup> (**Figure V.3**). In order to increase the steric bulk of the side arms  $t^{\text{Bu}}\text{PCN-C}_n$  ( $n = 2,4$ ) (**502a/b**) ligands were prepared, with the synthesis requiring use of NaH as the base instead of Et<sub>3</sub>N as was required for  $i^{\text{Pr}}\text{PCN-C}_n$ . Installing nickel on these ligands interestingly required use of an excess of NiCl<sub>2</sub> (3 equivalents) instead of 2 equivalents needed for the less bulky  $i^{\text{Pr}}\text{PCN-C}_n$  (**501a/b**) ligands. (**Figure V.3 (a)**) ( $t^{\text{Bu}}\text{PCN-C}_n$ )PdX ( $n = 2,4$  X = Cl, OTf) were prepared by procedures similar to that of analogous Pd complexes of the iso-propyl phosphine substituted ligands.

Efforts were also undertaken to incorporate functional groups into the flexible linkers to further facilitate interaction with small molecules. Linkers with pendant amines were targeted specifically because of the important role of pendant amines in facilitating activation of H<sub>2</sub> via M-H/N-H exchange with Ni<sup>203–206</sup> and Fe<sup>207,208</sup> phosphine complexes, demonstrated by Bullock and coworkers in the past few years. Efforts to make benzaldimines analogous to that for the  $^{\text{R}}\text{PCN-C}_n$  type ligands albeit with a pendant amine in the linker such as **505a'**, by the condensation of 3-hydroxybenzaldehyde and diethylenetriamine led to undesired products presumably due to the susceptibility of the desired product benzaldimine towards nucleophilic attack by the pendant amine.

Condensation of 3-hydroxyacetophenone with diethylenetriamine however, did proceed cleanly to yield the benzoketimine **504a'** in good yields which was subsequently converted to the binuclear pincer ligand  $t^{\text{Bu}}\text{PCN-C}_2\text{NC}_2$  (**504a**) by reacting with NaH and  $t^{\text{Bu}}_2\text{PCl}$ . Efforts to make the diisopropylphosphine derivative of the ligand proved

unsuccessful. Attempts to install Pd on this ligand failed despite trying different Pd<sup>II</sup> precursors and reaction conditions. The Ni complex (<sup>t</sup>BuPCN-C<sub>2</sub>NC<sub>2</sub>)NiCl (**504-NiCl**) was obtained by reacting the ligand with 2 equivalents each of NiCl<sub>2</sub> and 2,6-lutidine at 160 °C in *ortho*-dichlorobenzene. (**Figure V.4**)

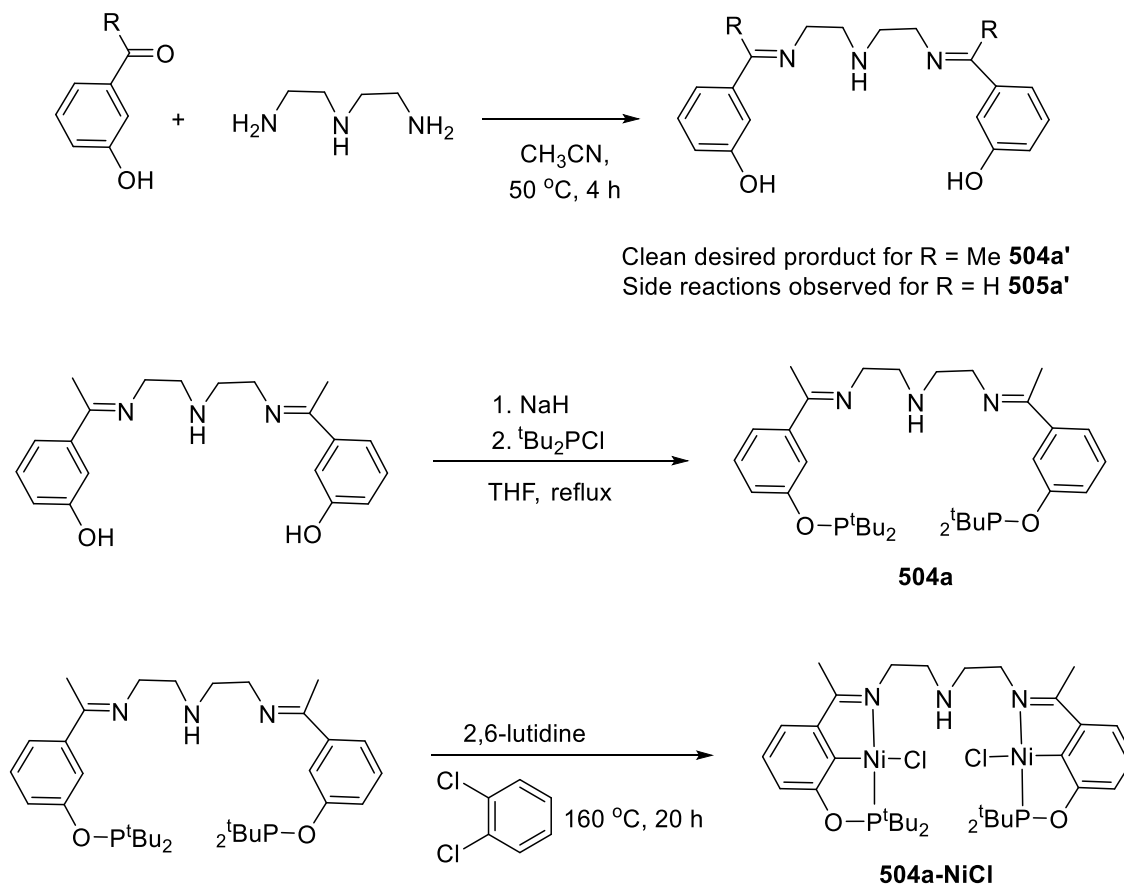


**Figure V.4** Synthesis of binuclear (PCN) Ni complex with a pendant amine linker

### 5.2.2. Synthetic details for PNN complexes

Complexes of the type (<sup>i</sup>PrPNN-C<sub>2</sub>)NiX (X = Cl, OAc) were synthesized by reacting the previously reported <sup>i</sup>PrPNN-C<sub>2</sub> ligand (**503a**) with NiCl<sub>2</sub>·6H<sub>2</sub>O/2,6-lutidine or Ni(OAc)<sub>2</sub>·4H<sub>2</sub>O respectively. (**Figure V.5**)

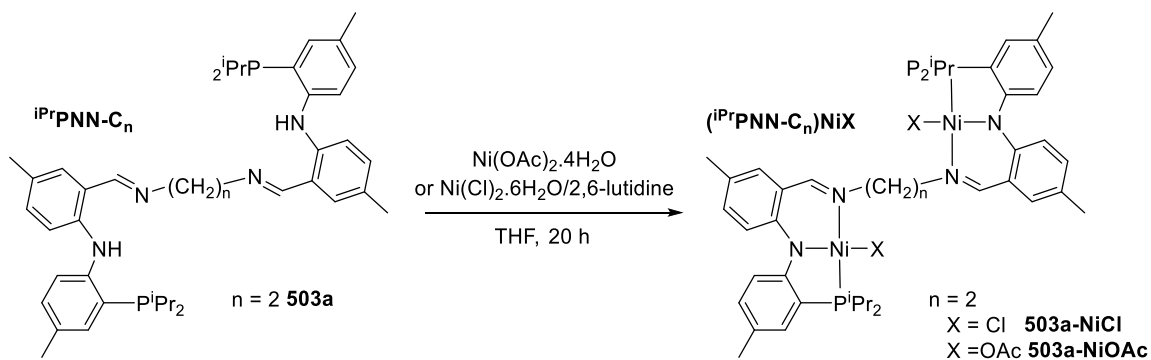


**Figure V.5** Synthesis of (PNN)NiX complexes

5.2.3. Solid-State structures of complexes of the type  $(^R\text{PCN-C}_n)\text{MX}$  and  $(^{iPr}\text{PNN-C}_2)\text{MX}^{**}$

X-ray crystallographic studies were undertaken to look at the arrangement of the binuclear complexes in solid state. Orange, X-ray quality crystals of the PCN complexes 1a-NiCl and 1b-NiCl were grown by slow diffusion of Et<sub>2</sub>O into a CH<sub>2</sub>Cl<sub>2</sub> solution at -35 °C. The asymmetric unit in both the structures contains only pincer core suggesting that the sites are crystallographically identical. In each unit, the environment around the Ni center is slightly distorted square planar with Ni-C, Ni-P and Ni-N distances comparable to those reported for analogous (PCN)Ni complexes by the groups of Zargarian<sup>209,210</sup> and Song<sup>211,212</sup>. The relative arrangement of the two pincer sites is such that they are pointing towards each other in parallel planes.

---

\*\* X-ray structures for  $(^{\text{tBu}}\text{PCN-C}_2)\text{PdCl}$  and  $(^{\text{tBu}}\text{PCN-C}_4)\text{PdCl}$  obtained by Dr. Dave Herbert, rest by C. M. Palit

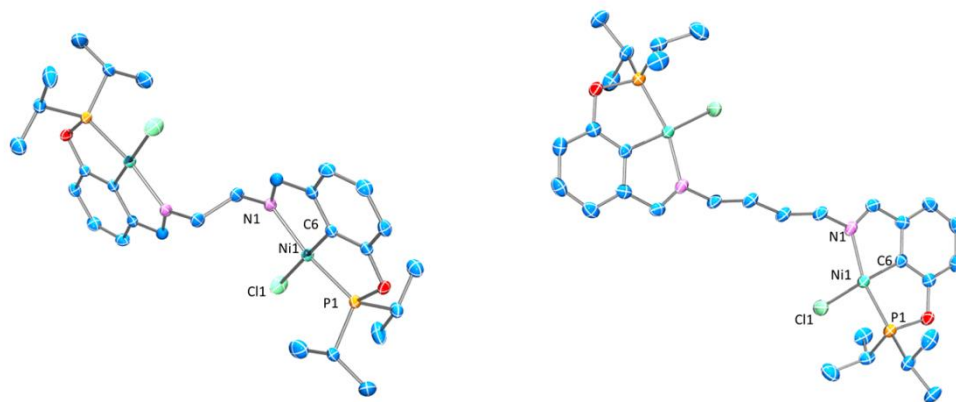


**Figure V.6** ORTEP drawing (50% probability ellipsoids) of (*i*PrPCN-C<sub>2</sub>)NiCl (**501a-NiCl**)(left) Selected bond distances (Å) and angles (deg) for **501a-NiCl** follow: Ni1-C6, 1.846(2); N1-Cl1, 2.199(1); Ni1-N1, 1.965(2); Ni1-P1, 2.114(1); N1-Ni1-P1, 163.39(5); N1-Ni1-Cl1, 98.69(5); P1-Ni1-Cl1, 97.82(2); C6-Ni1-P1, 80.95(7); C6-Ni1-N1, 82.44(8) (b) (*i*PrPCN-C<sub>4</sub>)NiCl (**501b-NiCl**) (right) Select atom labeling. Hydrogen atoms are omitted for clarity. Selected bond distances (Å) and angles (deg) for **501b-NiCl** follow: Ni1-Cl1, 2.199(3); Ni1-N1, 1.978(4); Ni1-P1, 2.128(3); Ni1-C6 1.847(4); C6-Ni1-N1, 82.7(1); C6-Ni1-P1, 80.9(1); C6-Ni1-Cl1, 175.3(1); P1-Ni1-Cl1, 97.84(4)

Crystals for the (<sup>t</sup>BuPCN-C<sub>n</sub>)PdCl complexes (**502a-PdCl** and **502b-PdCl**) were obtained using similar procedures and show crystallographic characteristics previously observed by us for the diisopropylphosphine substituted analogues.<sup>202</sup> The Pd-P, Pd-C, Pd-N bonds and N-Pd-P, Cl-Pd-C angles remain almost identical to those for the diisopropylphosphine substituted analogues suggesting increasing the bulk of the phosphine side arms has minimal effect on the pincer core geometry.

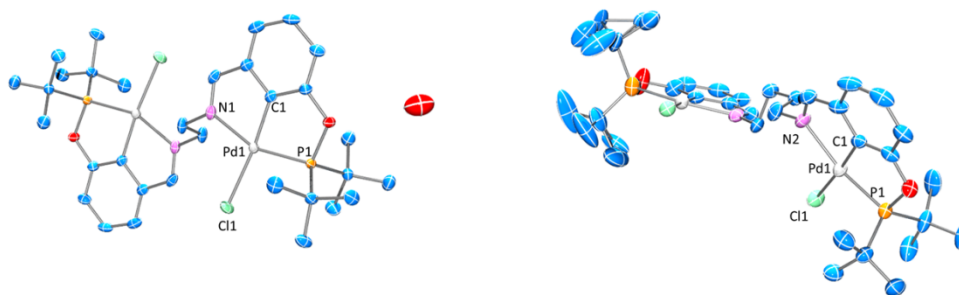


**Figure V.7** ORTEP drawing (50% probability ellipsoids) of  $(t\text{BuPCN-C}_2)\text{PdCl}$  (**502a-PdCl**) (left) Selected bond distances ( $\text{\AA}$ ) and angles (deg) for **502a-PdCl** follow: Pd1-Cl1, 2.391(1); Pd1-N1, 2.125(3); Pd1-P1, 2.220(1); Pd1-C1 1.952(3); P1-Pd1-C1, 79.6(1); C1-Pd1-N1, 79.3(1); C11-Pd1-C1, 174.2(1); P1-Pd1-Cl1, 105.24(3) and  $(t\text{BuPCN-C}_4)\text{PdCl}$  (**502b-PdCl**) (right) Selected bond distances ( $\text{\AA}$ ) and angles (deg) for **502b-PdCl** follow: Pd1-Cl1, 2.395(2); Pd1-N2, 2.142(4); Pd1-P1, 2.224(2); Pd1-C1 1.953(6); C1-Pd1-P1, 79.3(2); C1-Pd1-N2, 78.9(2); C11-Pd1-N2, 97.6(1); C11-Pd1-P1, 104.27(6)

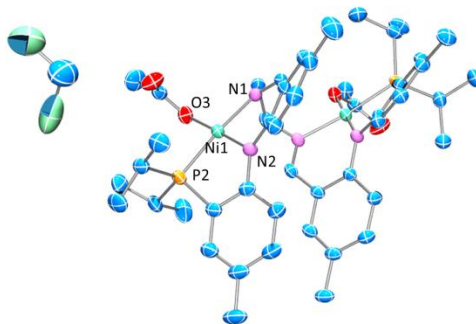


**Figure V.8** ORTEP drawing (50% probability ellipsoids) of  $(i\text{PrPNN-C}_2)\text{NiOAc}$  (**503a-NiOAc**) Select atom labeling. Hydrogen atoms are omitted for clarity. Selected bond distances ( $\text{\AA}$ ) and angles (deg) for **503a-NiOAc** follow: Ni1-N2, 1.882(3); N1-O3, 1.874(2); Ni1-N1, 1.941(2); Ni1-P2, 2.158(1); N1-Ni1-P2, 174.37(8); N2-Ni1-O3, 178.0(1); N2-Ni1-P2, 85.40(8)

A single green block-shaped crystal for  $(i\text{PrPNN-C}_2)\text{NiOAc}$  (**503a-NiOAc**) was obtained by slow diffusion of  $\text{Et}_2\text{O}$  into a  $\text{CH}_2\text{Cl}_2$  solution at  $-35\text{ }^\circ\text{C}$  with one molecule of

CH<sub>2</sub>Cl<sub>2</sub> co-crystallizing with the molecule. Each pincer site is square planar with the two moieties displaying aromatic stacking over the other pincer half.

### 5.3. Conclusions

In summary, we have synthesized binuclear complexes of Ni using binuclear PCN and PNN ligands previously reported by our group. In addition, we have expanded the library of such complexes by varying the steric bulk of the phosphine side arms, and we have also incorporated functionality into the linkers by using pendant amine linkers instead of simple alkyl linkers.

### 5.4. Experimental

#### 5.4.1. General considerations

Unless otherwise specified, all manipulations were performed under an argon atmosphere using standard Schlenk line or glove box techniques. Toluene, THF, pentane, and isooctane were dried and deoxygenated (by purging) using a solvent purification system and stored over molecular sieves in an Ar-filled glove box. C<sub>6</sub>D<sub>6</sub> and hexanes were dried over and distilled from NaK/Ph<sub>2</sub>CO/18-crown-6 and stored over molecular sieves in an Ar-filled glove box. Fluorobenzene was dried with and then distilled or vacuum transferred from CaH<sub>2</sub>. The binuclear ligands <sup>i</sup>PrPCN-C<sub>2</sub> (**501a**) and <sup>i</sup>PrPCN-C<sub>4</sub> (**501b**) were synthesized according to published procedures.<sup>202</sup> All other chemicals were used as received from commercial vendors. NMR spectra were recorded on a Varian NMRS 500 (<sup>1</sup>H NMR, 499.686 MHz; <sup>13</sup>C NMR, 125.659 MHz, <sup>31</sup>P NMR, 202.298 MHz, <sup>19</sup>F NMR, 470.111 MHz) spectrometer. For <sup>1</sup>H and <sup>13</sup>C NMR spectra, the residual solvent peak was used as an internal reference. <sup>31</sup>P NMR spectra were referenced externally using 85%

H<sub>3</sub>PO<sub>4</sub> at  $\delta$  0 ppm. <sup>19</sup>F NMR spectra were referenced externally using 1.0 M CF<sub>3</sub>CO<sub>2</sub>H in CDCl<sub>3</sub> at -78.5 ppm. Elemental analyses were performed by CALI Labs, Inc. (Parsippany, NJ).

#### 5.4.2. Synthesis of PCN compounds with alkyl linkers

**Synthesis of (<sup>i</sup>PrPCN-C<sub>2</sub>)NiCl (501a-NiCl).** <sup>i</sup>PrPCN-C<sub>2</sub> (**501a**) (1.010 gm, 2.02 mmol) was dissolved in ca. 20 mL of 1,2-dichlorobenzene. To this 2,6-lutidine (510  $\mu$ L, 471 mg, 4.41 mmol) and anhydrous NiCl<sub>2</sub> (570 mg, 4.41 mmol) were added and the flask was put in an oil bath at 160 °C and left to stir for 20 h when the solution turned bright orange. The volatiles were distilled off and the orange solid was extracted with ca. 50 mL of C<sub>6</sub>H<sub>6</sub> and filtered through a pad of celite on a glass frit. The volatiles were pumped off and the obtained solid was redissolved in ca. 10 mL of dichloromethane and layered with 20 mL of diethylether and put in the freezer at -35 °C. A yellow orange crystalline product (810 mg, 59% yield) was obtained overnight. A small amount of these crystals were taken and re-dissolved in ca. 2 mL of diethyl ether and xray quality crystals were obtained by slow evaporation. <sup>1</sup>H NMR (CD<sub>2</sub>Cl<sub>2</sub>, 500 MHz, 22°C):  $\delta$  = 8.23 (br s, 2H, HC=N), 6.890 (m, 2H, Ar CH), 6.80 (d, *J* = 7.0 Hz, 2H, Ar CH), 6.58 (d, *J* = 7.5 Hz, 2H, Ar CH), 4.03 (br, 4H, CH<sub>2</sub>), 2.36 (m, 4H, CH(CH<sub>3</sub>)<sub>2</sub>), 1.61-1.41 (m, 12H, CH(CH<sub>3</sub>)<sub>2</sub>), 1.40-1.23 (m, 12H, CH(CH<sub>3</sub>)<sub>2</sub>). (**Figure V.9**) <sup>13</sup>C{<sup>1</sup>H} NMR (CD<sub>2</sub>Cl<sub>2</sub>, 126 MHz, 22°C):  $\delta$  = 174.3 (d, *J* = 3.0 Hz, HC=N), 165.8 (d, *J* = 10.3 Hz, Ar C), 150.8 (d, *J* = 35.9 Hz, Ar C), 147.5 (Ar C), 126.8 (Ar CH), 121.1 (Ar CH), 113.4 (d, *J* = 12.4 Hz, Ar CH), 57.0 (CH<sub>2</sub>), 28.5 (d, *J* = 22.7 Hz, CH(CH<sub>3</sub>)<sub>2</sub>), 17.8 (d, *J* = 3.3 Hz, CH(CH<sub>3</sub>)<sub>2</sub>), 16.9 ppm (d, *J* = 1.8 Hz, CH(CH<sub>3</sub>)<sub>2</sub>). (**Figure V.10**) <sup>31</sup>P{<sup>1</sup>H} NMR (CD<sub>2</sub>Cl<sub>2</sub>, 200 MHz, 22°C):  $\delta$  = 197.7 ppm. (**Figure V.11**)



Elem. Anal. Calc. for  $C_{28}H_{40}Cl_2N_2Ni_2O_2P_2$ : C, 48.96; H, 5.87; N, 4.08. Found: C, 49.13; H, 5.85; N, 4.03.

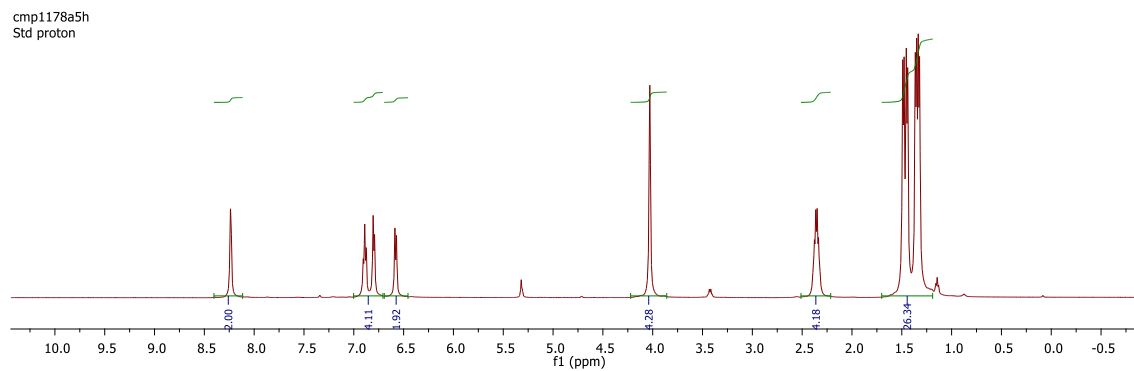


**Figure V.9**  $^1H$  NMR spectrum of  $(iPr)PCN-C_2NiCl$  (**1a-NiCl**) in  $CD_2Cl_2$ . Minor residual diethylether and dichloromethane present

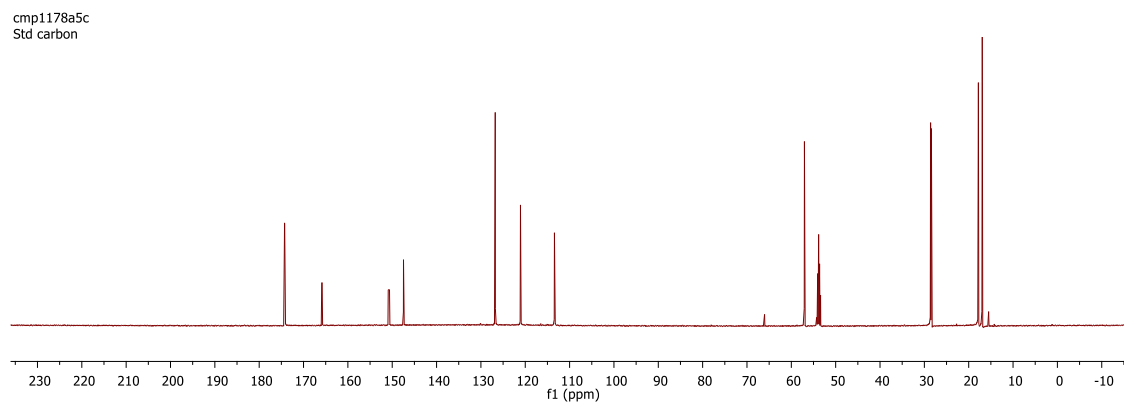


**Figure V.10**  $^{13}C\{^1H\}$  NMR spectrum of  $(iPr)PCN-C_2NiCl$  (**501a-NiCl**) in  $CD_2Cl_2$ . Minor residual diethylether and dichloromethane present.

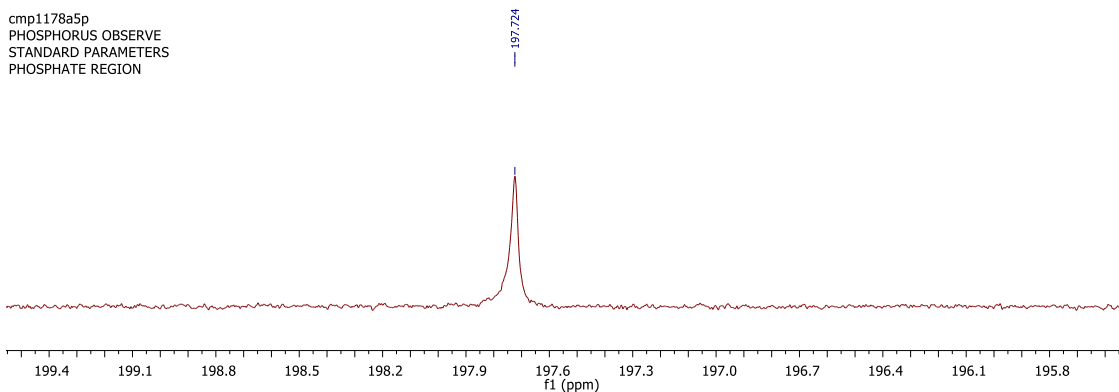


**Figure V.11**  $^{31}\text{P}\{^1\text{H}\}$  NMR spectrum of  $(i\text{PrPCN-C}_2)\text{NiCl}$  (**501a-NiCl**) in  $\text{CD}_2\text{Cl}_2$ .

**Synthesis of  $(i\text{PrPCN-C}_4)\text{NiCl}$  (**501b-NiCl**).**  $i\text{PrPCN-C}_4$  (**501b**) (1.41 gm, 2.67 mmol) was dissolved in ca. 40 mL of 1,2-dichlorobenzene. To this 2,6-lutidine (678  $\mu\text{L}$ , 628 mg, 5.87 mmol) and anhydrous  $\text{NiCl}_2$  (760 mg, 5.87 mmol) were added and the flask was put in an oil bath at 160  $^\circ\text{C}$  and left to stir for 20 h when the solution turned bright orange. The volatiles were distilled off and the orange solid was extracted with ca. 10 mL of  $\text{C}_6\text{H}_6$  and filtered through a pad of celite on a glass frit. The volatiles were pumped off and the obtained solid was redissolved in ca. 5 mL of diethylether and layered with 10 mL of pentane and put in the freezer at -35  $^\circ\text{C}$ . A yellow orange crystalline product (1.51 gm, 78% yield) was obtained overnight. A small amount of these crystals were taken and re-dissolved in ca. 2 mL of diethyl ether and xray quality crystals were obtained by slow evaporation.  $^1\text{H}$  NMR ( $\text{CD}_2\text{Cl}_2$ , 500 MHz, 22 $^\circ\text{C}$ ):  $\delta$  = 8.07 (d,  $J$  = 4.5 Hz, 2H,  $\text{HC}=\text{N}$ ), 6.97-6.87 (overlapped m, 4H, Ar  $\text{CH}$ ), 6.58 (dd,  $J$  = 8.0 Hz,  $J$  = 1.0 Hz, 2H, Ar  $\text{CH}$ ), 3.60 (br, 4H,  $\text{CH}_2$ ), 2.33 (m, 4H,  $\text{CH}(\text{CH}_3)_2$ ), 1.82 (br, 4H,  $\text{CH}_2$ ), 1.49-1.39 (m, 12H,  $\text{CH}(\text{CH}_3)_2$ ), 1.38-1.28 (m, 12H,  $\text{CH}(\text{CH}_3)_2$ ). (**Figure V.12**)  $^{13}\text{C}\{^1\text{H}\}$  NMR ( $\text{CD}_2\text{Cl}_2$ , 126 MHz, 22 $^\circ\text{C}$ ):  $\delta$  = 171.7 (d,  $J$  = 3.1 Hz,  $\text{HC}=\text{N}$ ), 165.8 (d,  $J$  = 10.6 Hz, Ar C), 150.7 (d,  $J$  =

36.2 Hz, Ar C), 148.1 (Ar C), 126.6 (Ar CH), 120.9 (d,  $J = 1.8$  Hz, Ar CH), 113.0 (d,  $J = 12.5$  Hz, Ar CH), 56.4 (CH<sub>2</sub>), 28.5 (d,  $J = 22.6$  Hz, CH(CH<sub>3</sub>)<sub>2</sub>), 28.3 (CH<sub>2</sub>), 17.7 (d,  $J = 4.6$  Hz, CH(CH<sub>3</sub>)<sub>2</sub>), 16.9 ppm (d,  $J = 1.8$  Hz, CH(CH<sub>3</sub>)<sub>2</sub>). **(Figure V.13)** <sup>31</sup>P{<sup>1</sup>H} NMR (CD<sub>2</sub>Cl<sub>2</sub>, 121 MHz, 22°C):  $\delta = 197.2$  ppm. **(Figure V.14)**

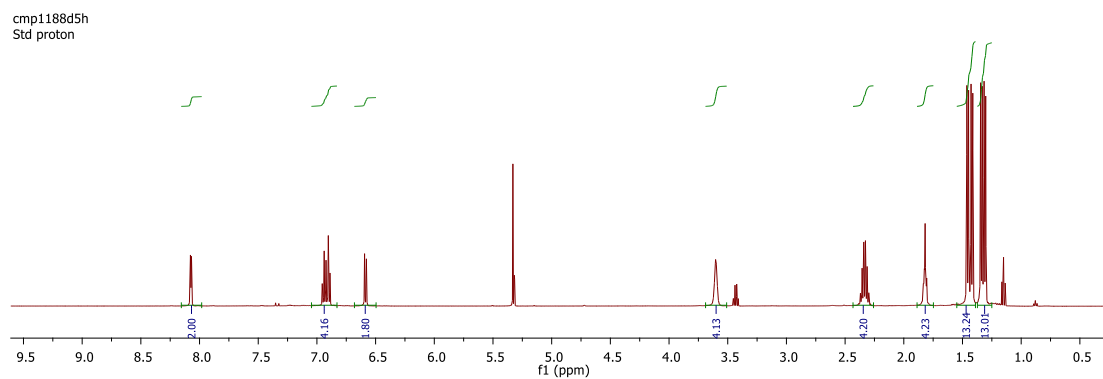


**Figure V.12** <sup>1</sup>H NMR spectrum of (iPr)PCN-C<sub>4</sub>NiCl (**501b-NiCl**) in CD<sub>2</sub>Cl<sub>2</sub>. Residual diethylether present.

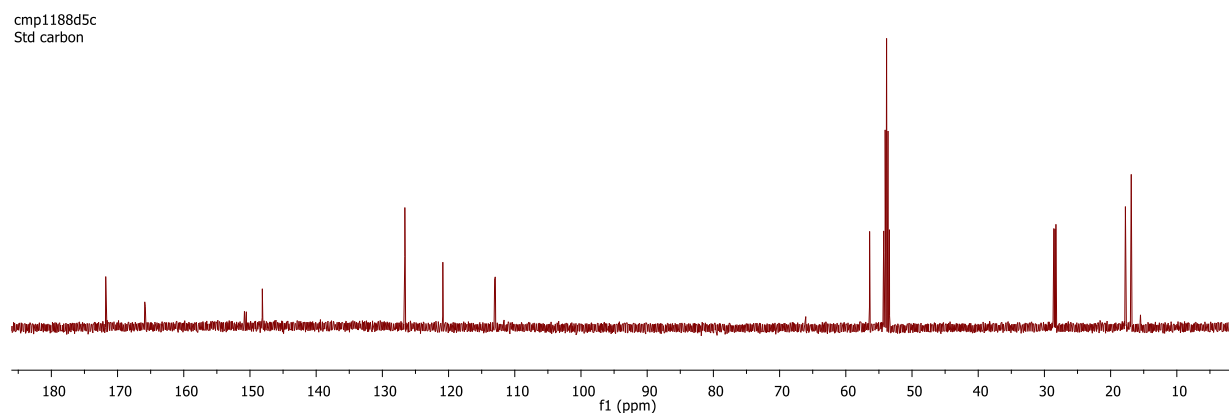


**Figure V.13** <sup>13</sup>C{<sup>1</sup>H} NMR spectrum of (iPr)PCN-C<sub>4</sub>NiCl (**501b-NiCl**) in CD<sub>2</sub>Cl<sub>2</sub>. Residual diethylether present.

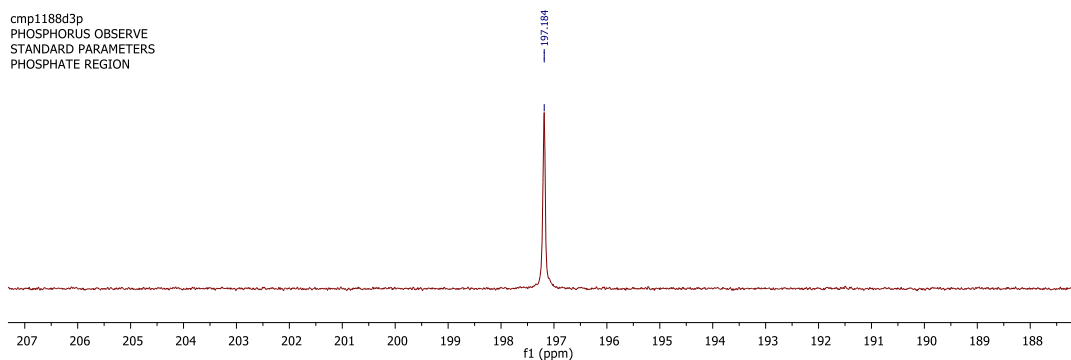


**Figure V.14**  $^{31}\text{P}\{^1\text{H}\}$  NMR spectrum of ( $i\text{PrPCN-C}_4$ )NiCl (**501b-NiCl**) in  $\text{CD}_2\text{Cl}_2$ .

**Synthesis of ( $i\text{PrPCN-C}_2$ )NiOTf (**501a-NiOTf**).** ( $i\text{PrPCN-C}_2$ )NiCl (**501a-NiCl**) (390 mg, 0.568 mmol) was dissolved in ca. 10 mL of toluene. To this  $\text{Me}_3\text{SiOTf}$  (620  $\mu\text{L}$ , 756 mg, 3.40 mmol) was added and the flask was put in an oil bath at 80  $^\circ\text{C}$  and left to stir for 12 h when the solution turned yellow. The volatiles were removed yielding a yellow solid (501 mg, 97% yield).  $^1\text{H}$  NMR ( $\text{CD}_2\text{Cl}_2$ , 500 MHz, 22 $^\circ\text{C}$ ):  $\delta$  = 8.21 (d,  $J$  = 3.5 Hz, 2H, HC=N), 6.97 (m, 2H, Ar CH), 6.86 (d,  $J$  = 7.5 Hz, 2H, Ar CH), 6.58 (d,  $J$  = 8.0 Hz, 2H, Ar CH), 3.70 (br, 4H,  $\text{CH}_2$ ), 2.54 (m, 4H,  $\text{CH}(\text{CH}_3)_2$ ), 1.57-1.42 (m, 12H,  $\text{CH}(\text{CH}_3)_2$ ), 1.38-1.28 (m, 12H,  $\text{CH}(\text{CH}_3)_2$ ). (**Figure V.15**)  $^{13}\text{C}\{^1\text{H}\}$  NMR ( $\text{CD}_2\text{Cl}_2$ , 126 MHz, 22 $^\circ\text{C}$ ):  $\delta$  = 175.3 (d,  $J$  = 2.7 Hz, HC=N), 166.8 (d,  $J$  = 8.8 Hz, Ar C), 147.4 (Ar C), 141.9 (d,  $J$  = 35.3 Hz, Ar C), 128.1 (Ar CH), 122.3 (d,  $J$  = 1.5 Hz, Ar CH), 114.4 (d,  $J$  = 12.0 Hz, Ar CH), 56.2 ( $\text{CH}_2$ ), 29.0 (d,  $J$  = 22.4 Hz,  $\text{CH}(\text{CH}_3)_2$ ), 18.2 (d,  $J$  = 6.0 Hz,  $\text{CH}(\text{CH}_3)_2$ ), 17.0 ppm (d,  $J$  = 3.5 Hz,  $\text{CH}(\text{CH}_3)_2$ ). (**Figure V.16**)  $^{31}\text{P}\{^1\text{H}\}$  NMR ( $\text{CD}_2\text{Cl}_2$ , 121 MHz, 22 $^\circ\text{C}$ ):  $\delta$  = 198.6 ppm. (**Figure V.17**)  $^{19}\text{F}$  NMR ( $\text{CD}_2\text{Cl}_2$ , 282 MHz, 22 $^\circ\text{C}$ ):  $\delta$  = -79.1 ppm. (**Figure V.18**)

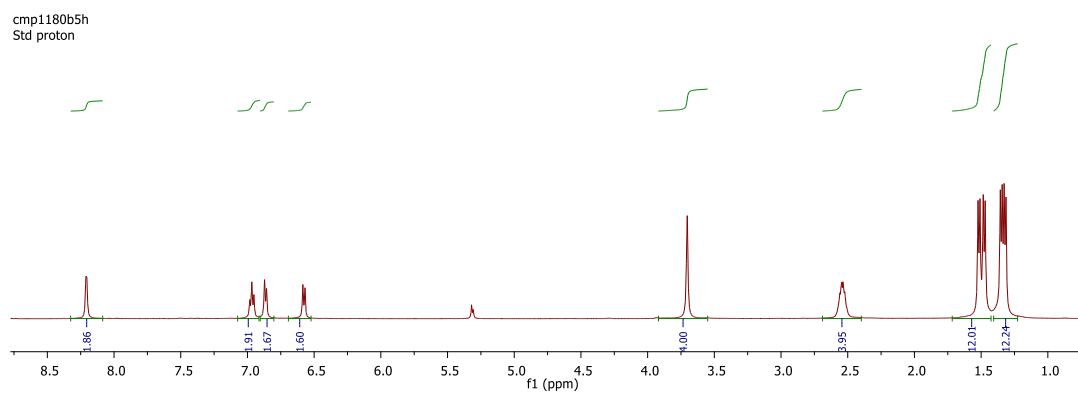


**Figure V.15**  $^1\text{H}$  NMR spectrum of ( $i\text{PrPCN-C}_2$ )NiOTf (**501a-NiOTf**) in  $\text{CD}_2\text{Cl}_2$ .

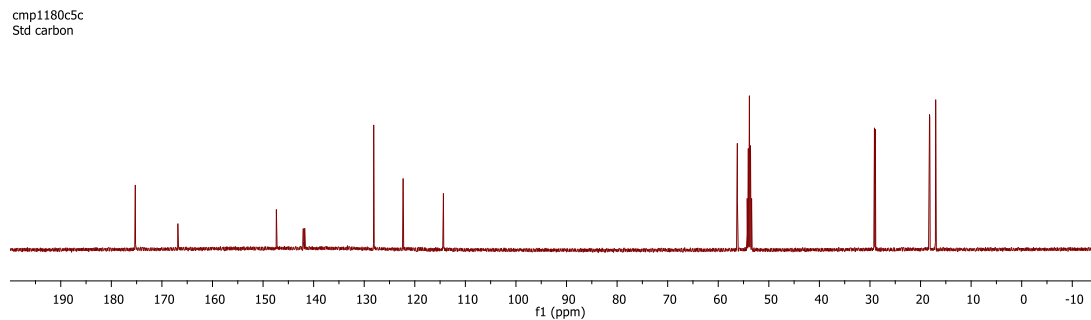


**Figure V.16**  $^{13}\text{C}\{^1\text{H}\}$  NMR spectrum of ( $i\text{PrPCN-C}_2$ )NiOTf (**501a-NiOTf**) in  $\text{CD}_2\text{Cl}_2$ .

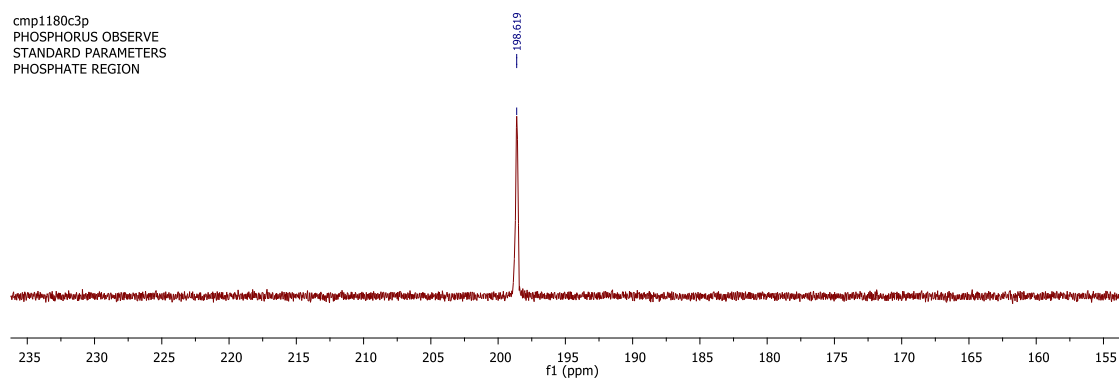


**Figure V.17**  $^{31}\text{P}\{^1\text{H}\}$  NMR spectrum of ( $i\text{PrPCN-C}_2$ )NiOTf (**501a-NiOTf**) in  $\text{CD}_2\text{Cl}_2$ .

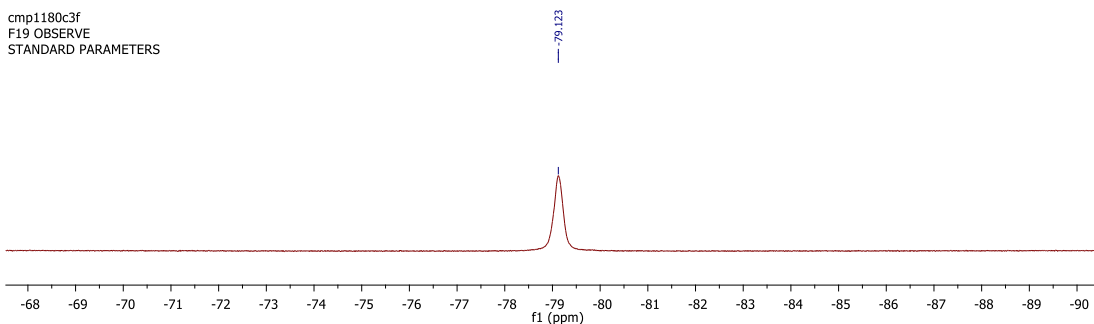


**Figure V.18**  $^{19}\text{F}$  NMR spectrum of ( $i\text{PrPCN-C}_2$ )NiOTf (**501a-NiOTf**) in  $\text{CD}_2\text{Cl}_2$ .

**Synthesis of ( $i\text{PrPCN-C}_4$ )NiOTf (501b-NiOTf).** **501b-NiCl** (160 mg, 0.225 mmol) was dissolved in ca. 5 mL of toluene. To this  $\text{Me}_3\text{SiOTf}$  (244  $\mu\text{L}$ , 298 mg, 1.35 mmol) was added and the flask was put in an oil bath at 80  $^\circ\text{C}$  and left to stir for 12 h when the solution turned yellow. The volatiles were removed yielding a yellow solid (240 mg, 97% yield).  $^1\text{H}$  NMR ( $\text{CD}_2\text{Cl}_2$ , 500 MHz, 22 $^\circ\text{C}$ ):  $\delta$  = 7.97 (d,  $J$  = 4.5 Hz, 2H,  $\text{HC}=\text{N}$ ), 6.99 (m, 2H, Ar  $\text{CH}$ ), 6.91 (d,  $J$  = 7.5 Hz, 2H, Ar  $\text{CH}$ ), 6.57 (dd,  $J$  = 8.0 Hz,  $J$  = 1.0 Hz, 2H, Ar  $\text{CH}$ ), 3.43 (br, 4H,  $\text{CH}_2$ ), 2.52 (m, 4H,  $\text{CH}(\text{CH}_3)_2$ ), 1.72 (br, 4H,  $\text{CH}_2$ ), 1.51-1.41 (m, 12H,  $\text{CH}(\text{CH}_3)_2$ ), 1.36-1.28 (m, 12H,  $\text{CH}(\text{CH}_3)_2$ ). (**Figure V.19**)  $^{13}\text{C}\{^1\text{H}\}$  NMR ( $\text{CD}_2\text{Cl}_2$ , 126 MHz, 22 $^\circ\text{C}$ ):  $\delta$  = 171.9 (d,  $J$  = 3.0 Hz,  $\text{HC}=\text{N}$ ), 166.8 (d,  $J$  = 8.8 Hz, Ar  $\text{C}$ ), 147.9 (Ar  $\text{C}$ ), 141.9 (d,  $J$  = 35.4 Hz, Ar  $\text{C}$ ), 127.9 (Ar  $\text{CH}$ ), 121.8 (d,  $J$  = 2.0 Hz, Ar  $\text{CH}$ ), 114.4 (d,  $J$  = 11.7 Hz, Ar  $\text{CH}$ ), 56.8 ( $\text{CH}_2$ ), 28.9 (d,  $J$  = 22.0 Hz,  $\text{CH}(\text{CH}_3)_2$ ), 27.7 ( $\text{CH}_2$ ), 18.0 (d,  $J$  = 5.9 Hz,  $\text{CH}(\text{CH}_3)_2$ ), 16.9 ppm (d,  $J$  = 3.4 Hz,  $\text{CH}(\text{CH}_3)_2$ ). (**Figure V.20**)  $^{31}\text{P}\{^1\text{H}\}$  NMR ( $\text{CD}_2\text{Cl}_2$ , 121 MHz, 22 $^\circ\text{C}$ ):  $\delta$  = 198.1 ppm. (**Figure V.21**)  $^{19}\text{F}$  NMR ( $\text{CD}_2\text{Cl}_2$ , 282 MHz, 22 $^\circ\text{C}$ ):  $\delta$  = -79.1 ppm. (**Figure V.22**)

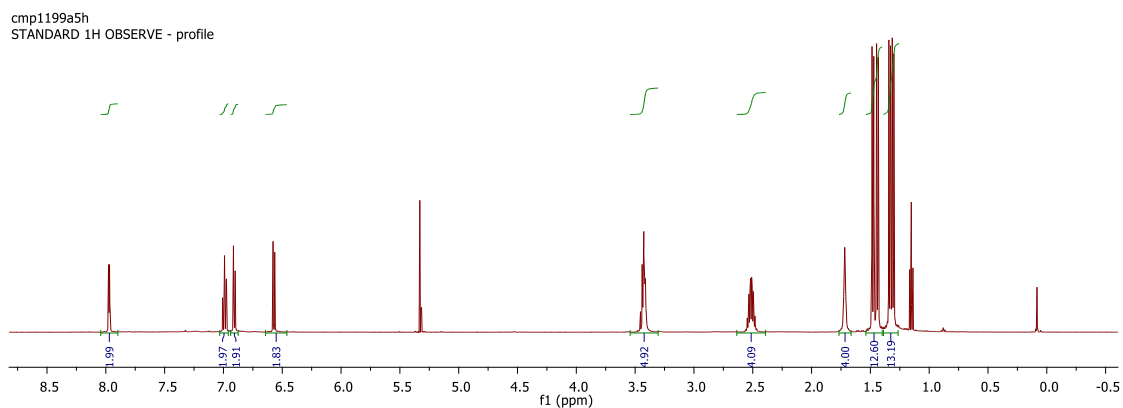


**Figure V.19**  $^1\text{H}$  NMR spectrum of  $(i\text{PrPCN-C}_4)\text{NiOTf}$  (**501b-NiOTf**) in  $\text{CD}_2\text{Cl}_2$ . Minor diethylether present

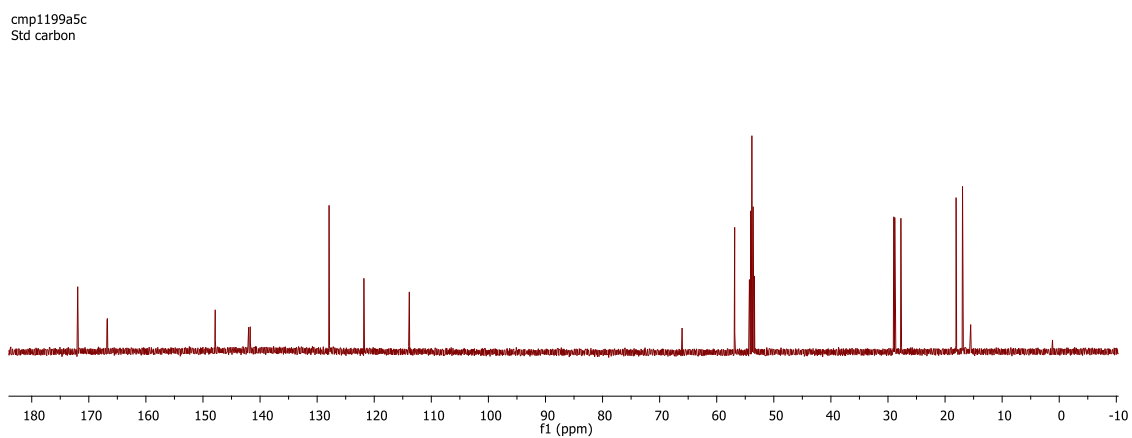


**Figure V.20**  $^{13}\text{C}\{^1\text{H}\}$  NMR spectrum of  $(i\text{PrPCN-C}_4)\text{NiOTf}$  (**501b-NiOTf**) in  $\text{CD}_2\text{Cl}_2$ . Minor diethylether present

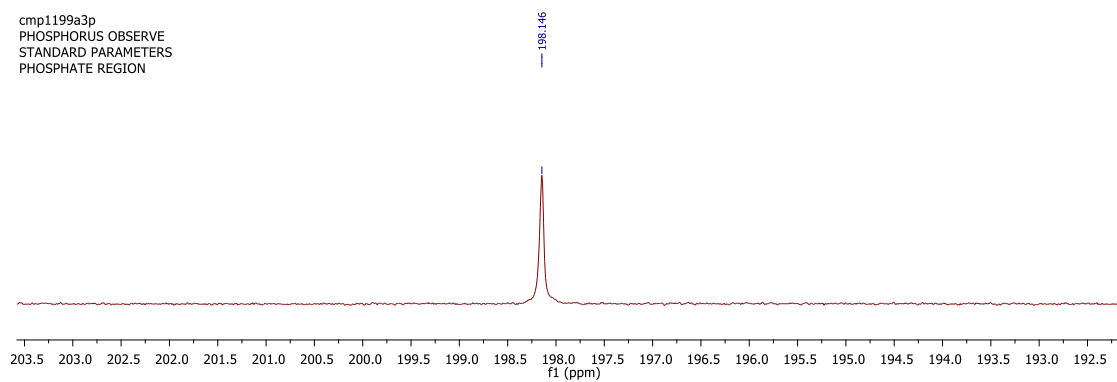


**Figure V.21**  $^{31}\text{P}\{^1\text{H}\}$  NMR spectrum of  $(i\text{PrPCN-C}_4)\text{NiOTf}$  (**501b-NiOTf**) in  $\text{CD}_2\text{Cl}_2$

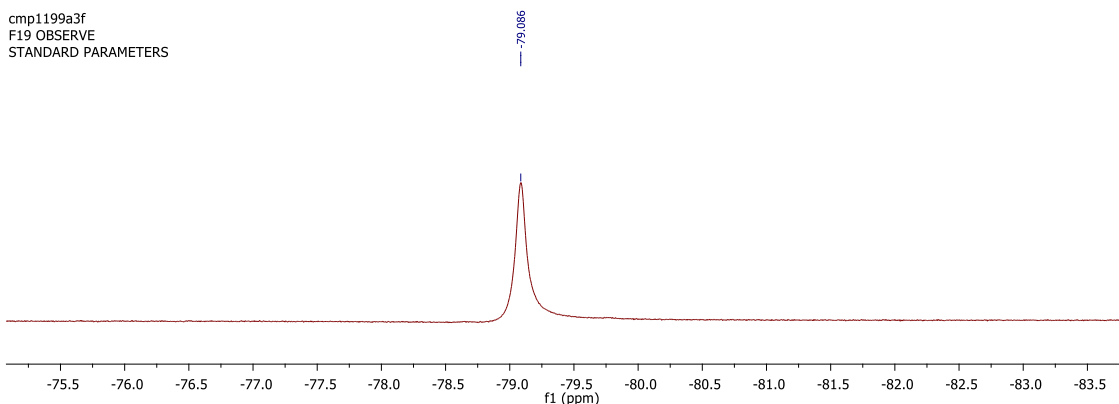


**Figure V.22**  $^{19}\text{F}$  NMR spectrum of ( $i\text{PrPCN-C}_4$ )NiOTf (**501b-NiOTf**) in  $\text{CD}_2\text{Cl}_2$

**Synthesis of  $t\text{BuPCN-C}_2$  (**502a**).** Solid NaH (0.189 g, 7.87 mmol) was added portion-wise to a rapidly stirring suspension of the ethylene-bridged benzaldimine (**502a'**) (1.05 g, 3.90 mmol) in THF (50 mL). The mixture was heated at reflux for 2 h then  $t\text{Bu}_2\text{PCl}$  (1.48 mL, 7.80 mmol) was added via syringe and heating was continued for 15 h. The mixture was then dried in vacuo to leave a brown-yellow oil and off-white solid. The product was extracted by stirring the residue in 50 mL of pentane for 30 min and filtered over a short plug of silica, which was then washed with 3 x 15 mL of  $\text{Et}_2\text{O}$ . The collected extracts were then dried to give a yellow oil which was further dried under vacuum at  $50^\circ\text{C}$  for 1 h to remove residual volatiles. Yield = 1.129 g (52%).  $^1\text{H}$  NMR ( $\text{CDCl}_3$ , 499 MHz,  $22^\circ\text{C}$ ):  $\delta$  = 8.26 (s, 2H,  $\text{HC}=\text{N}$ ), 7.49 (m, 2H, Ar CH) 7.28 (m – overlapped with solvent, 6H, Ar CH), 3.97 (s, 2H,  $\text{CH}_2$ ), 1.17 ppm (d,  $^2J_{\text{HP}} = 12.0$  Hz, 36H,  $t\text{Bu}$ ). (**Figure V.23**)  $^{13}\text{C}\{^1\text{H}\}$  NMR ( $\text{CDCl}_3$ , 126 MHz,  $22^\circ\text{C}$ ):  $\delta$  = 162.6 ( $\text{HC}=\text{N}$ ), 160.2 (d,  $J = 9.2$  Hz, Ar C), 137.7 (Ar C), 129.6 (Ar CH), 121.5 (Ar CH), 120.5 (d,  $J = 12.2$  Hz, Ar CH), 117.8 (d,  $J = 8.4$  Hz, Ar CH), 61.7 ( $\text{CH}_2$ ), 35.8 (d,  $J = 25.4$  Hz,  $t\text{Bu CMe}_3$ ), 27.5 ppm (d,  $J =$



15.4 Hz, *t*Bu CMe<sub>3</sub>). (Figure V.24) <sup>31</sup>P{<sup>1</sup>H} NMR (CDCl<sub>3</sub>, 202 MHz, 22°C): δ = 154.6 ppm. (Figure V.25)

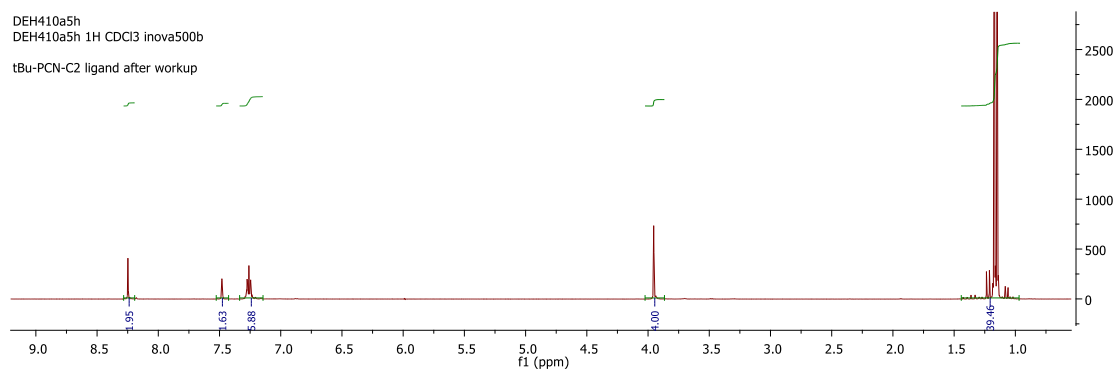


Figure V.23 <sup>1</sup>H NMR spectrum of (<sup>t</sup>BuPCN-C<sub>2</sub>) (502a) in CDCl<sub>3</sub>.

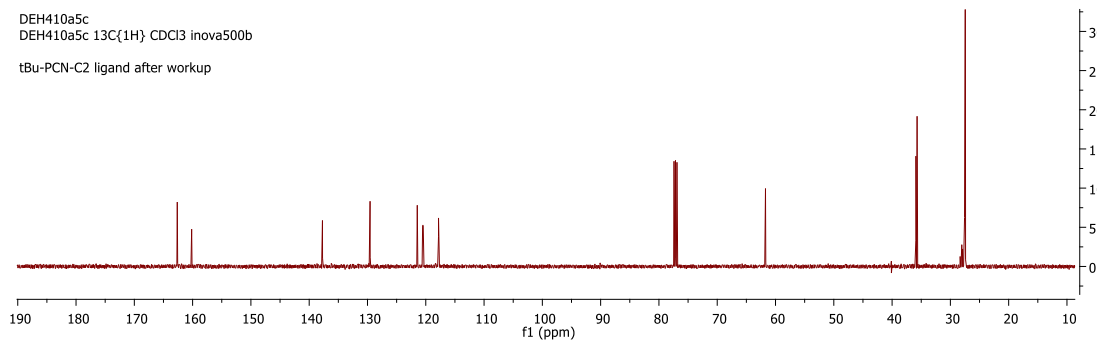


Figure V.24 <sup>13</sup>C{<sup>1</sup>H} NMR spectrum of (<sup>t</sup>BuPCN-C<sub>2</sub>) (502a) in CDCl<sub>3</sub>

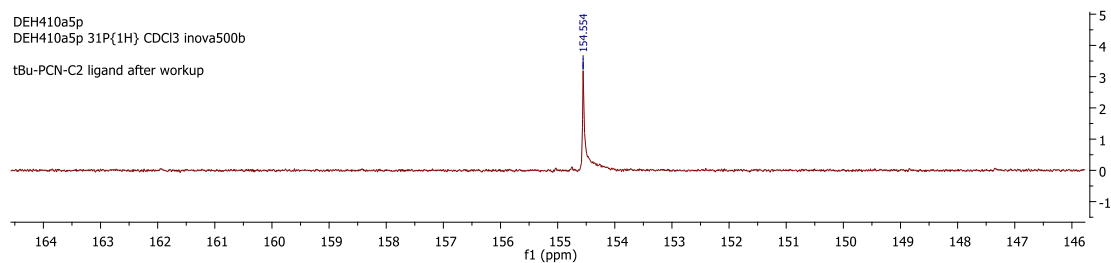
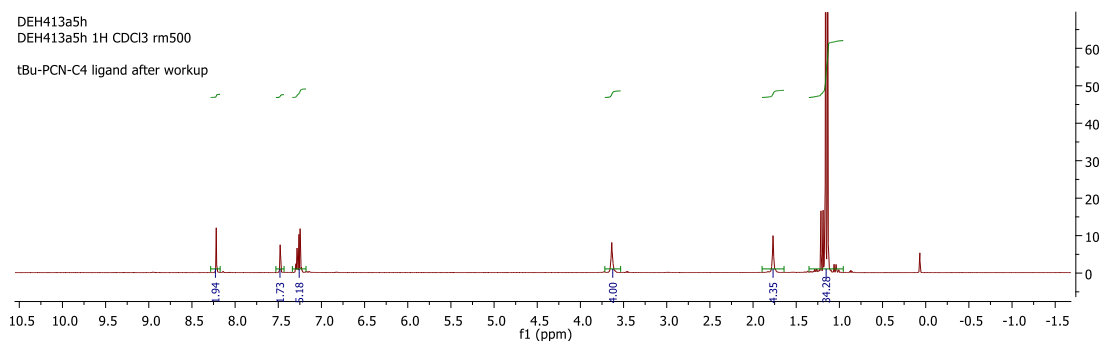


Figure V.25 <sup>31</sup>P{<sup>1</sup>H} NMR spectrum of (<sup>t</sup>BuPCN-C<sub>2</sub>) (502a) in CDCl<sub>3</sub>.

**Synthesis of <sup>t</sup>BuPCN-C<sub>4</sub> (502b).**<sup>††</sup> Solid NaH (0.245 g, 10.2 mmol) was added portion-wise to a rapidly stirring suspension of the C<sub>4</sub>-bridged benzaldimine (**502b'**) (1.50 g, 5.06 mmol) in THF (50 mL). The mixture was heated at reflux for 2 h then <sup>t</sup>Bu<sub>2</sub>PCl (1.92 mL, 10.2 mmol) was added via syringe and heating was continued for 15 h. The mixture was then dried in vacuo to leave a brown-yellow oil and off-white solid. The product was extracted by stirring the residue in 50 mL of pentane for 30 min and filtered over a short plug of silica, which was then washed with 3 x 15 mL of Et<sub>2</sub>O. The collected extracts were then dried to give a yellow oil which was further dried under vacuum at 50°C for 1 h to remove residual volatiles. Yield = 2.310 g (78%). <sup>1</sup>H NMR (CDCl<sub>3</sub>, 500 MHz, 22°C): δ = 8.22 (s, 2H, HC=N), 7.48 (br, 2H, Ar CH), 7.28 (m, 2H, Ar CH), 7.25 (m, 4H, Ar CH), 3.64 (br, 4H, CH<sub>2</sub>), 1.77 (br, 4H, CH<sub>2</sub>), 1.15 ppm (d, <sup>2</sup>J<sub>HP</sub> = 12.0 Hz, 36H, *t*Bu). (**Figure V.26**) <sup>13</sup>C{<sup>1</sup>H} NMR (CDCl<sub>3</sub>, 126 MHz, 22°C): δ = 160.9 (HC=N), 160.2 (d, *J* = 9.3 Hz, Ar C), 137.8 (Ar C), 129.6 (d, *J* = 2.1 Hz, Ar CH), 121.3 (d, *J* = 1.1 Hz, Ar CH), 120.3 (d, *J* = 12.8 Hz, Ar CH), 117.8 (d, *J* = 8.5 Hz, Ar CH), 61.6 (CH<sub>2</sub>), 35.8 (d, *J* = 25.3 Hz, *t*Bu CMe<sub>3</sub>), 28.8 (CH<sub>2</sub>), 27.5 ppm (d, *J* = 15.1 Hz, *t*Bu CMe<sub>3</sub>). (**Figure V.27**) <sup>31</sup>P{<sup>1</sup>H} NMR (CDCl<sub>3</sub>, 121 MHz, 22°C): δ = 154.2 ppm. (**Figure V.28**)

---

<sup>††</sup> <sup>t</sup>BuPCN-C<sub>2</sub> and <sup>t</sup>BuPCN-C<sub>4</sub> ligands and their Pd complexes first synthesized by Dr. Dave Herbert; further purification and characterization carried out by C. M. Palit



**Figure V.26**  $^1\text{H}$  NMR spectrum of ( $^t\text{BuPCN-C}_4$ ) (**502b**) in  $\text{CDCl}_3$ .

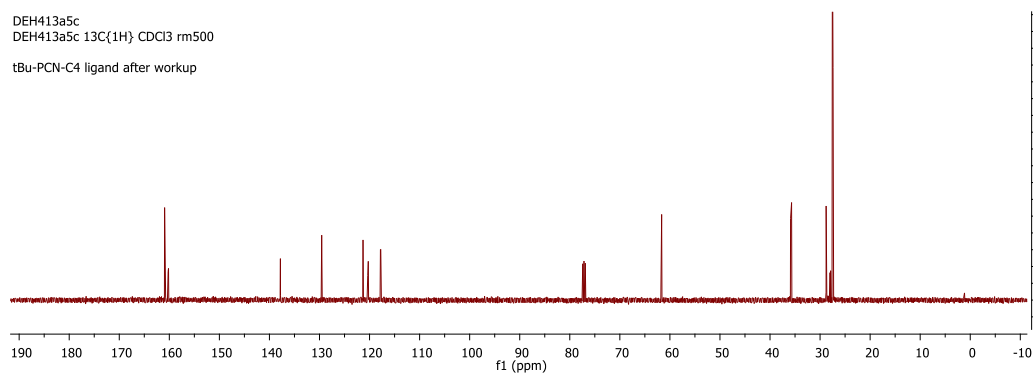


**Figure V.27**  $^{13}\text{C}\{^1\text{H}\}$  NMR spectrum of ( $^t\text{BuPCN-C}_4$ ) (**502b**) in  $\text{CDCl}_3$

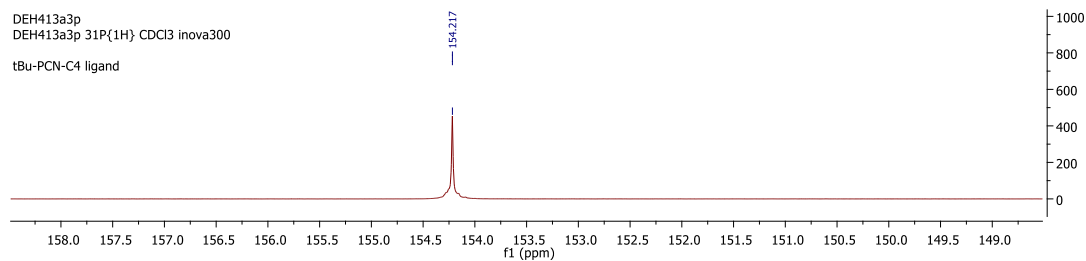


**Figure V.28**  $^{31}\text{P}\{^1\text{H}\}$  NMR spectrum of ( $^t\text{BuPCN-C}_4$ ) (**502b**) in  $\text{CDCl}_3$

**Synthesis of ( $^t\text{BuPCN-C}_2$ )NiCl (**502a-NiCl**).** **502a** (250 mg, 0.45 mmol) was dissolved in ca. 10 mL of 1,2-dichlorobenzene. To this 2,6-lutidine (104  $\mu\text{L}$ , 0.90 mmol) and anhydrous  $\text{NiCl}_2$  (175 mg, 1.35 mmol) were added and the flask was put in an oil bath at 160  $^\circ\text{C}$  and left to stir for 18 h when the solution turned bright orange. Then the volatiles

were distilled off and the orange solid was extracted with ca. 20 mL of C<sub>6</sub>H<sub>6</sub> and filtered through a pad of celite on a glass frit. The volatiles were pumped off and the obtained solid was redissolved in ca. 10 mL of diethylether and layered with 20 mL of pentane and put in the freezer at -35 °C. A yellow orange crystalline product (300 mg, 89% yield) was obtained overnight. <sup>1</sup>H NMR (CD<sub>2</sub>Cl<sub>2</sub>, 500 MHz, 22°C): δ = 8.22 (d, *J* = 4.0 Hz, 2H, HC=N), 6.90 (m, 2H, Ar CH), 6.77 (d, *J* = 7.0 Hz, 2H, Ar CH), 6.62 (d, *J* = 8.0 Hz, 2H, Ar CH), 4.04 (br, 4H, CH<sub>2</sub>), 1.52 ppm (d, *J* = 14.5 Hz, 36H, *t*Bu CMe<sub>3</sub>). (**Figure V.29**) <sup>13</sup>C{<sup>1</sup>H} NMR (CD<sub>2</sub>Cl<sub>2</sub>, 126 MHz, 22°C): δ = 174.2 (d, *J* = 2.4 Hz, HC=N), 166.6 (d, *J* = 9.1 Hz, Ar C), 150.4 (d, *J* = 33.5 Hz, Ar C), 147.3 (Ar C), 126.5 (Ar C), 120.7 (Ar C), 113.3 (d, *J* = 12.0 Hz, Ar CH), 56.9 (CH<sub>2</sub>), 39.5 (d, *J* = 14.4 Hz, *t*Bu CMe<sub>3</sub>), 28.0 ppm (d, *J* = 4.3 Hz, *t*Bu CMe<sub>3</sub>). (**Figure V.30**) <sup>31</sup>P{<sup>1</sup>H} NMR (CD<sub>2</sub>Cl<sub>2</sub>, 121 MHz, 22°C): δ = 203.9 ppm. (**Figure V.31**) Elem. Anal. Calc. for C<sub>32</sub>H<sub>48</sub> Cl<sub>2</sub>N<sub>2</sub>Ni<sub>2</sub>O<sub>2</sub>P<sub>2</sub>: C, 51.73; H, 6.51; N, 3.77. Found: C, 51.82; H, 6.43; N, 3.70.

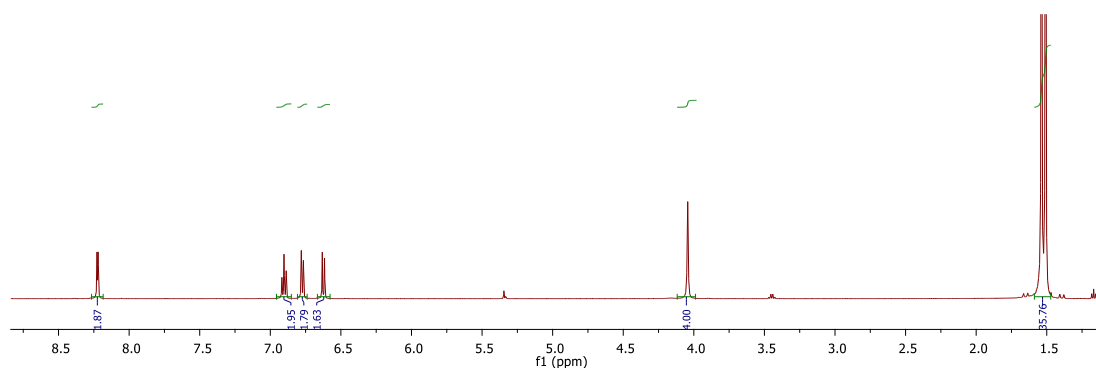


**Figure V.29** <sup>1</sup>H NMR spectrum of (<sup>t</sup>BuPCN-C<sub>2</sub>)NiCl (**502a-NiCl**) in CD<sub>2</sub>Cl<sub>2</sub>

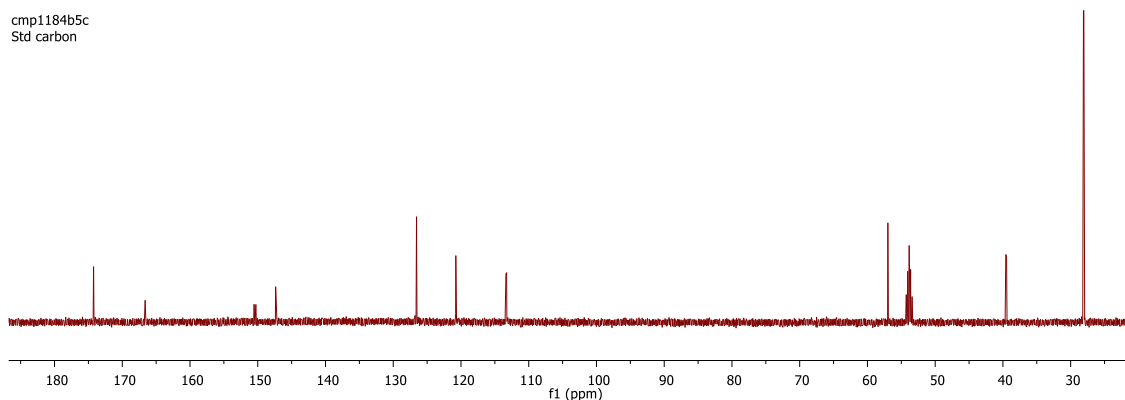


**Figure V.30**  $^{13}\text{C}\{^1\text{H}\}$  NMR spectrum of  $(^t\text{BuPCN-C}_2)\text{NiCl}$  (**502a-NiCl**) in  $\text{CD}_2\text{Cl}_2$ .

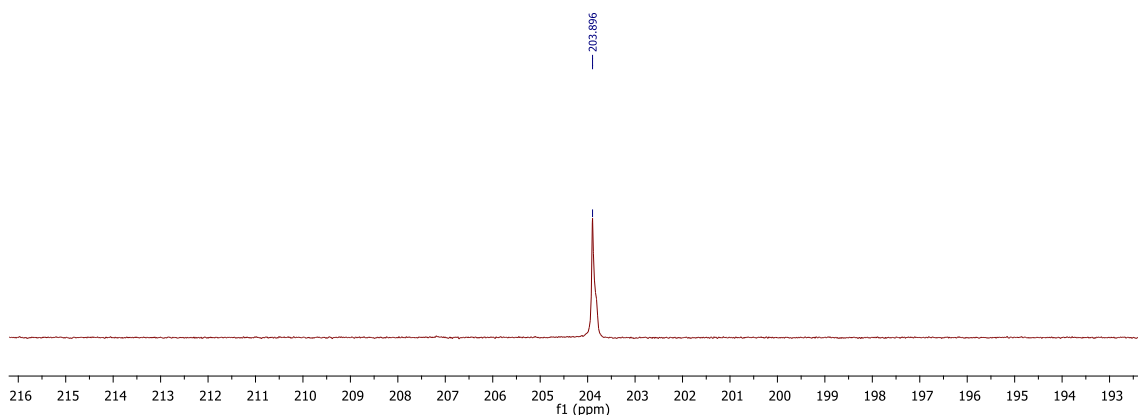


**Figure V.31**  $^{31}\text{P}\{^1\text{H}\}$  NMR spectrum of  $(^t\text{BuPCN-C}_2)\text{NiCl}$  (**502a-NiCl**) in  $\text{CD}_2\text{Cl}_2$ .

**Synthesis of  $(^t\text{BuPCN-C}_4)\text{NiCl}$  (**502b-NiCl**).** **502b** (500 mg, 0.859 mmol) was dissolved in ca. 30 mL of 1,2-dichlorobenzene. To this 2,6-lutidine (200  $\mu\text{L}$ , 1.72 mmol) and anhydrous  $\text{NiCl}_2$  (334 mg, 2.57 mmol) were added and the flask was put in an oil bath at  $160^\circ\text{C}$  and left to stir for 12 h when the solution turned bright orange. Then the volatiles were distilled off and the orange solid was extracted with ca. 10 mL of  $\text{C}_6\text{H}_6$  and filtered through a pad of celite on a glass frit. The volatiles were pumped off and the obtained solid was redissolved in ca. 5 mL of diethylether and layered with 10 mL of pentane and

put in the freezer at  $-35\text{ }^{\circ}\text{C}$ . A yellow orange crystalline product (450 mg, 68% yield) was obtained overnight. A small amount of these crystals were taken and re-dissolved in ca. 2 mL of diethyl ether and X-ray quality crystals were obtained by slow evaporation.  $^1\text{H}$  NMR ( $\text{CD}_2\text{Cl}_2$ , 500 MHz,  $22\text{ }^{\circ}\text{C}$ ):  $\delta = 8.05$  (d,  $J = 4.5$  Hz, 2H,  $\text{HC}=\text{N}$ ), 6.97-6.84 (overlapping m, 4H, Ar  $\text{CH}$ ), 6.61 (dd,  $J = 7.8$  Hz,  $J = 1.2$  Hz, 2H, Ar  $\text{CH}$ ), 3.59 (br, 4H,  $\text{CH}_2$ ), 1.80 (br, 4H,  $\text{CH}_2$ ), 1.47 ppm (d,  $J = 14.4$  Hz, 36H,  $t\text{Bu CMe}_3$ ). (**Figure V.32**)  $^{31}\text{P}\{^1\text{H}\}$  NMR ( $\text{CD}_2\text{Cl}_2$ , 121 MHz,  $22\text{ }^{\circ}\text{C}$ ):  $\delta = 203.7$  ppm (**Figure V.33**)

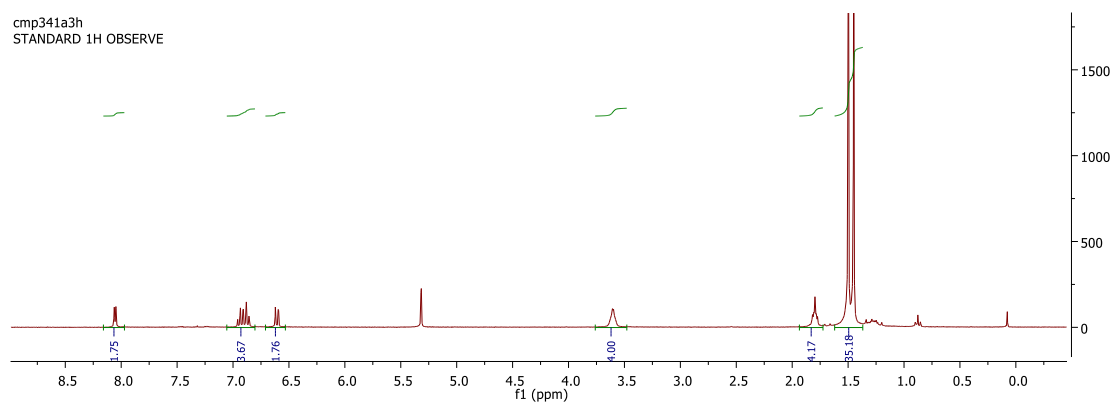


**Figure V.32**  $^1\text{H}$  NMR spectrum of  $(t\text{BuPCN-C}_4)\text{NiCl}$  (502b-NiCl) in  $\text{C}_6\text{D}_6$ .

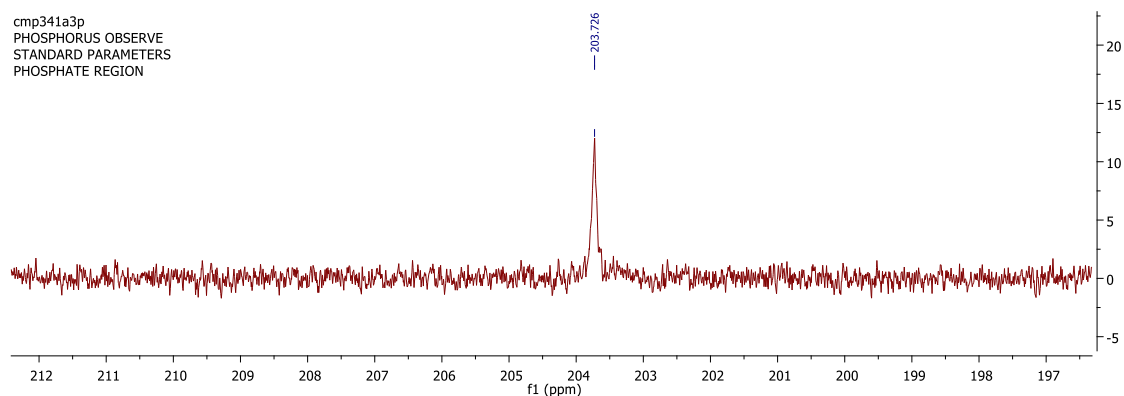


**Figure V.33**  $^{31}\text{P}\{^1\text{H}\}$  NMR spectrum of  $(t\text{BuPCN-C}_4)\text{NiCl}$  (502b-NiCl) in  $\text{C}_6\text{D}_6$ .

**Synthesis of (<sup>t</sup>BuPCN-C<sub>2</sub>)NiOTf (2a-NiOTf).** 502a-NiCl (300 mg, 0.406 mmol) was dissolved in ca. 20 mL of 1:1 C<sub>6</sub>H<sub>5</sub>F/CH<sub>2</sub>Cl<sub>2</sub>. To this AgOTf (208 mg, 0.813 mmol) was added and the solution was left to stir for 12 h when the solution turned yellow. The volatiles were removed, solids extracted with C<sub>6</sub>H<sub>6</sub> and filtered through a pad of celite on a glass frit. The volatiles were pumped off yielding a yellow solid (260 mg, 66% yield) .

<sup>1</sup>H NMR (CD<sub>2</sub>Cl<sub>2</sub>, 500 MHz, 22°C): δ = 8.19 (d, *J* = 4.0 Hz, 2H, HC=N), 6.95 (m, 2H, Ar CH), 6.78 (d, *J* = 7.0 Hz, 2H, Ar CH), 6.57 (d, *J* = 8.0 Hz, 2H, Ar CH), 3.84 (br, 4H, CH<sub>2</sub>), 1.50 ppm (d, *J* = 15.0 Hz, 36H, <sup>t</sup>Bu CMe<sub>3</sub>). (Figure V.34) <sup>13</sup>C{<sup>1</sup>H} NMR (CD<sub>2</sub>Cl<sub>2</sub>, 126 MHz, 22°C): δ = 175.4 (d, *J* = 2.7 Hz, HC=N), 167.5 (d, *J* = 7.7 Hz, Ar C), 147.2 (d, *J* = 1.4 Hz, Ar C), 140.1 (d, *J* = 34.7 Hz, Ar C), 128.0 (Ar C), 122.0 (d, *J* = 1.9 Hz, Ar C), 114.3 (d, *J* = 11.4 Hz, Ar CH), 56.9 (CH<sub>2</sub>), 39.5 (d, *J* = 14.4 Hz, <sup>t</sup>Bu CMe<sub>3</sub>), 27.7 ppm (d, *J* = 5.0 Hz, <sup>t</sup>Bu CMe<sub>3</sub>). (Figure V.35) <sup>31</sup>P{<sup>1</sup>H} NMR (CD<sub>2</sub>Cl<sub>2</sub>, 282 MHz, 22°C): δ = 202.2 ppm. (Figure V.36) <sup>19</sup>F NMR (CD<sub>2</sub>Cl<sub>2</sub>, 282 MHz, 22°C): δ = -78.7 ppm. (Figure V.37) Elem. Anal. Calc. for C<sub>34</sub>H<sub>48</sub>F<sub>6</sub>N<sub>2</sub>Ni<sub>2</sub>O<sub>8</sub>P<sub>2</sub>S<sub>2</sub>: C, 42.09; H, 4.99; N, 2.89.

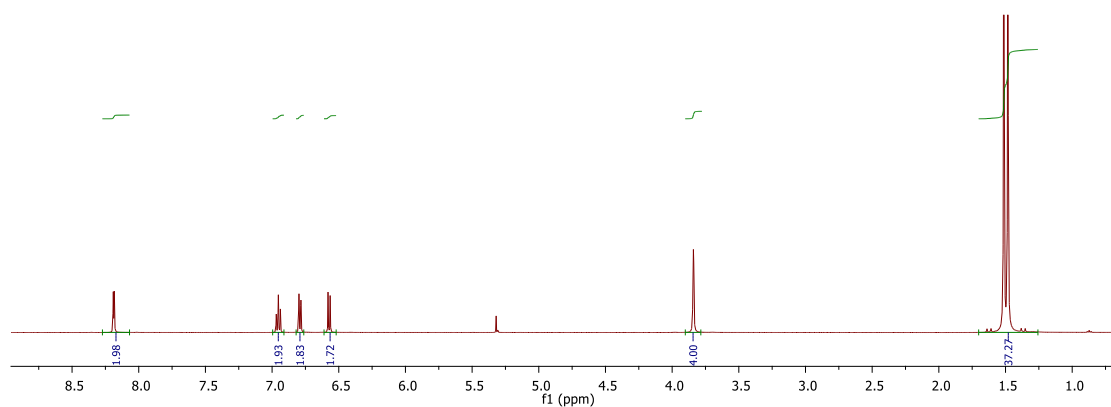


**Figure V.34** <sup>1</sup>H NMR spectrum of (<sup>t</sup>BuPCN-C<sub>2</sub>)NiOTf (502a-NiOTf) in CD<sub>2</sub>Cl<sub>2</sub>.

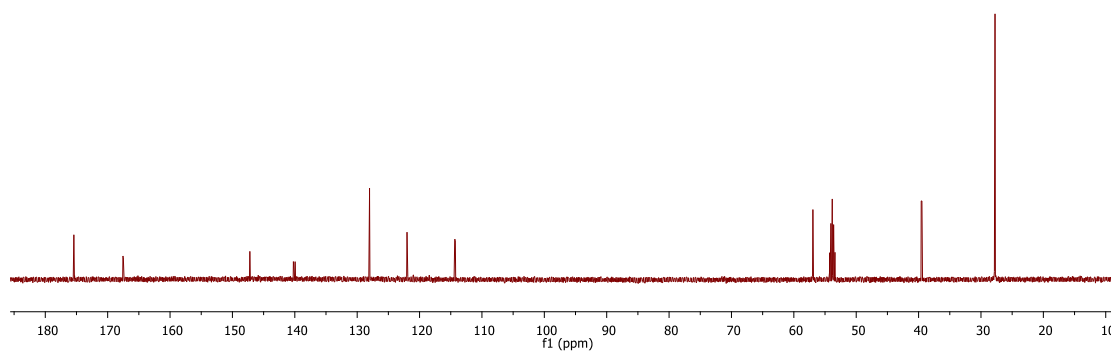


**Figure V.35**  $^{13}\text{C}\{^1\text{H}\}$  NMR spectrum of  $(^t\text{BuPCN-C}_2)\text{NiOTf}$  (**502a-NiOTf**) in  $\text{CD}_2\text{Cl}_2$

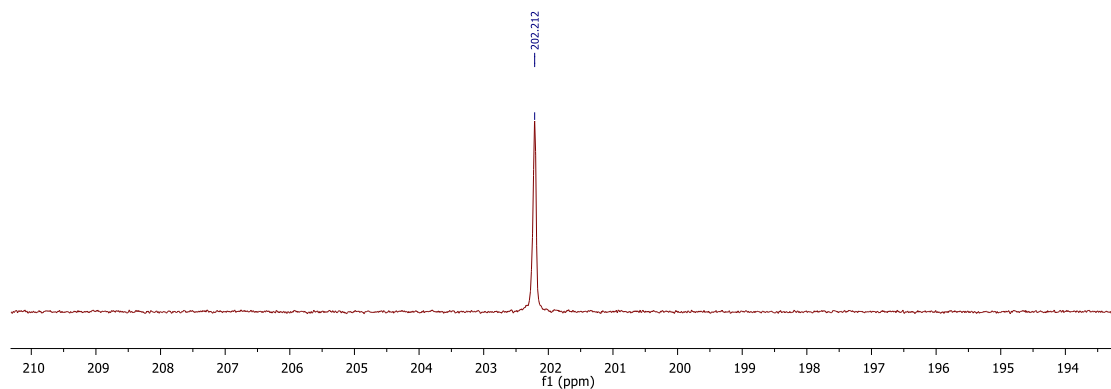


**Figure V.36**  $^{31}\text{P}\{^1\text{H}\}$  NMR spectrum of  $(^t\text{BuPCN-C}_2)\text{NiOTf}$  (**502a-NiOTf**) in  $\text{CD}_2\text{Cl}_2$

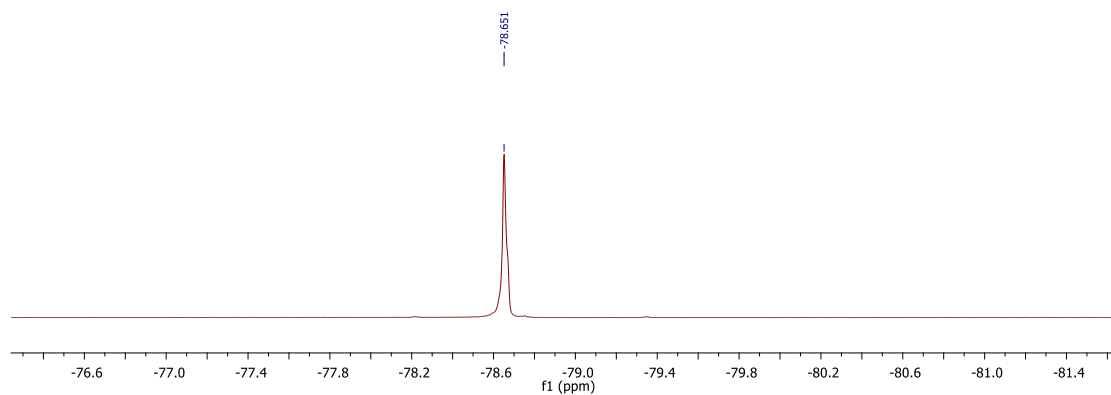


**Figure V.37**  $^{19}\text{F}$  NMR spectrum of  $(^t\text{BuPCN-C}_2)\text{NiOTf}$  (**502a-NiOTf**) in  $\text{CD}_2\text{Cl}_2$

**Synthesis of  $(^t\text{BuPCN-C}_4)\text{NiOTf}$  (**2b-NiOTf**).** **502b-NiCl** (200 mg, 0.260 mmol) was dissolved in ca. 20 mL of 1:1  $\text{C}_6\text{H}_5\text{F}/\text{CH}_2\text{Cl}_2$ . To this  $\text{AgOTf}$  (134 mg, 0.520 mmol) was



added and the solution was left to stir for 12 h when the solution turned yellow. The volatiles were removed, solids extracted with C<sub>6</sub>H<sub>6</sub> and filtered through a pad of celite on a glass frit. The volatiles were pumped off yielding a yellow solid (180 mg, 69% yield) .

<sup>1</sup>H NMR (CD<sub>2</sub>Cl<sub>2</sub>, 300 MHz, 22°C): δ = 7.93 (d, *J* = 3.6 Hz, 2H, HC=N), 6.99 (m, 2H, Ar CH), 6.89 (d, *J* = 7.2 Hz, 2H, Ar CH), 6.57 (d, *J* = 8.1 Hz, 2H, Ar CH), 3.54 (br, 4H, CH<sub>2</sub>), 1.76 (br, 4H, CH<sub>2</sub>), 1.47 ppm (d, *J* = 15.0 Hz, 36H, <sup>t</sup>Bu CMe<sub>3</sub>). **(Figure V.38)** <sup>31</sup>P{<sup>1</sup>H} NMR (CD<sub>2</sub>Cl<sub>2</sub>, 282 MHz, 22°C): δ = 201.8 ppm. **(Figure V.39)** <sup>19</sup>F NMR (CD<sub>2</sub>Cl<sub>2</sub>, 282 MHz, 22°C): δ = -78.8 ppm. **(Figure V.40)**

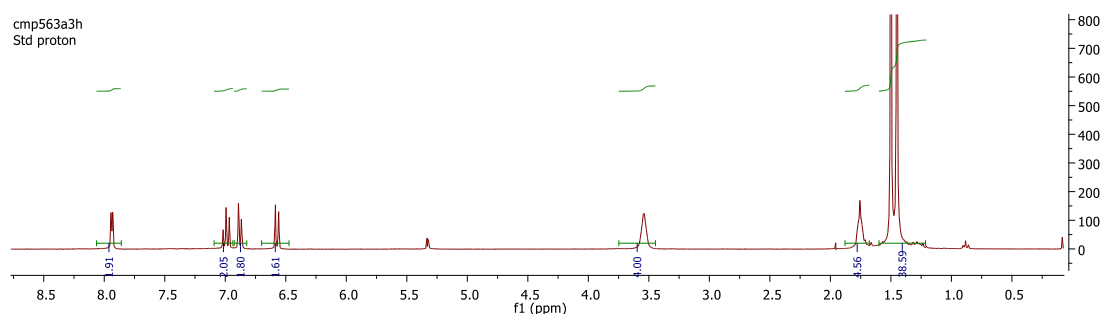


**Figure V.38** <sup>1</sup>H NMR spectrum of (<sup>t</sup>BuPCN-C<sub>4</sub>)NiOTf (**502b-NiOTf**) in CD<sub>2</sub>Cl<sub>2</sub>.

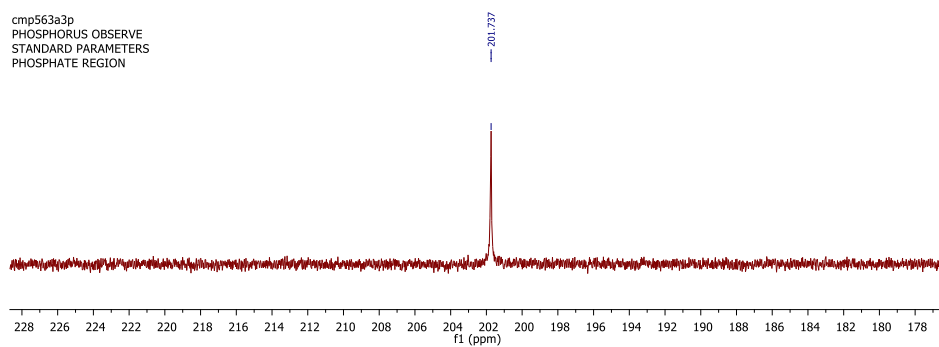


**Figure V.39** <sup>31</sup>P{<sup>1</sup>H} NMR spectrum of (<sup>t</sup>BuPCN-C<sub>4</sub>)NiOTf (**502b-NiOTf**) in CD<sub>2</sub>Cl<sub>2</sub>

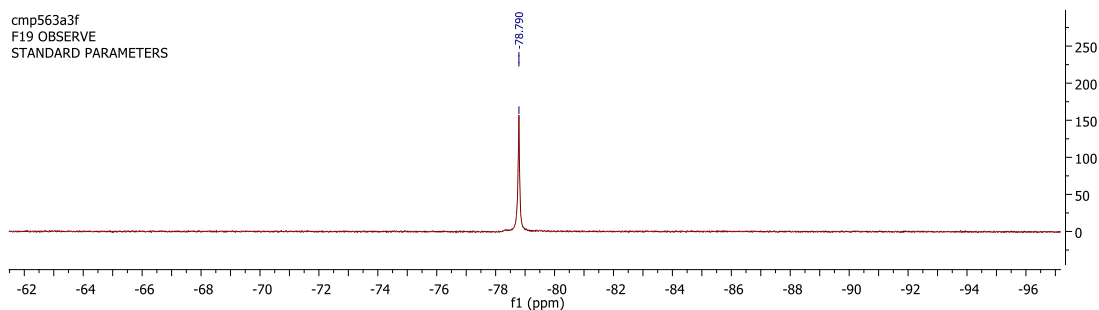


**Figure V.40**  $^{19}\text{F}$  NMR spectrum of  $(^t\text{BuPCN-C}_4)\text{NiOTf}$  (**502b-NiOTf**) in  $\text{CD}_2\text{Cl}_2$

**Synthesis of  $(^t\text{BuPCN-C}_2)\text{PdCl}$  (**502a-PdCl**).** A solution of the  $^t\text{BuPCN-C}_2$  ligand (**502a**) (0.443 g, 0.797 mmol) in ODCB (5 mL) was combined with a solution of  $\text{Pd}(\text{COD})\text{Cl}_2$  (0.454 g, 1.591 mmol) and 2,6-lutidine (0.184 mL, 1.591 mmol) in ODCB (95 mL) and the mixture was heated to reflux ( $160^\circ\text{C}$ ) for 3 h at which point the solution was homogeneous and golden yellow. After cooling to room temperature, 150 mL of  $\text{Et}_2\text{O}$  was added and the resulting white suspension was filtered over Celite and dried by distillation. The yellow-orange residue was taken up in dichloromethane, filtered and recrystallized from dichloromethane/pentane at  $0^\circ\text{C}$ . Yield = 0.370 g (54%).  $^1\text{H}$  NMR ( $\text{CD}_2\text{Cl}_2$ , 500 MHz,  $22^\circ\text{C}$ ):  $\delta$  = 8.33 (d,  $J$  = 4.6 Hz, 2H,  $\text{HC}=\text{N}$ ), 6.94 (t,  $J$  = 8.0 Hz, 2H, Ar CH), 6.85 (d,  $J$  = 7.5 Hz, 2H, Ar CH), 6.76 (d,  $J$  = 8.0 Hz, 2H, Ar CH), 4.40 (s br, 4H,  $\text{CH}_2$ ), 1.42 ppm (d,  $J$  = 15.6 Hz, 36H,  $t\text{Bu CMe}_3$ ). (**Figure V.41**)  $^{13}\text{C}\{^1\text{H}\}$  NMR ( $\text{CD}_2\text{Cl}_2$ , 126 MHz,  $22^\circ\text{C}$ ):  $\delta$  = 176.8 (d,  $J$  = 3.9 Hz,  $\text{HC}=\text{N}$ ), 164.4 (d,  $J$  = 5.4 Hz, Ar C), 153.4 (Ar C), 145.7 (Ar C), 126.5 (Ar CH), 122.0 (Ar CH), 114.3 (d,  $J$  = 14.7 Hz, Ar CH), 58.3 ( $\text{CH}_2$ ), 39.8 (d,  $J$  = 17.1 Hz,  $t\text{Bu CMe}_3$ ), 27.7 ppm (d,  $J$  = 5.9 Hz,  $t\text{Bu CMe}_3$ ). (**Figure V.42**)  $^{31}\text{P}\{^1\text{H}\}$  NMR ( $\text{CD}_2\text{Cl}_2$ , 121 MHz,  $22^\circ\text{C}$ ):  $\delta$  = 210.5 ppm. (**Figure V.43**)

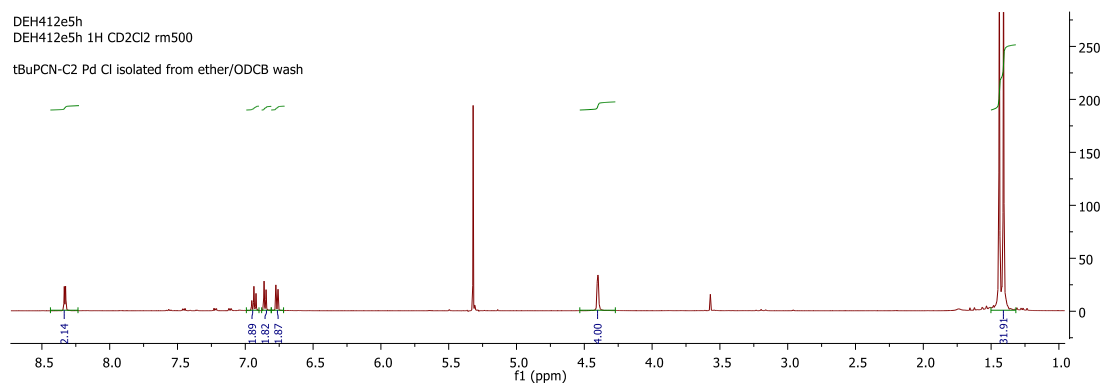


**Figure V.41**  $^1\text{H}$  NMR spectrum of  $(^t\text{BuPCN-C}_2)\text{PdCl}$  (**502a-PdCl**) in  $\text{CD}_2\text{Cl}_2$

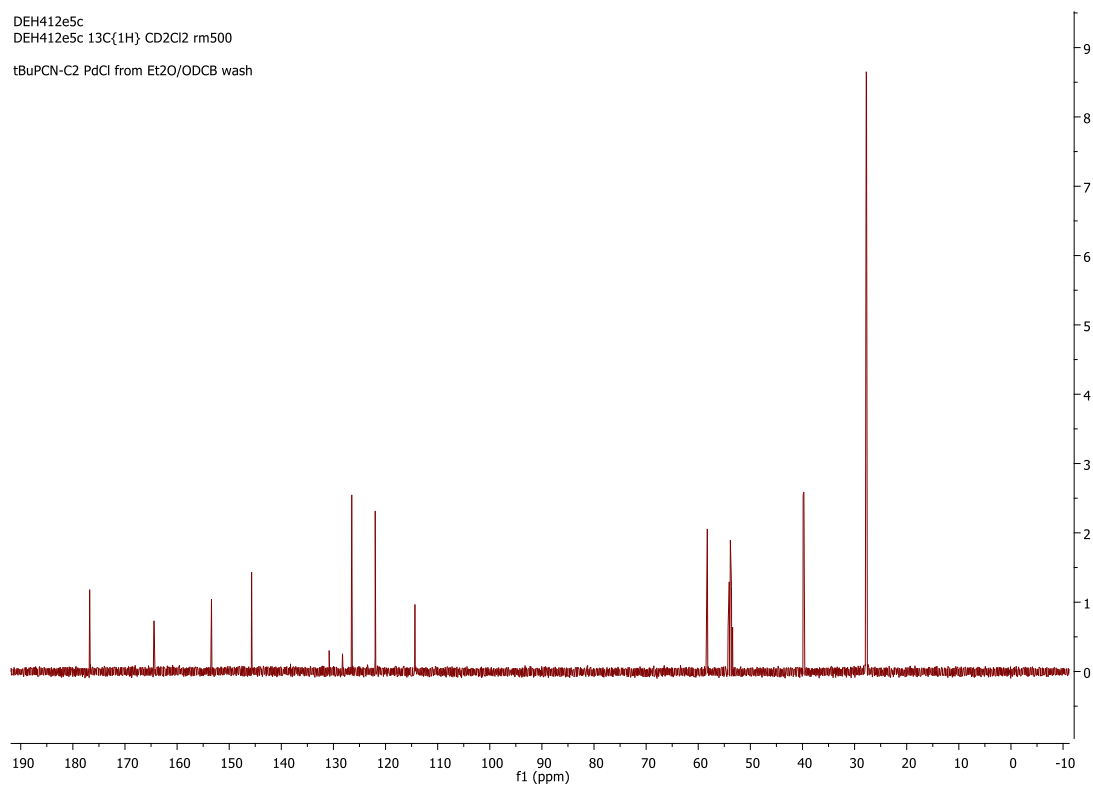


**Figure V.42**  $^{13}\text{C}\{^1\text{H}\}$  NMR spectrum of  $(^t\text{BuPCN-C}_2)\text{PdCl}$  (**502a-PdCl**) in  $\text{CD}_2\text{Cl}_2$

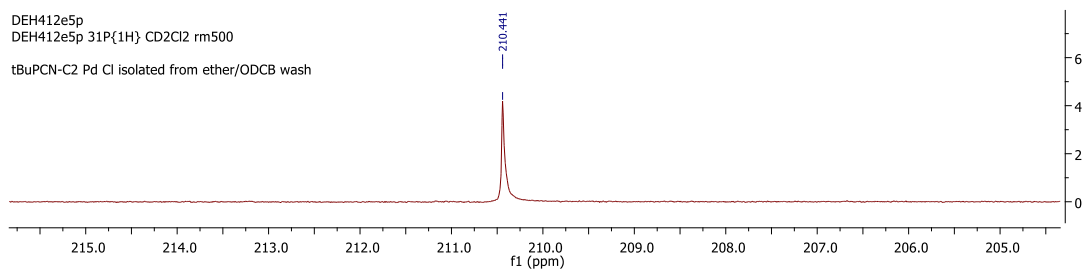


**Figure V.43**  $^{31}\text{P}\{^1\text{H}\}$  NMR spectrum of ( $t\text{BuPCN-C}_2$ )PdCl (**502a-PdCl**) in  $\text{CD}_2\text{Cl}_2$

**Synthesis of ( $t\text{BuPCN-C}_4$ )PdCl (**502b-PdCl**).** A solution of  $t\text{BuPCN-C}_4$  ligand (**502b**) (0.550 g, 0.940 mmol) in ODCB (5 mL) was combined with a solution of  $\text{Pd}(\text{COD})\text{Cl}_2$  (0.537 g, 1.881 mmol) and 2,6-lutidine (0.218 mL, 1.881 mmol) in ODCB (95 mL) and the mixture was heated to reflux ( $160^\circ\text{C}$ ) for 3 h at which point the solution was homogeneous and golden yellow. After cooling to room temperature, 150 mL of  $\text{Et}_2\text{O}$  was added and the resulting white suspension was filtered over Celite and dried by distillation. The yellow-orange residue was taken up in dichloromethane, filtered and recrystallized from dichloromethane/pentane at  $0^\circ\text{C}$ . Yield = 0.707 g (87%)  $^1\text{H}$  NMR ( $\text{CD}_2\text{Cl}_2$ , 500 MHz,  $22^\circ\text{C}$ ):  $\delta$  = 8.28 (d,  $J$  = 5.0 Hz,  $\text{HC}=\text{N}$ ), 7.03 (d overlapped,  $J$  = 8.0 Hz, 2H, Ar  $\text{CH}$ ), 7.01 (t overlapped,  $J$  = 8.0 Hz, 2H, Ar  $\text{CH}$ ), 6.81 (d,  $J$  = 7.5 Hz, 2H, Ar  $\text{CH}$ ), 3.82 (br, 4H,  $\text{CH}_2$ ), 1.93 (br, 4H,  $\text{CH}_2$ ), 1.43 ppm (d,  $J$  = 15.0 Hz, 36H,  $t\text{Bu CMe}_3$ ). (**Figure V.44**)  $^{13}\text{C}\{^1\text{H}\}$  NMR ( $\text{CD}_2\text{Cl}_2$ , 126 MHz,  $22^\circ\text{C}$ ):  $\delta$  = 174.3 (d,  $J$  = 3.9 Hz,  $\text{HC}=\text{N}$ ), 164.5 (d,  $J$  = 5.3 Hz, Ar  $\text{CH}$ ), 153.5 (Ar C), 146.5 (Ar C), 126.4 (Ar  $\text{CH}$ ), 122.0 (Ar  $\text{CH}$ ), 114.0 (d,  $J$  = 15.3 Hz, Ar  $\text{CH}$ ), 58.0 ( $\text{CH}_2$ ), 39.7 (d,  $J$  = 17.0 Hz,  $t\text{Bu CMe}_3$ ), 27.7 (d,  $J$  = 5.4 Hz,  $t\text{Bu CMe}_3$ ), 27.6 ppm ( $\text{CH}_2$ ).  $^{31}\text{P}\{^1\text{H}\}$  NMR ( $\text{CD}_2\text{Cl}_2$ , 121 MHz,  $22^\circ\text{C}$ ):  $\delta$  = 210.3 ppm. (**Figure V.45**)

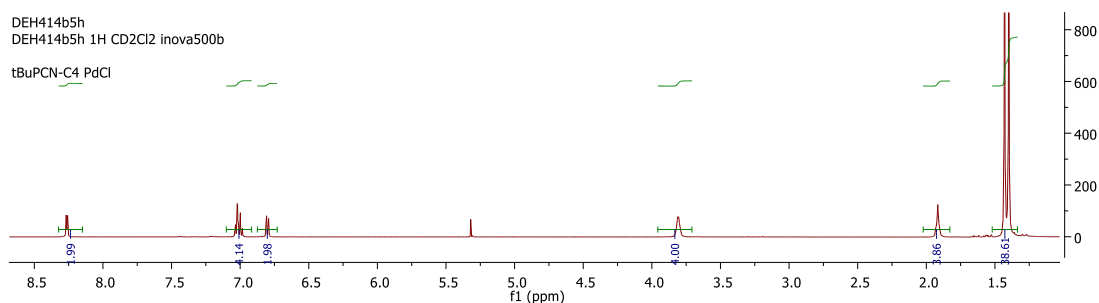


**Figure V.44**  $^1\text{H}$  NMR spectrum of  $(^t\text{BuPCN-C}_4)\text{PdCl}$  (**502b-PdCl**) in  $\text{CD}_2\text{Cl}_2$

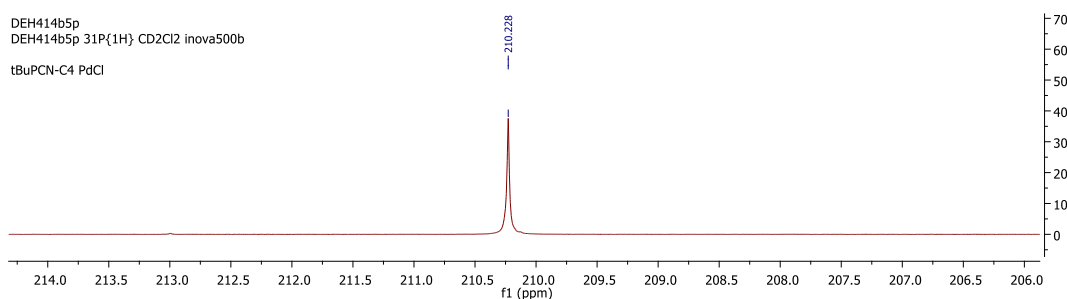


**Figure V.45**  $^{31}\text{P}\{^1\text{H}\}$  NMR spectrum of  $(^t\text{BuPCN-C}_4)\text{PdCl}$  (**502b-PdCl**) in  $\text{CD}_2\text{Cl}_2$

**Synthesis of  $(^t\text{BuPCN-C}_2)\text{PdOTf}$  (**502a-PdOTf**).**  $(^t\text{BuPCN-C}_2)\text{PdCl}$  (**502a-PdCl**) (0.192 g, 0.222 mmol) was dissolved in ca. 20 mL of  $\text{CH}_2\text{Cl}_2$  and to this  $\text{AgOTf}$  (0.114 g, 0.444 mmol) was added and the mixture was left to stir for 12 h. The volatiles were removed under vacuum and the solids were extracted with ca. 10 mL of  $\text{C}_6\text{H}_6$  and filtered through a plug of celite on a glass frit. The volatiles were removed to yield a pale yellow solid (210 mg, yield = 88%).  $^1\text{H}$  NMR ( $\text{CD}_2\text{Cl}_2$ , 500 MHz,  $22^\circ\text{C}$ ):  $\delta$  = 8.38 (d,  $J$  = 4.5 Hz, 2H,  $\text{HC}=\text{N}$ ), 7.05 (dd,  $J$  = 7.5, 7.0 Hz, 2H, Ar  $\text{CH}$ ), 6.99 (dd,  $J$  = 7.5, 1.0 Hz, 2H, Ar  $\text{CH}$ ), 6.79 (dd,  $J$  = 7.0, 1.0 Hz, 2H, Ar  $\text{CH}$ ), 4.15 (br, 4H,  $\text{CH}_2$ ), 1.42 ppm (d,  $J$  = 16.0 Hz, 36H,  $t\text{Bu CMe}_3$ ). (**Figure V.46**)  $^{13}\text{C}\{^1\text{H}\}$  NMR ( $\text{CD}_2\text{Cl}_2$ , 126 MHz,  $22^\circ\text{C}$ ):  $\delta$  = 177.5 (d,  $J$  = 3.8 Hz,  $\text{HC}=\text{N}$ ), 165.1 (d,  $J$  = 4.6 Hz, Ar C), 146.0 (d,  $J$  = 1.7 Hz, Ar C), 145.9 (Ar C), 127.8 (Ar  $\text{CH}$ ), 123.5 (Ar  $\text{CH}$ ), 115.4 (d,  $J$  = 14.3 Hz, Ar  $\text{CH}$ ), 58.4 ( $\text{CH}_2$ ), 40.1 (d,  $J$  = 16.6 Hz,

*t*Bu CMe<sub>3</sub>), 27.6 ppm (d, *J* = 6.0 Hz, *t*Bu CMe<sub>3</sub>). (Figure V.47) <sup>31</sup>P{<sup>1</sup>H} NMR (CD<sub>2</sub>Cl<sub>2</sub>, 121 MHz, 22°C): δ = 208.8 ppm. <sup>19</sup>F NMR (CD<sub>2</sub>Cl<sub>2</sub>, 470 MHz, 22°C): δ = -78.9 ppm.

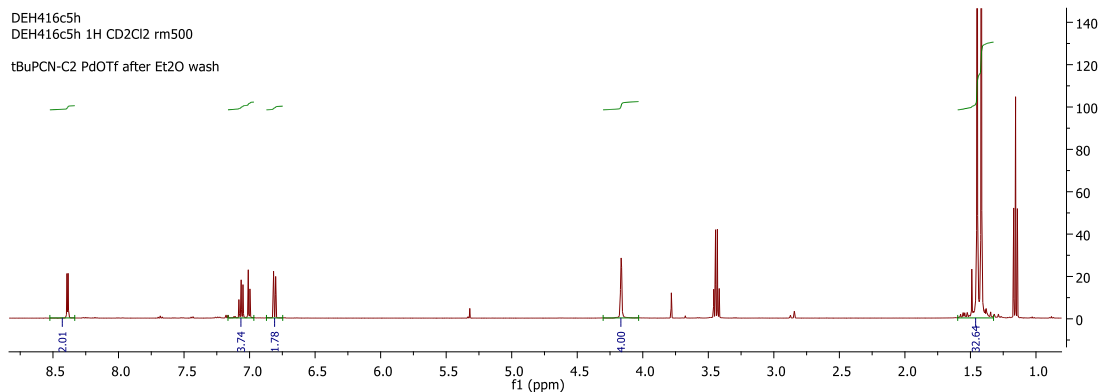


**Figure V.46** <sup>1</sup>H NMR spectrum of (*t*BuPCN-C<sub>2</sub>)PdOTf (**502a-PdOTf**) in CD<sub>2</sub>Cl<sub>2</sub>

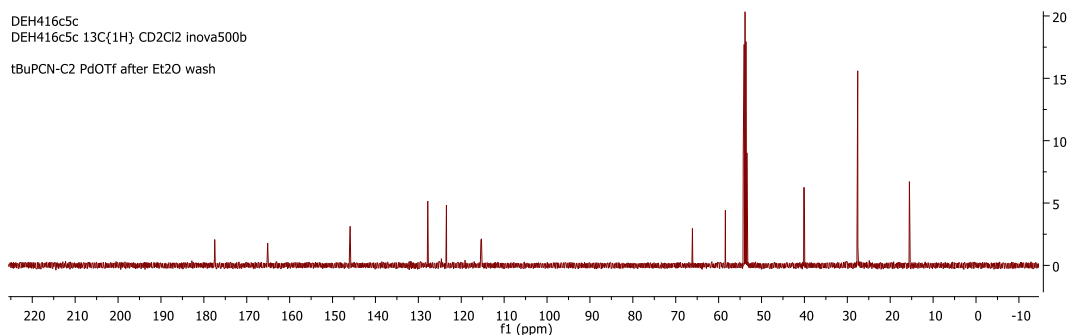


**Figure V.47** <sup>13</sup>C{<sup>1</sup>H} NMR spectrum of (*t*BuPCN-C<sub>2</sub>)PdOTf (**502a-PdOTf**) in CD<sub>2</sub>Cl<sub>2</sub>

**Synthesis of (*t*BuPCN-C<sub>4</sub>)PdOTf (**502b-PdOTf**).** (*t*BuPCN-C<sub>4</sub>)PdCl (**502b-PdCl**) (200 mg, 0.239 mmol) was dissolved in ca. 20 mL of CH<sub>2</sub>Cl<sub>2</sub> and to this AgOTf (135 mg, 0.526 mmol) was added and the mixture was left to stir for 12 h. The volatiles were removed under vacuum and the solids were extracted with ca. 10 mL C<sub>6</sub>H<sub>6</sub> and filtered through a plug of celite on a glass frit. The volatiles were removed to yield a pale yellow solid (212 mg, 83%). <sup>1</sup>H NMR (CD<sub>2</sub>Cl<sub>2</sub>, 500 MHz, 22°C): δ = 8.10 (d, *J* = 4.5 Hz, 2H,

HC=N), 7.09-7.06 (overlapped m, 2H, Ar CH), 7.06-7.02 (overlapped m, 2H, Ar CH), 3.80 (br, 4H, CH<sub>2</sub>), 1.84 (br, 4H, CH<sub>2</sub>), 1.42 ppm (d, *J* = 15.5 Hz, *t*Bu CMe<sub>3</sub>). (**Figure V.48**) <sup>13</sup>C{<sup>1</sup>H} NMR (CD<sub>2</sub>Cl<sub>2</sub>, 126 MHz, 22°C): δ = 173.5 (HC=N), 165.1 (Ar C), 146.3 (Ar C), 145.9 (Ar C), 127.6 (Ar CH), 122.9 (Ar CH), 114.9 (d, *J* = 14.4 Hz, Ar CH), 59.4 (CH<sub>2</sub>), 39.9 (d, *J* = 16.3 Hz, *t*Bu CMe<sub>3</sub>), 27.6 ppm (*t*Bu CMe<sub>3</sub> and CH<sub>2</sub> overlapped). (**Figure V.49**) <sup>31</sup>P{<sup>1</sup>H} NMR (CD<sub>2</sub>Cl<sub>2</sub>, 121 MHz, 22°C): δ = 208.4 ppm. (**Figure V.50**) <sup>19</sup>F NMR (CD<sub>2</sub>Cl<sub>2</sub>, 282 MHz, 22°C): δ = -79.0 ppm. (**Figure V.51**)

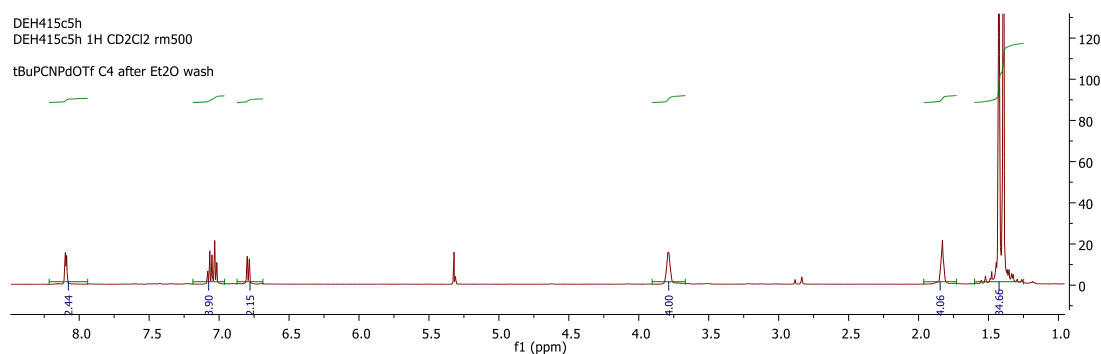


**Figure V.48** <sup>1</sup>H NMR spectrum of (<sup>t</sup>BuPCN-C<sub>4</sub>)PdOTf (**502b-PdOTf**) in CD<sub>2</sub>Cl<sub>2</sub>

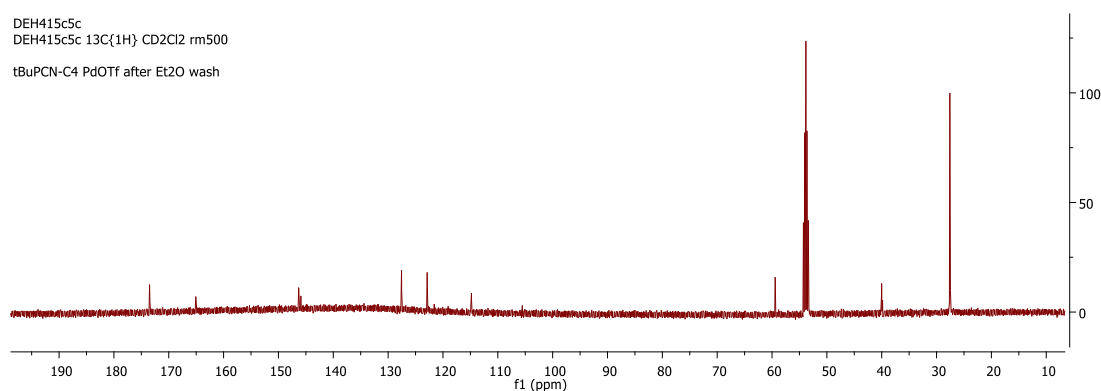


**Figure V.49** <sup>13</sup>C{<sup>1</sup>H} NMR spectrum of (<sup>t</sup>BuPCN-C<sub>4</sub>)PdOTf (**502b-PdOTf**) in CD<sub>2</sub>Cl<sub>2</sub>

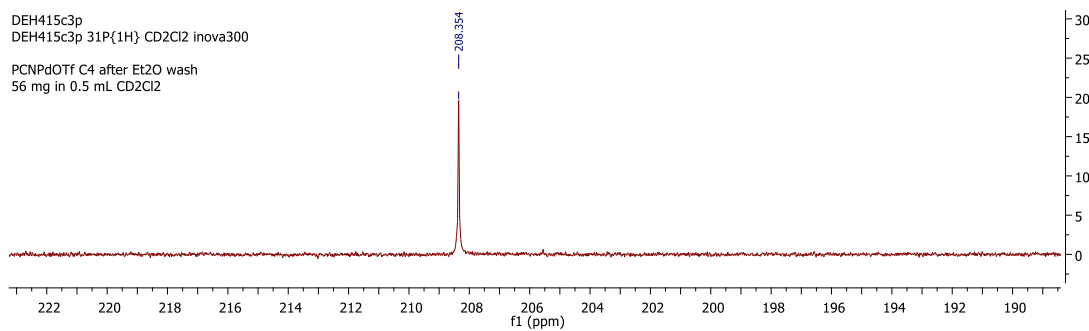


**Figure V.50**  $^{31}\text{P}\{^1\text{H}\}$  NMR spectrum of ( $^t\text{BuPCN-C}_4$ )PdOTf (**502b-PdOTf**) in  $\text{CD}_2\text{Cl}_2$

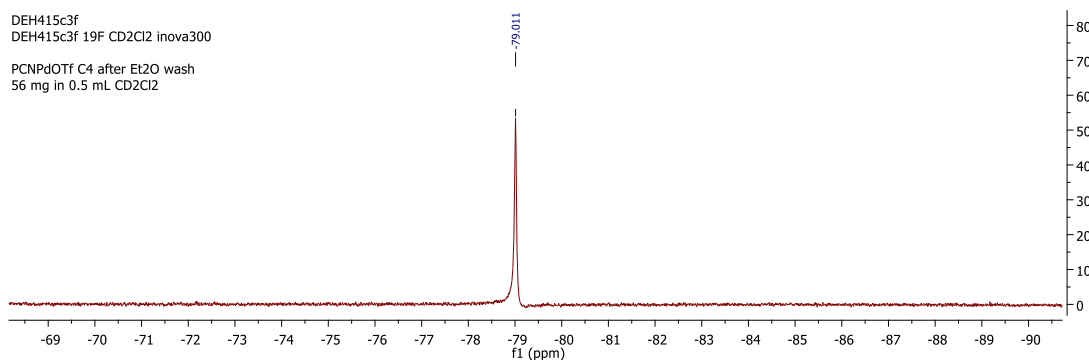


**Figure V.51**  $^{19}\text{F}$  NMR spectrum of ( $^t\text{BuPCN-C}_4$ )PdOTf (**502b-PdOTf**) in  $\text{CD}_2\text{Cl}_2$

#### 5.4.3. Synthesis of PNN compounds with alkyl linkers

**Synthesis of ( $^i\text{PrPNN-C}_2$ )NiCl (**503a-NiCl**).**  $^i\text{PrPNN-C}_2$  (**503a**) (201 mg, 0.281 mmol) was dissolved in ca. 10 mL of THF. To this 2,6-lutidine (72  $\mu\text{L}$ , 66 mg, 0.622 mmol) and  $\text{NiCl}_2 \cdot 6\text{H}_2\text{O}$  (147 mg, 0.621 mmol) were added and the solution was left to stir for 20 h when the solution turned green. The volatiles were pumped off and the green solid was extracted with ca. 20 mL of  $\text{CH}_2\text{Cl}_2$  and filtered through a pad of silica on a glass frit. The volatiles were pumped off and the obtained solid was redissolved in ca. 10 mL of dichloromethane and layered with 20 mL of pentane and put in the freezer at  $-35^\circ\text{C}$ . A green crystalline product (223 mg, 96% yield) was obtained overnight.  $^1\text{H}$  NMR ( $\text{CD}_2\text{Cl}_2$ ,



500 MHz, 22°C):  $\delta$  = 8.20 (d,  $J$  = 9.0 Hz, 2H, HC=N), 7.01 (d,  $J$  = 7.0 Hz, 2H, Ar-H), 6.92 (d,  $J$  = 8.5 Hz, 2H, Ar-H), 6.65-6.58 (overlapped m, 4H, Ar-H), 6.40 (br s, 2H, Ar-H), 6.02 (dd,  $J$  = 8.5 Hz,  $J$  = 4.0 Hz, 2H, Ar-H), 4.85 (d,  $J$  = 7.0 Hz, 2H, CH<sub>a</sub>H<sub>b</sub>), 4.39-4.24 (m, 2H, CH<sub>a</sub>H<sub>b</sub>), 2.37 (m, 2H, CHMe<sub>2</sub>), 2.24 (s, 6H, Ar-CH<sub>3</sub>), 2.13 (m, 2H, CHMe<sub>2</sub>), 2.02 (s, 6H, Ar-CH<sub>3</sub>), 1.78- 1.67 (m, 6H, CHMe<sub>2</sub>), 1.58- 1.42 (m, 12H, CHMe<sub>2</sub>), 1.18-1.09 ppm (m, 6H, CHMe<sub>2</sub>). (**Figure V.52**) <sup>31</sup>P{<sup>1</sup>H} NMR (CD<sub>2</sub>Cl<sub>2</sub>, 202 MHz, 22°C)  $\delta$  48.2 ppm. (**Figure V.53**)

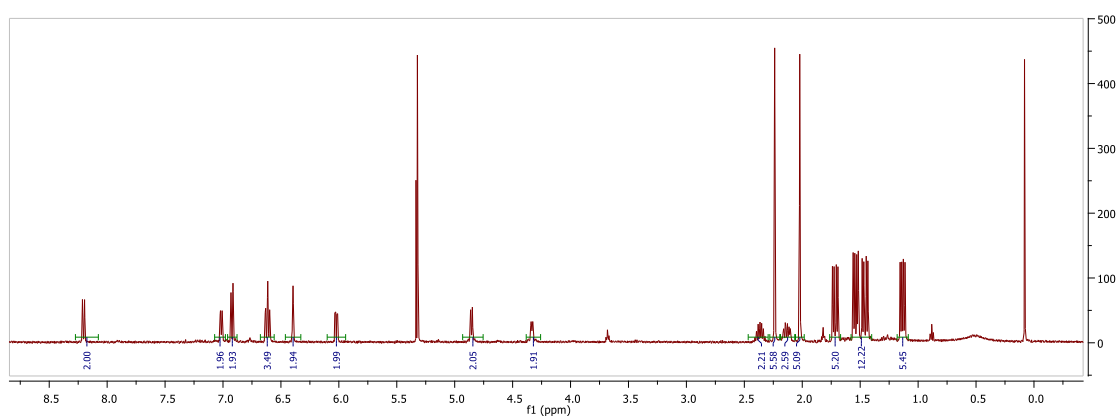


**Figure V.52** <sup>1</sup>H NMR spectrum of (iPrPNN-C<sub>2</sub>)NiCl (**503a-NiCl**) in CD<sub>2</sub>Cl<sub>2</sub>

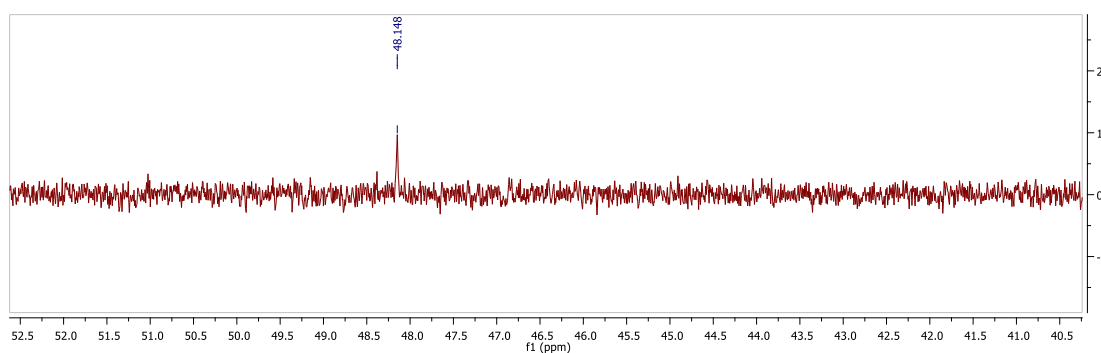


**Figure V.53** <sup>31</sup>P{<sup>1</sup>H} NMR spectrum of (iPrPNN-C<sub>2</sub>)NiCl (**503a-NiCl**) in CD<sub>2</sub>Cl<sub>2</sub>

**Synthesis of (<sup>i</sup>PrPNN-C<sub>2</sub>)NiOAc (503a-NiOAc).** <sup>i</sup>PrPNN-C<sub>2</sub> (**503a**) (128 mg, 0.181 mmol) was dissolved in ca. 10 mL of THF. To this Ni(OAc)<sub>2</sub>·4H<sub>2</sub>O (101 mg, 0.401 mmol) were added and the solution was left to stir for 18 h. The volatiles were pumped off and the green solid was extracted with ca. 20 mL of CH<sub>2</sub>Cl<sub>2</sub> and filtered through a pad of silica on a glass frit. The volatiles were pumped off and the obtained solid was redissolved in ca. 10 mL of dichloromethane and layered with 20 mL of pentane and put in the freezer at -35 °C. A green crystalline product (131 mg, 77 yield) was obtained overnight. <sup>1</sup>H NMR (C<sub>6</sub>D<sub>6</sub>, 300 MHz, 22°C): δ = 8.15 (d, *J* = 8.1 Hz, 2H, HC=N), 6.88-6.74 (m, 4H, Ar-H), 6.46 (d, *J* = 8.4 Hz, 4H, Ar-H), 6.27 (br s, 2H, Ar-H), 5.93 (dd, *J* = 8.1 Hz, *J* = 3.9 Hz, 2H, Ar-H), 3.99 (m, 4H, CH<sub>2</sub>), 2.31 (m, 2H, CHMe<sub>2</sub>), 2.13 (s, 6H, Ar-CH<sub>3</sub>), 1.98 (m, 2H, CHMe<sub>2</sub>), 1.89 (s, 6H, Ar-CH<sub>3</sub>), 1.78- 1.52 (overlapped m, 12H, CHMe<sub>2</sub> (6H), Ni-OC(O)CH<sub>3</sub> (6H)), 1.51- 1.34 (m, 6H, CHMe<sub>2</sub>), 1.21- 0.84 ppm (m, 12H, CHMe<sub>2</sub>). (**Figure V.54**) <sup>31</sup>P{<sup>1</sup>H} NMR (C<sub>6</sub>D<sub>6</sub>, 121 MHz, 22°C) δ 45.0 ppm. (**Figure V.55**)

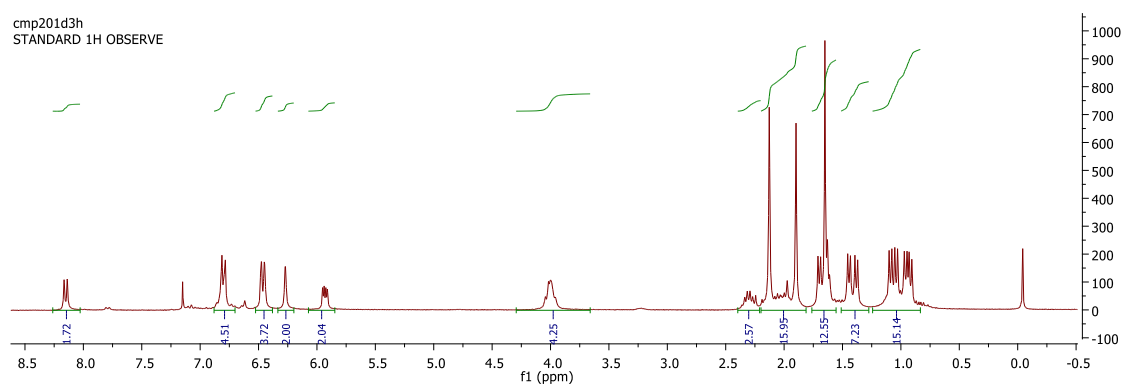


**Figure V.54** <sup>1</sup>H NMR spectrum of (<sup>i</sup>PrPNN-C<sub>2</sub>)NiOAc (**503a-NiOAc**) in C<sub>6</sub>D<sub>6</sub>

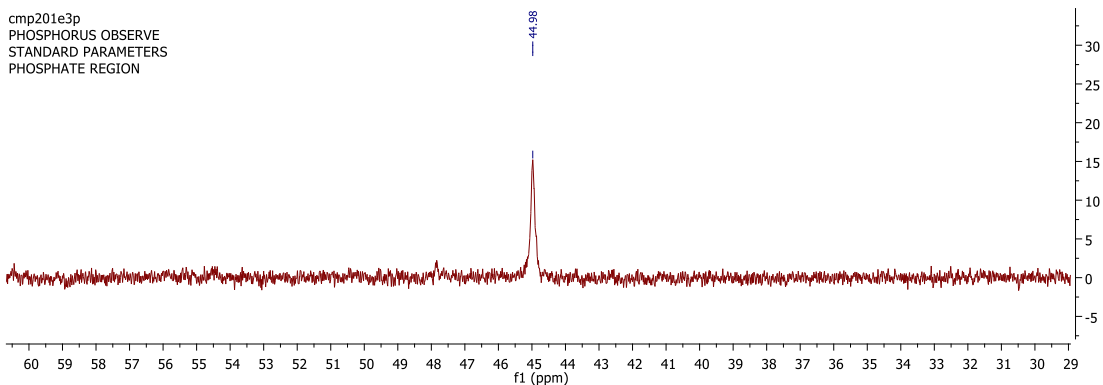


**Figure V.55**  $^{31}\text{P}\{^1\text{H}\}$  NMR spectrum of ( $^i\text{PrPNN-C}_2$ )NiOAc (**503a-NiOAc**) in  $\text{C}_6\text{D}_6$

#### 5.4.4. Synthesis of PCN ligand and Ni complex with pendant amine linker

**Synthesis of benzoketimine with pendant amine linker (504a').** 3'-hydroxyacetophenone (690 mg, 5.07 mmol) was dissolved in ca. 40 mL of acetonitrile. To this, diethylenetriamine (270  $\mu\text{L}$ , 261 mg, 2.54 mmol) was added using a syringe and the solution was placed in an oil bath at 50  $^\circ\text{C}$  and left to stir for 4 h. The volatiles were then pumped off and the solid was washed with cold acetone (3 x 5 mL) followed by cold pentane (3 x 5 mL). A tan solid was obtained (802 mg, 92%).  $^1\text{H}$  NMR ( $(\text{CD}_3)_2\text{SO}$ , 300 MHz, 22 $^\circ\text{C}$ ):  $\delta$  9.21 (br s, NH), 7.31-7.01 (overlapped m, 2H, Ar-H (2H), OH (1H)), 6.78 (d,  $J = 7.8$  Hz, 2H, ArH), 3.49 (t,  $J = 6.0$  Hz, 4H,  $\text{CH}_2$ ), 2.91 (t,  $J = 6.0$  Hz, 4H,  $\text{CH}_2$ ), 2.15 (s, 6H,  $\text{C}(=\text{N})\text{CH}_3$ ). (**Figure V.56**)

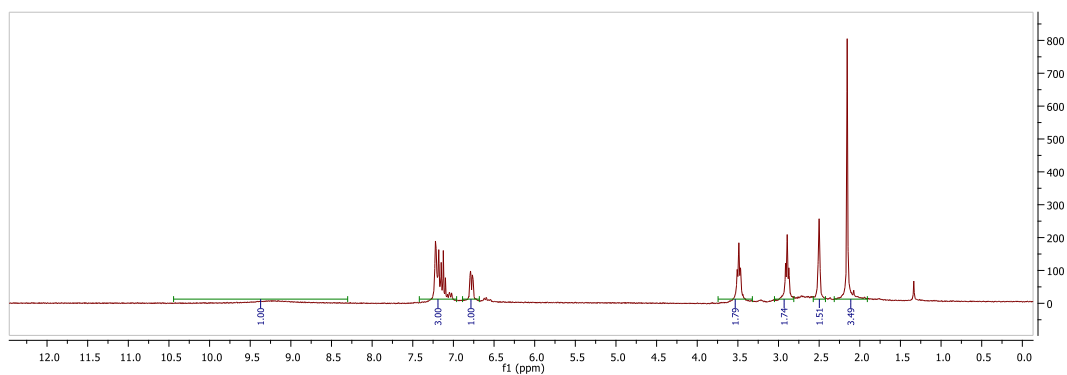


**Figure V.56**  $^1\text{H}$  NMR spectrum of **504a'** in  $(\text{CD}_3)_2\text{SO}$

**Synthesis of  $^t\text{BuPCN-C}_2\text{NC}_2$  (**504a**).** **504a'** (201 mg, 0.553 mmol) was dissolved in ca. 15 mL THF. To this solution, NaH (30 mg, 1.16 mmol) was added and the solution was left to stir for 1 h. Then  $^t\text{Bu}_2\text{PCl}$  (225  $\mu\text{L}$ , 209 mg, 1.16 mmol) was added using a syringe and the solution was set to reflux for 20 h. The volatiles were pumped off, the oily product was extracted with ca. 10 mL of diethylether and passed through a pad of celite on a glass frit. The volatiles were pumped off to get the ligand in 90% purity (300 mg, 86%).  $^1\text{H}$  NMR ( $\text{C}_6\text{D}_6$ , 500 MHz,  $22^\circ\text{C}$ ):  $\delta$  8.00 (br s, NH), 7.54 (d, 2H,  $J = 8.0$  Hz, Ar-H, 2H), 7.35 (d,  $J = 8.5$  Hz, 2H, Ar-H), 7.11 (t,  $J = 7.5$  Hz, 2H, Ar-H), 3.45 (t,  $J = 6.0$  Hz, 4H,  $\text{CH}_2$ ), 3.12 (m,  $J = 6.5$  Hz, 4H,  $\text{CH}_2$ ), 1.77 (s, 6H,  $\text{C}(=\text{N})\text{CH}_3$ ), 1.12 ppm (d,  $J = 12.0$  Hz, 36 H,  $\text{C}(\text{CH}_3)_3$ ). (**Figure V.57**)  $^{31}\text{P}\{^1\text{H}\}$  ( $\text{C}_6\text{D}_6$ , 202 MHz,  $22^\circ\text{C}$ )  $\delta$  153.0 ppm. (**Figure V.58**)

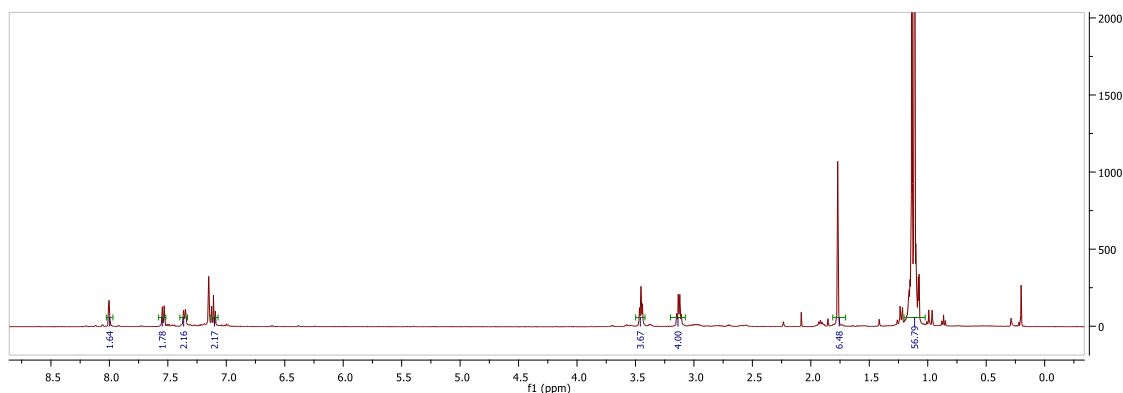


**Figure V.57**  $^1\text{H}$  NMR spectrum of **504a** in  $\text{C}_6\text{D}_6$

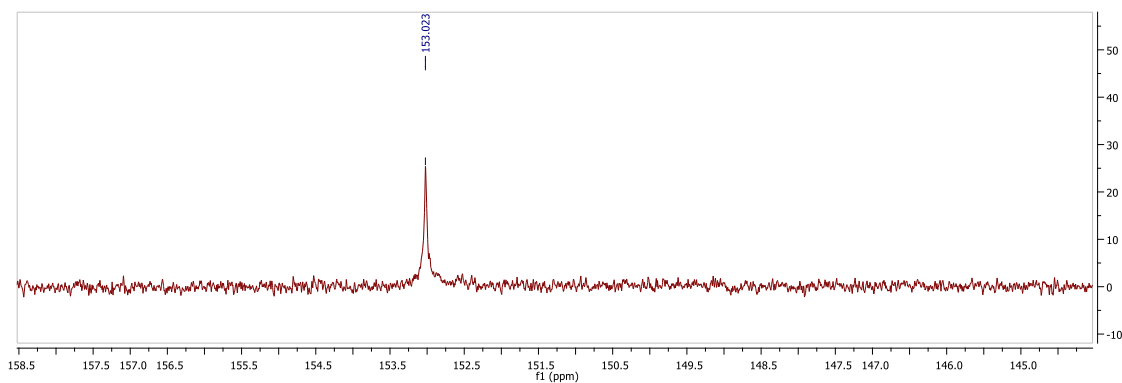


**Figure V.58**  $^{31}\text{P}\{^1\text{H}\}$  NMR spectrum of **504a** in  $\text{C}_6\text{D}_6$

**Synthesis of (*t*BuPCN- $\text{C}_2\text{NC}_2$ )NiCl (**504a-NiCl**).** *t*BuPCN- $\text{C}_2\text{NC}_2$  (**504a**) (350 mg, 0.554 mmol) was dissolved in ca. 15 mL of 1,2-dichlorobenzene. To this 2,6-lutidine (160  $\mu\text{L}$ , 129 mg, 1.21 mmol) and anhydrous  $\text{NiCl}_2$  (180 mg, 1.38 mmol) were added and the flask was put in an oil bath at 160  $^\circ\text{C}$  and left to stir for 18 h when the solution turned bright orange. Then the volatiles were distilled off and the orange solid was extracted with ca. 20 mL of  $\text{C}_6\text{H}_6$  and filtered through a pad of celite on a glass frit. The volatiles were pumped off and the obtained solid was redissolved in ca. 10 mL of diethylether and layered with 20 mL of pentane and put in the freezer at -35  $^\circ\text{C}$ . A yellow orange crystalline product

(402 mg, 89% yield) was obtained overnight.  $^1\text{H}$  NMR ( $\text{CD}_2\text{Cl}_2$ , 300 MHz,  $22^\circ\text{C}$ ):  $\delta$  8.86 (br s, NH), 7.06-6.87 (overlapped m, 4H, Ar-H), 6.65 (d,  $J = 7.5$  Hz, 2H, Ar-H), 4.01 (br, 4H,  $\text{CH}_2$ ), 3.17 (br, 4H,  $\text{CH}_2$ ), 2.51 (s, 6H,  $\text{C(=N)CH}_3$ ), 1.43 ppm (d,  $J = 14.4$  Hz, 36 H,  $\text{C(CH}_3)_3$ ). **(Figure V.59)**  $^{31}\text{P}\{^1\text{H}\}$  ( $\text{CD}_2\text{Cl}_2$ , 202 MHz,  $22^\circ\text{C}$ )  $\delta$  204.8 ppm. **(Figure V.60)**

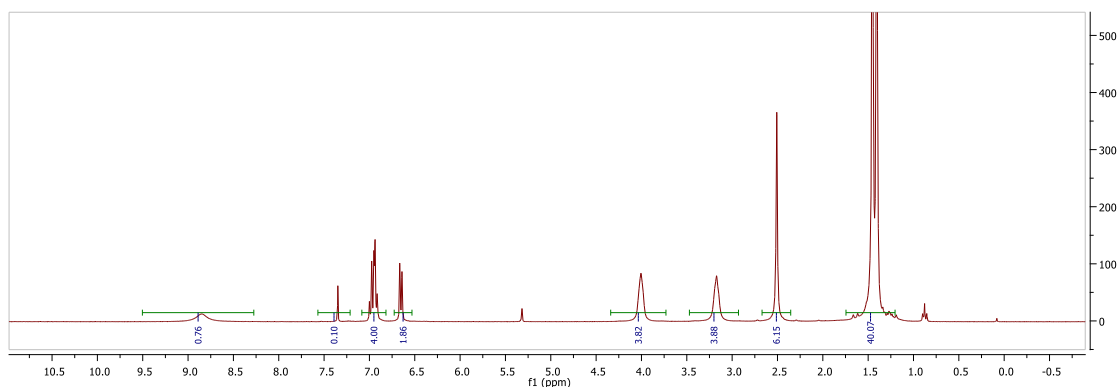


**Figure V.59**  $^1\text{H}$  NMR spectrum of ( $t\text{BuPCN-C}_2\text{NC}_2$ )NiCl (**504a-NiCl**) in  $\text{CD}_2\text{Cl}_2$

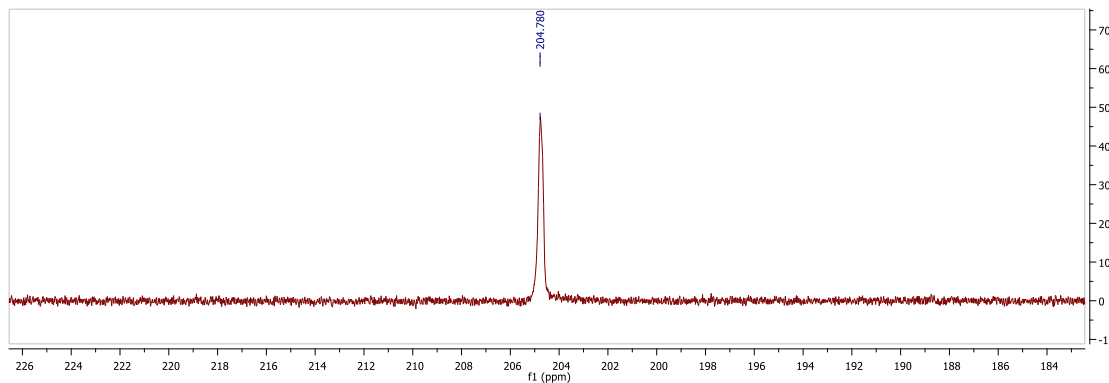


**Figure V.60**  $^{31}\text{P}\{^1\text{H}\}$  NMR spectrum of ( $t\text{BuPCN-C}_2\text{NC}_2$ )NiCl (**504a-NiCl**) in  $\text{CD}_2\text{Cl}_2$

#### 5.4.5. X-ray crystallography

**X-Ray data collection, solution, and refinement for ( $i\text{PrPCN-C}_2$ )NiCl.** An orange, multi-faceted crystal of suitable size and quality (**0.180 x 0.140 x 0.080** mm) was selected using an optical microscope and mounted onto a nylon loop. Low temperature (**110 K**) X-

ray data were obtained on a Bruker APEXII CCD based diffractometer (Mo sealed X-ray tube,  $K_{\alpha} = 0.71073 \text{ \AA}$ ). All diffractometer manipulations, including data collection, integration and scaling were carried out using the Bruker APEXII software.<sup>181</sup> An absorption correction was applied using SADABS.<sup>182</sup> The structure was initially solved in the **monoclinic  $P2_1/n$**  space group using XS<sup>183</sup> (incorporated in SHELXTL). The solution was refined by full-matrix least squares on  $F^2$ . No additional symmetry was found using ADDSYMM incorporated into the PLATON program.<sup>184</sup> All non-hydrogen atoms were refined with anisotropic thermal parameters. All hydrogen atoms were placed in idealized positions and refined using a riding model. The structure was refined (weighted least squares refinement on  $F^2$ ) and the final least-squares refinement converged to  $R_1 = \mathbf{0.0310}$  ( $I > 2\sigma(I)$ , **3626** data) and  $wR_2 = \mathbf{0.0820}$  ( $F^2$ , **17017** data, **176** parameters).

**X-Ray data collection, solution, and refinement (<sup>i</sup>PrPCN-C<sub>4</sub>)NiCl.** An orange , multi-faceted crystal of suitable size and quality (**0.25 x 0.06 x 0.04** mm) was selected using an optical microscope and mounted onto a nylon loop. Low temperature (**150 K**) X-ray data were obtained on a Bruker APEXII CCD based diffractometer (Mo sealed X-ray tube,  $K_{\alpha} = 0.71073 \text{ \AA}$ ). All diffractometer manipulations, including data collection, integration and scaling were carried out using the Bruker APEXII software.<sup>181</sup> An absorption correction was applied using SADABS.<sup>182</sup> The structure was initially solved in the **monoclinic  $P2_1/n$**  space group using XS<sup>183</sup> (incorporated in SHELXTL). The solution was refined by full-matrix least squares on  $F^2$ . No additional symmetry was found using ADDSYMM incorporated into the PLATON program.<sup>184</sup> All non-hydrogen atoms were refined with anisotropic thermal parameters. All hydrogen atoms were placed in idealized

positions and refined using a riding model. The structure was refined (weighted least squares refinement on  $F^2$ ) and the final least-squares refinement converged to  $R_1 = \mathbf{0.0466}$  ( $I > 2\sigma(I)$ , **3829** data) and  $wR_2 = \mathbf{0.0820}$  ( $F^2$ , **18029** data, **185** parameters).

**X-Ray data collection, solution, and refinement (<sup>t</sup>BuPCN-C<sub>2</sub>)PdOTf.** A pale yellow, multi-faceted crystal of suitable size and quality (0.15 x 0.12 x 0.08 mm) was selected using an optical microscope and mounted onto a nylon loop. Low temperature (110 K) X-ray data were obtained on a Bruker APEXII CCD based diffractometer (Mo sealed X-ray tube,  $K_\alpha = 0.71073 \text{ \AA}$ ). All diffractometer manipulations, including data collection, integration and scaling were carried out using the Bruker APEXII software.<sup>181</sup> An absorption correction was applied using SADABS.<sup>182</sup> The structure was initially solved in the triclinic  $P\bar{1}$  space group using XS<sup>183</sup> (incorporated in SHELXTL). The solution was refined by full-matrix least squares on  $F^2$ . No additional symmetry was found using ADDSYM incorporated into the PLATON program.<sup>184</sup> All non-hydrogen atoms were refined with anisotropic thermal parameters. All hydrogen atoms on the main residue were placed in idealized positions and refined using a riding model. The structure was refined (weighted least squares refinement on  $F^2$ ) and the final least-squares refinement converged to  $R_1 = 0.0353$  ( $I > 2\sigma(I)$ , 4180 data) and  $wR_2 = 0.0907$  ( $F^2$ , 10741 data, 205 parameters). A molecule of water, likely incorporated during crystallization, was found in the lattice.

**X-Ray data collection, solution, and refinement (<sup>t</sup>BuPCN-C<sub>4</sub>)PdOTf.** A pale yellow, multi-faceted crystal of suitable size and quality (0.130 x 0.040 x 0.005 mm) was selected using an optical microscope and mounted onto a nylon loop. Low temperature



(150 K) X-ray data were obtained on a Bruker APEXII CCD based diffractometer (Mo sealed X-ray tube,  $K_{\alpha} = 0.71073 \text{ \AA}$ ). All diffractometer manipulations, including data collection, integration and scaling were carried out using the Bruker APEXII software.<sup>181</sup> An absorption correction was applied using SADABS.<sup>182</sup> The structure was initially solved in the monoclinic  $P2_1/c$  space group using XS<sup>183</sup> (incorporated in SHELXTL). The solution was refined by full-matrix least squares on  $F^2$ . No additional symmetry was found using ADDSYMM incorporated into the PLATON program.<sup>184</sup> All non-hydrogen atoms were refined with anisotropic thermal parameters. All hydrogen atoms were placed in idealized positions and refined using a riding model. The structure was refined (weighted least squares refinement on  $F^2$ ) and the final least-squares refinement converged to  $R_1 = 0.0590(I > 2\sigma(I), 8820 \text{ data})$  and  $wR_2 = 0.1219(F^2, 43724 \text{ data}, 442 \text{ parameters})$ . One set of *tert*-butyl groups on a phosphine arm were found to be disordered over two sites and accordingly, restraints were employed to restrain distances within the two disordered components to similar values.

**X-Ray data collection, solution, and refinement for (<sup>i</sup>PrPNN-C<sub>2</sub>)NiOAc.** A green, multi-faceted crystal of suitable size and quality (**0.110 x 0.080 x 0.070** mm) was selected using an optical microscope and mounted onto a nylon loop. Low temperature (**150 K**) X-ray data were obtained on a Bruker APEXII CCD based diffractometer (Mo sealed X-ray tube,  $K_{\alpha} = 0.71073 \text{ \AA}$ ). All diffractometer manipulations, including data collection, integration and scaling were carried out using the Bruker APEXII software.<sup>181</sup> An absorption correction was applied using SADABS.<sup>182</sup> The structure was initially solved in the **monoclinic  $P2_1/c$**  space group using XS<sup>183</sup> (incorporated in SHELXTL). The solution

was refined by full-matrix least squares on  $F^2$ . No additional symmetry was found using ADDSYMM incorporated into the PLATON program.<sup>184</sup> All non-hydrogen atoms were refined with anisotropic thermal parameters. All hydrogen atoms were placed in idealized positions and refined using a riding model. The structure was refined (weighted least squares refinement on  $F^2$ ) and the final least-squares refinement converged to  $R_1 = \mathbf{0.0497}$  ( $I > 2\sigma(I)$ , **9381** data) and  $wR_2 = \mathbf{0.1563}$  ( $F^2$ , **11381** data, **582** parameters).

## CHAPTER VI

### SUMMARY AND CONCLUSIONS

This dissertation looked at the utility of pincer complexes in diverse applications such as reduction of CO<sub>2</sub> to CO and cross-coupling reactions with cobalt. For reduction of CO<sub>2</sub> to CO, a bis(*p*-fluoroaryl)amido based PNP ligand supported Pd<sup>I</sup>-Pd<sup>I</sup> dimer [(<sup>F</sup>PNP)Pd]<sub>2</sub> was tested. Use of trimethylsilyl reagents for O-atom abstraction was found to be vital following the reduction of CO<sub>2</sub> with the Pd<sup>I</sup>-Pd<sup>I</sup> bond as a 2e<sup>-</sup> source. The evolved CO was trapped and quantified by the use of a PNP supported Ir complex, (<sup>Me</sup>PNP)Ir(D)(C<sub>6</sub>D<sub>5</sub>) as an *in-situ* trap. Various control reactions were also carried out to ensure that the presence of the Ir complex does not affect the chemistry with CO<sub>2</sub>. It was observed that although (<sup>Me</sup>PNP)Ir(D)(C<sub>6</sub>D<sub>5</sub>) reacts with CO<sub>2</sub>, these reactions do not interfere with the reduction of CO<sub>2</sub> to CO by [(<sup>F</sup>PNP)Pd]<sub>2</sub>.

Utility of pincer complexes of transition metals for catalytic C-C and C-heteroatom coupling has been a hot topic for research owing to the diverse applications of such reactions. Our group has specifically focused on the use of metals like Ir and Rh for various catalytic processes. Due to cobalt being in the same group as Ir and Rh and motivated by its high abundance and low cost, we envision the use of cobalt pincer complexes as catalysts in cross coupling reactions. We hypothesize cobalt based catalytic coupling involving mechanisms similar to those illustrated for Ir and Rh in previous reports by us and others, hence our efforts were focused on isolating proposed catalytic intermediates and seeing their interconversion.

POCOP type pincer ligands were tested first due to our recent success with catalytic C-S, C-N and Kumada-Corriu type C-C coupling reactions with (POCOP)Rh complexes. Our efforts resulted in the successful isolation of catalytically relevant Co<sup>III</sup> complexes such as (POCOP)Co(Ar)(X) and (POCOP)Co(Ar)(SAr') for the first time. C-S RE from (POCOP)Co(Ar)(SAr') however was not observed upon thermolysis, C<sub>ligand</sub>-C<sub>Ar</sub> being observed instead. The higher rates of C-C RE vs C-S RE were attributed as the cause for these observations and a move to pincer ligands without central C donors was deemed necessary.

PNP complexes of Co<sup>III</sup> such as (PNP)Co(Ar)(X) and (PNP)Co(Ar)(SAr') were synthesized and isolated following procedures analogous to those for POCOP. Thermolysis of (PNP)Co(Ar)(SAr') did afford elimination of Ar-S-Ar' but it was accompanied by the formation of Co<sup>II</sup> species of the type, (PNP)Co(Ar) and (PNP)Co(SAr') raising concerns about the prevalence and mechanism of the formation of Ar-S-Ar'. A set of preliminary experiments suggest that a concerted RE mechanism might be more plausible than a radical elimination based mechanism but further studies need to be performed to provide this hypothesis more credence.

In a separate effort, we strived to expand the library of available binuclear pincer ligands and their metal complexes to facilitate use of such ligands and complexes in catalytic applications. Successful modification of ligands to incorporate more steric bulk and functionality on the linker connecting the pincer sites was observed. Nucleation of Ni instead of previously reported Pd was also achieved.

## REFERENCES

- (1) Morales-Morales, D., Jensen, C. M., Eds.; *The chemistry of pincer compounds*, 1st ed.; Elsevier: Amsterdam ; Boston, 2007.
- (2) Ozerov, O. V.; Guo, C.; Papkov, V. A.; Foxman, B. M. *J. Am. Chem. Soc.* **2004**, *126*, 4792.
- (3) DeMott, J. C.; Basuli, F.; Kilgore, U. J.; Foxman, B. M.; Huffman, J. C.; Ozerov, O. V.; Mindiola, D. J. *Inorg. Chem.* **2007**, *46*, 6271.
- (4) Fan, L.; Foxman, B. M.; Ozerov, O. V. *Organometallics* **2004**, *2*, 326.
- (5) Fan, L.; Yang, L.; Guo, C.; Foxman, B. M.; Ozerov, O. V. *Organometallics* **2004**, *23*, 4778.
- (6) Liang, L.-C.; Lin, J.-M.; Hung, C.-H. *Organometallics* **2003**, *22*, 3007.
- (7) Crocker, C.; Errington, R. J.; McDonald, W. S.; Odell, K. J.; Shaw, B. L.; Goodfellow, R. J. *J. Chem. Soc. Chem. Commun.* **1979**, *11*, 498.
- (8) Moulton, C. J.; Shaw, B. L. *J. Chem. Soc. Dalton Trans.* **1976**, *11*, 1020.
- (9) Miller, E. M.; Shaw, B. L. *J. Chem. Soc. Dalton Trans.* **1974**, *5*, 480.
- (10) Shih, W.-C.; Ozerov, O. V. *Organometallics* **2015**, *34*, 4591.
- (11) Leis, W.; Mayer, H. A.; Kaska, W. C. *Coord. Chem. Rev.* **2008**, *252*, 1787.
- (12) Morales-Morales, D.; Grause, C.; Kasaoka, K.; Redón, R.; Cramer, R. E.; Jensen, C. M. *Inorganica Chim. Acta* **2000**, *300–302*, 958.
- (13) Salem, H.; Ben-David, Y.; Shimon, L. J. W.; Milstein, D. *Organometallics* **2006**, *25*, 2292.

- (14) Bedford, R. B.; Draper, S. M.; Scully, P. N.; Welch, S. L. *New J. Chem.* **2000**, *24*, 745.
- (15) Fryzuk, M. D.; Leznoff, D. B.; Thompson, R. C.; Rettig, S. J. *J. Am. Chem. Soc.* **1998**, *120*, 10126.
- (16) Fryzuk, M. D.; MacNeil, P. A. *J. Am. Chem. Soc.* **1981**, *103*, 3592.
- (17) Fryzuk, M. D.; MacNeil, P. A.; Rettig, S. J. *Organometallics* **1985**, *4*, 1145.
- (18) Chen, X.; Femia, F. J.; Babich, J. W.; Zubieta, J. *Inorganica Chim. Acta* **2000**, *307*, 88.
- (19) Bligh, S. W. A.; Bashall, A.; Garrud, C.; McPartlin, M.; Wardle, N.; White, K.; Padhye, S.; Barve, V.; Kundu, G. *Dalton Trans.* **2003**, *2*, 184.
- (20) Alyea, E. C.; Ferguson, G.; Restivo, R. J.; Merrell, P. H. *J. Chem. Soc. Chem. Commun.* **1975**, *8*, 269.
- (21) Restivo, R. J.; Ferguson, G. *J. Chem. Soc. Dalton Trans.* **1976**, *6*, 518.
- (22) Morales-Morales, D. *Mini-Rev. Org. Chem.* **2008**, *5*, 141.
- (23) Chakraborty, S.; Bhattacharya, P.; Dai, H.; Guan, H. *Acc. Chem. Res.* **2015**, *48*, 1995.
- (24) Fan, L.; Foxman, B. M.; Ozerov, O. V. *Organometallics* **2004**, *23*, 326.
- (25) Winter, A. M.; Eichele, K.; Mack, H.-G.; Potuznik, S.; Mayer, H. A.; Kaska, W. *C. J. Organomet. Chem.* **2003**, *682*, 149.
- (26) Liang, L.-C. *Coord. Chem. Rev.* **2006**, *250*, 1152.

- (27) Davidson, J. J.; DeMott, J. C.; Douvris, C.; Fafard, C. M.; Bhuvanesh, N.; Chen, C.-H.; Herbert, D. E.; Lee, C.-I.; McCulloch, B. J.; Foxman, B. M.; Ozerov, O. V. *Inorg. Chem.* **2015**, *54*, 2916.
- (28) Lee, C.-I.; DeMott, J. C.; Pell, C. J.; Christopher, A.; Zhou, J.; Bhuvanesh, N.; Ozerov, O. V. *Chem. Sci.* **2015**, *6*, 6572.
- (29) Pell, C. J.; Ozerov, O. V. *ACS Catal.* **2014**, *4*, 3470.
- (30) Smith, D. A.; Herbert, D. E.; Walensky, J. R.; Ozerov, O. V. *Organometallics* **2013**, *32*, 2050.
- (31) Huacuja, R.; Graham, D. J.; Fafard, C. M.; Chen, C.-H.; Foxman, B. M.; Herbert, D. E.; Alliger, G.; Thomas, C. M.; Ozerov, O. V. *J. Am. Chem. Soc.* **2011**, *133*, 3820.
- (32) Fafard, C. M.; Adhikari, D.; Foxman, B. M.; Mindiola, D. J.; Ozerov, O. V. *J. Am. Chem. Soc.* **2007**, *129*, 10318.
- (33) Fan, L.; Ozerov, O. V. *Chem. Commun.* **2005**, *35*, 4450.
- (34) Liang, L.-C.; Li, C.-W.; Lee, P.-Y.; Chang, C.-H.; Lee, H. M. *Dalton Trans.* **2011**, *40*, 9004.
- (35) King, A. O.; Yasuda, N.; In *Organometallics in Process Chemistry*; Topics in Organometallic Chemistry; Springer Berlin Heidelberg, 2004; pp 205–245.
- (36) Torborg, C.; Beller, M. *Adv. Synth. Catal.* **2009**, *351*, 3027.
- (37) Mizoroki, T.; Mori, K.; Ozaki, A. *Bull. Chem. Soc. Jpn.* **1971**, *44*, 581.
- (38) Mori, K.; Mizoroki, T.; Ozaki, A. *Bull. Chem. Soc. Jpn.* **1973**, *46*, 1505.
- (39) Heck, R. F.; Nolley, J. P. *J. Org. Chem.* **1972**, *37*, 2320.

- (40) Heck, R. F. *J. Am. Chem. Soc.* **1968**, *90*, 5518.
- (41) Dieck, H. A.; Heck, R. F. *J. Am. Chem. Soc.* **1974**, *96*, 1133.
- (42) Miyaura, N.; Suzuki, A. *J. Chem. Soc. Chem. Commun.* **1979**, *19*, 866.
- (43) Miyaura, N.; Yamada, K.; Suzuki, A. *Tetrahedron Lett.* **1979**, *20*, 3437.
- (44) Miyaura, N.; Suzuki, A. *Chem. Rev.* **1995**, *95*, 2457.
- (45) Baba, S.; Negishi, E. *J. Am. Chem. Soc.* **1976**, *98*, 6729.
- (46) King, A. O.; Okukado, N.; Negishi, E. *J. Chem. Soc. Chem. Commun.* **1977**, *19*, 683.
- (47) Sonogashira, K.; Tohda, Y.; Hagihara, N. *Tetrahedron Lett.* **1975**, *16*, 4467.
- (48) Hartwig, J. F. *Acc. Chem. Res.* **1998**, *31*, 852.
- (49) Hartwig, J. F. *Angew. Chem. Int. Ed.* **1998**, *37*, 2046.
- (50) Muci, A. R.; Buchwald, S. L. In *Cross-Coupling Reactions*; Miyaura, P. N., Ed.; Topics in Current Chemistry; Springer Berlin Heidelberg, 2002; pp 131–209.
- (51) Old, D. W.; Wolfe, J. P.; Buchwald, S. L. *J. Am. Chem. Soc.* **1998**, *120*, 9722.
- (52) The Nobel Prize in Chemistry 2010  
[http://www.nobelprize.org/nobel\\_prizes/chemistry/laureates/2010/](http://www.nobelprize.org/nobel_prizes/chemistry/laureates/2010/) (accessed Apr 30, 2016).
- (53) Negishi, E., Meijere, A. de, Eds.; *Handbook of organopalladium chemistry for organic synthesis*; Wiley-Interscience: New York, 2002.
- (54) Yamaguchi, J.; Muto, K.; Itami, K. *Eur. J. Org. Chem.* **2013**, *2013*, 19.
- (55) Wang, Z.-X.; Liu, N. *Eur. J. Inorg. Chem.* **2012**, *2012*, 901.



- (56) Meijere, A. de; Diederich, F. *Metal-catalyzed cross-coupling reactions*, 2nd, completely and enl. ed ed.; Wiley-VCH: Weinheim, 2004.
- (57) Takahashi, T.; Kanno, K. In *Modern Organonickel Chemistry*; Tamaru, Y., Ed.; Wiley-VCH Verlag GmbH & Co. KGaA, 2005; pp 41–55.
- (58) Joshi-Pangu, A.; Biscoe, M. *Synlett* **2012**, *23*, 1103.
- (59) *Synfacts* **2011**, *2011*, 897.
- (60) *Synfacts* **2011**, *2011*, 662.
- (61) Ullmann, F.; Bielecki, J. *Berichte Dtsch. Chem. Ges.* **1901**, *34*, 2174.
- (62) Ullmann, F. *Berichte Dtsch. Chem. Ges.* **1903**, *36*, 2382.
- (63) Ullmann, F.; Maag, R. *Berichte Dtsch. Chem. Ges.* **1906**, *39*, 1693.
- (64) Goldberg, I. *Berichte Dtsch. Chem. Ges.* **1906**, *39*, 1691.
- (65) Beletskaya, I. P.; Cheprakov, A. V. *Coord. Chem. Rev.* **2004**, *248*, 2337.
- (66) Evano, G.; Blanchard, N.; Toumi, M. *Chem. Rev.* **2008**, *108*, 3054.
- (67) Ley, S. V.; Thomas, A. W. *Angew. Chem. Int. Ed.* **2003**, *42*, 5400.
- (68) Monnier, F.; Taillefer, M. *Angew. Chem. Int. Ed.* **2009**, *48*, 6954.
- (69) Grushin, V. V.; Alper, H. *Organometallics* **1991**, *10*, 1620.
- (70) Ishiyama, T.; Hartwig, J. *J. Am. Chem. Soc.* **2000**, *122*, 12043.
- (71) Murata, M.; Ishikura, M.; Nagata, M.; Watanabe, S.; Masuda, Y. *Org. Lett.* **2002**, *4*, 1843.
- (72) Bedford, R. B.; Limmert, M. E. *J. Org. Chem.* **2003**, *68*, 8669.
- (73) Ueura, K.; Satoh, T.; Miura, M. *Org. Lett.* **2005**, *7*, 2229.
- (74) Wang, X.; Lane, B. S.; Sames, D. *J. Am. Chem. Soc.* **2005**, *127*, 4996.

- (75) Wu, J.; Zhang, L.; Gao, K. *Eur. J. Org. Chem.* **2006**, 2006, 5260.
- (76) Shintani, R.; Yamagami, T.; Hayashi, T. *Org. Lett.* **2006**, 8, 4799.
- (77) Ito, J.; Miyakawa, T.; Nishiyama, H. *Organometallics* **2008**, 27, 3312.
- (78) Yamanoi, Y.; Nishihara, H. *J. Org. Chem.* **2008**, 73, 6671.
- (79) Lewis, J. C.; Bergman, R. G.; Ellman, J. A. *Acc. Chem. Res.* **2008**, 4, 1013.
- (80) Kim, M.; Chang, S. *Org. Lett.* **2010**, 12, 1640.
- (81) Lewis, J. C.; Wiedemann, S. H.; Bergman, R. G.; Ellman, J. A. *Org. Lett.* **2004**, 6, 35.
- (82) Surawatanawong, P.; Ozerov, O. V. *Organometallics* **2011**, 30, 2972.
- (83) Timpa, S. D.; Fafard, C. M.; Herbert, D. E.; Ozerov, O. V. *Dalton Trans.* **2011**, 40, 5426.
- (84) Timpa, S. D.; Pell, C. J.; Zhou, J.; Ozerov, O. V. *Organometallics* **2014**, 33, 5254.
- (85) Timpa, S. D.; Pell, C. J.; Ozerov, O. V. *J. Am. Chem. Soc.* **2014**, 136, 14772.
- (86) Amatore, M.; Gosmini, C. *Angew. Chem. Int. Ed.* **2008**, 47, 2089.
- (87) Hojilla Atienza, C. C.; Milsmann, C.; Semproni, S. P.; Turner, Z. R.; Chirik, P. J. *Inorg. Chem.* **2013**, 52, 5403.
- (88) Wong, Y.-C.; Jayanth, T. T.; Cheng, C.-H. *Org. Lett.* **2006**, 8, 5613.
- (89) Hartwig, J. F. *Organotransition metal chemistry: from bonding to catalysis*; University Science Books: Sausalito, Calif, 2010.
- (90) Crabtree, R. H. In *The Organometallic Chemistry of the Transition Metals*; John Wiley & Sons, Inc., 2005; pp 159–182.
- (91) Hartwig, J. F.; Paul, F. *J. Am. Chem. Soc.* **1995**, 117, 5373.

- (92) Amatore, C.; Pflüger, F. *Organometallics* **1990**, *9*, 2276.
- (93) Fauvarque, J.-F.; Pflüger, F.; Troupel, M. *J. Organomet. Chem.* **1981**, *208*, 419.
- (94) Amatore, C.; Jutand, A.; Khalil, F.; M'Barki, M. A.; Mottier, L. *Organometallics* **1993**, *12*, 3168.
- (95) Otsuka, S.; Yoshida, T.; Matsumoto, M.; Nakatsu, K. *J. Am. Chem. Soc.* **1976**, *98*, 5850.
- (96) Paul, F.; Patt, J.; Hartwig, J. F. *Organometallics* **1995**, *14*, 3030.
- (97) Barrios-Landeros, F.; Carrow, B. P.; Hartwig, J. F. *J. Am. Chem. Soc.* **2009**, *131*, 8141.
- (98) Driver, M. S.; Hartwig, J. F. *J. Am. Chem. Soc.* **1997**, *119*, 8232.
- (99) Driver, M. S.; Hartwig, J. F. *J. Am. Chem. Soc.* **1995**, *117*, 4708.
- (100) Mann, G.; Shelby, Q.; Roy, A. H.; Hartwig, J. F. *Organometallics* **2003**, *22*, 2775.
- (101) Jones, W. D.; Kuykendall, V. L. *Inorg. Chem.* **1991**, *30*, 2615.
- (102) Johansson Seechurn, C. C. C.; Kitching, M. O.; Colacot, T. J.; Snieckus, V. *Angew. Chem. Int. Ed.* **2012**, *51*, 5062.
- (103) Chen, S.; Li, Y.; Zhao, J.; Li, X. *Inorg. Chem.* **2009**, *48*, 1198.
- (104) Grushin, V. V.; Marshall, W. J. *J. Am. Chem. Soc.* **2004**, *126*, 3068.
- (105) Hoogervorst, W. J.; Goubitz, K.; Fraanje, J.; Lutz, M.; Spek, A. L.; Ernsting, J. M.; Elsevier, C. J. *Organometallics* **2004**, *23*, 4550.
- (106) Macgregor, S. A.; Roe, D. C.; Marshall, W. J.; Bloch, K. M.; Bakhmutov, V. I.; Grushin, V. V. *J. Am. Chem. Soc.* **2005**, *127*, 15304.

- (107) de Pater, B. C.; Zijp, E. J.; Frühauf, H.-W.; Ernsting, J. M.; Elsevier, C. J.; Vrieze, K.; Budzelaar, P. H. M.; Gal, A. W. *Organometallics* **2004**, *23*, 269.
- (108) Willems, S. T. H.; Budzelaar, P. H. M.; Moonen, N. N. P.; de Gelder, R.; Smits, J. M. M.; Gal, A. W. *Chem. – Eur. J.* **2002**, *8*, 1310.
- (109) Douglas, T. M.; Chaplin, A. B.; Weller, A. S. *Organometallics* **2008**, *27*, 2918.
- (110) Gatard, S.; Çelenligil-Çetin, R.; Guo, C.; Foxman, B. M.; Ozerov, O. V. *J. Am. Chem. Soc.* **2006**, *128*, 2808.
- (111) Gatard, S.; Guo, C.; Foxman, B. M.; Ozerov, O. V. *Organometallics* **2007**, *26*, 6066.
- (112) Puri, M.; Gatard, S.; Smith, D. A.; Ozerov, O. V. *Organometallics* **2011**, *30*, 2472.
- (113) Ghosh, R.; Emge, T. J.; Krogh-Jespersen, K.; Goldman, A. S. *J. Am. Chem. Soc.* **2008**, *130*, 11317.
- (114) Timpa, S. D.; Pell, C. J.; Ozerov, O. V. *J. Am. Chem. Soc.* **2014**, *136*, 14772.
- (115) van Leeuwen, P. W. N. M.; Freixa, Z. In *Activation of Small Molecules*; Tolman, W. B., Ed.; Wiley-VCH Verlag GmbH & Co. KGaA, 2006; pp 319–356.
- (116) Higman, C.; Burgt, M. van der. *Gasification*; Elsevier/Gulf Professional Pub: Boston, 2003.
- (117) *Wikipedia, the free encyclopedia*. <https://en.wikipedia.org/wiki/Syngas> (accessed July 14, 2016).
- (118) *Wikipedia, the free encyclopedia*. [https://en.wikipedia.org/wiki/Steam\\_reforming](https://en.wikipedia.org/wiki/Steam_reforming) (accessed July 14, 2016)

- (119) Barton Cole, E.; Bocarsly, A. B. In *Carbon Dioxide as Chemical Feedstock*; Aresta, M., Ed.; Wiley-VCH Verlag GmbH & Co. KGaA, 2010; pp 291–316.
- (120) Fontecilla-Camps, J. C.; Amara, P.; Cavazza, C.; Nicolet, Y.; Volbeda, A. *Nature* **2009**, *460*, 814.
- (121) Benson, E. E.; Kubiak, C. P. *Chem. Commun.* **2012**, *48*, 7374.
- (122) Schneider, J.; Jia, H.; Kobihiro, K.; Cabelli, D. E.; Muckerman, J. T.; Fujita, E. *Energy Environ. Sci.* **2012**, *5*, 9502.
- (123) DuBois, D. L.; Miedaner, A.; Haltiwanger, R. C. *J. Am. Chem. Soc.* **1991**, *113*, 8753.
- (124) Steffey, B. D.; Miedaner, A.; Maciejewski-Farmer, M. L.; Bernatis, P. R.; Herring, A. M.; Allured, V. S.; Carperos, V.; DuBois, D. L. *Organometallics* **1994**, *13*, 4844.
- (125) Steffey, B. D.; Curtis, C. J.; DuBois, D. L. *Organometallics* **1995**, *14*, 4937.
- (126) Raebiger, J. W.; Turner, J. W.; Noll, B. C.; Curtis, C. J.; Miedaner, A.; Cox, B.; DuBois, D. L. *Organometallics* **2006**, *25*, 3345.
- (127) Chen, Z.; Chen, C.; Weinberg, D. R.; Kang, P.; Concepcion, J. J.; Harrison, D. P.; Brookhart, M. S.; Meyer, T. J. *Chem. Commun.* **2011**, *47*, 12607.
- (128) Silvia, J. S.; Cummins, C. C. *J. Am. Chem. Soc.* **2010**, *132*, 2169.
- (129) Williams, V. A.; Manke, D. R.; Wolczanski, P. T.; Cundari, T. R. *Inorganica Chim. Acta* **2011**, *369*, 203.
- (130) Jayarathne, U.; Chandrasekaran, P.; Jacobsen, H.; Mague, J. T.; Donahue, J. P. *Dalton Trans.* **2010**, *39*, 9662.

- (131) Fachinetti, G.; Floriani, C.; Chiesi-Villa, A.; Guastini, C. *J. Am. Chem. Soc.* **1979**, *101*, 1767.
- (132) Hall, K. A.; Mayer, J. M. *J. Am. Chem. Soc.* **1992**, *114*, 10402.
- (133) Castro-Rodriguez, I.; Meyer, K. *J. Am. Chem. Soc.* **2005**, *127*, 11242.
- (134) Ménard, G.; Gilbert, T. M.; Hatnean, J. A.; Kraft, A.; Krossing, I.; Stephan, D. W. *Organometallics* **2013**, *32*, 4416.
- (135) Li, J.; Hermann, M.; Frenking, G.; Jones, C. *Angew. Chem. Int. Ed.* **2012**, *51*, 8611.
- (136) Ménard, G.; Stephan, D. W. *Angew. Chem. Int. Ed.* **2011**, *50*, 8396.
- (137) Gau, D.; Rodriguez, R.; Kato, T.; Saffon-Merceron, N.; de Cózar, A.; Cossío, F. P.; Baceiredo, A. *Angew. Chem. Int. Ed.* **2011**, *50*, 1092.
- (138) Laitar, D. S.; Müller, P.; Sadighi, J. P. *J. Am. Chem. Soc.* **2005**, *127*, 17196.
- (139) Walensky, J. R.; Fafard, C. M.; Guo, C.; Brammell, C. M.; Foxman, B. M.; Hall, M. B.; Ozerov, O. V. *Inorg. Chem.* **2013**, *52*, 2317.
- (140) Fafard, C. M.; Adhikari, D.; Foxman, B. M.; Mindiola, D. J.; Ozerov, O. V. *J. Am. Chem. Soc.* **2007**, *129*, 10318.
- (141) Huacuja, R.; Herbert, D. E.; Fafard, C. M.; Ozerov, O. V. *J. Fluor. Chem.* **2010**, *131*, 1257.
- (142) Kullberg, M. L.; Kubiak, C. P. *Inorg. Chem.* **1986**, *25*, 26.
- (143) Cameron, T. S.; Gardner, P. A.; Rundy, K. R. *J. Organomet. Chem.* **1981**, *212*, C19.
- (144) Cámpora, J.; Palma, P.; del Río, D.; Álvarez, E. *Organometallics* **2004**, *23*, 1652.

- (145) Bennett, M. A.; Robertson, G. B.; Rokicki, A.; Wickramasinghe, W. A. *J. Am. Chem. Soc.* **1988**, *110*, 7098.
- (146) Kubiak, C. P.; Woodcock, C.; Eisenberg, R. *Inorg. Chem.* **1982**, *21*, 2119.
- (147) Zhu, Y.; Fan, L.; Chen, C.-H.; Finnell, S. R.; Foxman, B. M.; Ozerov, O. V. *Organometallics* **2007**, *26*, 6701.
- (148) Ozerov, O. V.; Guo, C.; Fan, L.; Foxman, B. M. *Organometallics* **2004**, *23*, 5573.
- (149) Suh, H.-W.; Schmeier, T. J.; Hazari, N.; Kemp, R. A.; Takase, M. K. *Organometallics* **2012**, *31*, 8225.
- (150) Levy, G. C.; Cargioli, J. D.; Juliano, P. C.; Mitchell, T. D. *J. Magn. Reson.* **1969** *1972*, *8*, 399.
- (151) *Palladium-catalyzed coupling reactions: practical aspects and future developments*; Molnár, Á., Ed.; Wiley-VCH: Weinheim, Germany, 2013.
- (152) Tsuji, J. *Palladium reagents and catalysts: new perspectives for the 21st century*; Wiley: Hoboken, NJ, 2004.
- (153) Trost, B. M.; Van Vranken, D. L.; Bingel, C. *J. Am. Chem. Soc.* **1992**, *114*, 9327.
- (154) Miao, J.; Ge, H. *Eur. J. Org. Chem.* **2015**, *2015*, 7859.
- (155) Su, B.; Cao, Z.-C.; Shi, Z.-J. *Acc. Chem. Res.* **2015**, *48*, 886.
- (156) Han, F.-S. *Chem. Soc. Rev.* **2013**, *42*, 5270.
- (157) Netherton, M. R.; Fu, G. C. *Adv. Synth. Catal.* **2004**, *346*, 1525.
- (158) Rudolph, A.; Lautens, M. *Angew. Chem. Int. Ed.* **2009**, *48*, 2656.
- (159) Tasker, S. Z.; Standley, E. A.; Jamison, T. F. *Nature* **2014**, *509*, 299.
- (160) Gosmini, C.; Bégouin, J.-M.; Moncomble, A. *Chem. Commun.* **2008**, *28*, 3221.

- (161) Tsou, T. T.; Kochi, J. K. *J. Am. Chem. Soc.* **1979**, *101*, 6319.
- (162) Breitenfeld, J.; Wodrich, M. D.; Hu, X. *Organometallics* **2014**, *33*, 5708.
- (163) Smith, A. L.; Hardcastle, K. I.; Soper, J. D. *J. Am. Chem. Soc.* **2010**, *132*, 14358.
- (164) Bowman, A. C.; Milsmann, C.; Bill, E.; Lobkovsky, E.; Weyhermüller, T.; Wiegardt, K.; Chirik, P. J. *Inorg. Chem.* **2010**, *49*, 6110.
- (165) Obligacion, J. V.; Chirik, P. J. *J. Am. Chem. Soc.* **2013**, *135*, 19107.
- (166) Yu, R. P.; Darmon, J. M.; Milsmann, C.; Margulieux, G. W.; Stieber, S. C. E.; DeBeer, S.; Chirik, P. J. *J. Am. Chem. Soc.* **2013**, *135*, 13168.
- (167) Hojilla Atienza, C. C.; Milsmann, C.; Lobkovsky, E.; Chirik, P. J. *Angew. Chem. Int. Ed.* **2011**, *50*, 8143.
- (168) Hulley, E. B.; Wolczanski, P. T.; Lobkovsky, E. B. *J. Am. Chem. Soc.* **2011**, *133*, 18058.
- (169) Volpe, E. C.; Wolczanski, P. T.; Lobkovsky, E. B. *Organometallics* **2010**, *29*, 364.
- (170) Brennan, M. R.; Kim, D.; Fout, A. R. *Chem. Sci.* **2014**, *5*, 4831.
- (171) Xu, H.; Bernskoetter, W. H. *J. Am. Chem. Soc.* **2011**, *133*, 14956.
- (172) Przyojski, J. A.; Arman, H. D.; Tonzetich, Z. J. *Organometallics* **2013**, *32*, 723.
- (173) Timpa, S. D.; Zhou, J.; Bhuvanesh, N.; Ozerov, O. V. *Organometallics* **2014**, *33*, 6210.
- (174) Cho, C.-H.; Chien, T.-Y.; Chen, J.-H.; Wang, S.-S.; Tung, J.-Y. *Dalton Trans.* **2010**, *39*, 2609.
- (175) Addison, A. W.; Rao, T. N.; Reedijk, J.; Rijn, J. van; Verschoor, G. C. *J. Chem. Soc. Dalton Trans.* **1984**, *7*, 1349.



- (176) Fout, A. R.; Basuli, F.; Fan, H.; Tomaszewski, J.; Huffman, J. C.; Baik, M.-H.; Mindiola, D. J. *Angew. Chem. Int. Ed.* **2006**, *45*, 3291.
- (177) Drulis, H.; Dyrek, K.; Hoffmann, K. P.; Hoffmann, S. K.; Weselucha-Birczynska, A. *Inorg. Chem.* **1985**, *24*, 4009.
- (178) Trávníček, Z.; Klanicová, A.; Popa, I.; Rolčík, J. *J. Inorg. Biochem.* **2005**, *99*, 776.
- (179) Greig, L. M.; Slawin, A. M. Z.; Smith, M. H.; Philp, D. *Tetrahedron* **2007**, *63*, 2391.
- (180) Hebden, T. J.; St. John, A. J.; Gusev, D. G.; Kaminsky, W.; Goldberg, K. I.; Heinekey, D. M. *Angew. Chem. Int. Ed.* **2011**, *50*, 1873.
- (181) *Apex2, Version 2 User Manual, M86-E01078*; Bruker Analytical Systems: Madison, WI, 2006.
- (182) Sheldrick, G. M. University of Goettingen 2008,.
- (183) Sheldrick, G. M. *Acta Crystallogr. A* **2008**, *64*, 112.
- (184) Spek, A. L. *J. Appl. Crystallogr.* **2003**, *36*, 7.
- (185) Hartwig, J. F. *Nature* **2008**, *455*, 314.
- (186) Tran, B. L.; Adhikari, D.; Fan, H.; Pink, M.; Mindiola, D. J. *Dalton Trans.* **2009**, *39*, 358.
- (187) Semproni, S. P.; Milsmann, C.; Chirik, P. J. *J. Am. Chem. Soc.* **2014**, *136*, 9211.
- (188) Semproni, S. P.; Atienza, C. C. H.; Chirik, P. J. *Chem. Sci.* **2014**, *5*, 1956.
- (189) Zhang, G.; Yin, Z.; Tan, J. *RSC Adv.* **2016**, *6*, 22419.
- (190) Zhang, G.; Scott, B. L.; Hanson, S. K. *Angew. Chem. Int. Ed.* **2012**, *51*, 12102.

- (191) Zhang, G.; Vasudevan, K. V.; Scott, B. L.; Hanson, S. K. *J. Am. Chem. Soc.* **2013**, *135*, 8668.
- (192) Zhang, G.; Yin, Z.; Zheng, S. *Org. Lett.* **2016**, *18*, 300.
- (193) Weng, W.; Yang, L.; Foxman, B. M.; Ozerov, O. V. *Organometallics* **2004**, *2*, 4700.
- (194) Sumbly, C. J.; Steel, P. J. *Organometallics* **2003**, *22*, 2358.
- (195) Chan, C.-W.; Mingos, D. M. P.; White, A. J. P.; Williams, D. J. *Chem. Commun.* **1996**, *1*, 81.
- (196) Lagunas, M.-C.; Gossage, R. A.; Spek, A. L.; van Koten, G. *Organometallics* **1998**, *17*, 731.
- (197) Steenwinkel, P.; Kooijman, H.; Smeets, W. J. J.; Spek, A. L.; Grove, D. M.; van Koten, G. *Organometallics* **1998**, *17*, 5411.
- (198) Chattopadhyay, S.; Sinha, C.; Choudhury, S. B.; Chakravorty, A. *J. Organomet. Chem.* **1992**, *427*, 111.
- (199) Tsubomura, T.; Tanihata, T.; Yamakawa, T.; Ohmi, R.; Tamane, T.; Higuchi, A.; Katoh, A.; Sakai, K. *Organometallics* **2001**, *20*, 3833.
- (200) Göttker-Schnetmann, I.; White, P.; Brookhart, M. *J. Am. Chem. Soc.* **2004**, *126*, 1804.
- (201) Göttker-Schnetmann, I.; White, P. S.; Brookhart, M. *Organometallics* **2004**, *23*, 1766.
- (202) Herbert, D. E.; Ozerov, O. V. *Organometallics* **2011**, *30*, 6641.

- (203) Chen, S.; Ho, M.-H.; Bullock, R. M.; DuBois, D. L.; Dupuis, M.; Rousseau, R.; Raugei, S. *ACS Catal.* **2014**, *4*, 229.
- (204) Wiese, S.; Kilgore, U. J.; Ho, M.-H.; Raugei, S.; DuBois, D. L.; Bullock, R. M.; Helm, M. L. *ACS Catal.* **2013**, *3*, 2527.
- (205) O'Hagan, M.; Shaw, W. J.; Raugei, S.; Chen, S.; Yang, J. Y.; Kilgore, U. J.; DuBois, D. L.; Bullock, R. M. *J. Am. Chem. Soc.* **2011**, *133*, 14301.
- (206) Yang, J. Y.; Smith, S. E.; Liu, T.; Dougherty, W. G.; Hoffert, W. A.; Kassel, W. S.; DuBois, M. R.; DuBois, D. L.; Bullock, R. M. *J. Am. Chem. Soc.* **2013**, *135*, 9700.
- (207) Liu, T.; Liao, Q.; O'Hagan, M.; Hulley, E. B.; DuBois, D. L.; Bullock, R. M. *Organometallics* **2015**, *34*, 2747.
- (208) Liu, T.; DuBois, D. L.; Bullock, R. M. *Nat. Chem.* **2013**, *5*, 228.
- (209) Spasyuk, D. M.; Zargarian, D. *Inorg. Chem.* **2010**, *49*, 6203.
- (210) Spasyuk, D. M.; Zargarian, D.; van der Est, A. *Organometallics* **2009**, *28*, 6531.
- (211) Zhang, B.-S.; Wang, W.; Shao, D.-D.; Hao, X.-Q.; Gong, J.-F.; Song, M.-P. *Organometallics* **2010**, *29*, 2579.
- (212) Yang, M.-J.; Liu, Y.-J.; Gong, J.-F.; Song, M.-P. *Organometallics* **2011**, *30*, 3793.